Pyrolyse de précurseurs organosiliciés en vue de l'élaboration de fibres céramiques base SiC

Eric Bouillon

N° d'ordre : 307

THESE

PRESENTEE A

L' UNIVERSITE DE BORDEAUX I

POUR OBTENIR LE GRADE DE

DOCTEUR

Spécialité : SCIENCES DES MATERIAUX

PAR

Eric BOUILLON

Ingénieur ENSCPB

PYROLYSE DE PRECURSEURS ORGANOSILICIES EN VUE DE L'ELABORATION DE FIBRES CERAMIQUES BASE SiC

Soutenue le 20 avril 1989, devant la commission d'examen :

MM.	P. HAGENMULLER.....	*Président*
M. me	A. OBERLIN.....	
MM.	J. DUNOGUES.....	
	J. ETOURNEAU.....	
	P. OLRY.....	*Examinateurs*
	E. MARCE.....	
	R. NASLAIN.....	
	R. PAILLER.....	

- 1989 -

N° d'ordre : 307

THESE

PRESENTEE A

L' UNIVERSITE DE BORDEAUX I

POUR OBTENIR LE GRADE DE

DOCTEUR

Spécialité : SCIENCES DES MATERIAUX

PAR

Eric BOUILLON

Ingénieur ENSCPB

PYROLYSE DE PRECURSEURS ORGANOSILICIES EN VUE DE L'ELABORATION DE FIBRES CERAMIQUES BASE SiC

Soutenue le 20 avril 1989, devant la commission d'examen :

MM.	P. HAGENMULLER.....	*Président*
M. mc	A. OBERLIN.....	
MM.	J. DUNOGUES.....	
	J. ETOURNEAU.....	
	P. OLRY.....	*Examinateurs*
	E. MARCE.....	
	R. NASLAIN.....	
	R. PAILLER.....	

- 1989 -

Ce travail a été réalisé au Laboratoire de Chimie du Solide du CNRS, sous la direction de Monsieur le Professeur P. HAGENMULLER. Je tiens à lui exprimer ma profonde reconnaissance pour l'acceuil qu'il m'a réservé dans son laboratoire et pour avoir accepté la présidence de mon jury de thèse.

Monsieur le Professeur J. ETOURNEAU, Directeur du Laboratoire de Chimie du Solide du CNRS, m'a fait l'honneur de juger ce mémoire. Je lui adresse mes remerciements les plus sincères.

Madame A. OBERLIN, Directrice du Laboratoire Marcel Mathieu à bien voulu me faire l'honneur de juger mon travail et de me guider dans l'exploitation des résultats de microscopie en transmission, qu'elle trouve ici l'expression de ma respectueuse reconnaissance.

Monsieur le Professeur J. DUNOGUES, Directeur de Recherche au Laboratoire de Chimie Organique et Organométallique du CNRS a bien voulu me faire l'honneur de juger ce travail. Il m'a prodigué conseils et encouragements, qu'il en soit ici vivement remercié.

Monsieur le Professeur R. NASLAIN, Directeur du Laboratoire des Composites Thermostructuraux, a dirigé le présent travail en me faisant profiter de ses précieux conseils. Je tiens à lui exprimer ma profonde gratitude pour tout ce qu'il m'a enseigné au cours de ces années de recherche.

Monsieur P. ORLY, Ingénieur en chef à la Société Européenne de Propulsion a bien voulu suivre et juger ce travail, qu'il trouve ici l'expression de ma sincère gratitude.

Monsieur E. MARCE, Directeur de l'Agence Française pour la Maîtrise de l'Energie a bien voulu juger mon travail, je le remercie vivement.

Je tiens à remercier tout particulièrement, Messieurs F. LANGLAIS et R. PAILLER qui, grâce à leurs compétences scientifiques mais aussi leur gentillesse et leur disponibilité, m'ont permis de mener à bien ce travail. Je tiens à les assurer de ma très profonde reconnaissance et de ma sincère amitié.

Mes remerciements s'adressent aussi à tous ceux du groupe "Matériaux Composites" qui par leur sympathie et leur bonne humeur ont crée une ambiance de travail agréable.

De même, je tiens à remercier Mademoiselle C. DUPOUY qui a contribué largement à la réalisation de ce mémoire.

Enfin, ce travail ayant fait appel à une très large collaboration, je tiens à remercier ici tous ceux qui y ont contribué, en particulier ceux du Laboratoire de Chimie du Solide du CNRS, notamment MM. VIDEAU, DORDOR et MARQUESTAUT.

Je remercie la Société Européenne de Propulsion et l'Agence Française de l'Energie (AFME/CEFI) qui ont permis la réalisation de ces recherches.

SOMMAIRE

CHAPITRE II

Relations between microtexture and electrical properties during heat-treatment of SiC fibre precursor

CHAPITRE III

Composition-microstructure-property relationships in ceramic monofilaments resulting from the pyrolysis of a polycarbosilane precursor at 800-1400°C

CHAPITRE IV

New polycarbosilane models. 5 :
Pyrolysis of series of functional polycarbosilanes

INTRODUCTION

1 - GENERALITES

L'évolution des secteurs aéronautique et aérospatial a nécessité des matériaux présentant simultanément une **faible densité** et de **bonnes caractéristiques mécaniques** (e.g. rigidité, résistance à la rupture statique et dynamique). Les matériaux traditionnels ne pouvant satisfaire ces exigences, c'est une solution "**Composite**" qui a été retenue. En fait, la conception des ces matériaux, ainsi que le choix multiple de leurs constituants leur confèrent un ensemble de propriétés spécifiques et modulables, ce qui explique leur présence dans beaucoup d'autres secteurs d'applications.

L'attrait des matériaux renforcés par des fibres réside principalement dans le fait qu'ils offrent la possibilité **d'associer deux matériaux aux propriétés complémentaires** dans une structure unique dont les propriétés sont supérieures à celles de chacun des constituants pris isolement [1].

L'intérêt qu'on leur porte provient aussi de leur anisotropie très marquée. En effet il est parfois suffisant qu'une structure donnée présente de bonnes propriétés mécaniques dans une seule direction, on réalisera alors un **composite dit unidirectionnel** (i.e. 1D), de façon à ce que toutes les fibres contribuent à supporter la charge, la matrice servira à maintenir les fibres alignées et à transférer les efforts qu'elle reçoit par l'intermédiaire de **l'interphase**. Pour des chargements plus complexes on est amené à réaliser des architectures bidimensionnelles ou multidirectionnelles (i.e. nD avec n = 3,4,5...etc). L'isotropie des matériaux de structure traditionnel ne permet pas d'adopter ce type de démarche. Ainsi pour concevoir et réaliser un matériau composite, il faut connaître avant tout l'utilisation qu'en sera faite de manière à configurer judicieusement le renfort fibreux : on réalise ainsi une **préforme**. Enfin, on peut moduler le taux de fibre et de matrice suivant les applications. On peut ainsi concilier légèreté et résistance mécanique plus des propriétés spécifiques liées à la matrice et/ou aux fibres (résistance à la corrosion, conductivité thermique et/ou électrique etc...) au sein d'un même système [2-5].

Cependant l'utilisation des composites à grande échelle est encore freinée par des problèmes d'élaboration et par le prix du renfort. Nous noterons toutefois que pour des applications "basses températures", les composites à matrice organique (e.g matrice polyester ou polyépoxyde) renforcée par des fibres de verre ou de carbone ont déjà trouvé de nombreuses applications [6]. Ainsi s'imposent-ils dans la réalisation d'articles de sport ou de loisirs, mais le plus gros consommateur de composites à hautes performances reste actuellement l'industrie aéronautique et spatiale. Si ces matériaux présentent des **résistances mécaniques spécifiques** (rapportées à l'unité de masse) excellentes, il n'en demeure pas moins vrai qu'au-dessus de 250°C, la stabilité thermique des matrices organiques devient insuffisante. Il faut faire appel à d'autres types de matrice.

Ce sont les composites à matrice métallique qui sont utilisés aux moyennes températures, i.e. jusque vers 600°C pour des composites à matrice titane. Il semblerait toutefois que les applications des composites à matrice métallique restent relativement limitées étant données les difficultés de mise en oeuvre. Certaines pièces de moteurs peuvent être réalisées avec ce type de composites. Il s'agit plus précisémment d'alliages d'aluminium renforcés par des fibres courtes, sur la base de leur résistance à l'usure et à la fatigue. Les composites à fibres longues de carbone à haut module et à matrice de magnésium, quant à eux pourraient trouver des applications spatiales comme les antennes déployables grâce à leur grande stabilité dimensionnelle et leur faible densité .

Pour les applications à hautes et très hautes températures, e.g. dans les moteurs alternatifs ou les turbines à gaz, les seuls matériaux envisageables sont à base de céramique.

C'est à partir de cette constatation que le regain d'intérêt pour les céramiques est apparu. En effet, elles bénéficient, par rapport aux métaux d'une tenue mécanique supérieure aux températures élevées : c'est le cas, par exemple du carbure et du nitrure de silicium. La densité des céramiques reste faible, et de manière générale elles présentent une bonne inertie chimique. En atmosphère oxydante, par exemple, le carbure de silicium résiste au-delà de 1400°C. De plus, leur dureté est souvent élevée.

En revanche, les céramiques frittées possèdent un gros défaut qui pénalise fortement leur utilisation en tant que matériau de structure : c'est leur fragilité. Une fois créée, une microfissure ne necessite une énergie bien plus faible que dans les métaux pour se propager [7]. Il a été montré récemment que l'addition de fibres longues continues susceptibles de former des liaisons interfaciales particulières constitue une solution efficace pour améliorer la tenacité des céramiques, et dans certains cas la contrainte à rupture. Il est à noter que les composites à matrice céramiques (CMC) présentent par rapport à leurs homologues à matrices métallique et organique un comportement original puisque celle-ci a une déformation à rupture inférieure à celles des fibres. On les qualifie souvent de composites à comportement inverse par rapport aux autres composites dits réguliers.

2 - LES COMPOSITES A MATRICE CERAMIQUE (CMC)

Les composites à matrice céramique font actuellement l'objet de nombreux programmes de recherche/développement car ils sont appelés dans un proche avenir à répondre à des fonctions thermostructurales (boucliers de protection thermique réutilisables, moteur des avions super ou hypersoniques) qui paraissent inéluctables pour les besoins de l'industrie aérospatiale, et à plus long terme au besoin des industries de transports terrestres.Même si les combinaisons semblent multiples et non moins intéressantes au niveau du choix de la matrice et de la fibre [8-12], il n'en demeure pas moins vrai, à notre connaissance, que seuls les composites fibreux C-C (le premier terme se rapporte à la fibre et le second à la matrice) et les composites fibreux C-SiC et SiC-SiC sont l'objet d'une production industrielle. Cette restriction au niveau de l'industrialisation doit probablement provenir, d'une part, des difficultés qui caractérisent les procédés de densification actuels (i.e. CVI, voie liquide, etc...) et, d'autre part,du fait que les fibres actuellement sur le marché (principalement carbone et carbure de silicium) ne semblent pas répondre parfaitement aux exigences des applications thermostructurales.

2.1 - Les composites à matrices non-oxydes

Les composites Carbone-Carbone bénéficient actuellement d'applications importantes. Compte tenu de leur grande réfractérité, de leur faible densité, de leur résitance à l'ablation et de leurs performances mécaniques, l'industrie

aérospatiale en a fait un candidat de choix pour l'élaboration de tuyères, de divergents ou bien encore de protections thermiques non réutilisables. Ils sont aussi utilisés en tant que dispositifs de freinage étant donné leur coéfficient de friction élevé à moyenne température. Ces composites sont obtenus soit par infiltration chimique en phase vapeur (CVI), la source gazeuse étant souvent le méthane, soit par voie liquide à partir d'une résine phénolique ou furanique [13-16].

Au regard de la mauvaise tenue à l'oxydation des composites Carbone-Carbone les composites SiC-SiC semblent mieux adaptés pour l'élaboration de protections thermiques réutilisables devant travailler en milieu oxydant ou de pièces chaudes de moteurs. La Société Européenne de Propulsion a développé industriellement le procédé de dépôt chimique en phase vapeur imaginé par F. Christin et al. en 1975, pour obtenir la matrice carbure de silicium. La source gazeuse est le méthyltrichlorosilane mélangé à de l'hydrogène ou de l'argon [17-19]. La matrice SiC pourrait être également obtenue par imprégnations-pyrolyses successives d'un polymère organosilicié mais il ne semble pas que ce procédé soit l'objet à l'heure actuelle d'une production industrielle.

Les travaux de recherche effectués au sein du groupe Matériaux Composites du Laboratoire de Chimie du Solide ont démontré qu'il était possible d'étendre le procédé d'infiltration chimique par voie gazeuse à d'autre matrice réfractaire telles que : C-SiC, C-TiC, C-BN, C-B_4C [20-22]. De manière générale, ces matériaux dits composites à matrice hybride présentent des propriétés mécaniques améliorées ainsi qu'une tenue à l'oxydation accrue vis-à-vis des composites Carbone-Carbone.

2.2 - Les composites à matrice d'oxydes

Certains composites à matrice constituée d'un oxyde réfractaire peuvent être obtenus par la voie gazeuse comme Al_2O_3/Al_2O_3, Al_2O_3/ZrO_2 ou C/ZrO_2 mais la plupart d'entre eux font appel à la voie liquide. La matrice est mise en oeuvre soit à l'état fondu (ce qui est le cas de matrice à bas point de fusion comme les verres) soit formée à partir d'un précurseur liquide (précurseurs organométalliques comme les alcoolates, barbotines, sols, etc...).

Les premiers composites à matrice silicatée (verre ou vitrocéramique) ont été développés par UKEA à HARWELL (fibre de carbone) puis par UTRC à EAST HARTFORD (fibre SiC).

Les matériaux obtenus présentent de trés bonnes caractéristiques mécaniques ($\sigma R > 1000$ MPa, tenacité élevée) jusqu'à 1000°C pour des matrices vitrocéramiques, et une stabilité dimensionnelle exceptionnelle dans le cas d'association fibres de carbone-matrice vitreuse borosilicatée. Leur application est envisagée pour la réalisation de pièces d'optique spatiales et pour celle des composants de moteur.

Leur tenue à l'oxydation à haute température dépend essentiellement de la nature des fibres et des interphases et du rôle joué par la matrice pour leur protection contre l'oxydation.

3 - LES POLYMERES ORGANOMETALLIQUES : PRECURSEURS DE CERAMIQUE

La voie pyrolytique qui consiste à transformer un polymère organométallique en un solide minéral a dans le domaine des matériaux composites, suscité un interêt tout particulier durant ces dix dernières années aussi bien au niveau du renfort fibreux que de la matrice. Cette voie a été plutôt utilisée jusqu'à présent pour l'élaboration de fibres céramiques, cependant les potentialités que semblent posséder les précurseurs de céramique sont multiples, étant donné que des polymères sont connus pour la plupart des matériaux réfractaires susceptibles d'être utilisés dans le domaine des matériaux composites thermostructuraux. Comme l'indique le tableau n°1, des céramiques à base de SiC, B_4C, BN, Si_3N_4 seules ou en combinaison peuvent être obtenues avec des taux de conversion convenables. On notera enfin que des précurseurs organométalliques existent aussi pour les céramiques à base d'oxydes ; il s'agit par exemple, des alkoxysilanes pour SiO_2, du tributhylate secondaire d'aluminium pour Al_2O_3 ou bien encore du tétraméthylorthotitanate pour TiO_2.

En dehors de la diversité des matériaux obtenus par la voie des précurseurs organométalliques, l'intérêt que l'on porte à ce procédé provient aussi des coûts généralement élevés des méthodes de synthèse de matrice céramique telle que la CVI. En effet sur la base des travaux déjà réalisés dans le domaine des Carbone-Carbone sur la voie liquide, on peut penser que

PRECURSEURS ORGANO-METALLIQUES	RESIDUS MINERAUX	RENDEMENTS (WT. %) THEOR.	EXP.
(1) Carborane-siloxane	SiC/B C	64,5	60
(2) 1,1,1,2,3,3,3- Heptaméthyl 2-vinyltrisilane	SiC	60	50
(3) Poly(borodiphényl)siloxane	SiC/B_4C	43	43
(4) Polycarbosilanes	SiC/C	-	-
(5) Polysilastyrène : phénylméthylsilane-diméthylsilane	SiC/C	-	-
(6) Hexaméthyldisilazane/MTS	Si_3N_4 /SiC/C	-	-
(7) MTS/méthylamine	Si_3N_4 /SiC/C	-	-
(8) Ammonioborane	BN	81	65

TABLEAU I : Quelques précurseurs organo-métalliques de céramiques d'après (23,24,25,26)

d'autres matrices (SiC, Si_3N_4 etc...) pourraient être obtenues suivant quatre étapes principales : (i) la synthèse d'un précurseur organométallique approprié, (ii) l'imprégnation de la préforme fibreuse par le précurseur en solution ou à l'état fondu, (iii) la polymérisation in-situ du précurseur et iv sa pyrolyse à température modérée sous atmosphère généralement inerte. On peut penser que plusieurs cycles imprégnation/polymérisation/pyrolyse seront nécessaires pour aboutir à une densification importante. Selon ce procédé FITZER [27] et al. ont préparé des composites à matrice à base SiC, mais il ne semble pas qu'il y ait eu pour le moment de développements industriels basés sur ces travaux.

De manière générale, pour être utilisés de manière effective pour l'élaboration de matrice, les précurseurs doivent être solubles ou/et liquides à température(s) relativement basse(s), mouiller le renfort fibreux, posséder une viscosité compatible avec les techniques d'imprégnation en phase liquide, conduire après réticulation pyrolyse, avec un rendement aussi élevé que possible, à un solide minéral ayant de bonnes propriétés chimiques et thermomécaniques.

La recherche sur les précurseurs organiques a été jusqu'ici plutôt orientée vers la production de fibres que vers la préparation de matrice. Dans ce cas le polymère doit présenter une bonne aptitude au filage et présenter après réticulation-pyrolyse une faible porosité résiduelle, une bonne tenue à l'oxydation ainsi qu'une bonne stabilité microstructurale à haute température. Parmi ces fibres, celles à base de carbure de silicium présentent un intérêt tout particulier pour l'élaboration de matériaux thermostructuraux. Ainsi des polycarbosilanes furent élaborés par S. Yajima et al. en vue de fabriquer ces nouvelles fibres [28].

4 - FIBRES MULTIBRINS A BASE DE CARBURE DE SILICIUM

La fibre à base de carbure de silicium commercialisée à l'heure actuelle par NIPPON CARBON sous la marque NICALON est le premier exemple de fibres céramiques industrielles obtenues à partir de précurseurs organosiliciés. Elle fait partie aujourd'hui d'une famille plus vaste de fibres réfractaires issues de polymères de type polycarbosilane (PCS) et/ou polycarbosilazane (PCSZ), s'inscrivant dans le système quaternaire Si-C-N-O

(voir dans un système encore plus complexe à la suite d'addition en petite quantité d'autres hétéroatomes comme le titane).

4.1. - Méthode de préparation

La synthèse des fibres multibrins à base de carbure de silicium a été rendue possible grâce à l'existence de polymères organosiliciés filables et donnant après pyrolyse un haut rendement en céramique. Ce sont les travaux de S. Yajima et al. qui font autorité dans ce domaine [28-33]. A l'origine, il semblerait que le polycarbosilane (PCS) ait été obtenu par traitement thermique du polydiméthylsilane (PDMS) à pression atmosphérique [34]. Le PDMS est quant à lui obtenu par déchloruration de diméthyldichlorosilane (Me_2SiCl_2) au sodium dans un bain de xylène au reflux [35]. Par la suite, S. Yajima ne fera plus mention de la "polymérisation à pression atmosphérique" dans ses publications. Il parlera d'une autre voie permettant d'accéder au polycarbosilane qui est la **thermolyse du PDMS en autoclave** vers 470°C [31]. Celle-ci conduit après divolatilisation à 300°C, au PCS filable appelé MARKI et qui est sans doute le précurseur de la fibre NICALON actuellement commercialisée. Il est à noter que pour limiter la quantité d'oxygène dans le précurseur, toutes les opérations sont conduites à l'aide de réactifs anhydres et en atmosphère inerte.

Le PCS est caractérisé par la répétition de motifs carbosilanes $Si\text{-}CH_2$ et représenté par la formulation $-(MeHSiCH_2)-_n$ (ou Me représente le groupe méthyl). La formule brute serait proche de $SiC_{1.8}O_{0.03}H_4$, donc peu éloignée du **polysilapropylène** [31-36], ce qui fait apparaitre un **excés de carbone par rapport au SiC**. Les études effectuées sur ce polymère et plus particulièrement les données RMN [31] montrent que celui-ci est loin de présenter une structure linéaire puisqu'il possède un certain nombre de branchements au niveau des atomes de silicium. Cette configuration complexe du PCS provient d'un mécanisme de réactions radicalaires se produisant lors de la thermolyse. Suivant la température de traitement la masse moléculaire du PCS obtenue augmente [31-33]. Enfin par mesure de viscosité intrinsèque [9] Y. Hasegawa a démontré que l'hypothèse d'une structure plane constituée d'enchaînements cycliques et linéaires (Fig. 1) semblait bien correspondre à ce polymère. Ce polymère bien que possédant une faible masse moléculaire (Mn = 1000 à 2000) est filable vers 300-350°C.

L'étape de filage s'effectue sous azote par extrusion et étirage du précurseur à une vitesse de l'ordre de 200 m min^{-1} (réduction du diamètre à 15 µm environ). De manière à **rendre les fils infusibles** pour qu'ils puissent subir la pyrolyse ultérieure sans dommage, ceux-ci subissent un traitement de stabilisation sous air ou sous oxygène jusque vers 200°C. Il est à noter que, pour des raisons de protection industrielle ce traitement demeure relativement peu connu. Il semblerait toutefois que l'on forme préférentiellement des **ponts Si-O-Si** par réaction des liaisons Si-H, mais aussi des liaisons Si-O-C par réaction des liaisons $Si-CH_3$. Après cette étape la teneur en oxygène lié est de l'ordre de 15 % en poids [32].

La dernière étape du procédé est une **pyrolyse effectuée sous gaz inerte** et à température allant jusque vers 1300°C. Durant cette pyrolyse, d'importantes modifications s'opérent au sein du polymère qui évolue progressivement vers une céramique microcristallisée [33,37,38]. D'après les travaux d'Hasegawa et d'Okamura, la transition fibre polymère-fibre céramique peut se décomposer en six stades [33] (Fig. 2) : 1) le polymère perd des molécules légères et sa masse moléculaire moyenne augmente (T inférieur à 400°C) ; 2) il se produit un changement de structure par réaction de condensation (400-550°C) ; 3 et 4) un départ de gaz (i.e. principalement H_2 et CH_4) est observé, on évolue vers un matériau minéral comportant un réseau tridimensionnel amorphe et ceci jusque vers 900°C ; 5) entre 900 et 1200°C, la phase SiC-β microcristalline se forme au sein de la céramique contenant aussi du carbone libre et une phase oxydée ; 6) après 1200°C, il y a augmentation de la taille des grains de SiC, diminution du nombre de liaisons Si-O par réaction de celles-ci avec du carbone libre pour donner CO.

Le mode opératoire de la synthèse de la fibre est reporté à la figure 3

4.2. Caractéristiques de la fibre NICALON

Avant d'aborder l'étude physico-chimique et mécanique des fibres à base de carbure de silicium, une remarque préliminaire s'impose : NIPPON CARBON (le seul fabricant de ce type de renfort) commercialise des produits qui diffèrent suivant les applications. Citons pour exemple les fibres **NLP-102 et NLM-202.** Dans la nomenclature du fabricant, P est relatif aux applications en matrices plastiques et M est relatif aux applications en matrices métalliques.

Ces deux nuances diffèrent seulement par la nature de l'ensimage des torons. Les premiers chiffres 1 et 2 signifiant respectivement "Standart Grade" et "Ceramic Grade" et correspondent surtout à différentes teneur en oxygène (voir tableau 2). A chaque type de fibre correspond un process bien défini et donc des propriétés spécifiques. Or, de nombreux articles parus il y a quelques années, ne font pas mention du type de fibres étudiées ou utilisent une autre nomenclature. Ceci rend bien évidemment les comparaisons entre résultats délicates.

Quel qu'en soit le type, les fibres sont constituées de silicium, de carbone, d'oxygène et aussi d'une faible quantité d'hydrogène, témoin de l'origine de ces matériaux. L'analyse élémentaire de ces fibres (tableau 2, [39 et 40]) montre très clairement les différences de teneur en oxygène suivant les nuances. Il faut remarquer d'autre part que depuis leurs origines le taux d'oxygène dans ces fibres a nettement diminué. Celui-ci est passé de 18-20 %, d'après les premiers travaux de S. Yajima [40], à une valeur inférieure à 13 % pour les dernières générations de fibres. Ceci résulte directement de différentes améliorations apportées dans le procédé de fabrication.

Les fibres type NICALON ont été décrites à l'origine, en partant de leur analyse élémentaire par S. Yajima comme un mélange de phases SiC, SiO_2, C avec pour conséquence une surestimation importante de la silice [40]. Actuellement beaucoup d'auteurs s'accordent pour les définir plutôt comme une phase amorphe d'oxycarbure de silicium enrobant des microcristaux de carbure de silicium et de carbone [41-42].

Leurs caractéristiques mécaniques à température ambiante (E = 200 GPa, σ^R = 2800 MPa) associées à une faible densité (2,56) , à une mise en oeuvre aisée et à une meilleure tenue à l'oxydation (vis à vis des fibres de carbone) les prédisposent à occuper une place de choix dans l'élaboration de matériaux composites à matrice céramique.

Cependant, le système complexe que constitue la fibre a tendance à évoluer lorsqu'il est porté en température [43], la contrainte à rupture des fibres chute rapidement au dessus de 1200°C alors que le module d'Young décroît progressivement avec la température [39-44].

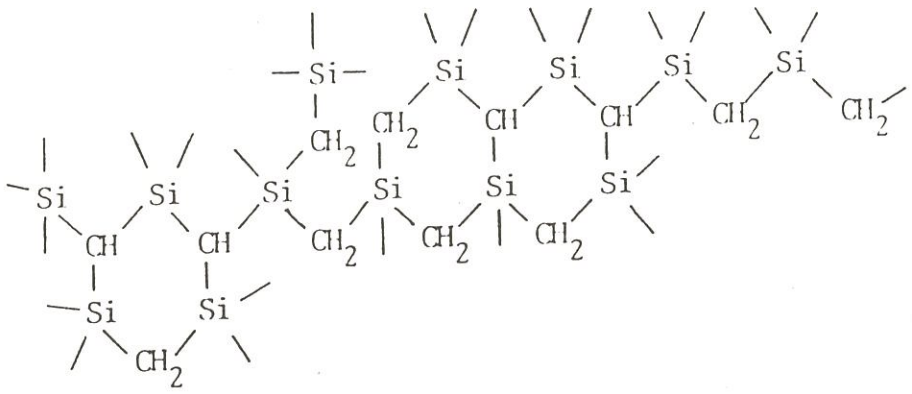

Substituants : H ou Me

Fig 1 : Modèle de structure du PCS obtenu par thermolyse du polydiméthylsilane selon la voie Yajima [31]

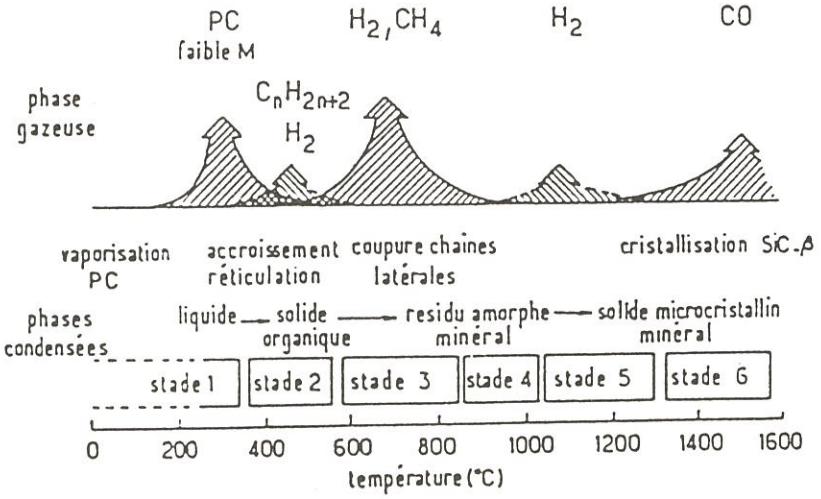

Fig 2 : Les principales étapes de la pyrolyse d'une fibre de PCS stabilisé selon [33]

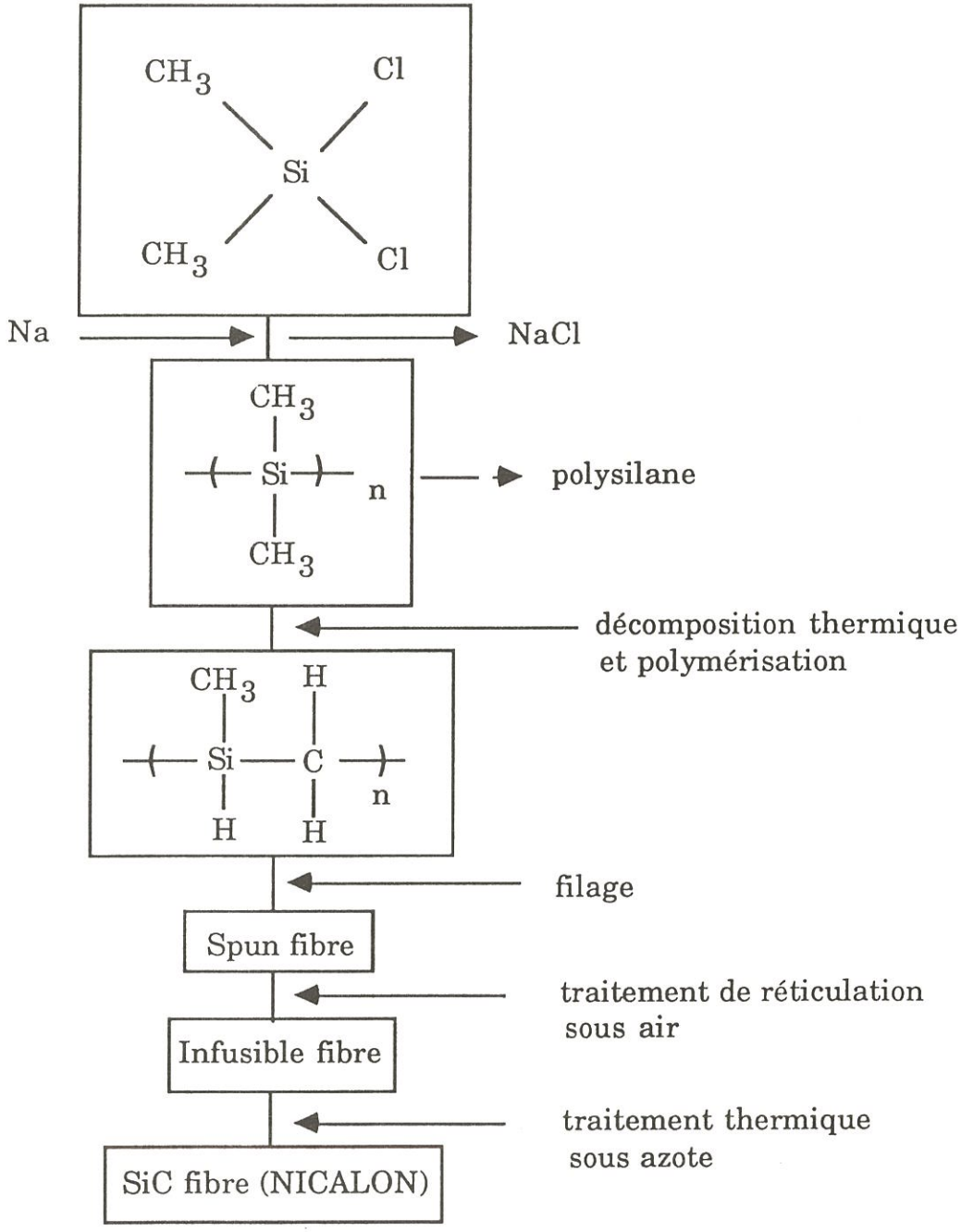

Fig 3 : Shéma de principe de la fabrication d'une fibre à base de SiC à partir d'un précurseur de type carbosilane, selon la voie S. Yajima

Nuances de fibres Nicalon	Si (% pond.)	C (% pond.)	O (% pond.)	Références
NLP 101	60	27	13	(39)
NLM 102	56	35	9	(39)
Fibres SiC première génération	51	24	18	(40)

Tableau 2 : Analyse élémentaire de quelques fibres ex - PCS

De plus comme l'ont montré divers auteurs, leur résistance à l'oxydation en température pour des temps d'exposition prolongés est relativement faible et intimement liée à la pression d'oxygène [45-46].

5 - OBJECTIFS ET CONTENU DU PRESENT TRAVAIL

Il est apparu clairement, après une étude bibliographique sur les fibres du système Si-C-N-O ou plus généralement des céramiques issues de la pyrolyse d'un précurseur organosilicié, qu'il était nécessaire de mieux appréhender, d'une part, la transformation organique-minérale et, d'autre part, les relations existantes entre polymères et céramiques résultantes, de manière à comprendre et essayer de résoudre le mauvais comportement mécanique à haute température des fibres base-SiC existantes.

Le présent travail avait pour objectif d'approfondir la connaissance de la transformation des précurseurs de type polycarbosilanes (PCS) et polycarbilazanes (PCSZ) en céramiques a base de SiC et de Si-(C,N) et de tenter de faire le lien entre la structure du précurseur, la microstructure de la céramique obtenue par pyrolyse et ses propriétés mécaniques. Il s'est orienté autour trois axes principaux :

(i) nous avons mis en évidence les diverses étapes ainsi que les mécanismes intervenant lors de la pyrolyse et de la céramisation d'un précurseur commercial de type polycarbosilane (NC_2). Il est à noter, qu'avant d'être pyrolysé, celui-ci a subi un resserement des masses moléculaires afin d'être filable. Cette étude a fait l'objet de **trois publications** qui constituent respectivement le chapitre I, le chapitre II et l'annexe I.

- **Le chapitre I** concerne, dans un premier temps, la transformation du polymère jusqu'au solide minéral amorphe (vers 850°C) ; celle-ci a été suivie sur la base d'une étude détaillée de l'évolution des gaz de pyrolyse et de l'évolution des différentes liaisons incluses dans les résidus solides par spectroscopie **Infrarouge**. En second lieu, nous nous sommes attachés à mettre en évidence les différentes phases présentes dans ce type de céramique et à suivre l'évolution physico-chimique et microstructurale du système en fonction du traitement thermique. Pour cela, nous avons étudié l'environnement du silicium par **EXAFS** (Extanded X-Ray Absorption Fine Structure) ainsi que les liaisons présentes dans les matériaux par spectroscopie **XPS** (X-Ray

Photoelectron Spectroscopy). L'analyse de l'évolution microstructurale a été réalisée par diffraction des rayons X **(XRD)**, microscopie électronique en transmission **(TEM)** et par microanalyse Raman **(RSMA)** (en ce qui concerne le carbone libre).

- **Le second chapitre** traite plus spécifiquement d'une étude fine réalisée par microscopie électronique en transmission . Celle-ci a permis sur la base de l'évolution de la phase "carbone libre" d'établir une corrélation entre l'évolution de la microstructure et celle du comportement électrique des résidus pyrolysés à différentes températures (Cette partie a fait l'objet d'une publication).

(ii) L'élaboration **d'éprouvettes cylindriques monofilamentaires** à partir du NC_2 a permis de suivre l'évolution des propriétés mécaniques d'une céramique de type ex-PCS en fonction de la température par mesure de la contrainte à rupture, du module d'Young et du module de cisaillement. Nous avons tenté d'expliquer les comportements mécaniques sur la base de l'évolution des phases, de l'évolution microstructurale et de l'évolution des propriétés électriques des éprouvettes en fonction de la température de pyrolyse. Cette étude est reportée au **chapitre III** et fait l'objet d'une publication.

(iii) **Le chapitre IV** a pour objet la définition de **précurseurs modèles** et l'étude de leur pyrolyse ainsi que des céramiques résultantes. Deux publications sont proposées sur ce thème ; celle concernant la minéralisation est présentée au chapitre 4 et celle concernant la synthèse des précurseurs est donnée à l'annexe 2. Nous avons, en particulier mis en évidence le rôle joué par l'azote sur l'état de cristallisation d'une céramique issue de précurseurs modèles de type polycarbosilazane. Nous avons tenté de dégager les corrélations existant entre, d'une part, le rapport C/Si et le type de fonctions carbonées dans le polymère et, d'autre part, le rapport C/Si dans les céramiques résultantes.

REFERENCES

1 - Introduction aux Matériaux Composites ; R. NASLAIN, Ed. CNRS/IMC Bordeaux, 2 (1985), Chap 1.

2 - A. BERGHEZAN ; Matériaux et techniques, Novembre 1976, pp 369-375.

3 - A. BERGHEZAN ; Matériaux et techniques, Janvier-Février 1977, pp 27-32.

4 - A. BERGHEZAN ; Matériaux et techniques, Janvier-Février 1978, pp 17-23.

5 - A.R. BUNSELL, Ann. Chim. Fr., 1980, 5, pp 307-325.

6 - Introduction aux Matériaux Composites ; R. NASLAIN, Ed. CNRS/IMC Bordeaux, 1.

7 - J.F. JAMET, L. ANGUEZ, M. PARLIER, M.H. RITTI, P. PERES, L. GRATEAU, L'Aéronautique et l'Astronautique, 1987- 2/3 N° 123/124 pp 128-142.

8 - I.W. DONALD, P.W. Mc WILLIAM, J. Mat. Sci. 11 (1976) pp 949-972.

9 - L.J. SCHIOLER, Ceram. Bul, Vol 25, N°2 (1986) pp 288-292.

10 - S. JANES, Ceramics Monographs, (1979) Verlag Schmid GmbH Freiburg i. Bry.

11 - G. BERNHART, P. LAMICQ, J. MACE, L'industrie Céramique, N° 790, 1/85 pp 51-56.

12 - A.C. PIERRE, L'Aéronautique et l'Astronautique, N° 75, (1979)- 2, pp 47-75.

13 - P. DELHAES, A. MARCHAND,A. PALCAULT, M. TRINQUECOSTE, B. CHATTERJEE, Rev. Chim. Min., 18 (1981) 476-485.

14 - W.V. KOTLENSKY et D.H. LEEDS, Proc. 3rd Int. Conf. CVD (F.A. Glaski Eds.), The Electrochem. Soc., Princeton (1972) 574-589.

15 - W.V. KOTLENSKY, Proc. 16 th Nat Sampe, Soc. Aerosp. Mater. Process. Eng. Azusa. (1971) pp 257)265.

16 - J.D. THEIS, 3rd Int. Conf. CVD (F.A. Glaski Eds.), The Electrochem. Soc., Princeton (1972) 561-573.

17 - F. CHRISTIN, Thèse de Doctorat d'Etat, N° 641, Univ. Bordeaux I, 1979.

18 - P. LAMICQ, G. BERNHART, M.M. DAUCHIER, J. MACE, Am. Ceram. Soc. Bul., 65 [2] 336-338 (1986).

19 - L.H. HERAULD, F. CHRISTIN, R. NASLAIN, P. HAGENMULLER, Proc. 8th Int. Conf. CVD (J.M. Blocher and alls eds) (1981) 782-789.

20 - C. MALLET, Thèse de Doctorat de 3 ème cycle, N°1811, Univ. Bordeaux I, 1982.

21 - J.Y. ROSSIGNOL, R. NASLAIN, P. HAGENMULLER, L. HERAULT et J.J. CHOURY, Proc. EURO CVD III, Neuchâtel (H.E. Hintermann, Eds) LSRH, (1980) 162-168.

22 - H. HANNACHE, R. NASLAIN et C. BERNHART, J. of Less Common Metal, 95 (1983) 221-246.

23 - S.YAJIMA, Ceram. Bull. , 62/8 (1983) 893-915.

24 - R. WEST, L.D. DAVID, P. I. DJUROVICH, H. YU, et R. SINCLAIR, Ceram. Bull., 62/8 (1983) 899.903.

25 - R.R. WILLS, R.A. MARKLE, et S.P. MAKHERJEE, Ceram. Bull., 62/8 (1983) 904-915.

26 - B.E. WALKER, R.W. RICE, P.F. BECHER, B.A. BERDER et W.S. GOBLENZ, Ceram. Bull., 62/8 (1983) 916-923.

27 - E. FITZER, W. FRITZ, et R. Gadow, Actes Réunion "Advanced Ceramic Materials" Tokyo Inst. Technol. , Yokohama, Oct. 1983.

28 - S. YAJIMA, "Advanced fibres and Composites for elevated temperatures", AIME, p. 30 (1979).

29 - S. YAJIMA, J. HAYASHI, M. OMORI, Chem. Lett., pp 931-934 (1975).

30 - S. YAJIMA, K.OKAMURA, J. HAYASHI, Chem. Lett., pp 1209-1212 (1975).

31 - S. YAJIMA, Y. HASEGAWA, J. HAYASHI, M. IIMURA, J. Mat. Sci. ,13 (1978) 2569-2576.

32 - Y. HASEGAWA, M. IIMURA, S. YAJIMA, J. Mat. Sci. , 15 (1980) 720-728.

33 - Y. HASEGAWA, K.OKAMURA, J. Mat. Sci. , 18 (1983) 3633-3648.

34 - S. YAJIMA, M. OMORI, J. HAYASHI, K.OKAMURA,T. MATSUZAWA, C. LIAW, Chem. Lett., 551 (1976).

35 - C.A. BURKHARD, J. Am. Chem. Soc. , 71, 963 (1964).

36 - Y. HASEGAWA, K.OKAMURA, J. Mat. Sci. , 21 (1986) 321-328.

37 - S. YAJIMA, K.OKAMURA, J. HAYASHI et M. OMORI, J. Amer. Ceram. Soc. , 59 (7-8) 324-77.

38 - K. OKAMURA, M. SATO, Y. HASEGAWA, J. Mater. Sci. Lett. 2 (1983) 769-771.

39 - G. SIMON, A.R. BUNSELL, J. Mat. Sci. 19 (1984) 3649-3657.

40 - S. YAJIMA, K.OKAMURA, Y. HASEGAWA, T. SHISHIDO, Nature, Vol 279, 21 Juin 1979.

41 - L. PORTE et A. SARTRE, J. Mater. Sci. 24 (1989) 271-275

42 - C. LAFFON , A.M. FLANK , R. HAGEGE, P.OLRY, J. COTTERET, M. LARIDJANI, S. DIXMIER, H. HOMMEL, A.P. LEGRAND, J. Mater. Sci. ,24,(1989) 1503-1512.

43 - K.L. LUTHRA J. Am. Ceram. Soc. , 69 (1986) C-231-C-233.

44 - D.J. PHYSHER, K.C. GORETTA, R.S. HODDER et R.E. TRESSLER J. Am. Ceram. Soc., 72 [2] 284-88 (1989)

45 - M. H. JASKOWIAK et J.A. DICARLO, J. Am. Ceram. Soc. 72 [2], 192-197 (1989)

46 - T.J. CLARK, E.R. PRACK, M.I. HAIDER et L.C. SAWYER, Ceram. Eng. Sci. Proc., 8 [7-8], 717-731 (1987).

47 - S. YAJIMA, Handbook of Composites, Vol 1 - Strong Fibers Ed. W. Watt et B.V. Perov, 1985, Elsevier Science Publishers B.V.

48 - K. OKAMURA, Composites, Vol 18, N°2 (1987) 107-120.

CHAPITRE I

On the conversion mechanisms of a polycarbosilane precursor into a SiC-based ceramic materials

INTRODUCTION AU CHAPITRE I

Aucune investigation n'avait été menée sur le thème "**pyrolyse de précurseurs organosiliciés**" au sein du groupe "Matériaux Composites" du Laboratoire de chimie du Solide du CNRS, avant ce travail de thèse. Il nous a donc paru primordial, avant d'aborder une étude de précurseurs originaux synthétisés par l'UA 35, de suivre avec précision les phénomènes physico-chimiques intervenant lors de la pyrolyse d'un polymère commercial. Ce précurseur commercialisé par la Société NIPPON CARBON et qui nous a été fourni par la **Société Européenne de Propulsion** est probablement le précurseur de la fibre NICALON. Cependant pour que celui-ci soit rendu filable, on procéde à un resserement des masses moléculaires, cette étape ayant été réalisée conjointement par la SEP et l'UA 35. L'ensemble des travaux exposés dans le premier chapitre a donc été réalisé sur ce **polycarbosilane** (PCS) **modifié** que nous appelons par la suite $\mathbf{NC_2}$.

L'analyse fine de la transformation du PCS en un solide minéral amorphe a été réalisée jusqu'à une température de pyrolyse (Tp) de 1000°C. Une approche original a consisté à suivre avec précision l'**évolution des espèces gazeuses** au cours du traitement thermique par couplage chromatographie/ spectrométrie de masse et de corréler les résultats obtenus avec l'analyse par **spectroscopie Infra rouge** réalisée sur les résidus solides. Cette première étape a été réalisée en collaboration avec Messieurs J.C. SARTHOU et A. DELPUECH au CEA/CESTAS. Nous avons mis en évidence une transition organométallique-minérale se situant entre 550 et 800°C. Les espèces gazeuses qui se dégagent, sont : (i) des PCS de faibles masses moléculaires avant la transition, qui donnent lieu à une perte de masse importante, (ii) des gaz organosiliciés et hydrocarbonés au cours de la transition et (iii) essentiellement du méthane et de l'hydrogène après la transition.

La deuxième partie de ce travail a été consacrée à l'évolution chimique et microstructurale du résidu minéral amorphe jusqu'à 1600°C. Une analyse fine réalisée par ESCA nous a permis de mettre en évidence les phases SiC, C libre et silice ainsi qu'une phase intermédiaire constituée d'atomes de silicium dans un environnement mixte carbone et oxygène. Cette phase **"oxycarbure de silicium"** est vraissemblablement à l'origine de l'état faiblement cristallisé de ces matériaux. En effet, les études réalisées aussi bien par microscopie électronique en transmission que par EXAFS montre bien que la phase SiC est microcristallisée jusqu'à environ 1400°C. Au-dessus de cette température une cristallisation importante s'opère et parallèlement la phase oxycarbure évolue provoquant le départ des espèces gazeuses SiO et CO.

Une approche originale a consisté à mesurer l'évolution de la conductivité électrique de ces matériaux en fonction de Tp. Elle nous a permis de mettre en évidence une transition entre 1000 et 1200°C de type **isolant-métallique.** Une étude détaillée réalisée par microscopie électronique en transmission et qui fait l'objet du **chapitre II** nous a permis de comprendre ce comportement électrique. Il serait dû essentiellement à un phénomène de percolation du carbone libre.

Enfin l'étude réalisée par EXAFS a donné lieu à une **communication** à "International Symposium EXAFS 5". Celle-ci a été réalisée en étroite collaboration avec C. LAFFON, A.M. FLANCK et P.LAGARDE et est présentée à l'**Annexe 1.**

Soumis à "Journal of Materials Science"

ON THE CONVERSION MECHANISMS OF A POLYCARBOSILANE PRECURSOR INTO A SiC-BASED CERAMIC MATERIAL

E. BOUILLON(*) , F. LANGLAIS(*) , R. PAILLER(*) , R. NASLAIN(*)
Laboratoire de Chimie du Solide du CNRS, Université de Bordeaux 1
33405 Talence, France

J.C SARTHOU, A. DELPUECH
CEA, Centre d'Etudes Scientifiques et Techniques d'Aquitaine,
33114 Le Barp, France

C. LAFFON, P. LAGARDE
LURE, Bt 209D, Université de Paris-Orsay
91405 Orsay, France.

F. CRUEGE, P.V. HUONG
Laboratoire de Spectroscopie Moléculaire et Cristalline, Université de Bordeaux 1, 33405 Talence, France

M. MONTHIOUX and A. OBERLIN
Laboratoire Marcel Mathieu,Université de Pau
2 av. du Pdt. P. Angot, 64000 Pau France.

ABSTRACT

The pyrolysis of a PCS precursor has been studied up to 1600°C through the analysis of the gas phase and the characterization of the solid residue by TGA, X-ray diffraction, EXAFS, ESCA, TEM, Raman and AES microanalyses as well as electrical conductivity measurements. The pyrolysis mechanism involves three main steps : (1) an organometallic mineral transition (550 < Tp < 800°C) leading to an amorphous hydrogenated solid built on tetrahedral SiC, SiO_2 and silicon oxycarbide entities, (2) a nucleation of SiC (1000 < Tp < 1200°C) resulting in SiC nuclei (less than 3 nm in size) surrounded with aromatic carbon layers and (3) a SiC grain size coarsening (Tp > 1400°C) consuming the residual amorphous phases and giving rise simultaneously to a probable evolution of SiO and CO. The formation of free carbon results in a sharp insulator-quasimetal transition with a percolation effect.

(*) Present address : Laboratoire des Composites Thermostructaux (UM 47-CNRS-SEP-UB1), Europarc, 3 Av. Léonard de Vinci, 33600. Pessac, France.

1-INTRODUCTION

Several important ceramic materials can be obtained by pyrolysis from organic or organometallic polymeric precursors. This method was first applied to carbon and then extended to a variety of refractory materials (e.g. SiC, Si_3N_4, B_4C or BN). The pyrolysis processing route has some important advantages with respect to more conventional techniques : (1) it requires lower temperatures, (2) polymeric precursors can be obtained under different states before firing (e.g. as bulk bodies, green films or fibers), (3) polymeric precursors are available with a variety of compositions as single species or as mixtures, a feature allowing the design of ceramics with specific properties [1].

In the field of composite materials, the organometallic polymer route has been widely developed for producing SiC-based fibers from a variety of organosilicon precursors, the most important contribution being due to S. Yajima and his coworkers [2]. The processing route of the Nicalon fiber involves four steps : (1) an adjustement of the molecular weight spectrum of the polymer by distillation under vacuum or an inert gas, (2) melt spinning at about 300°C, (3) a curing treatment by oxidation in air at about 200°C and (4) a pyrolysis at 1200-1300°C in an inert gas or under vacuum. Nicalon and related fibers have been widely studied and some correlations between their chemical nature, microstructure and mechanical behavior have been recently suggested [3-12]. Thus, the lowering of the tensile strength of the fibers after annealing at 1200°C has been associated with local and bulk structural features, crystallization state and chemical composition. SiC-based fibers could be described as a continuum made of SiC_4 and $SiC_{4-x}O_x$ tetrahedral species containing clusters of carbon atoms. The size of the domain of homogeneity varies from fiber grade to fiber grade and is of the order of 1 nm [13]. Both chemical and microstructural heterogeneities vary from the surface to the bulk from fiber grade to fiber grade and as function of the pyrolysis conditions. The oxygen content, silicon oxide surface layer, CO evolution, free carbon elimination as well as β-SiC grain growth are thought to be some determining factors in the thermal stability of Nicalon-type fibers.

Up to now, the mechanisms which are involved in both the synthesis of the fibers and the evolution of their behavior during high temperature annealing, are not well known. As far as we know, the only detailed analysis of

the successive steps of the polycarbosilane pyrolysis has been given by S. Yajima and his coworkers [14]. On the basis of TGA-DTA, IR, X-ray diffraction and chemical analysis as well as gas pressure measurements, they suggested a pyrolysis mechanism involving six steps : (1) at 20-350°C, an evaporation of low molecular weight species, (2) at 350-550°C, a dehydrogenation and dehydrocarbonation condensation, (3) at 550-850°C, a decomposition of the side chains of the polymer giving rise to an amorphous inorganic material with a 3D-network, (4) at 850-1050°C end of formation of the amorphous residue, (5) at 1050-1300°C, crystallization of β–SiC with a mean grain size of 20-30 Å. and occurence of free carbon and α-quartz and finally (6) at 1300-1600°C, coarsening of the α-SiC microstructure and decrease in the amount of Si-O bonds.

The aim of the present study was to bring out additional informations on the pyrolysis of a given polycarbosilane precursor, used as a reference material, on the basis of a variety of characterization techniques either new or already used in this field.

2- EXPERIMENTAL

The polycarbosilane (PCS)(*) used in this study was thought to have been prepared according to the S. Yajima route (i.e. by thermal decomposition and condensation of polydimethylsilane at about 450°C in autoclave) [14-16]. Its molecular structure can thus be described, at least in a first approximation, by the theoretical formula -[$HSiCH_3$-CH_2]-n. Its molecular weight distribution was slightly modified (i.e. the large mass fractions were eliminated by distilation).

Most pyrolysis experiments were performed in a RF induction furnace maintened under a pressure of 1 to 100 kPa of argon carefully purified. The apparatus has a water cooled stainless steel jacket and a rotating sample holder equipped with a set of small alumina crucibles containing the polymeric precursor. With this device, several experiments could be successively performed, in one single run, at different pyrolysis temperatures. The most commonly used temperature-time pyrolysis conditions are given in fig.1. The

(*) from Shinetsu, Japan

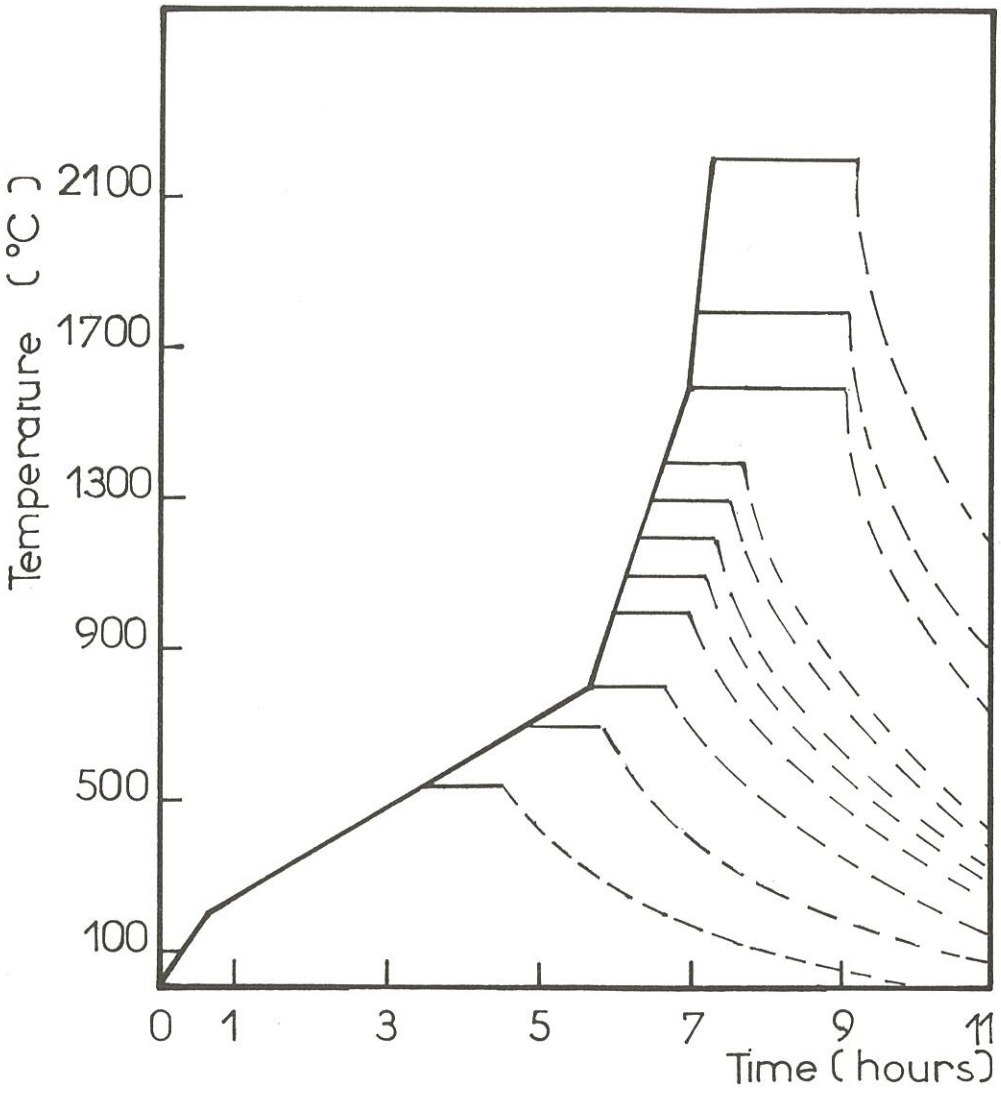

Fig. 1 - Various heat-treatment cycles for pyrolysis experiments

samples were first regularly heated to a temperature Tp (slowly for 200 < Tp < 800°C and then more rapidly) and maintained at this temperature 0.5 to 1 hour (in a few cases, the temperature plateau was as long as 20 hours). From one sample to the other, Tp was increased from 500 to 2200°C.

The analysis of the gaseous species resulting from the polycarbosilane pyrolysis was performed under very different temperature-time conditions (i.e. by flash pyrolysis). A small sample (usually 0.5 mg) was heated very rapidly, with a platinum resistor microfurnace, at a given temperature (ranging from 400 to 1000°C) which was further maintained constant for 10s. The gaseous species formed during the pyrolysis were transported with a helium flow to a chromatograph(*) where the different molecules were separated. Finally, the identification of the gaseous species was performed with a mass-spectrometer coupled with a computer for the treatment of the data. The gaseous species resulting from both types of pyrolysis procedures have been found to be the same. However, in the flash pyrolysis, the evolution of a given species takes place with a shift of 150-200°C towards the high temperatures.

The Electron Spectroscopy for Chemical Analysis (ESCA) was performed with an X-ray microbeam, 300 μm in diameter, under ultra high vacuum (10^{-6} Pa). The Auger Electron Spectroscopy (AES) analysis was carried out with a 250 nm probe. Both spectrometers were equipped with ion guns used to etch the sample surface. The Extented X-ray Absorption Fine Structure (EXAFS) study was performed with the ACO storage ring at LURE operated at 540 MeV and an average current of 100 mA. The RAMAN spectra were recorded with a 1 μm microprobe (laser wave length. : 514.5 nm). The other analyses, i.e. chemical analyses, TEM, TGA, IR, X-ray diffraction and electrical conductivity were performed according to conventional procedures.

3 -RESULTS

During the successive steps of the pyrolysis of a polycarbosilane two kinds of phenomena have to be studied : (1) the evolution of gaseous species and (2) the transformations occurring in the condensed phase

(*) Poropak Q column

3.1- Analysis of the gaseous species

The chromatograms and mass spectra recorded during the flash pyrolysis of the polycarbosilane, at increasing Tp temperatures, are given in fig. 2. The main species which have been clearly identified are alcanes (i.e.methane and ethane) and methylsilane as well as ethylene and carbon monoxide for the highest temperatures (800-1000°C). Assuming that hydrogen and heavy molecules do not contribute significantly to the gas evolution (the former due to its low molecular weight, the latter to their small amount), a tentative quantitative analysis of which results are shown in fig.3 has been performed. Up to 600°C, very little gas evolution is observed although TGA analysis evidences already a 40 % weight loss, as shown in fig. 4, in agreement with the results previously reported by S. Yajima et al. and by J.J. Poupeau et al. [3, 14, 18]. Besides the shift in temperature already mentioned between pyrolyses performed conventionnally (e.g. TGA) and under flash conditions, the evolution of heavy molecular weight gaseous species, easily recondensable, and corresponding to a very small gas volume hardly detectable by 700°C, an evolution of various methylsilanes (and to a less extent, light alcanes) occurs. Above about 800°C, the relative concentrations of the gas phase in methylsilanes decrease and the light carbon containing species (i.e. mainly CH_4 and C_2H_6) are produced preferentially. At least small amounts of carbon monoxide and hexamethylcyclotrisiloxane are identified due either to the oxygen present in the starting material (i.e. 1-1.5 %) or to some contamination during the experiment (PCS are very sensitive to moisture and oxygen).

3.2- The organic-inorganic transition

The occurence of an organic-inorganic transition established on the basis of the gas species analysis (the gas species result from broken organic bonds and recombination processes) is also confirmed by the IR characterization of the condensed phases. As a matter of fact, the evolution of the IR spectra with respect to the pyrolysis temperature (fig. 5), is very similar to that previously reported by S. Yajima et al. [3,14]. Up to 550°C under conventional pyrolysis conditions (and 700-750°C for flash pyrolysis), all the expected absorption peaks corresponding to the theoretical formula of the polymer are observed (i.e. C-H at 2900 and 2950 cm^{-1} ; Si-H at 2100 cm^{-1} ; $Si-CH_3$ at 1400 cm^{-1} and $Si-CH_2-Si$ at 1355 cm^{-1}). The peak intensities decrease slowly up to Tp = 550°C, a feature which confirms that the polymer is only weakly degraded up to this

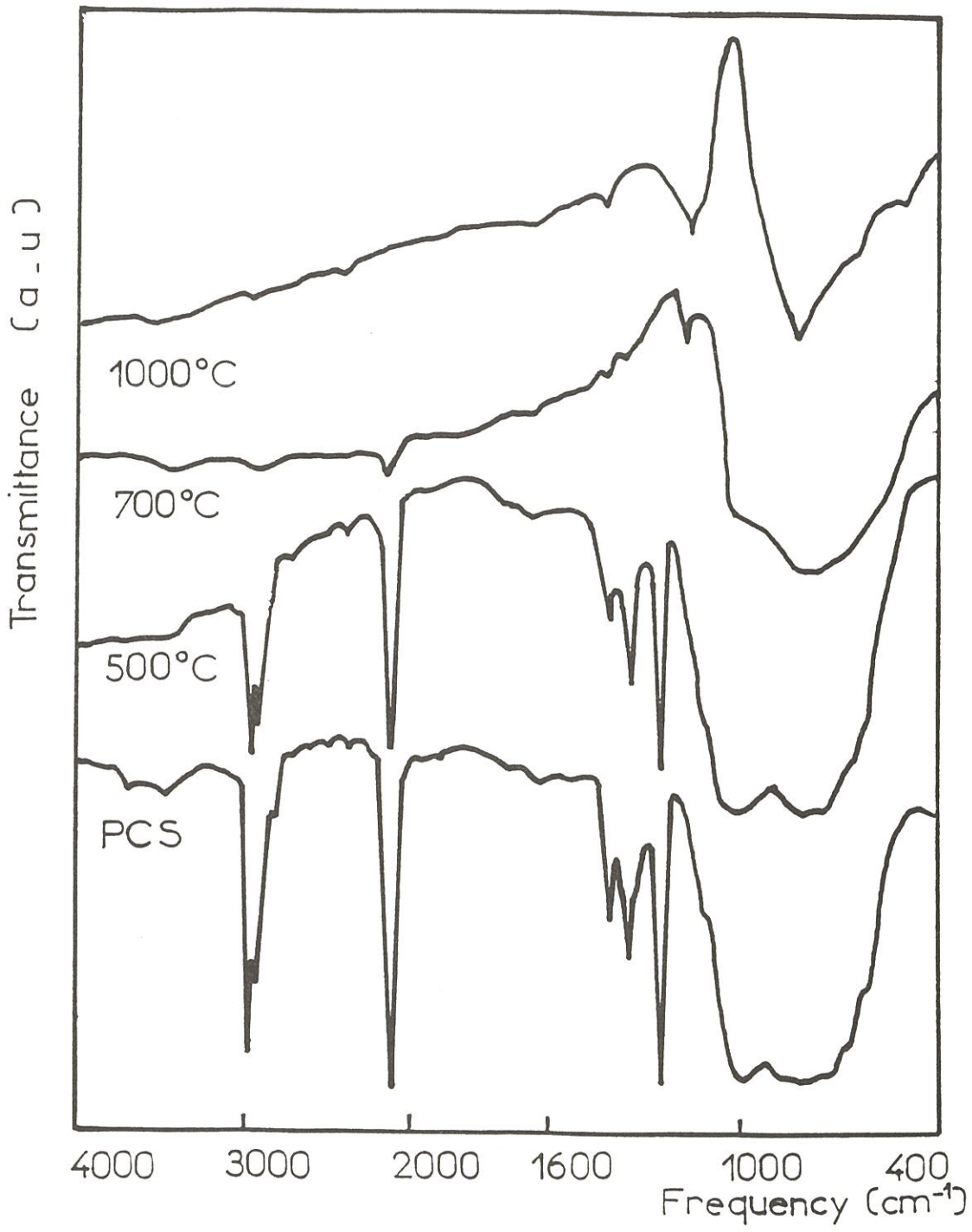

Fig. 5 - The organic-inorganic transition during the pyrolysis of polycarbosilane as evidenced from the IR spectra of the pyrolysis residues.

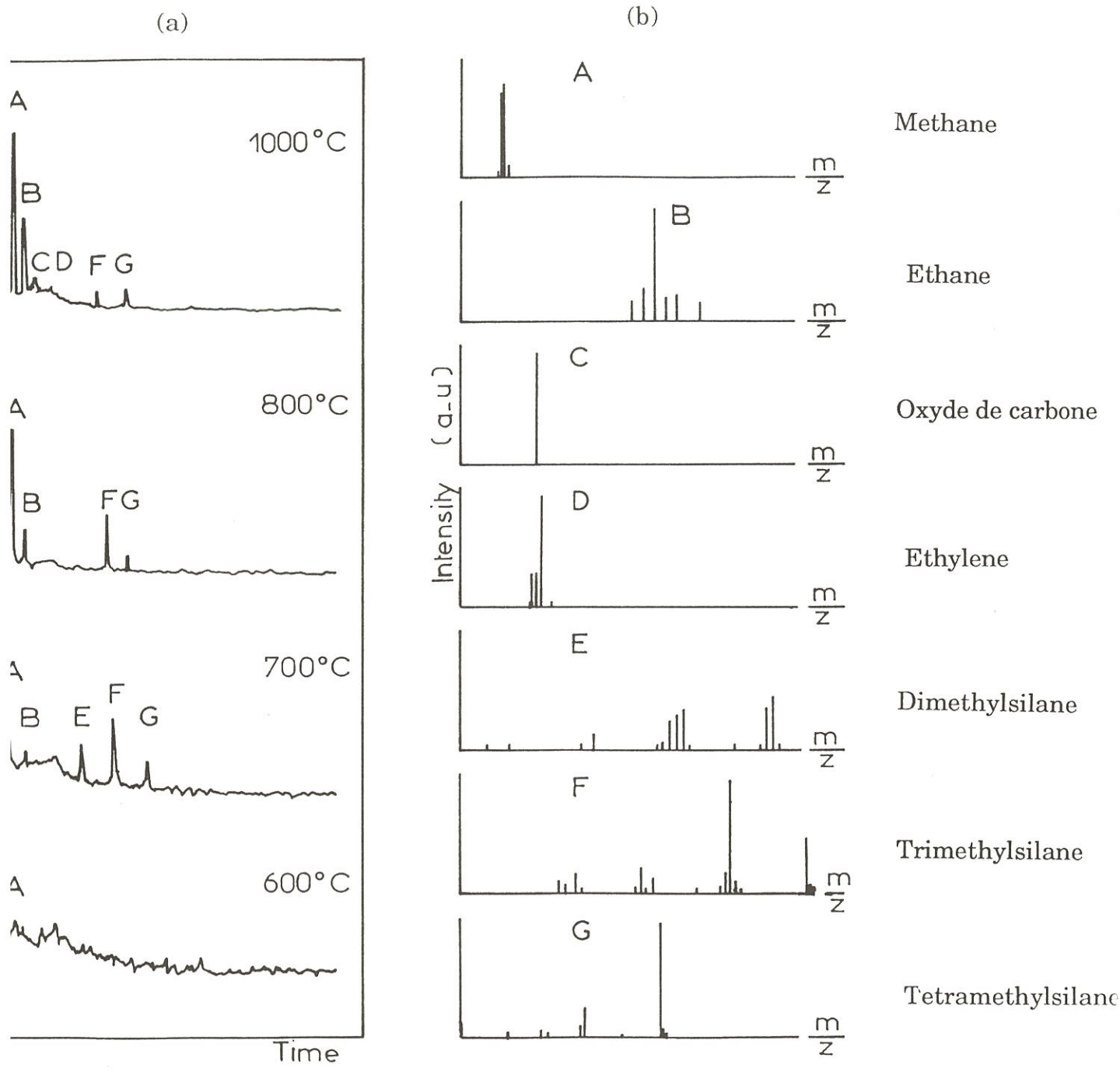

Fig. 2 - Identification of the gaseous species resulting from the flash-pyrolysis of polycarbosilane : (a) chromatograms, (b) mass spectra

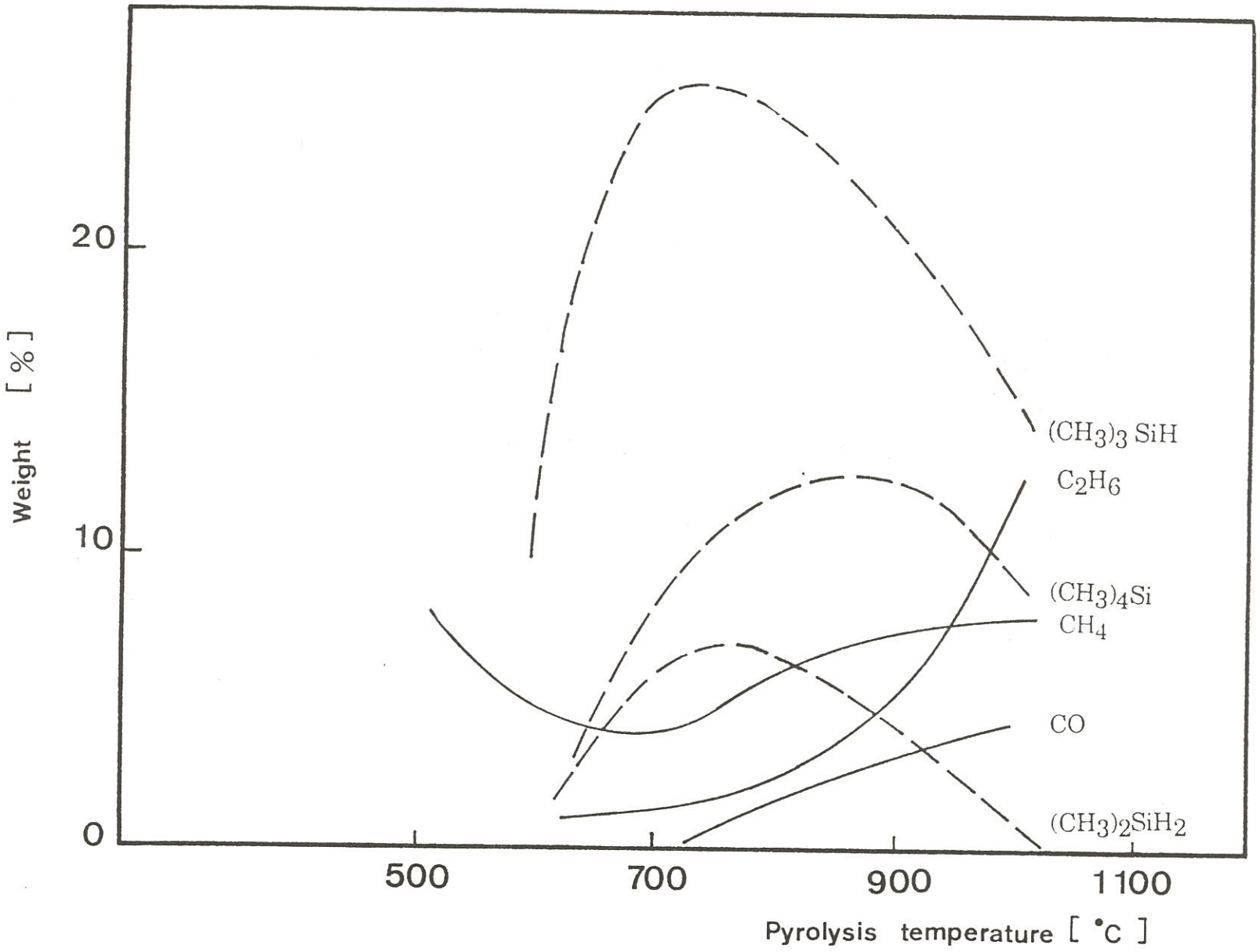

Fig. 3 - Tentative quantitative analysis of the gaseous species resulting from the pyrolysis of polycarbosilane as a function of temperature (the massic percentages are given with respect to the pyrolysed mass).

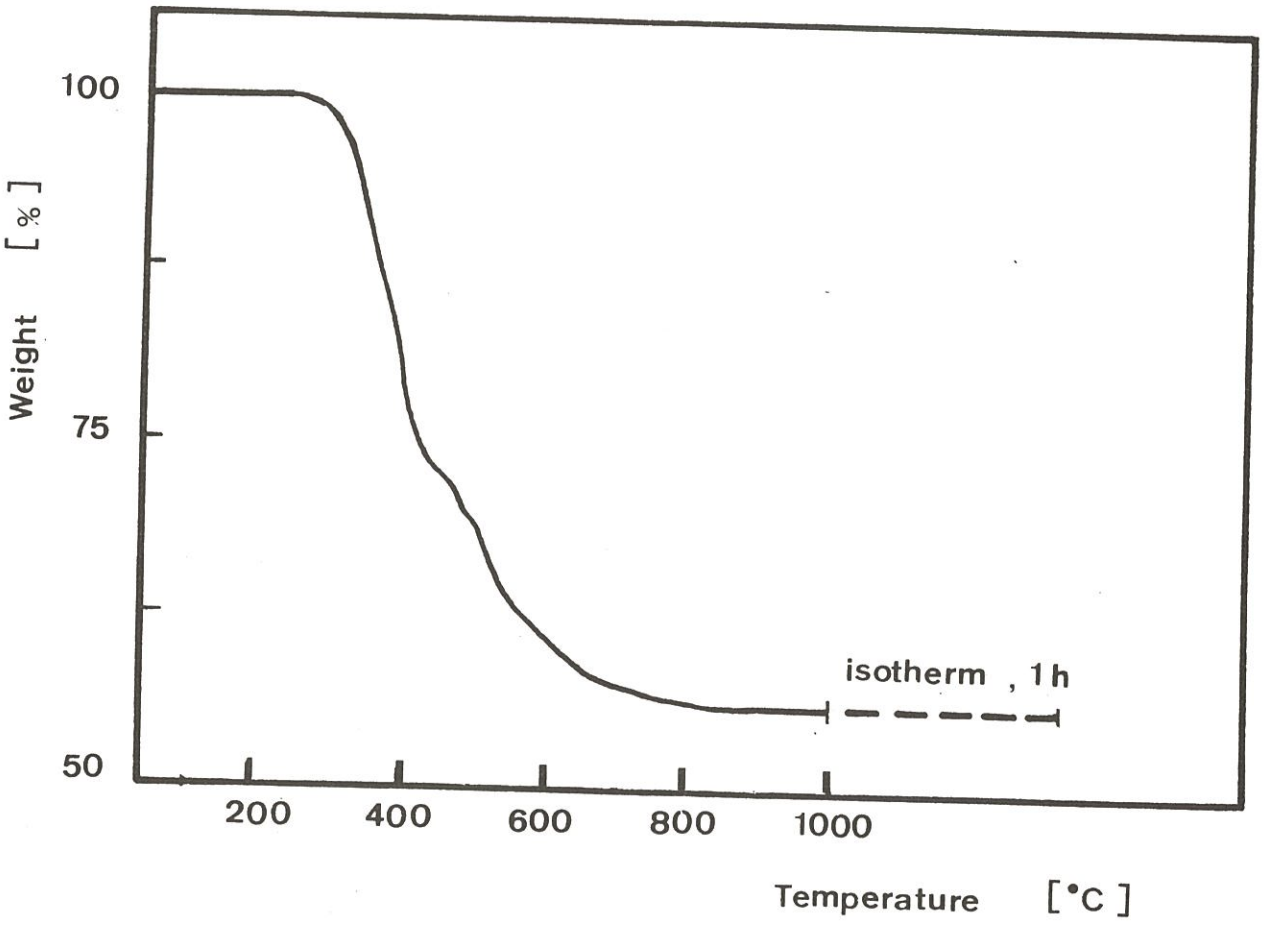

Fig. 4 - TGA of the weight loss observed during the pyrolysis of a polycarbosilane

temperature, as already identified from the gas species analysis. Under such conditions only few organic bonds are broken resulting in the formation of low molecular weight polymers. Between 550 and 700°C, the absorption bands due to the organic bonds decrease in a dramatic manner, a feature which evidences a strong degradation of the polycarbosilane. It seems reasonable to assume that the broken hydrocarbon and silane side entities form, by recombination, those species which have been identified by gas phase analysis. Above 700°C (or 850-900°C in flash pyrolysis), the IR spectra do not change markedly, i.e. the bonds between hydrogen and carbon (or silicon) which are characteristic of the organic state are no longer detected while Si-C and Si-O large bands (between 800 and 1100 cm^{-1}) are observed.

3.3- Chemical analysis of the pyrolysis residues

The results of chemical analyses performed on the residues resulting from pyrolyses run at increasing Tp are given in Table I. It appears that the thermal degradation of the organometallic polymer, which has been already established to be significant at 800°C from gas analysis and TGA, is achieved only above 1000°C as evidenced from the variation of the hydrogen concentration versus temperature. As Tp is raised, both silicon and carbon concentrations increase whereas there is a marked decrease in the oxygen and hydrogen contents. Finally, at 1600°C, the residue is almost free of oxygen and hydrogen. thus, by assuming that SiC is stochiometric, it appears that the final residue of the pyrolysis of the polycarbosilane is **a mixture of SiC and free carbon.**

The pyrolysis residues were also characterized by ESCA and AES. For all pyrolysis conditions, the ESCA spectra of the residues exhibit peaks characteristic of silicon, carbon and oxygen, as shown in fig. 6. From the deconvolution of the Si 2p and C1s peaks of the high resolution spectra, a semi-quantitative analysis of the chemical bonds has been tried.

The 2p silicon peak can be analysed on the basis of three components : the first one, occuring for a binding energy of 100.8 eV corresponds to the Si-C bond in silicon carbide, the second at 103.5 eV is assigned as recently suggested by several authors [13-19] to the Si-O bond in silica and the third at an intermediate energy of 101.8 eV could be assigned to silicon atoms bound to both carbon and oxygen (fig. 7). Similarly, the 1s carbon peak can be analysed

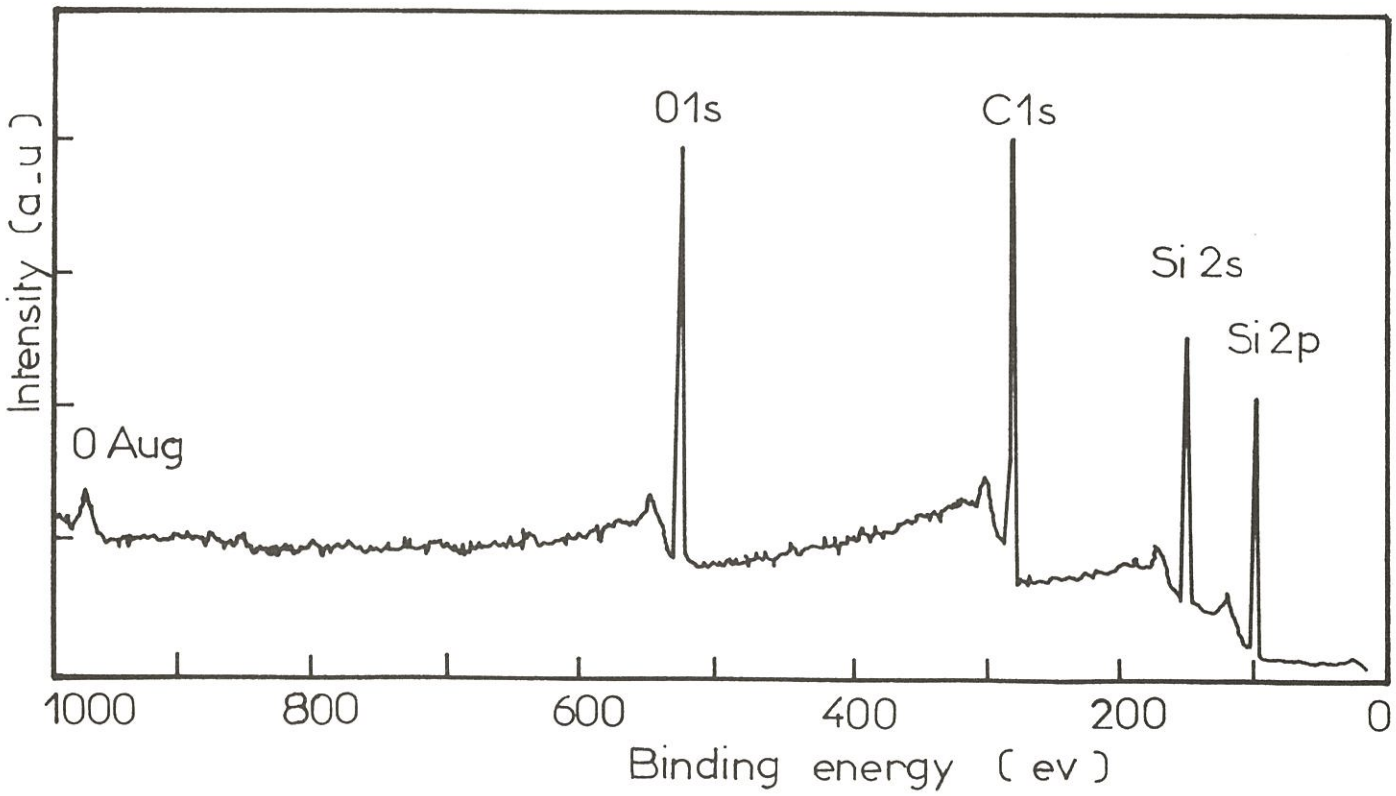

Fig. 6 - ESCA spectrum of the pyrolysis residue of polycarbosilane

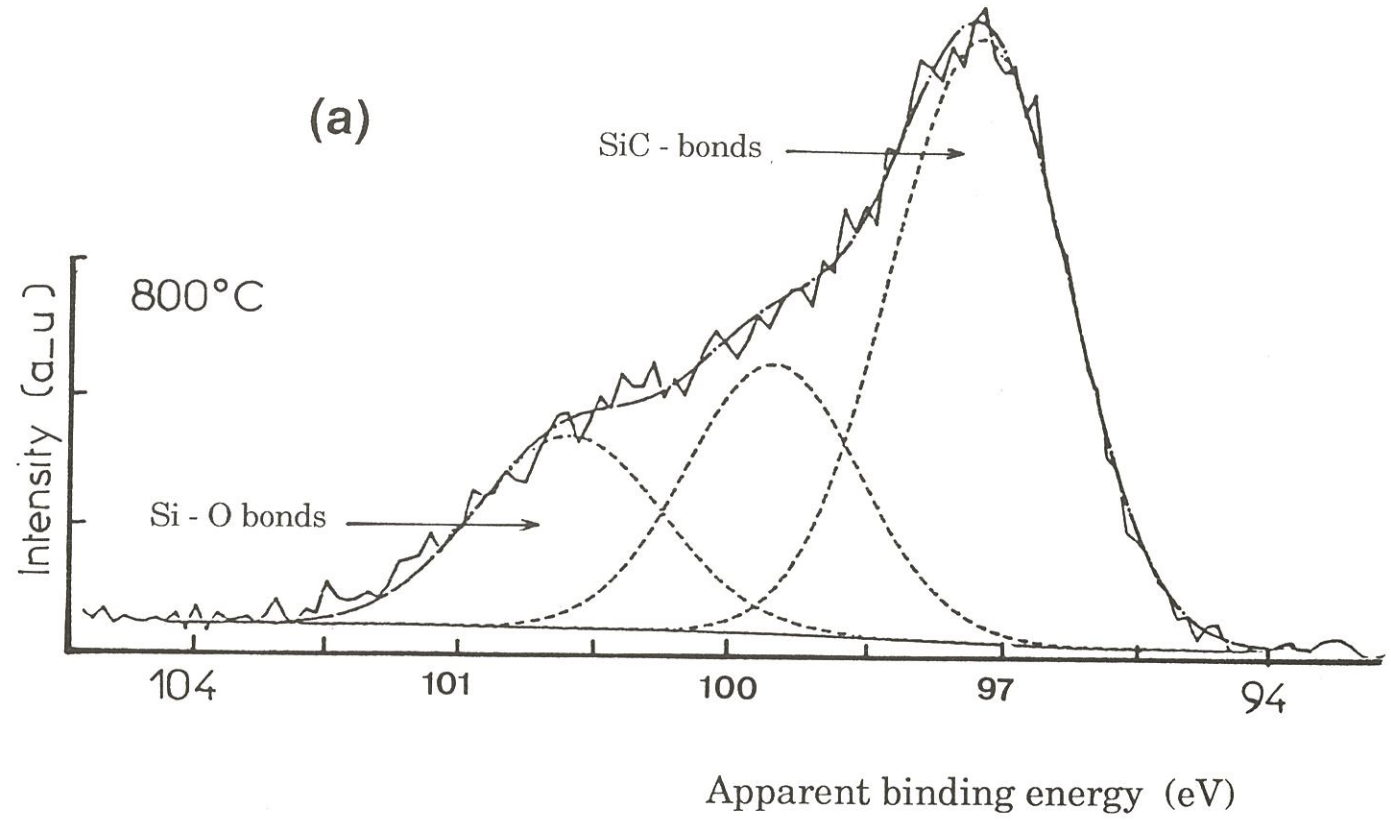

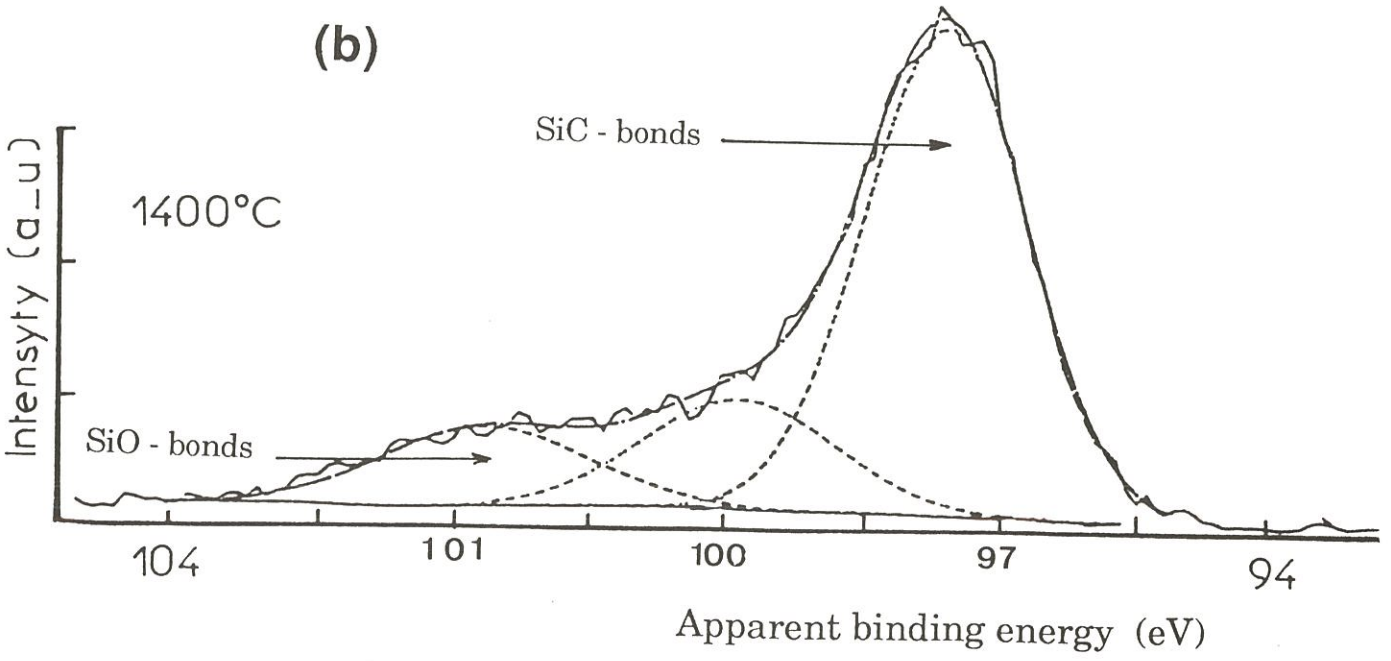

Fig. 7 - Deconvolution of the ESCA 2p silicon peak of pyrolysis residue : (a) Tp = 800°C ; (b) Tp = 1400°C.

on the basis of four components : the first one at 282.8 eV corresponds to carbon bound to silicon, the second at 284.2 eV could be assigned to the oxycarbide Si (C,O) species or to free aromatic carbon (and to a less extent to C-H bonds) [13, 19, 20] and the other two, occurring at higher binding energy can be attributed to carbon-oxygen bonds (i.e. C-O and C=O) (fig. 8). Furthermore, the analysis of the 1s oxygen peak reveals a shoulder (on the high binding energy side of the peak) whose intensity increases with raising Tp. Its assignement to a given bond is difficult regarding the very low chemical shifts observed for this element. Thus, ESCA evidences the occurence in the pyrolysis residues of chemical species which are not well defined and could be regarded as species intermediate between SiC and SiO_2 (e.g. related to Si(O,C) tetrahedra). Such species, sometimes referred to as Si-X (or O-Si-C), have been already reported by L.C. Sawyer et al. [9] or by J. Lipowitz et al. [21] and more recently by R. Hagege et al. as well as L. Porte and A. Sartre [13,19]. The occurence of species intermediate between SiC and SiO2 has also been ascertained by AES analysis. As shown in fig.9, the E.N (E) direct Auger electron spectra, recorded in the energy range corresponding to the LVV transition of silicon after ion etching of increasing duration, clearly show a fine structure with two shoulders between the 74 eV peak characteristic of silicon in SiO_2 and the 86 eV peak characteristic of silicon in SiC [22] .

A semi-quantitative analysis of the chemical bonds present in the pyrolysis residues has been made from the ESCA spectra. The results for unetched samples are given in Table 2. There is an acceptable agreement between the Si-C bond contents derived from the Si 2p and C 1s peaks regarding the difficulty of an accurate separation of the peak components. Moreover, the oxygen content appears to be very high, with respect to that obtained by chemical analysis of the bulk (table 1), at any Tp. At last, the hydrogen concentration, known to be not negligible for Tp < 1400°C, has not been taken into account.

In order to study the possible occurence of concentration gradients near the sample surface, ESCA spectra were recorded after a deep etching (i.e. 20 min of ion etching) on a residue obtained at Tp = 1400°C. As shown in table 2, the ESCA semi-quantitative analysis appears to be in rather good agreement with the composition of the bulk (table 1). This is particularly true for oxygen. Furthermore, the vanishing of the high energy components of the carbon 1s peak (assigned to both C-O and C=O bonds) suggests that part of the oxygen

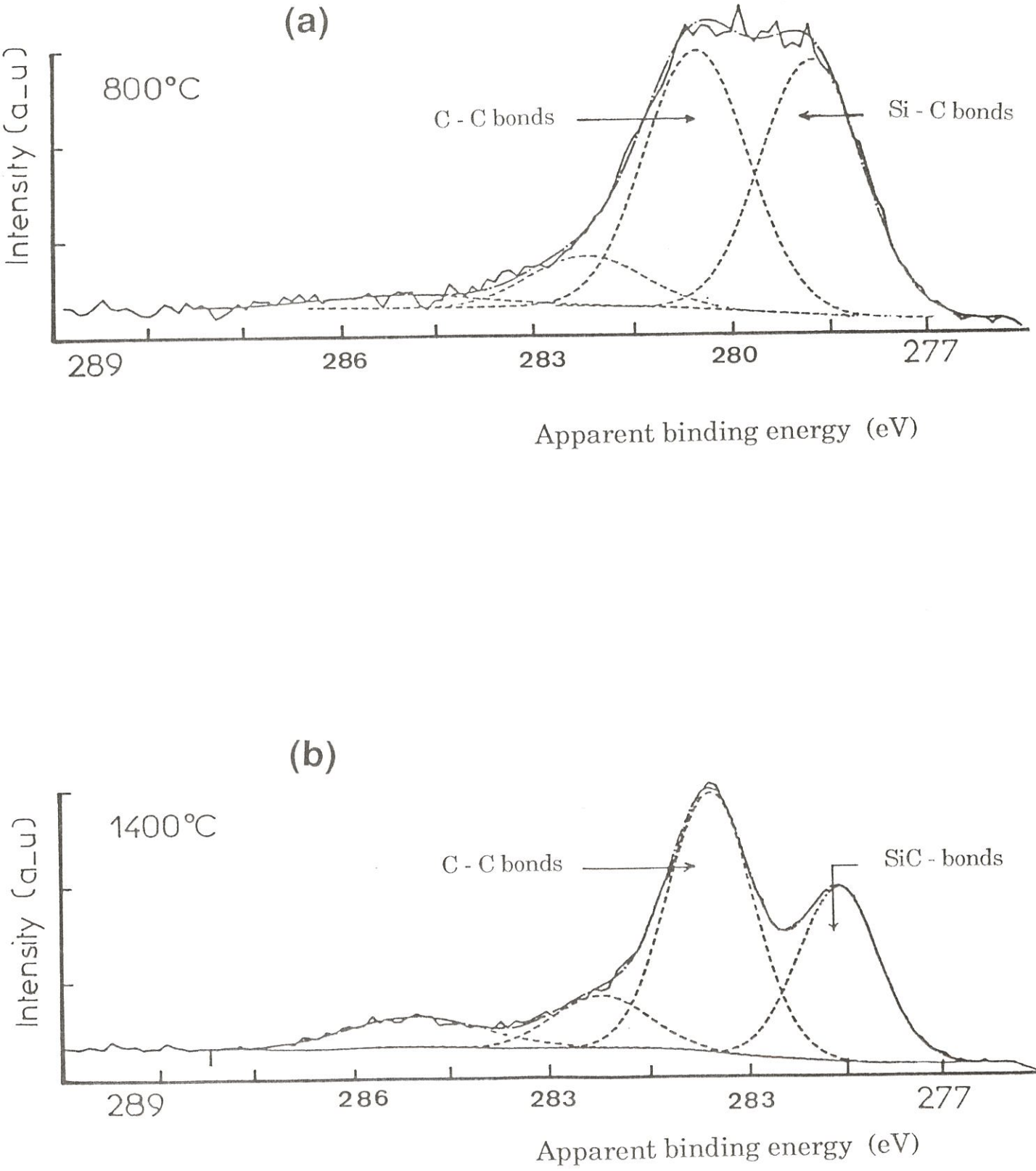

Fig. 8 - Deconvolution of the ESCA 1s-carbon peak of pyrolysis residue : (a) Tp = 800°C ; (b) Tp = 1400°C.

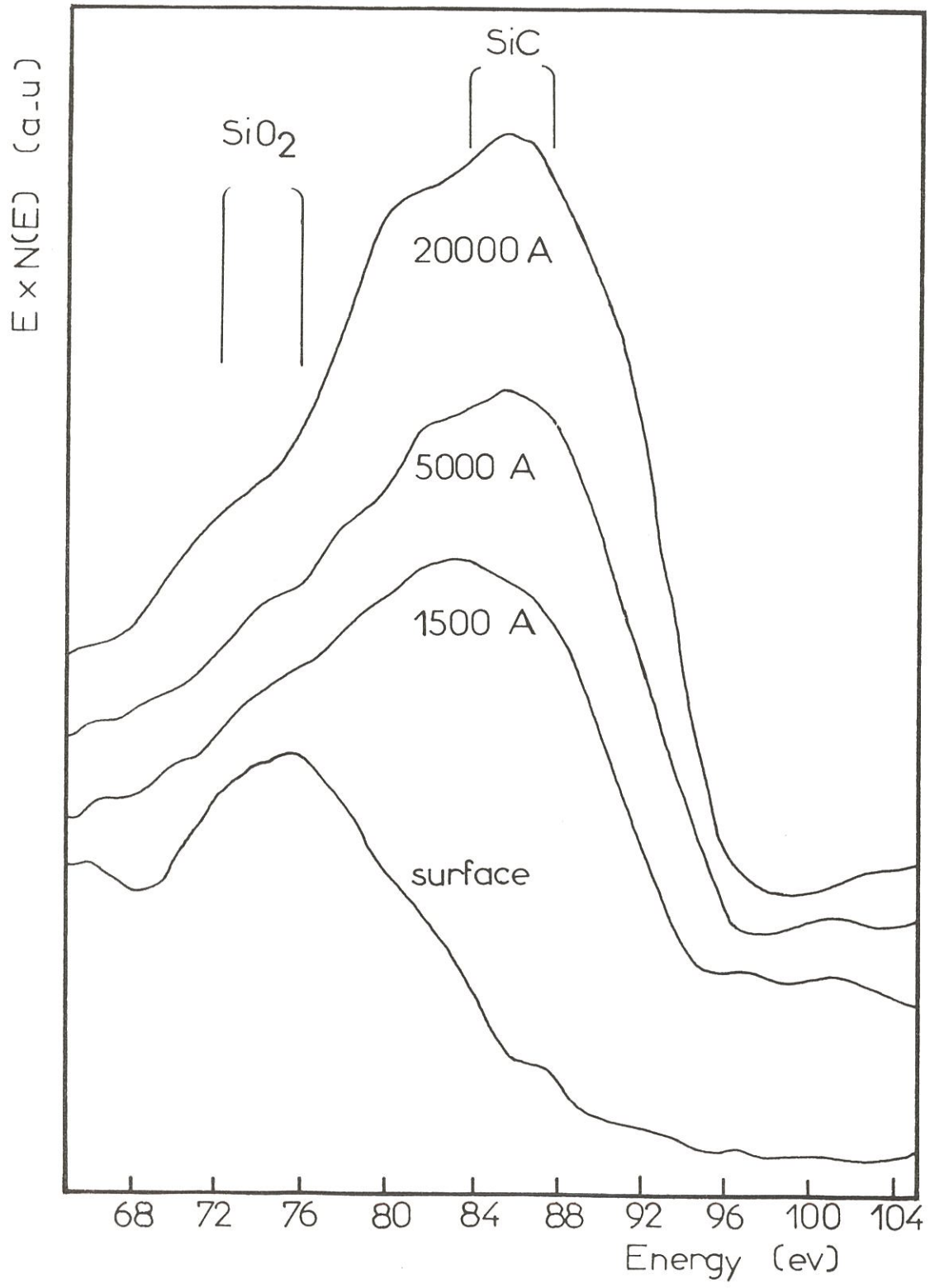

Fig. 9 - Auger electron peaks corresponding to the LVV transition of silicon recorded from a pyrolysis residue after etching of increasing duration.

Pyrolysis temperature / atomic %	Si	C	O	H
800°C *	31 *	33 *	18 *	18 *
1000°C	31	44	13	12
1400°C	34	52	12	2
1600°C	38	59	2	1

Table 1 Chemical analysis of various pyrolysis products (* at 800°C, the results should be taken with care due to uncontrolled evolution of light hydrocarbon molecules during the analysis procedure).

Pyrolysis temperature / atomic %	Si			C				O
					C-C			
	Si-C	Si-X	Si-O	C-Si	C-H	"C-O"	"C=O"	
800°C		26.8			42.3			30.9
	15.1	6.6	5.1	18.3	18.5	4.0	1.5	
1000°C		27.0			47.0			26.0
	17.0	4.8	5.2	17.8	24.2	3.8	1.2	
1200°C		25.9			48.2			25.9
	16.8	4.6	4.5	16.2	24.5	5.3	2.2	
1400°C		25.8			49.9			24.3
	17.5	4.6	3.7	15.4	25.6	4.7	4.2	
1400°C after etching		39.9			47.5			12.6
	28.7	8.3	2.9	23.6	19.9	4.0		

Table 2 analysis of the chemical bonds of various unetched pyrolysis products from ESCA experiments (the result corresponding to an etched sample obtained at 1400°C is given for the purpose of comparison).

near the surface is present in adsorbed chemical species, such as CO_2. On the basis of the ESCA data and assuming that the species present in the residues are SiC, SiO_2, Si-X and free carbon (including carbon from the hydrocarbon compounds), the relative atomic concentrations were calculated. Their variations as a function of Tp near the sample surface (full symbols) and after etching (open symbols) are shown in fig. 10. It is noteworthy that there is, near the surface, both a rapid increase in the free carbon content and a decrease in Si-X species as Tp is raised up to about 1000°C. Furthermore, it appears, from the data obtained on the etched 1400°C, that the content in free carbon is much higher near the sample surface than in the bulk and that it is the reverse for Si-X. These results are in agreement with the occurence of a carbon-rich thin layer often found around Nicalon-type fibers annealed at high temperatures and support the hypothesis that it could result from the thermal decomposition of a ternary Si (C,O) phase.

3.4- Microstructural analysis of the pyrolysis residues

The solids resulting from the pyrolysis of polycarbosilane are amorphous for Tp < 1000°C as shown by X-ray diffraction analysis (fig. 11). Above this temperature, broad diffraction peaks corresponding to β-SiC are observed. Assuming that the pyrolysis residues are not microstrained, the line broadening effect (i.e. the Scherrer equation) has been used to assess the mean grain size. As illustrated in fig. 11 the diffraction peaks become sharper and sharper as Tp increases suggesting a progressive crystallization process. The variations of the apparent grain size as a function of Tp are shown in fig. 12. Up to Tp = 1400°C, the apparent grain size increases slowly and remains smaller than about 50 Å, then it undergoes an important increase (i.e. at 1600°C, the mean grain size is of the order of 500 Å). The kinetics of growth of β-SiC have been roughly estimated by plotting the variations of the mean apparent grain size as function of the duration of the Tp plateau (from 1 to 20 hours) (fig. 13). At a given temperature, the apparent grain size increases rapidly during the first two hours, then very slowly.

The short range order around silicon has been investigated by EXAFS experiments carried out on the Si-K edge. The samples resulting from pyrolyses performed at Tp ranging from 800 to 1600°C were reduced to powders (mean particule size : less than 1 μm) and deposited on a menbrane as a thin

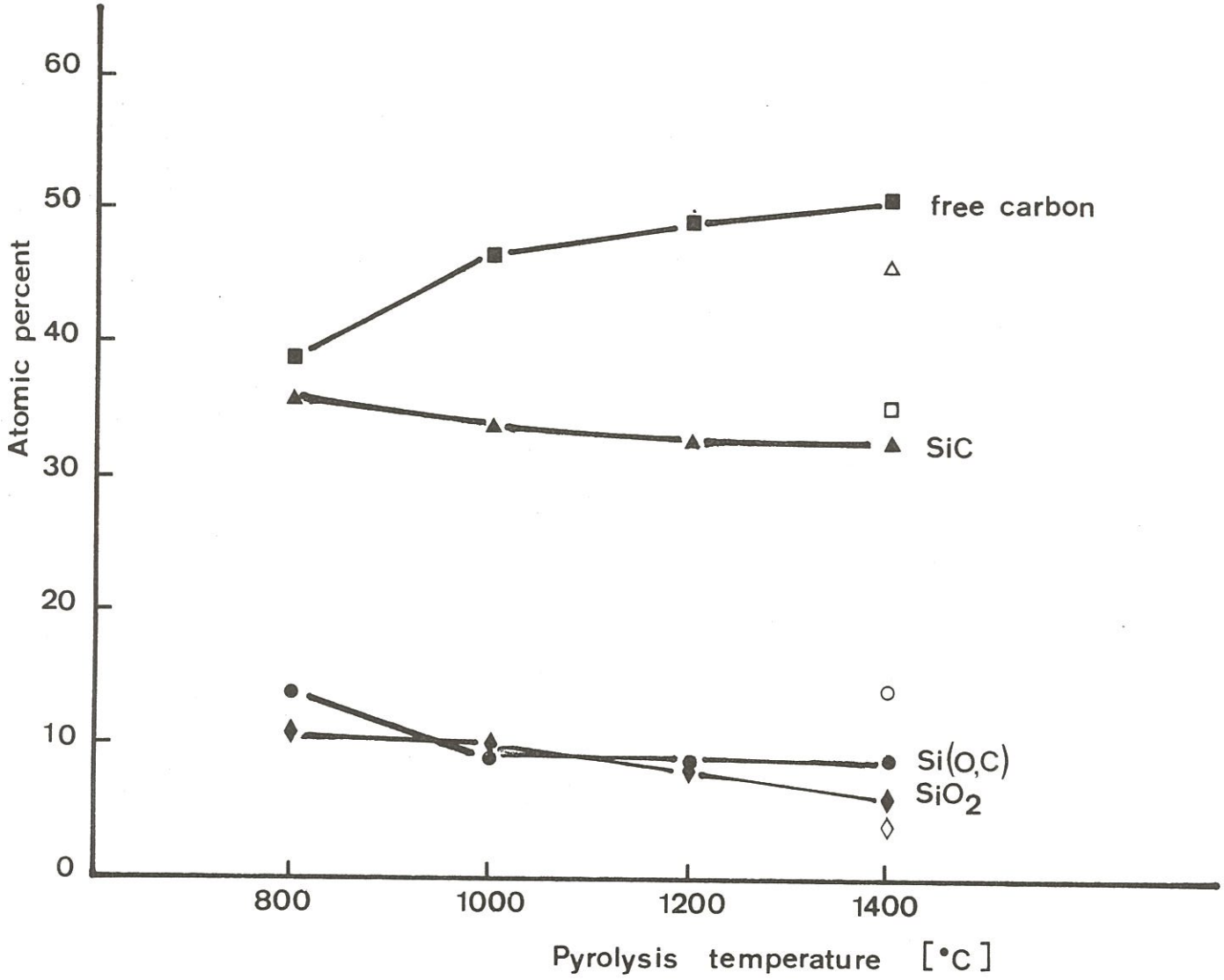

Fig. 10 - Variations of the atomic concentrations of the various species present in the residues as a function of the pyrolysis temperature (full symbols before etching and open symbols after etching).

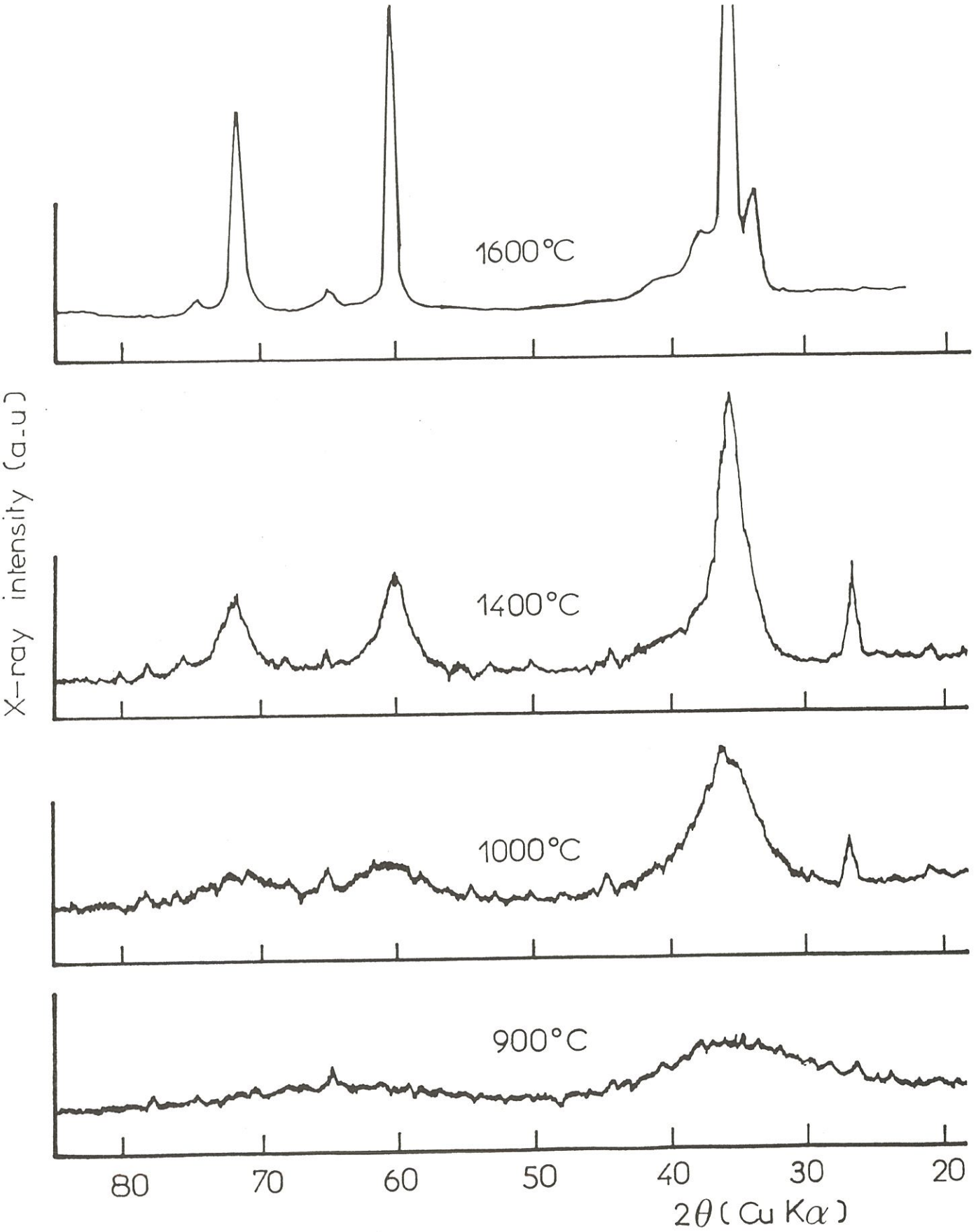

Fig. 11 - X-ray diffraction patterns of the solids resulting from the pyrolysis of polycarbosilane for increasing temperatures.

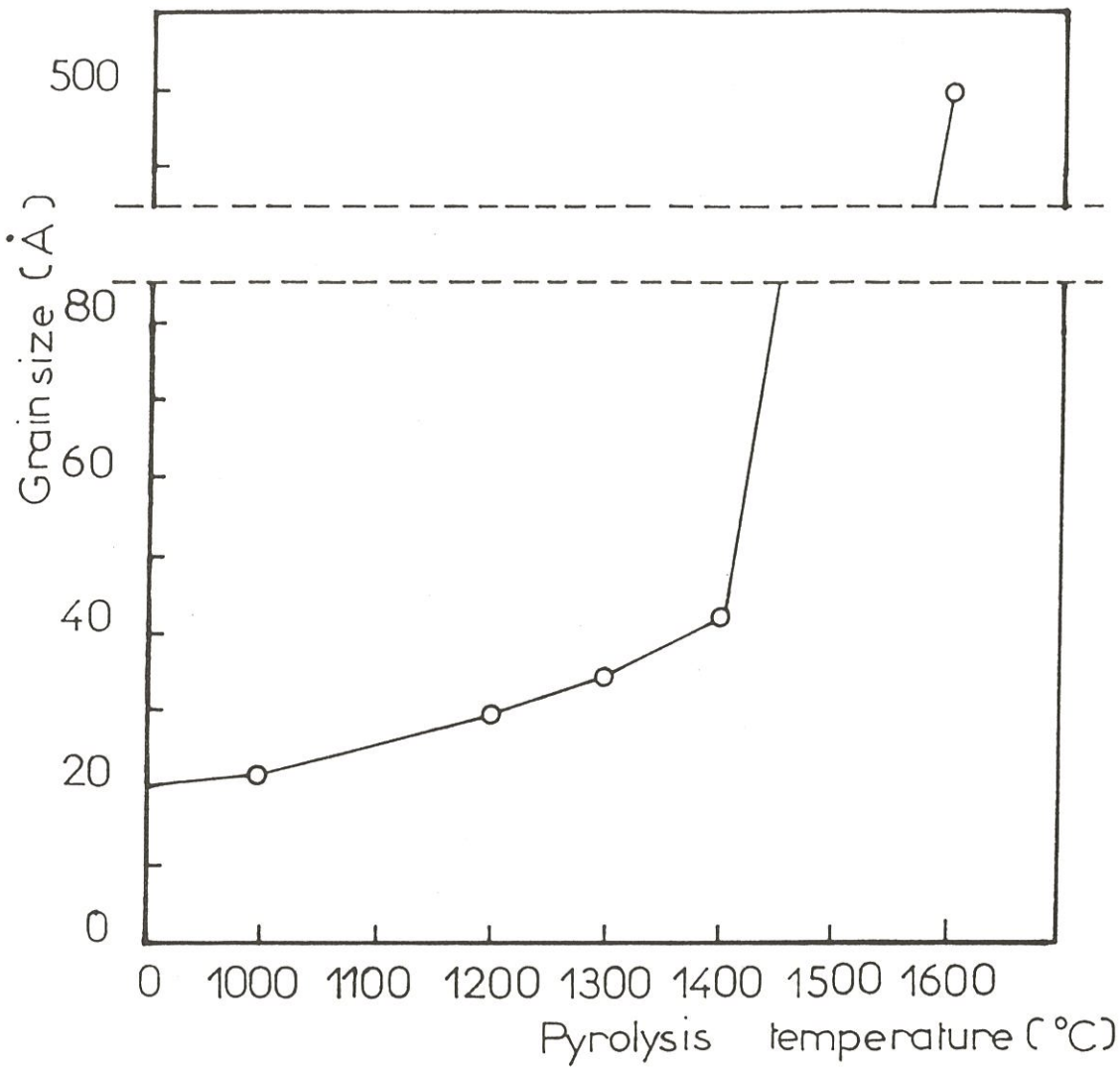

Fig. 12 - Variations of the mean grain size of β-SiC in the solids resulting from the pyrolysis of polycarbosilane as a function of the pyrolysis temperature.

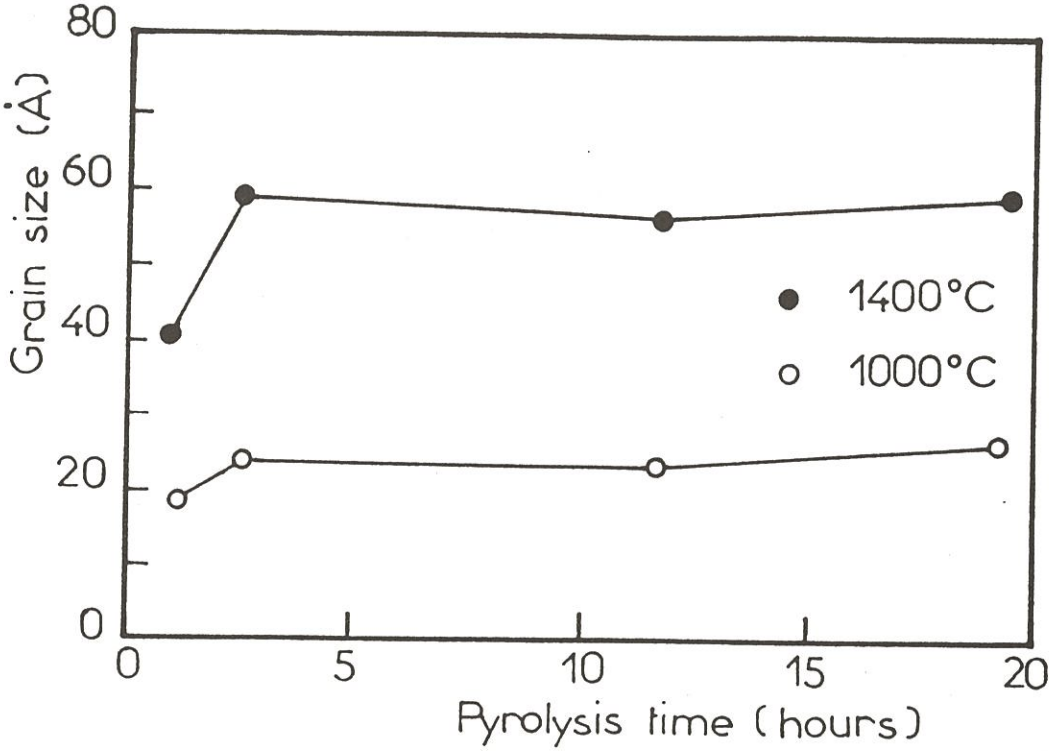

Fig. 13 - Kinetics of growth of β-SiC grain size in the solids resulting from the pyrolysis of polycarbosilane

film for experiments in the transmission mode. Amorphous silica and crystalline β-SiC were used as standards for quantitative analysis. For Tp = 800-1000°C, the residues resulting from the pyrolysis of PCS do not exhibit a defined structure beyond 3 Å (fig. 14 a). It is interesting to notice that the short range order around silicon is limited, as it is in the PCS precursor, to the first shell (which corresponds to both tetrahedral Si-C and Si-O distances) and to the second shell (associated with Si-Si distances found in both crystalline SiC and amorphous silica). Thus, a memory effect during the organic-inorganic transition occurs.A similar conclusion was drawn by R. Hagege et al. for the Nicalon NLP grade fiber [13]. Futhermore, in all the samples obtained at Tp > 1200°C, a crystalline ordering occurs which extends well beyond 15 Å (fig. 14 b). This structure is very close to that of crystallized β–SiC but SiO_2-type short distance surronding is always observed. The amount of silica is found to decrease from about 13 % to 7 % with increasing Tp. From the EXAFS data, the ceramization threshold (i.e. the transition from the amorphous state to a crystalline material) has been estimated to lie between 1000 and 1200°C.

Raman microprobe has been used, rather recently, to characterize pyrolytic carbon [23-26] as well as CVD thin films of amorphous silicon carbide [27-29] or SiC-based CVD filaments [30]. According to P. Lespade et al., the graphitization of carbons can be followed through the variations of four indices : the wave number and width of the E_{2g} line (1580-1600 cm^{-1}) which characterizes the extent of the two dimensional graphitic domains, the occurence of a 1350 cm^{-1} line due to lattice defects and the width of the 2700 cm^{-1} line (second order) which permits to follow the final stage of the graphitization process (tridimensional ordering) [23]. Amorphous silicon carbide films give rise to three groups of bands corresponding to Si-Si, Si-C and C-C bonds [28]. Even when containing low percentages of free carbon, the intensity of the C-C band (1300-1600 cm^{-1}) in the films is much higher than those related to the Si-Si band (300-600 cm^{-1}) and the Si-C band (700-1000 cm^{-1}) due to a better Raman efficiency. As a result, Raman analysis was preferentially used to structurally characterize the free carbon in the films. Only a few work has been carried out in the field of the ordering state of SiC itself. Two lines are usually observed at 789 and 967 cm^{-1} assigned to the cubic low temperature β-modification, the former being often stronger than the latter as reported by P. Martineau et al. for SiC CVD filaments [30].

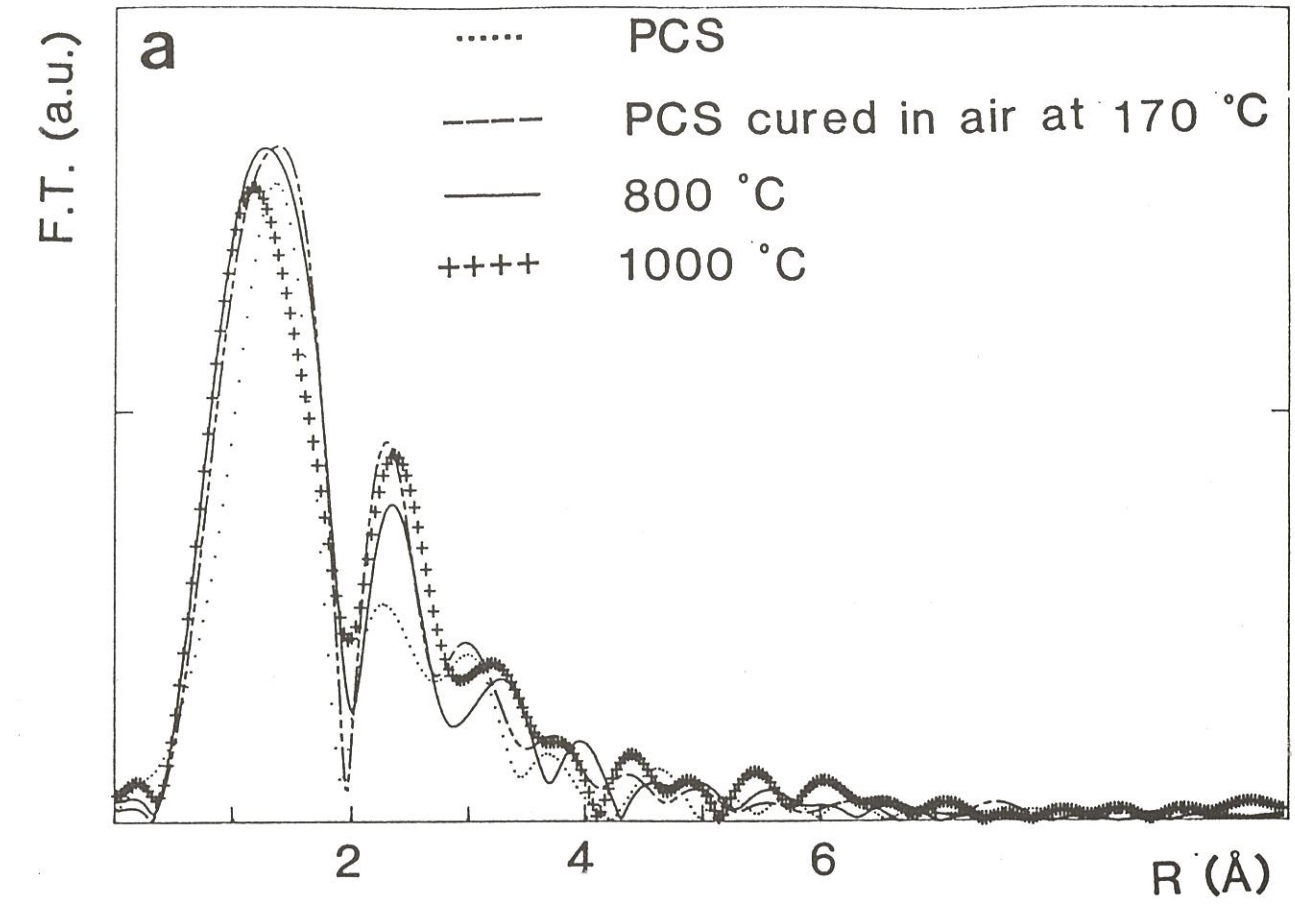

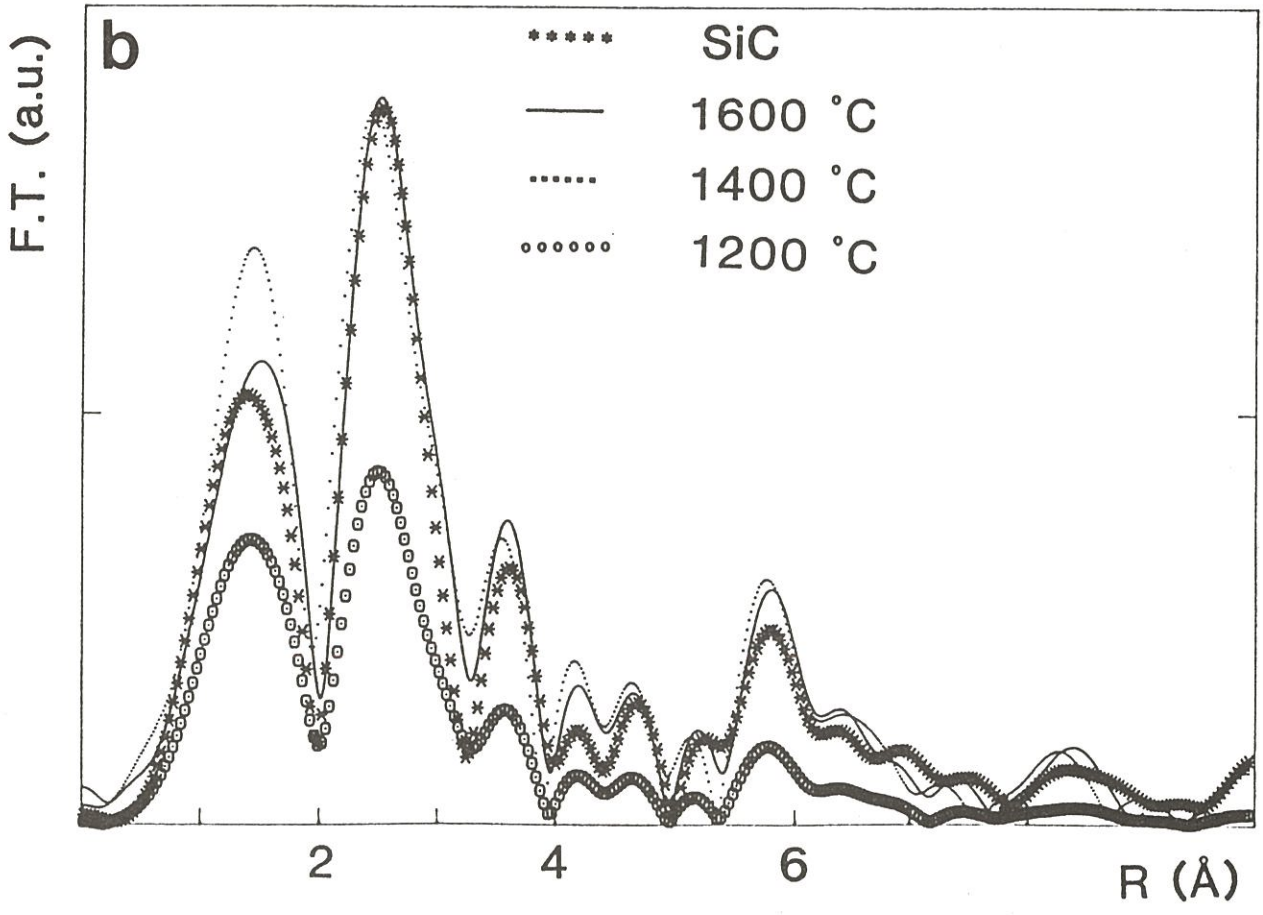

Fig. 14 - EXAFS analysis : (a) of the materials resulting from the pyrolysis of PCS at 800°C, (b) of the ceramics obtained by pyrolysis at increasing temperatures.

Raman microprobe analyses were performed on the residues obtained under different pyrolysis conditions with the following main features : (1) the presence of free carbon in all the sample, (2) a better definition of the SiC lines as Tp is increased and (3) the occurence of heterogeneites (in both concentration and crystallization state) within the samples. Some of the most representative Raman spectra corresponding to increasing Tp are shown in fig. 15. As far as free carbon is concerned, a single broad asymmetric band at about 1500 cm^{-1} is observed for Tp = 850°C, suggesting that carbon is totally amorphous or still bound to hydrogen atoms [28]. The splitting of this band, which begins at 1000°C (giving rise to the classical 1580 and 1350 cm^{-1} lines), evidences the formation of true free carbon. Then the Raman spectrum of carbon does not change markedly up to 1600°C (with the exception of a progressive narrowing of the lines). Finally, above 1800°C, the respective intensities of the two lines reverse (e.g. at 2200°C the one at 1350 cm^{-1} line is much lower) suggesting an evolution of the free carbon towards carbon crystallites of larger size (fig.16). Similarly, the Raman lines characteristic of crystalline SiC are almost not observed for the lowest Tp values (fig. 15). On the contrary, for Tp > 1200°C two broad lines occur at about 795 and 975 cm^{-1} becoming sharper as Tp increases due to a better crystallization state. As it can be seen on fig. 15 and 17, the spectrum definition was not good enough, even for Tp = 1600°C, to ascertain the occurence of a small amount of α-SiC (whose higher lattice symmetry results in a third Raman line of low intensity at 780 cm^{-1}).

In order to confirm the occurence of chemical and structural heterogeneity within the residues resulting from PCS pyrolysis, already partly established by ESCA, point analyses (made possible by the space resolution of Raman microprobe) were performed on a cross section. Due to the high Raman efficiency of the C-C bonds (which give lines of high intensity even for low carbon concentrations), it has not been possible to observe any heterogeneity in the free carbon distribution. On the contrary, the crystallization state of SiC within residues obtained at Tp = 1400°C was found to be dependent upon the analysed area, i.e. both 789 and 967 cm^{-1} lines exhibit variable intensities and even totally vanish. For Tp = 1600°C, the heterogeneity of the residues seems to be less significant, the SiC lines being always observed whatever the analysed area is.

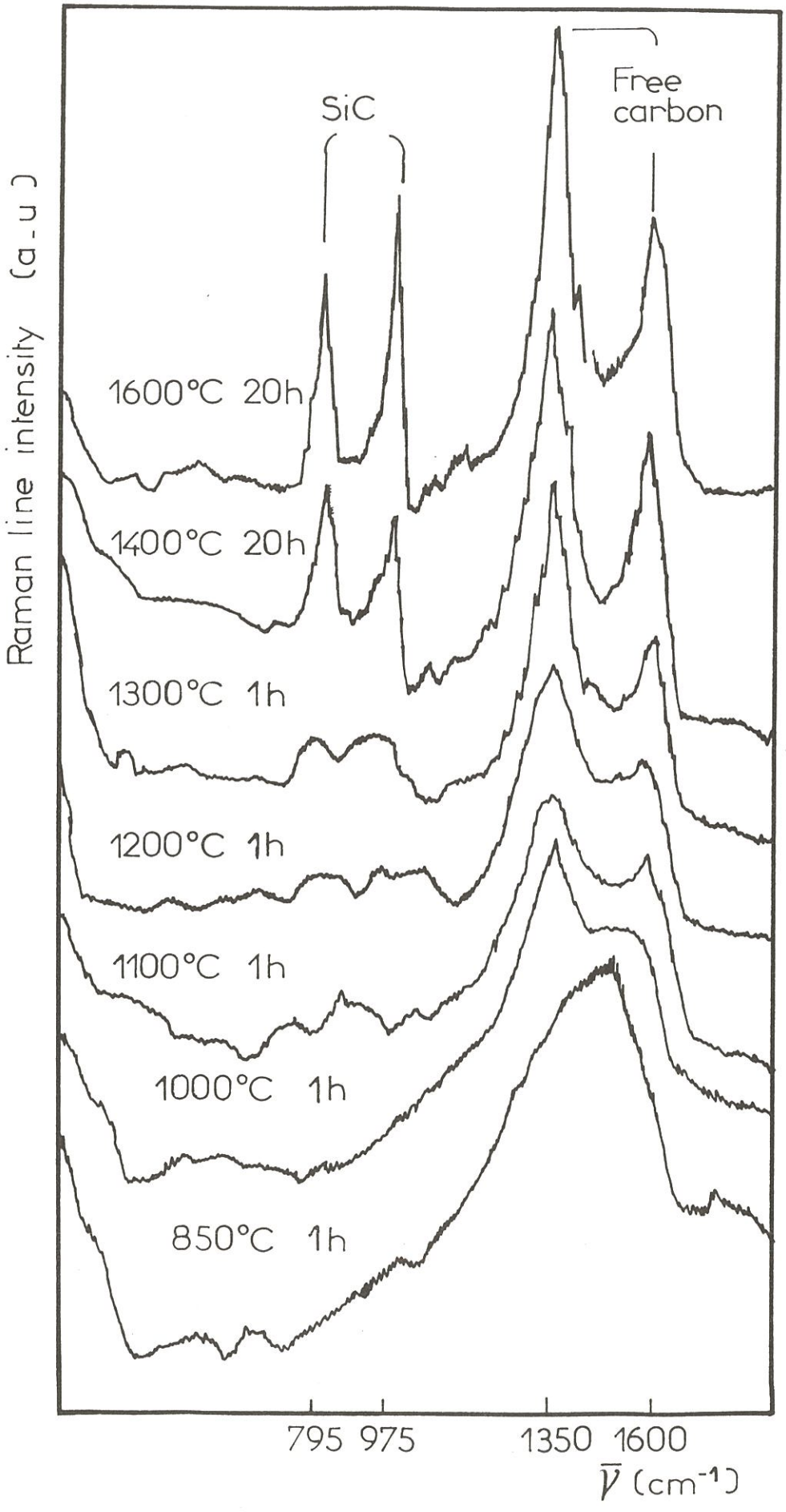

Fig. 15 - Evolution with Tp of the Raman spectra of the residues resulting from the pyrolysis of PCS.

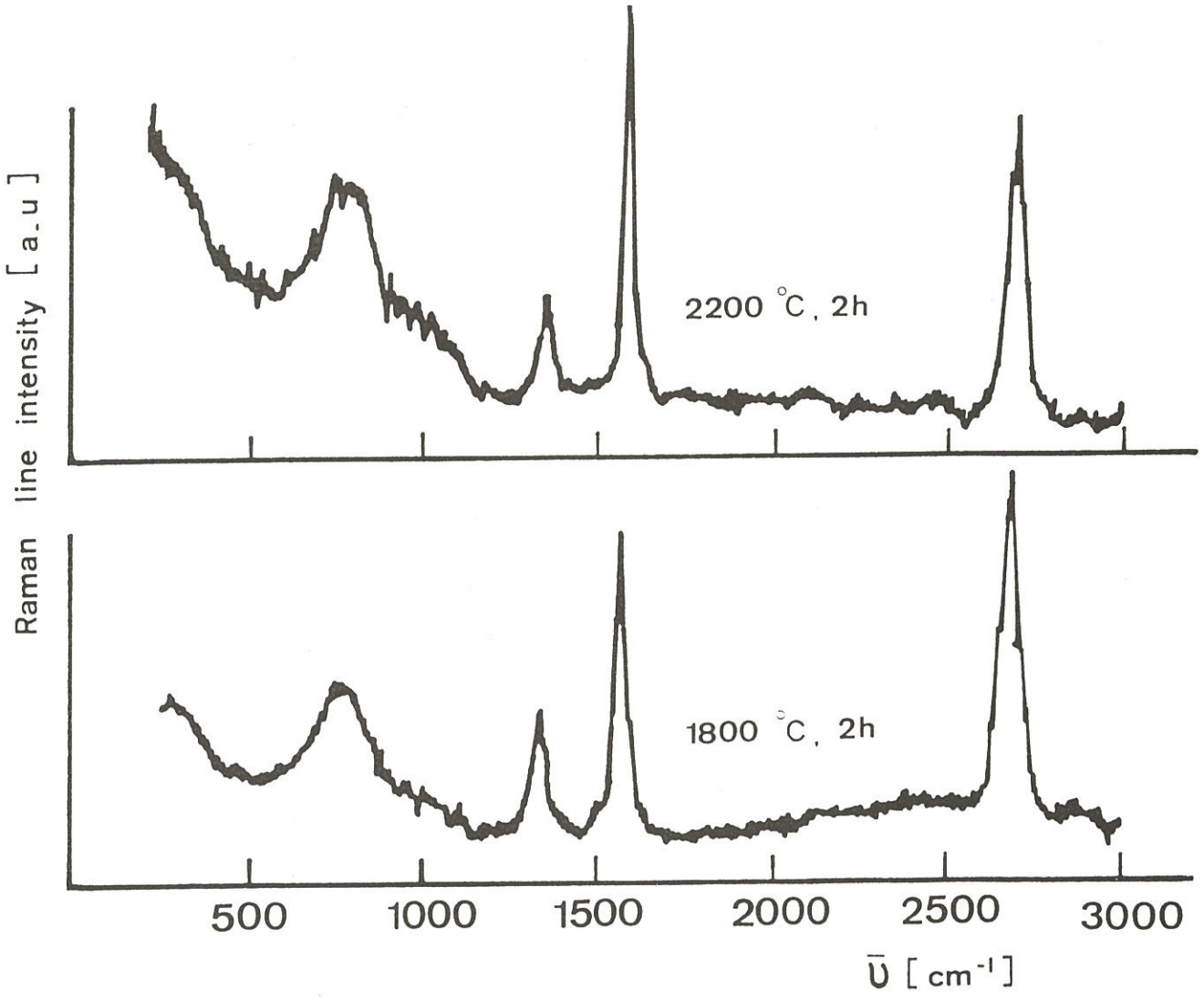

Fig. 16 - Raman spectra of the residues resulting from the high temperature pyrolysis of PCS.

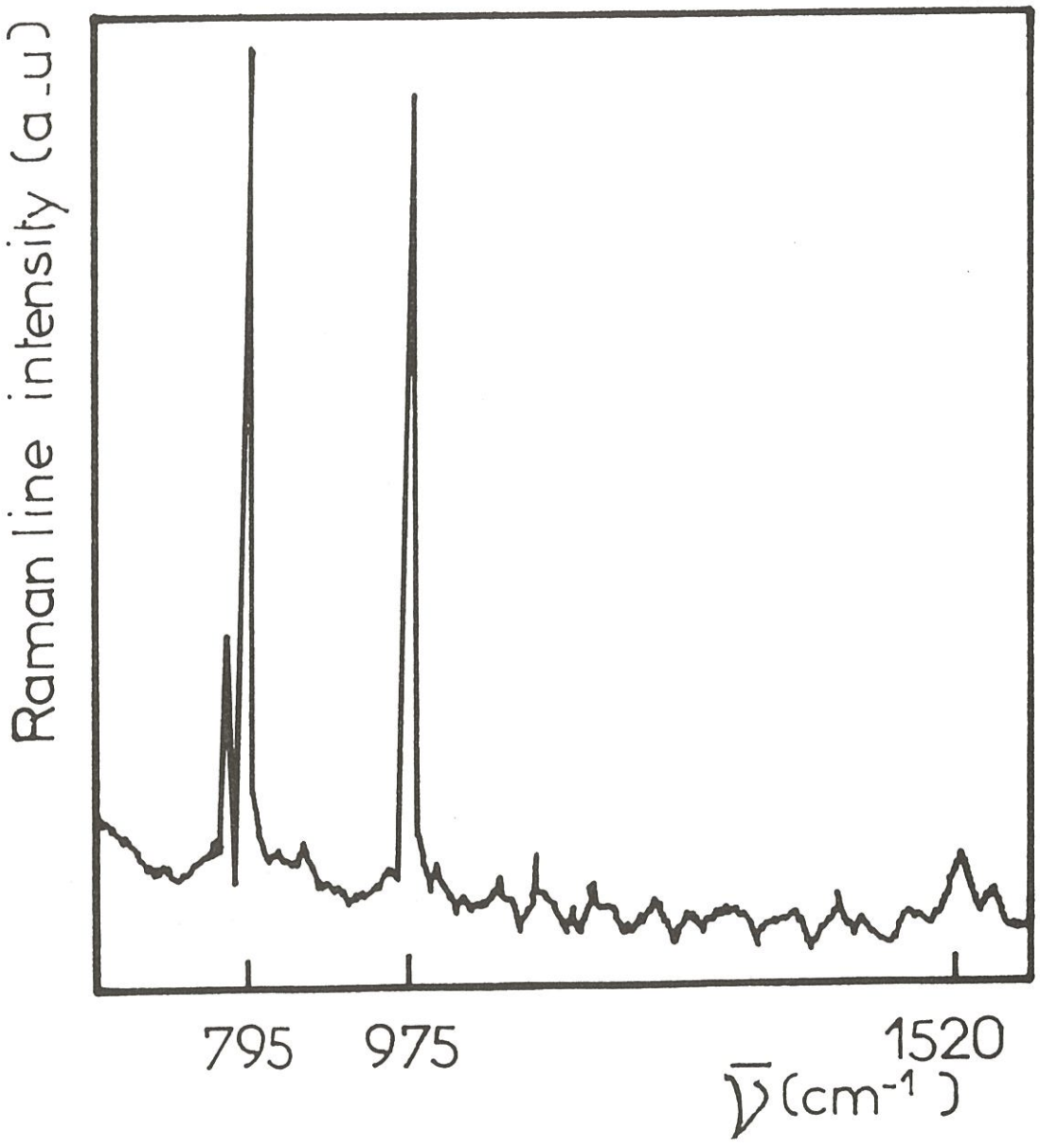

Fig. 17 - Raman spectrum of the high temperature α-modification of SiC.

The PCS pyrolysis residues were also analysed by transmission electron microscopy (bright field, dark field, high resolution lattice fringes, selected area electronic diffraction). The results of this detailed analysis will be reported elsewhere and are only summarized here for the purpose of the discussion [31]. The heterogeneity of the pyrolysis residues discussed above is confirmed by the results of the TEM analyses carried out on crushed samples except for those resulting from pyrolyses performed at Tp < 850°C. As an example, the material resulting from pyrolysis at 1400°C contains the four kinds of particules which can be seen on the micrographs of fig.18. For Tp < 850°C, the pyrolysis residue appears to a SiC-based amorphous phase in wich it is impossible to ascertain whether free carbon or silica are present. For Tp = 1000°C, this amorphous phase (which corresponds to particle 4 in fig. 18 a) gives rise partly to a microcrystalline phase containing SiC crystals 3 nm in size (like in particle 3) and to a less extent to crystals 10 nm in size (corresponding to particle 2). Finally, for Tp = 1400°C, the residues exhibit a more pronounced microstructural heterogeneity with "large" crystals (of about 15 nm in size, particle 1) and smaller ones which are surrounded by thin films of aromatic carbon (observed on dark field (fig. 18-c) and lattice fringe imaging), resulting in a sponge-like microtexture. The above results are in rather good agreement with the apparent grain size values calculated from X-ray diffraction patterns (the small difference being due to the fact that the latter are mean values while the former are measured on individual grains). On the basis of the TEM-analysis, the crystallization threshold of the pyrolysis residues of PCS, already established by EXAFS to be in the 1000-1200°C temperature range, rather occurs at 1000°C.

3.5 - Electrical properties of the pyrolysis residues of PCS

The variations of the electronic conductivity appear to be a very sensitive way to follow the transition taking place between the PCS precursor and the SiC-based ceramic material by pyrolysis at increasing Tp. Conductivity measurements have been performed, according to the four contact method, on PCS pyrolysis residues obtained at Tp ranging from 700 to 1600°C, Nicalon fibers (NLP 101 grade) as well as polycrystalline and monocrystalline SiC were used as standards. For each sample, the variations of the electrical conductivity between 20 and 600°C are plotted, as a function of the reciprocal temperature, in a semi-logarithmic scale in fig. 19. Since the data follow

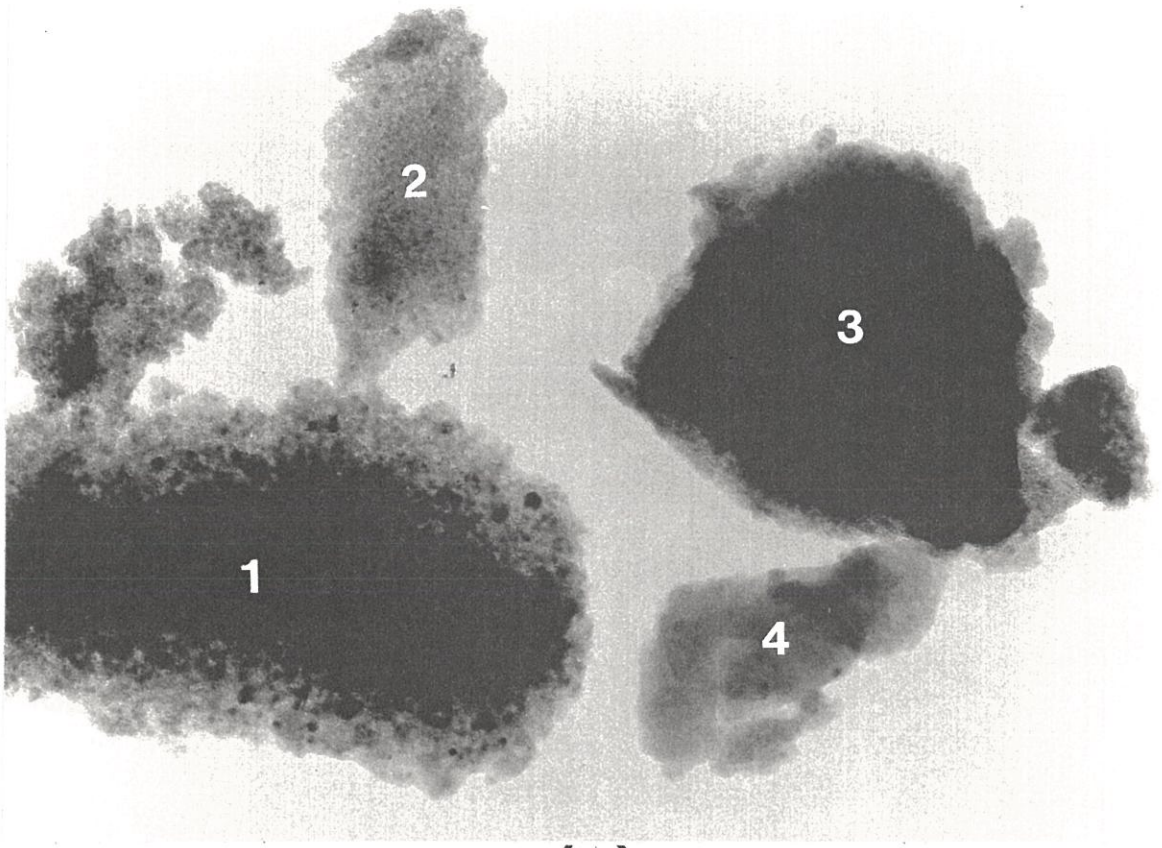

(a)

1000 Å

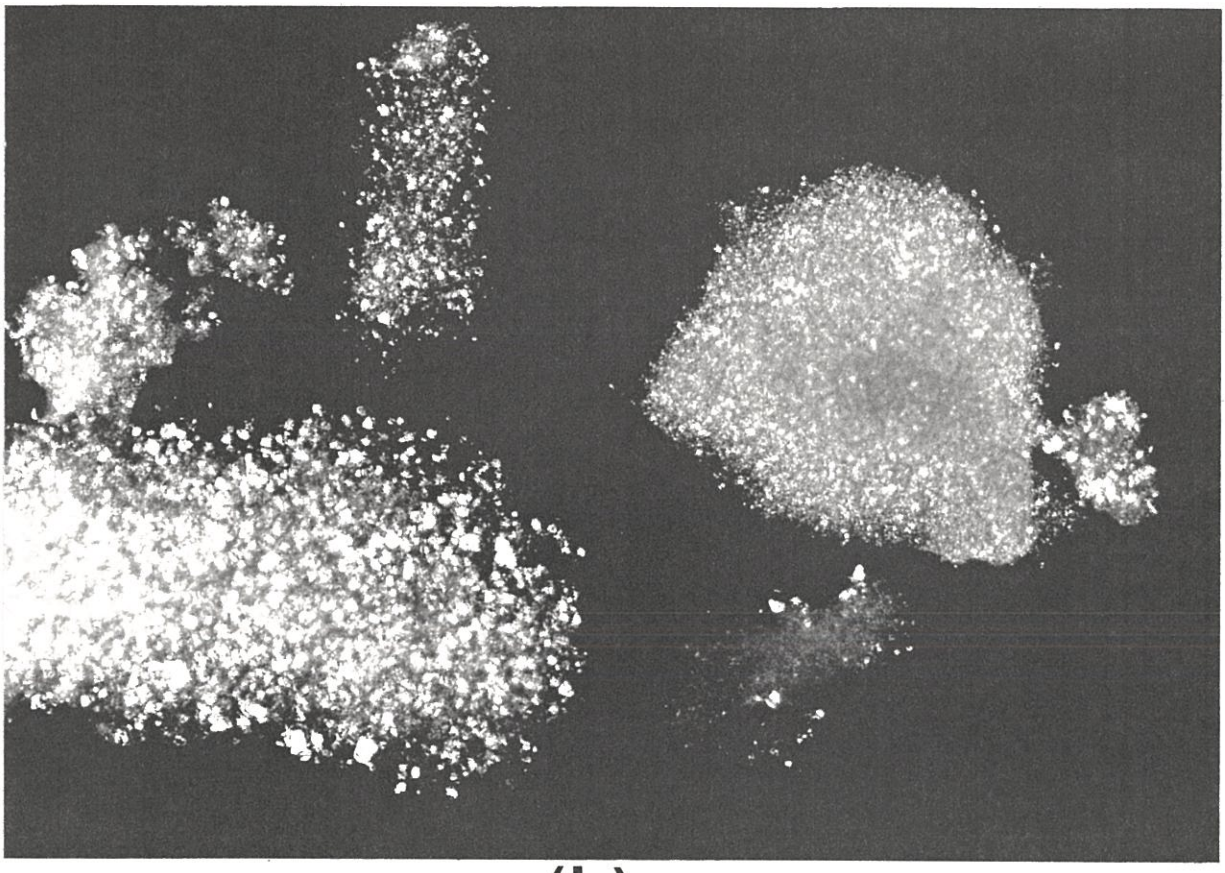

(b)

Fig. 18 - TEM analysis of residues resulting from PCS pyrolysis : (a) bright-field ; (b) dark-field showing SiC microcrystals.

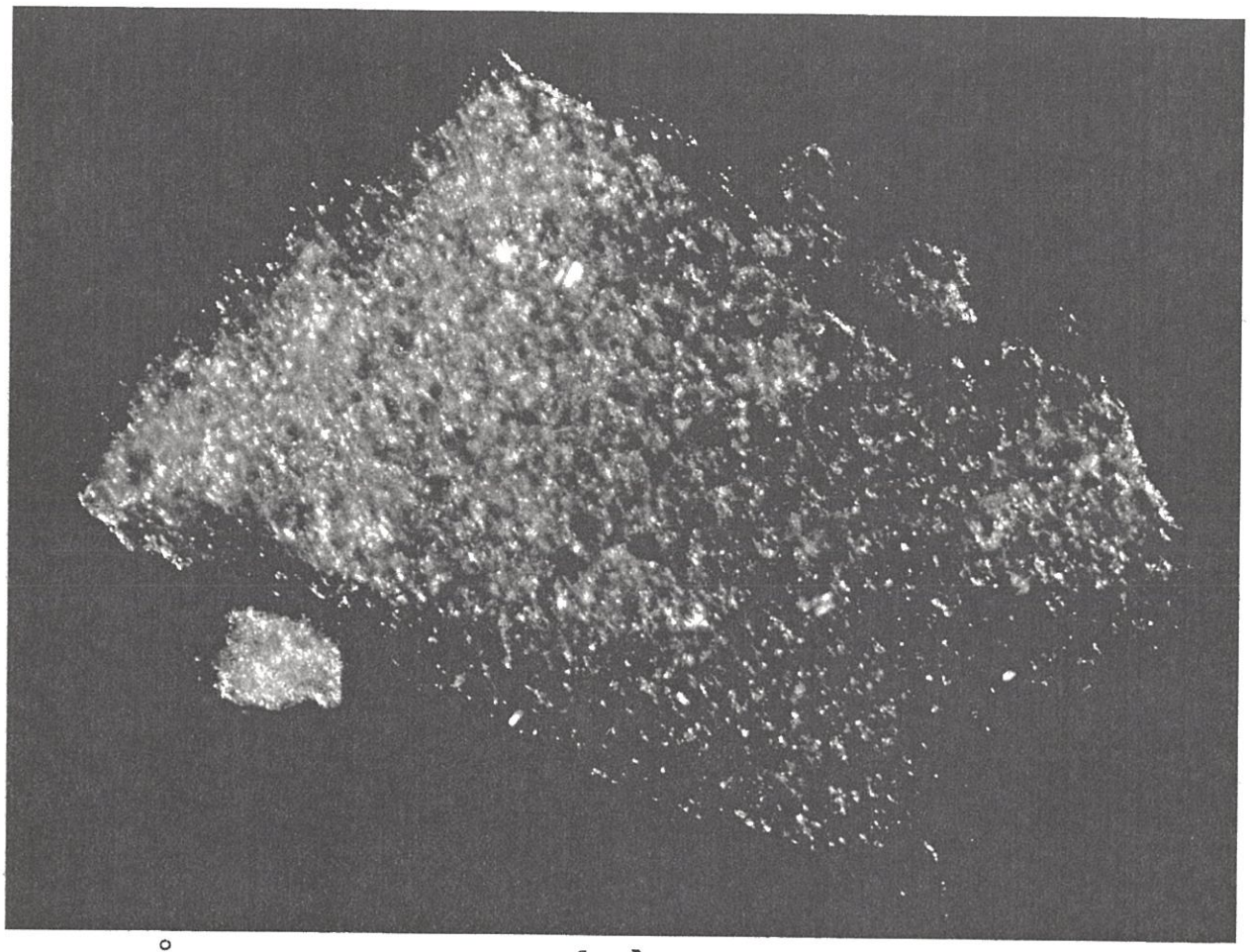

1000 Å

(c)

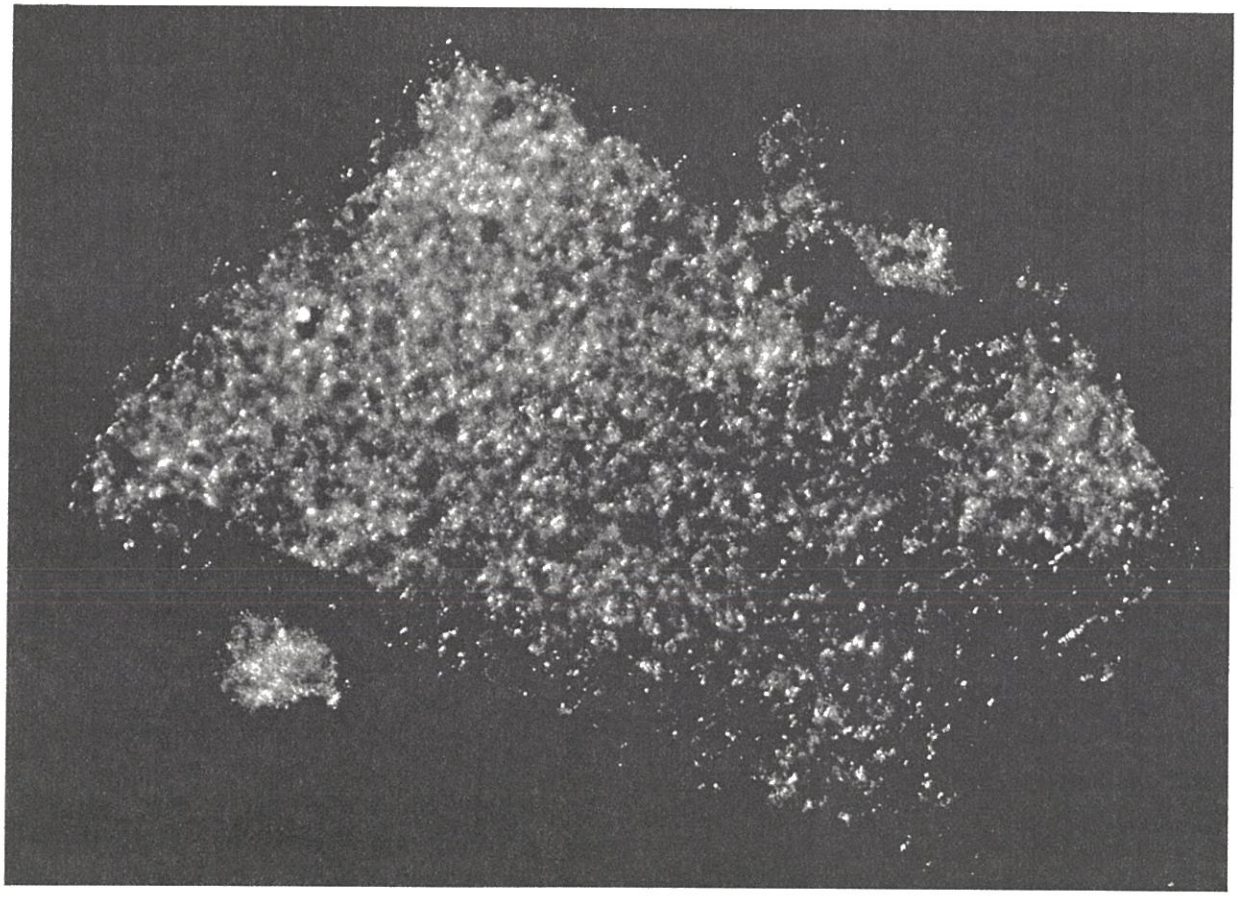

Fig. 18 - TEM analysis of residues resulting from PCS pyrolysis : (a) bright-field ; (b) dark-field showing SiC microcrystals ; (c) dark-field in two orthogonal positions showing C distribution.

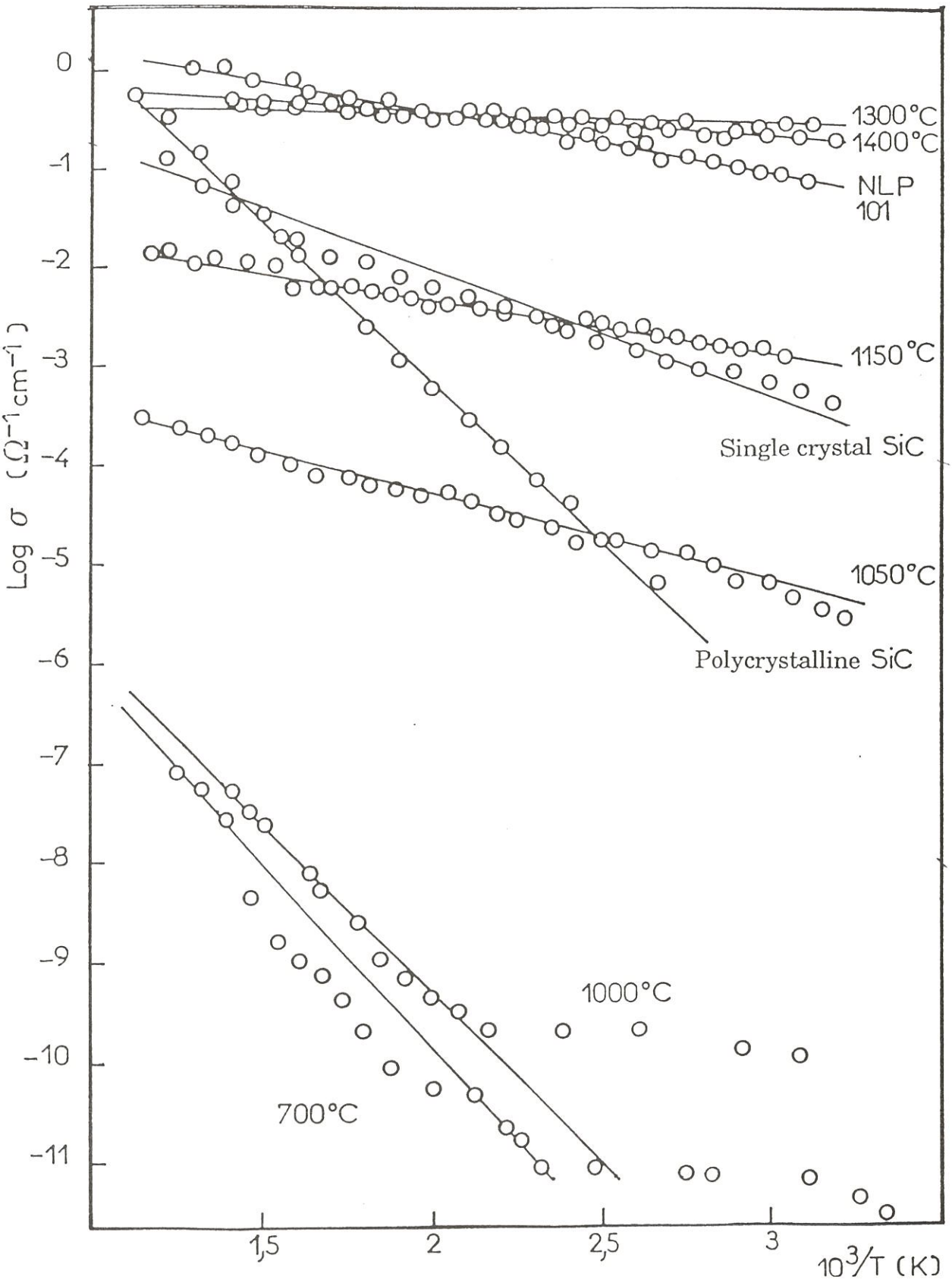

Fig. 19 - Temperature dependance of the electrical conductivity of materials resulting from the pyrolysis of PCS precursors.

Arrhenius laws, activation energies characterizing the conduction mechanism have been derived from the slopes of the straight lines. The reversibility of the electrical behavior has been verified for all samples, a feature which evidences that the materials are stable up to 600°C and exhibit an electronic-type conductivity. The variations of the activation energy as well as those of the conductivity at 20°C as a function of Tp are given in fig. 20.

For Tp < 1000°C, the pyrolysis residues are insulating materials with a conductivity lower than 10^{-10} Ω^{-1} cm^{-1} at 20°C and an apparent activation energy of 0.7 eV. The low conductivity could be due either to a low mobility or a low concentration of charge carriers. For 900 < Tp < 1200°C, the electrical conductivity undergoes a dramatic variation, i.e. the ambient conductivity increases by a factor of 10 orders of magnitude and the activation energy decreases to values lower than 0.01 eV. Finally, for Tp > 1200°C, the electrical characteristics remain almost constant, the ambient conductivity being close to 1 Ω^{-1} cm^{-1} and the activation energy almost zero, a feature which suggests a partly metallic behavior as in the related case of Nicalon fibers. On the contrary, crystalline SiC exhibits properties which are intermediate between those of residues resulting from PCS pyrolysis performed at high or low temperatures.

The evolution of the electrical behavior of the PCS pyrolysis residues with respect to Tp has some similarity with that reported for the pyrolysis of hydrocarbon polymers into pyrocarbons. Such a process can be explained for instance on the basis of the following mechanism [32-33] : (1) for Tp < 600°C, volatile species (e.g. CH_4) give rise to aggregates of sp^2 aromatic carbons bound to free radicals with single electron, (2) for 600 < T < 1200°C, the radicals capture the electrons of the aromatic network and leave corresponding holes which results in a rapid increase in conductivity as Tp is raised, a marked decrease in the activation energy and simultaneously an extension of the aromatic carbon domains as well as a strong decrease in the hydrogen content, (3) finally, for Tp > 1200°C, the carbons (which are no longer bound to any hydrogen atoms) undergo no futher change in their crystallization state up to the graphitization temperature.

In the case of the pyrolysis of PCS, the insultator-quasi metal transition occurs at a slightly higher temperature (i.e. between 1000 and 1200°C). Regarding the semiconducting behavior of crystalline SiC, that transition could be explained by both a segregation of free carbon at the external surface of the SiC-particles and an increase in the carbon concentration at raising Tp, which

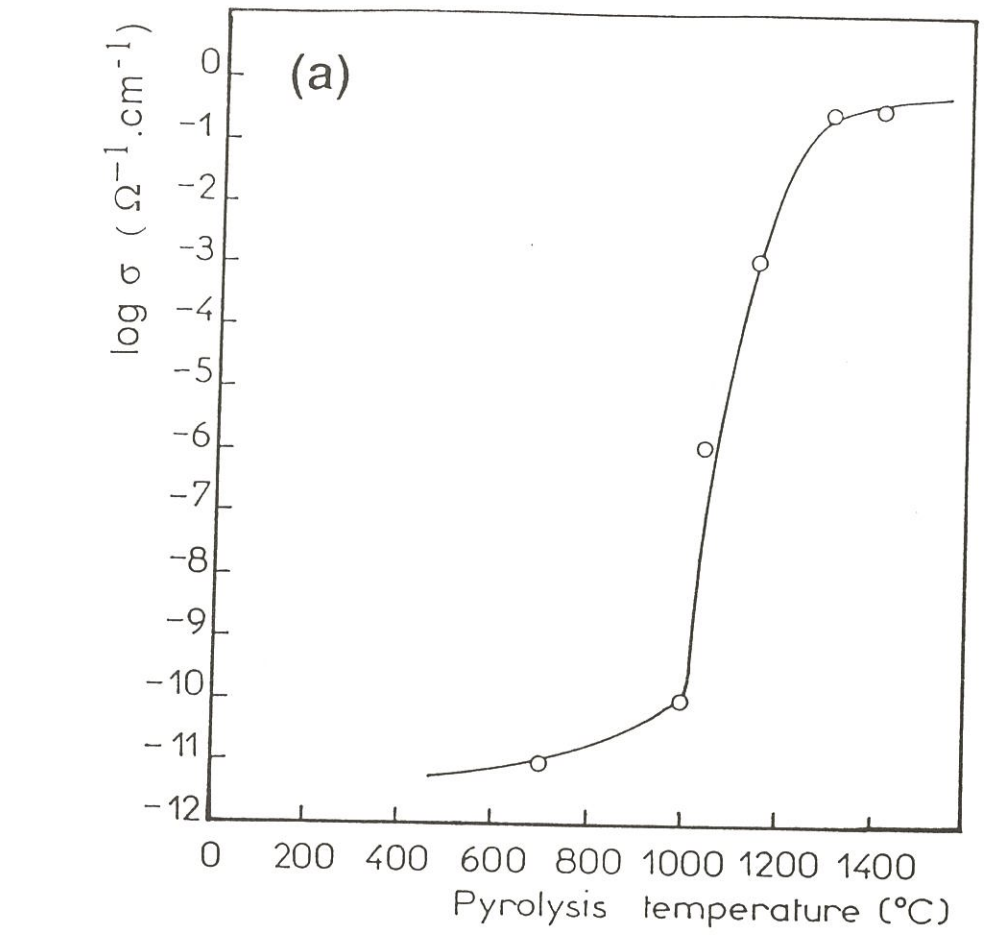

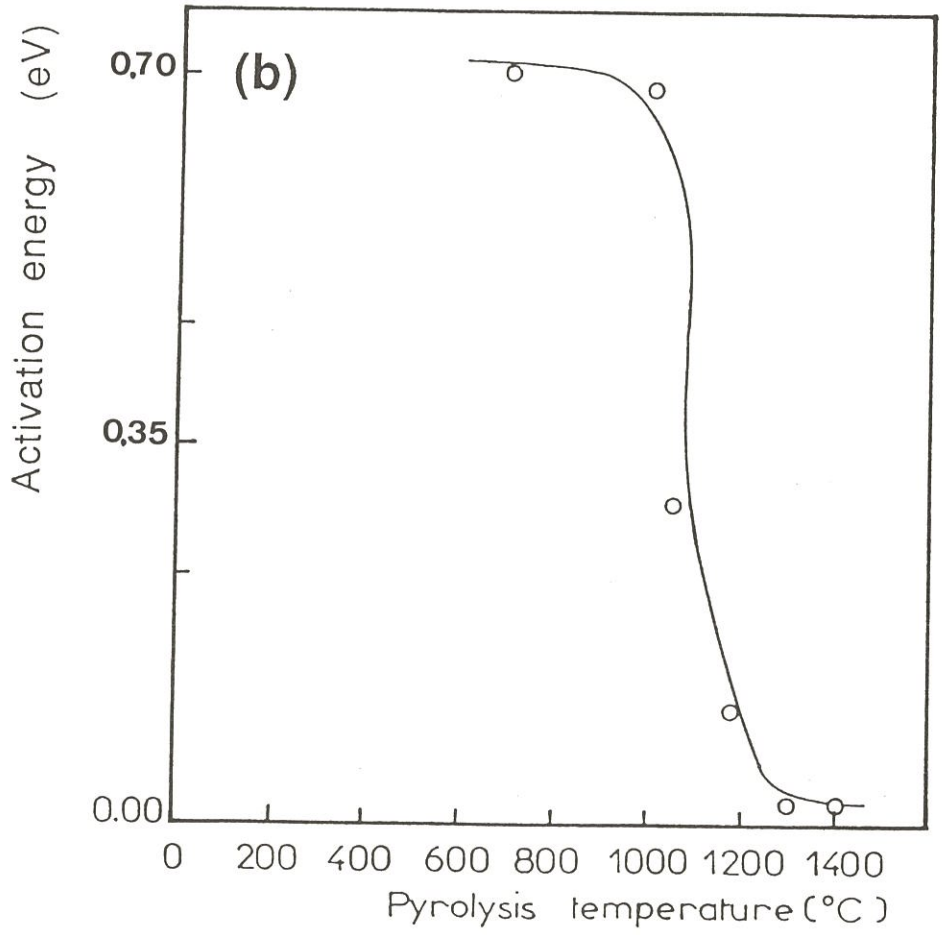

Fig. 20 - Variations, as a function of the pyrolysis temperature Tp, of the electrical conductivity at 20°C (a) and the activation energy (b).

induces a percolation effects [34]. This effect seems to take place at about Tp = 1100°C. This outstanding behavior is entirely consistent with the results of all the chemical analyses reported above, concerning the amount and microstructural state of free carbon (ESCA, Raman spectroscopy and TEM).

4- DISCUSSION AND CONCLUSION

The large variety of chemical and microstructural analyses all performed on residues resulting from the pyrolysis of the same PCS precursor has permitted, on the one hand, to enlarge our knowledge of the different stages occuring during the transformation process of PCS into SiC-based ceramic materials and, on the other hand, to suggest a general procedure for studying other similar transitions that take place between organometallic precursors and ceramics.

Three fundamental steps occur during the pyrolysis of PCS : (1) the organometallic-mineral transition (at 550 < Tp < 800°C), (2) the crystallization threshold of the amorphous residue (at 1000 < Tp < 1200°C) and (3) a grain coarsening above 1400°C. The intermediate steps (i.e. for 800 < Tp < 1000°C and 1200 < Tp < 1400°C) correspond to more limited changes in the composition or microstructure of the pyrolysis residues.

The experimental results which have been presented above support the following pyrolysis mechanism for the PCS precursor which has been studied here (and which is close to those used for the synthesis of Nicalon-type fibers) :

- For 20 < Tp < 550°C, the structure of the polymer precursor does not change markedly as evidenced from IR analysis. Lateral organic functions do not seem to be broken significantly as shown by the gas phase analysis (i.e. absence of light gaseous species). The only important phenomenon which occurs within this temperature range is the evolution of heavy gaseous products corresponding to polymers of low molecular weight which results in a large weight loss as established from the TGA analysis. At this stage, the polymer becomes infusible, probably due to an increase in the reticulation degree resulting from (i) the effect of temperature and (ii) some accidental addition of oxygen taken from the atmosphere of the pyrolysis furnace.

- For 550 < Tp < 800°C, the main part of the organometallic-mineral transition is effective. Most of the Si-H and C-H bonds are broken, as shown by the IR analysis. The tetrahedral environment of silicon as well as the polymer Si-C skeleton are probably maintained (i.e. the short range atomic order) as suggested by the EXAFS results.An important evolution of gaseous species is observed mainly consisting of light hydrocarbon molecules (i.e. CH_4, C_2H_6,...) and methylsilanes (i.e. $(CH_3)_4Si$, $(CH_3)_3SiH$, $(CH_3)_2SiH_2$) resulting respectively from the broken lateral chains and chain ends, as well as probably a large amount of hydrogen (which has not been analysed).

- For 800 < Tp < 1000°C, the material is essentially mineral but still contains some hydrogen which may have a role to play during the ceramization process. The pyrolysis residues must be regarded as homogeneous being totally amorphous. It can be described on the basis of three chemical tetrahedral entities : (1) hydrogenated amorphous silicon carbide (including some residual hydrocarbon groupments (e.g. CH, CH_2, CH_3) (2) hydrogenated amorphous silicon oxycarbide and (3) amorphous silica, the former being widely predominant in the bulk. As Tp increases up to 1000°C, the hydrogen content decreases, the free carbon percentage raises, the SiX oxycarbide amount decreases and the following phenomena are thought to occur : (1) volatile hydrocarbon molecules (e.g. CH_4, C_2H_6,...) resulting from breaking of Si-C bonds are decomposed in situ instead of being evolved, when their cracking temperature is reached, i.e. probably when Tp is close to 1000°C ; (2) this decomposition proceeds at a microscopic scale (e.g. in the microvoids of the residue or near the surface) giving rise to both a few nuclei of crystalline SiC and the heterogeneity of compostiion which has been evidenced by ESCA and TEM analyses. The insulating electrical behavior of the material obtained within this temperature range could be attributed either to a low mobility of the charge carriers if the Fermi level lies close to localized states or to a low charge carrier concentration if the Fermi level is close to narrow bands. Finally, the evolution of a small amount of light species (e.g. silanes or carbon monoxide) could be related to a partial decomposition of the amorphous hydrogenated silicon oxycarbide whose concentration decreases (according to S.M. Johnson et al. SiO remains the main gaseous species resulting from the heat-treatment of ex-PCS Nicalon fibers in the 1100-1400°C temperature range [35]).

- For 1000 < Tp < 1200°C, the number of SiC nuclei (less than 3 nm in size), which was very low at Tp = 1000°C, notably increases while their mean size hardly raises. This nucleation of SiC in the overall material becomes detectable by EXAFS (which shows, for Tp = 1200°C, a radial distribution function around silicon well defined beyond 1 nm). As the hydrogen content decreases, hydrogenated amorphous SiC vanishes, the only residual amorphous phases being both silica (when present) and silicon oxycarbide whose stoichiometry is very difficult to determine (from the ESCA chemical shifts between SiC and SiO_2, a tentative formula for the intermediate tetrahedra could be close to SiC_3O). As SiC nuclei grow from the amorphous medium, the free carbon content slowly increases, leading to a heterogeneous material with an extremely divided microtexture : SiC nuclei are thought to be surrounded with a thin film of aromatic carbon arranged as a stack of a few layers. As a consequence of the high enough free carbon concentration, the electrical properties of the material undergo a sharp insulating-quasimetallic behavior transition according to a percolation mechanism from a concentration threshold.

- For 1200 < Tp < 1400°C, as last hydrogen atoms are removed, a slow continuous crystallization of SiC is observed, the mean grain size reaching a value of about 10 nm. Simultaneously, the percentage of silica or Si (C,O) species decreases slowly (possibly due to an evolution of SiO) while the percentage of free carbon slightly raises. However, free carbon remains aromatic and the overall electrical behavior quasimetallic.

- For 1400 < Tp < 1600°C, a marked grain coarsening of the SiC microstructure is observed (the average grain size reaching a value higher than 50 nm). Simultaneously, a rapid decrease in both the amorphous silica (or silicon oxycarbide) contents occur with a probable evolution of silicon and carbon monoxides.

In summary, the various steps taking place during the pyrolysis of PCS precursor have been investigated. Interestingly, a correlation between a macroscopic behavior,i.e. the insulator-metal transition, and a microscopie scale change, i.e. the amorphous-microcrystalline state transition related to chemical composition, has been pointed out for the first time in this field. The former, which requires simple experimental procedures, could be applied in

the future to a variety of similar precursors while the latter which supposes the use of heavy analytical techniques (e.g. TEM, EXAFS,...) could be better limited to the detailed study of a few chosen organometallic polymers.

ACKNOLWLEDGEMENTS

This article is the result of a cooperative research programme which has been supported by SEP, the French ministry of Defence (DRET) CNRS, CEFI, AFME and Conseil Régional d'Aquitaine. The authors would like to acknowledge the contribution of : Dr. J. Dunogues, E. Bacqué, J.P. Pillot and M. Birot (CNRS-UA 35) for the supply of the PCS precursor and assistance in understanding different problems related to organometallic chemistry, P. Orly (SEP) for his help in interpreting the structure of the pyrolysis residues, E. Marquestaud for the conductivity measurements, J.J. Videau for IR spectra recording and M. Lahaye for the AES analyses. The ESCA analyses were performed by A. Sartre from Science et Surface Co.

REFERENCES

1 - R.W. RICE, Ceram. Bull., **62**, 8 (1983) 889.

2 - S. YAJIMA, Handbook of Composites, vol. 1 - Strong Fibers, W. Watt and B.V. Perov eds., Elsevier Science Publishers (1985) 201.

3 - Y.HASEGAWA, M. IIMURA and S. YAJIMA, J. Mater. Sci., **15** (1980) 720.

4 - T. MAH, N.L. HECHT, D.E. Mc CALLUM, J.R. HOENIGMAN, H.M. KIM, A.P. KATZ and H.A. LIPSITT, J. Mater. Sci., **19** (1984) 1191.

5 - G. SIMON and A.R. BUNSELL, J. Mater. Sci., **19** (1984) 3649.

6 - G. SIMON and A.R. BUNSELL, J. Mater. Sci., **19** (1984) 3658.

7 - T.J. CLARK, R. ARONS, J. RABE and J.B. STAMATOFF, Ceram. Eng. Sci. Proc., **6**, 7-8 (1985) 576.

8- T.J. CLARK, M. JAFFE, J. RABE and N.R. LANGLEY, Ceram. Eng. Sci. Proc., **7,** 7-8 (1986) 901.

9 - L.C. SAWYER, R.T. CHEN, F. HAIMBACH, P.J. HARGET, E.R. PRACK and M. JAFFE, Ceram. Eng. Sci. Proc., **7,** 7-8 (1986) 914.

10 - K. OKAMURA, Composites, **18**, 2 (1987) 107.

11 - A.S. FAREED, P. FANG, J. KOCZAK and F.M. KO, Ceram. Bull., **66,** 2 (1987) 353.

12 - L.C. SAWYER, M. JAMIESON, D. BRIKOWSKI, M.I. HAIDER and R.T. CHEN, J. Am. Ceram. Soc. **70**, 11 (1987) 798.

13 - C. LAFFON, P. LAGARDE, A.M. FLANK, R. HAGEGE, P.OLRY, J. COTTERET, S. DIXMIER, M. LARIDJANI, A.P. LEGRAND and B. HOMELLE, J. Mater. Sci. 24 (1989) 1503-1512

14 - Y.HASEGAWA and K. OKAMURA, J. Mater. Sci., **18** (1983) 3633.

15 - S. YAJIMA, Y.HASEGAWA, J. HAYASHI and M. IIMURA, J. Mater. Sci., **13** (1978) 2569.

16 - Y.HASEGAWA and K. OKAMURA, J. Mater. Sci., **21** (1986) 321.

17 - J.C. SARTHOU, University thesis n°155, Bordeaux (1984).

18 - J.J. POUPEAU, D. ABBE and J. JAMET, ONERA Report (1982).

19 - L. PORTE and A. SARTRE, J. Mater. Sci., 24 (1989) 271-275.

20 - Y. MISOKAWA, K.M. GEIB and C.W. WINSEM, J. Vac. Sci. Technol. A, **4**, 3 (1986) 1696.

21 - J. LIPOWITZ, H.A. FREEMAN, R.T. CHEN and E.R. PRACK, Advanced Ceramic Materials, **2**, 2 (1987) 121.

22 - D. BOUCHIER and A. BOSSEBOEUF, Thin Solid Films, **139** (1986) 95.

23 - P. LESPADE, A. MARCHAND, M. COUZI and F. CRUEGE, Carbon, **22**, 4-5 (1984) 375.

24 - F. TUINSTRA and J.L. KOENIG, J. Chem. Phys., **53**, 3 (1970) 1126.

25 - B.S. ELMAN, M.S. DRESSELHAUS, G. DRESSELHAUS, E.W. MABY and H. MAZUREK, Phys. Rev. B, **24**, 2 (1981) 1027.

26 - T.C. CHIEU, M.S. DRESSELHAUS and M. ENDO, Phys. Rev. B, **26**, 10 (1982) 5867.

27 - M. GORMAN and S.A. SOLIN, Solid State Commun. **15**, 4 (1974) 761.

28 - Y. INOUE, S; NAKASHIMA, A. MITSUISHI, S. TABATA and S. TSUBOI, Solid State Commun. **48**, 12 (1983) 1071.

29 - A. MORIMOTO, T. KATAOKA, M. KUMEDA and T. SHIMIZU, Philosophical Magazine B, **50**, 4 (1984) 517.

30 - P. MARTINEAU, M. LAHAYE, R. PAILLER, R. NASLAIN, M. COUZI and F. CRUEGE, J. Mater. Sci., **19** (1984) 2731.

31 - A. OBERLIN, M. MONTHIOUX, E. BOUILLON, Composite Science and Technology (in press)

32 - H.A. POHL, in Modern Aspects of the Vitrous State, J.D. Mackenzie ed., London, **2** (1972) 72.

33 - M. RODOT, " Les Matériaux Semi conducteurs", Dunod ed., Paris, **2** (1965).

34 - F. CARMONA, P. DELHAES, F. BARREAU, D. ORDIERA, R. CANET, L. LAFEYCHINE, J. Phys., **41** (1980) 531.

35 - S.M. JOHNSON, R.D. BRITTAIN, R.H. LAMOREAUX, D.J. RAWCLIFFE, J. Am. Ceram. Soc. **71**, [3] (1988) C-132,C-135.

CHAPITRE II

Relations between microtexture and electrical properties during heat-treatment of SiC fibre precursor

INTRODUCTION AU CHAPITRE II

Les résidus minéraux correspondants à différentes températures de pyrolyse du polymère NC_2 ont fait l'objet d'une étude détaillée, faisant appel à **de nombreuses techniques d'analyses fines**. L'ensemble des principaux résultats a été exposé au **chapitre I**. Ainsi **différentes transitions** ont été mises en évidence dans le processus de transformation du polymère en **solide minéral amorphe** puis en solide **partiellement cristallisé**.

Cependant, nous avons pensé que les résultats obtenus par mesure de **conductivité électrique** méritaient une analyse fine afin de mieux comprendre le comportement électrique original des résidus de pyrolyse. Pour cela, nous avons réalisé une étude détaillée par **microscopie électronique en transmission** grâce à une collaboration étroite avec M^{me} A. Oberlin et M^{r} M. Monthioux du Laboratoire Marcel Mathieu. L'ensemble des résultats obtenus fait l'objet du **chapitre II**.

Pour des températures de pyrolyse (Tp) inférieures à **1000°C**, les matériaux sont **homogènes et amorphes**. Ils deviennent **microcristallisés et hétérogènes** pour 1000 < Tp < 1400°C avec une taille moyenne de cristallites de SiC de l'ordre de 2-3 nm à 1000°C et 5-6 nm à 1400°C. Quelques **unités structurales de base de carbone** (UBS) sont présentes pour Tp = 1000°C. Ces USB vont devenir de plus en plus présentes autour des cristallites de SiC lorsque Tp augmente allant jusqu'à former un ensemble de cages de carbone jointives pour Tp > 1050°C et permettant ainsi un phénomène de conduction par **percolation**. Ceci explique le **saut de conductivité électrique** observé et le **comportement métallique** des résidus correspondants.

Enfin, au dessus de 1400°C, on observe une cristallisation importante de la phase SiC.

Accepté par "Composite Science and Technology "Numéro Spécial sur Composites à matrice céramique.

RELATIONS BETWEEN MICROTEXTURE AND ELECTRICAL PROPERTIES DURING HEAT-TREATMENT OF SiC FIBRE PRECURSOR

M. MONTHIOUX*, A. OBERLIN*, E. BOUILLON**(°)

* Laboratoire Marcel Mathieu. UA 1205 CNRS.
2, Avenue du Président P. Angot.
F-64000 Pau.

** Laboratoire de Chimie du Solide du CNRS, Université de Bordeaux-I
351, cours de la Libération, F-33405 Talence

ABSTRACT

During the heat treatment from 800 to 1400°C of a polycarbosilane, a dramatic increase in conductivity occurs. High resolution transmission electron microscopy (including specific techniques such as the radial and azimuthal exploration of the reciprocal space) was used to reveal what structural or textural changes could explain the electrical behaviour of the material. Carbon in excess was found to rearrange in small turbostractic stacks lying flat upon the SiC crystal faces. Between 1000 and 1020°C, the turbostractic carbon stacks form a continuous network of uncomplete cages surrounding the SiC crystals. The increase in conductivity is assumed to be due to the release of heteroatoms (mainly hydrogen) which insures the contact between the turbostractic carbon stacks, and to the completion of the carbon cages.

(°) Present address : Laboratoire des Composites Thermostructuraux (UMR 47 CNRS-SEP-UB1) Europarc, 3, av. Léonard de Vinci F-33600 PESSAC.

1-INTRODUCTION

The physical properties of materials largely depend on the three-dimensional arrangement of their elemental units (crystallites or coherent scattering domains). This is true for carbons as an example [1]. This is also true for SiC, for which the properties and among them the electrical properties vary according to the thermal evolution of the precursor between 800 and 1400°C. These variations were already studied in a previous paper [2]. The aim of the present paper is to explain the mechanism by which the conductivity of a given SiC percursor [2] increases abruptly with an inflexion point at 1020°C. Since the elemental units of the heat treated material are very small and since their arrangement changes at a nanometric scale, high resolution transmission electron microscopy (TEM) is one of the most informative analytical techniques to be used. All the modes of TEM were carried on : bright field (BF), dark field (DF), lattice fringes (LF) and selected area diffraction (SAD). They are described in full details elsewhere both for specific improvements of DF imaging [3] and peculiar applications to SiC [4,5].

The precursor studied is a commercial polycarbosilane (PCS) slightly modified then heated as described in the previous paper [2].

2-RESULTS

2.1. Possible phases

In a ceramed PCS the most probable phases are β–SiC, SiO_2 and free carbon. These phases are either crystalline, turbostratic i.e. two dimensionaly crystallized (for carbon) or amorphous. X-ray diffraction or electron diffraction studies give accurate data for all these phases.

A β-SiC crystal yields 111 (0.251 nm), 220 (0.154 nm), 311 (0,131 nm) and possibly 200 (0.217 nm) scattered beams (Fig. 1a). When amorphous [6,7], SiC yields only a diffuse but intense ring at 0.251nm and a haloe around 0.14nm (Fig.1b).

Whatever the crystalline form of SiO_2, the most intense reflection occurs at 0.41nm, whereas amorphous silica [8] gives a relatively intense ring at 0.44 nm and a faint plateau up to 0.12 nm (Fig.1c).

The crystalline modifications of carbon (graphite or diamond) are excluded but both turbostratic and amorphous carbons are plausible. Turbostractic carbons are formed by aromatic layer stacks where the aromatic layers are piled up in parallel but slightly rotated at random one to another. Correspondingly the 002 reflections remain Bragg reflections whereas hkl reflections disappear and are replaced by two dimensional hk lines [9]. The 002 interlayer spacing is always ≥ 0.344 nm (d_{002} of graphite being 0.3354 nm). The hk rings occur in the vicinity of hk0 of graphite, i.e. 0.213 nm (10 asymmetric band) and 0.123 nm (11 asymmetric band). 002 scattered beam is very intense and 10 and 11 bands very faint (Fig. 1d).

Amorphous carbons [10] yield a quasi constant intensity as the scattering vector increases, weakly modulated mainly at 0,216 nm and 0,114 nm.

Fig.2 sketches the combination of the above mentioned scattered beams. It shows also how it is possible, with a suitable aperture (2 nm^{-1} diameter), to image separately C_{002} and SiO_2 in position 1 (aperture centered at 2.4 nm^{-1}), SiC_{111} and C_{10} in position 2 (aperture centered at 4.2 nm^{-1}), and SiC_{220} in position 3 (aperture centered at 6.3 nm^{-1}). Since C_{10} is negligible in intensity relative to SiC, position 2 and 3 image selectively various orientations of SiC crystals, whereas position 1 images both C and SiO_2.

For position 1, 2 and 3 respectively, the radial tolerance of the 2 nm^{-1} aperture admits scattered beams corresponding to interplanar distance ranges of 0.29-0.71 nm, 0.19-0.31 nm and 0.13-0.19 nm. Likewise, the azimuthal twist tolerance are respectively $\pm$ 22°, 14,5° and 9,5°.

2.2. PCS heat-treated at 800°C

In BF mode used with the 2 nm^{-1} aperture, a fine granular texture occurs (Fig. 3a). The granulation scale is about 2-5 nm. The contrast of this texture increases with underfocussing and disappears when the aperture

used is 10 nm^{-1} diameter instead of 2 nm^{-1}. This peculiar contrast is thus not due to interference image but is a normal diffraction contrast since most of the diffused intensity is withdrawn by the smallest aperture. It can be attributed to local differences of thickness, expressed by optical density differences in the micrograph, and revealed that the material is porous. These data well agree with X-ray small angle scattering [11] which concludes to the occurence of heterogeneities in the 1-5 nm range.

The images obtained in high resolution mode (LF) only show the granularity due to the transfer function of the lens and are absolutely free from fringes (Fig. 3b). **The material is thus amorphous.**

The SAD patterns are illustrated by Fig. 1 b suggesting the occurence of only amorphous SiC.

The radial exploration of the reciprocal space (Fig.2) also yields DF images characteristic of amorphous materials [12], i.e. faint bright dots appear for any aperture location (Fig. 4abc). The size of these bright domains is below 1 nm, i.e. equals to the resolution limit. As the incident beam is rotated along a cone (equivalent to the aperture rotated along a circle) the bright dots remain homogeneously distributed, which means that there is no preferred orientation. Comparing SAD and DF data on amorphous SiC could be assumed. If SiC would be the only phase, the number of bright dots occuring in position 1 should be lower than for position 2 since the SiC scattering intensity is very low in position 1. However, the intensity of the dots remains coarsly constant as the aperture is displaced from position 1 to 3. Therefore, the occurence of another phase has to be assumed to account for the experimental data. Carbon in excess could cause additionnal intensity in the SAD pattern, but too low to be noticed in the pattern image itself. The occurence of $SiO_{4-x}C_x$ tetrahedra (revealed by ESCA and Auger experiments [2,11] could also contribute. These various contributions to DF imaging yield a quasi-constant distribution of bright dots of constant intensity whatever the aperture position.

In conclusion, the PCS heat-trated at 800°C can be described as an **homogeneous SiC-based amorphous and porous material**, containing oxygen and carbon in excess.

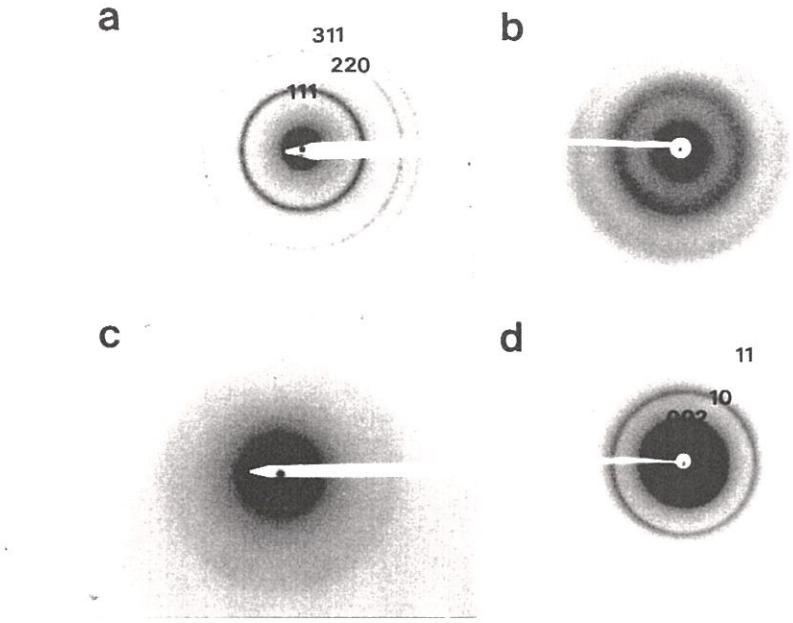

Fig. 1 : SAD patterns of : a-crystallized - SiC, b-amorphous SiC, c-amorphous SiO_2, d-turbostractic aromatic carbon.

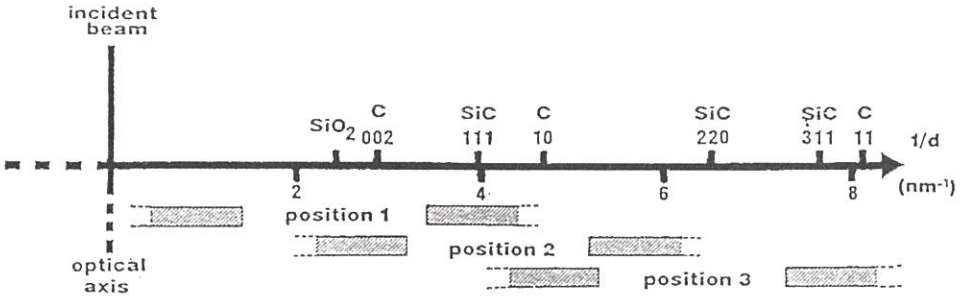

Fig. 2 : The main scattered beams to be expected in a SAD pattern of a SiC-based material, as compared with the objective aperture size. Successive positions of the objective aperture relative to the SAD pattern used for the radial exploration of the reciprocal space in DF imaging.

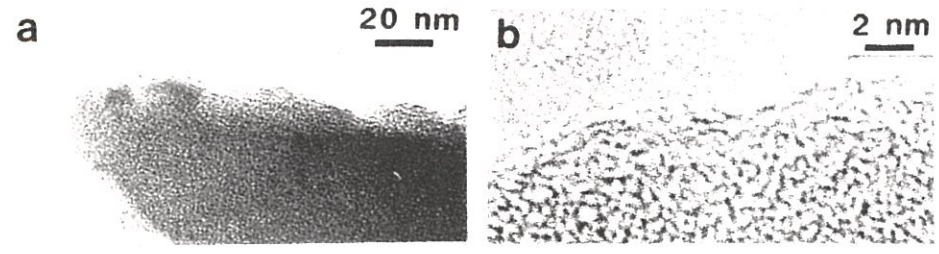

Fig. 3 : PCS heat-treated at 800°C : a-BF image, b-LF image.

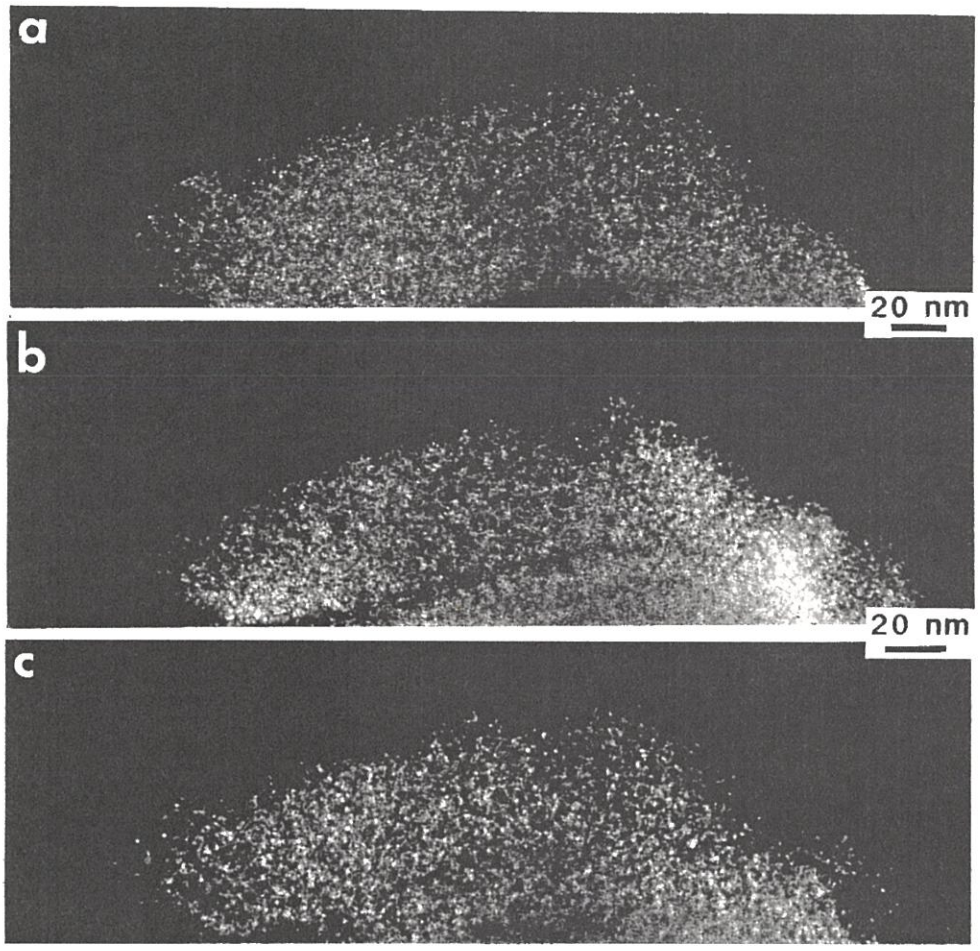

Fig. 4 : PCS heat-treated at 800°C : a- to c-sequence of DF images (positions 1 to 3 of the objective aperture).

2.3. PCS heat-treated at 1000°C

Besides amorphous SiC-based particles identical to those described above (about 20 % in number), all other fragments are different in texture (compare Fig.5a to Fig. 3a). They yield SAD patterns of crystallized SiC (Fig. 1a). A small number of these particles are covered by a thin layer (10-15 nm) of amorphous silica [13] (Fig. 5b).

The radial exploration of the reciprocal space yields the DF images of Fig. 6abc. As expected , position 1 (Fig. 6a) which excludes SiC imaging is entirely different from position 2 (Fig. 6b : SiC_{111}) or 3 (Fig. 6c : SiC_{220}). The bright dots observed in SiC_{111} and SiC_{220} DF range from 1 to 5 nm in size with a mode around 2 nm. These bright dots are **SiC microcrystals, i.e. coherent domains with a three-dimensional order.** This is evidenced by the occurence of Bragg fringes (arrows in Fig. 6b). The DF images obtained from the positions 2 and 3 (Fig. 6b and 6c) both illustrate SiC microcrystals, but which present different cristallographic orientations. In addition to these images, other ones were obtained for orthogonal 2 and 3 positions of the aperture (not represented). They show identical repartition of bright dots, which indicates that the distribution of the SiC crystals is perfectly random in the bulk.

This explains the texture observed in Fig. 5a, since the granular texture is produced by the boundaries between adjacent SiC crystals.

The DF image obtained in position 1 (Fig. 6a) entirely differs from the SiC DF images (Fig. 6b and 6c). It shows bright dots about 1 nm in size, indicating the particule to contain an other phase associated with SiC crystals. The size of these dots is too large for attributing them to an amorphous phase. In addition, when the aperture is displaced along a circle corresponding to the position 1 (azimuthal exploration of the reciprocal space), many thick particles show bright rims appearing then disappearing for two orthogonal positions of the aperture arrow in Fig. 7a and 7b. This necessarily indicates the occurence of a family of lattice planes having a preferred orientation normal to the scattering vector selected by the aperture (the direction of these lattice planes are indicated in Fig. 7 by double bars). Thus, the bright rims cannot be made of an amorphous material. Position 1 DF images then revealed either crystalline silica or turbostractic carbon (in latter case, the aromatic layers are imaged edge on). The position of the double bars in Figure 7 indicates that, at least

along the particle edge, the projections of the lattice planes of the new phase (silica or carbon) lie parallel to the external contour of SiC crystals, i.e. the lattice planes lie flat on some of the SiC crystal faces.

LF images (Fig.5c) show very short (≤ 1nm) stacks of two to four fringes. Some are agregated along the free edge of the particle where they form an oriented rim (single arrow). Others are randomly found in the bulk (double arrow) where they are more hardly seen. They are compatible with **poorly organized turbostractic carbons** [1]. The interlayer spacing cannot be measured by laser beam optical diffraction in this case, but will be measured latter for better organized materials, allowing carbon to be identified. Each fringe corresponds to the projection of an aromatic carbon layer oriented edge on two or three such layers are piled up in parallel forming basic structural units (BSU).

In conclusion, most of the 1000°C heat-treated PCS is made of **microcrystalline β-SiC** (about 2nm), and of a **carbon aromatic layer stacks** (BSU). In the bulk, the BSU do not form a dense array and thus appear single. On the contrary, the oriented rims occupy only the free edges of thick fragments. Indeed, during the sample grinding the cracks follow the lesser cohesion joints, i.e. occur between aromatic layers. In these regions, series of single BSU images issued from neighbouring SiC crystals align edge to edge. Series of single BSU images are also superimposed due to the thickness of the free surface. Apparent continuous carbon layer stacks are thus observed all along the particle edge, forming the oriented rims. Such rims were observed in other ceramic materials (either heated PCS or fibres) prepared by grinding or thin sectioning [4,5].

The 1000°C heat-treated PCS is **highly heterogeneous**, not only because a noticeable amount of amorphous phase remains, but also because a small number of particles wearing the characteristics of higher heat-treatments (for example 1400°C) are found.

2.4 PCS heat treated at 1050°C

Amorphous SiC-based particles have disappeared. The material is now made of **β-SiC crystals associated with free aromatic carbon**. The size of SiC

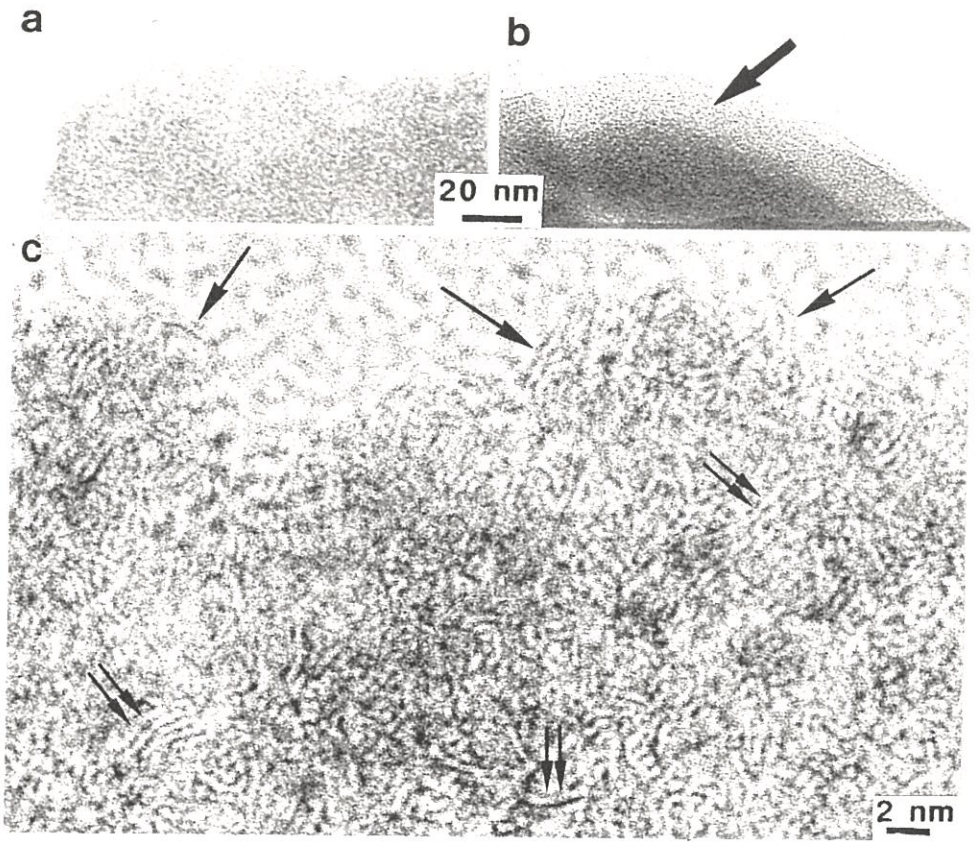

Fig. 5 : PCS heat-treated at 1000°C : a and b-BF image : the arrow shows an external amorphous SiO_2 layer, c-LF image : short stacks of turbostratic carbon evidenced either in the bulk (double arrows) or on the particule edge (single arrows).

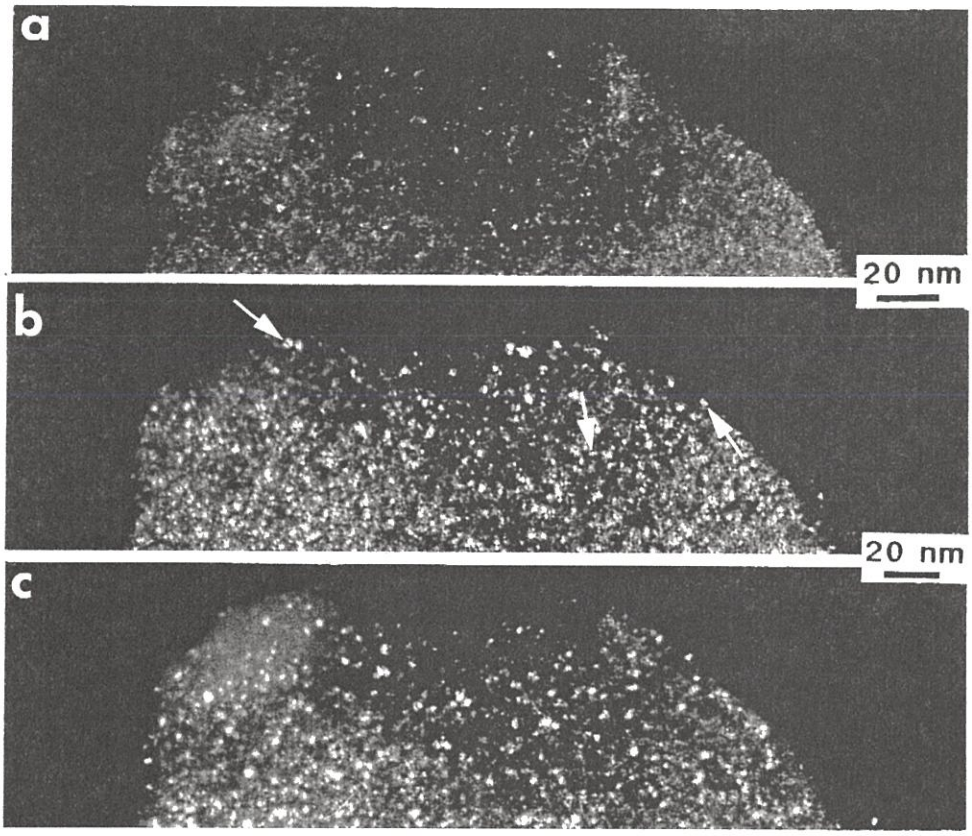

Fig. 6 : PCS heat-treated at 1000°C. Sequence of DF images : a-position 1 of the objectice aperture (carbon); b and c-positions 2 and 3 (SiC). Arrows show Bragg fringes.

crystals in the major particule type (Fig.8b) ranges from 1 to 5 nm with a mode around 3 nm, wich is not so different from the particles described in 2.3 (1000°C heat-treated PCS). The main difference lies in carbon . At first, carbon is now visible in the overexposed SAD patterns (Fig. 9). Faint 002 ring and hk bands are observed, associated with Debye Scherrer SiC rings. The structural organization of free aromatic carbon has thus improved. In position 1 DF images (Fig. 8a), the isometrical 1nm bright dots (which always image BSU) are now sometimes aligned (arrow). These short alignments have the same range of length than the SiC-crystal edges (up to 4-5 nm). Since the aromatic layers are parallel to the length of the alignments (see the double bar direction changes by 90° when two orthogonal DF images are compared). They form oriented rims along the broken edges of the particles.

Lattice fringe images (Fig. 10) are different from that of the 1000°C heated PCS (compare Fig. 10 with Fig. 5c). Stacks of 2 to 6 distorted continuous fringes are observed. They are made of small units (about 1nm) aligned edge-to-edge, with a length which again is about the same range than SiC-crystal faces. Then, these stacks of fringes are the alignments seen in the DF images. Some of these distorted stacks underline almost entirely an "empty" area (arrow in Fig. 10) The size and shape of these areas well correspond to the SiC-crystal external contours.

In conclusion, the above observations suggest that **SiC crystals have grown up** and **carbon BSU** have coalesced into distorted continuous layer stacks, forming **uncomplete open cages around each SiC crystal**. These cages are produced by the increase in size of SiC which brings two BSU edges into contact from place-to-place. The defects (dangling bonds, sp_3 bonds, ...) trapped at the BSU boundaries insure the lateral binding.

PCS heat-treated at 1050°C is not homogeneous despite no amorphous phase occurs, since a small number of more evolved particles is observed.

2.5. PCS heat treated at 1400°C

Figure 18 in ref. 2 gives example of BF and DF images obtained for this temperature. Figure 11 (LF mode) shows both SiC_{111} fringes and aromatic turbostratic carbon 002 fringes in the major particle type (50-60 % in number).

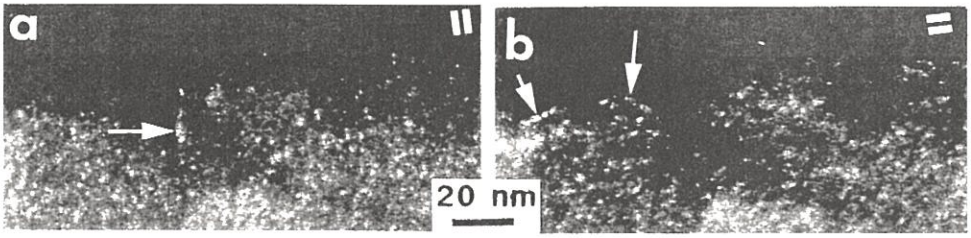

Fig. 7 : PCS heat-treated at 1000°C : a and b - DF images for two orthogonal position 1 of the objective aperture. Arrows show rims of oriented turbostratic carbon. The double bars indicate the coarse orientation of the aromatic planes.

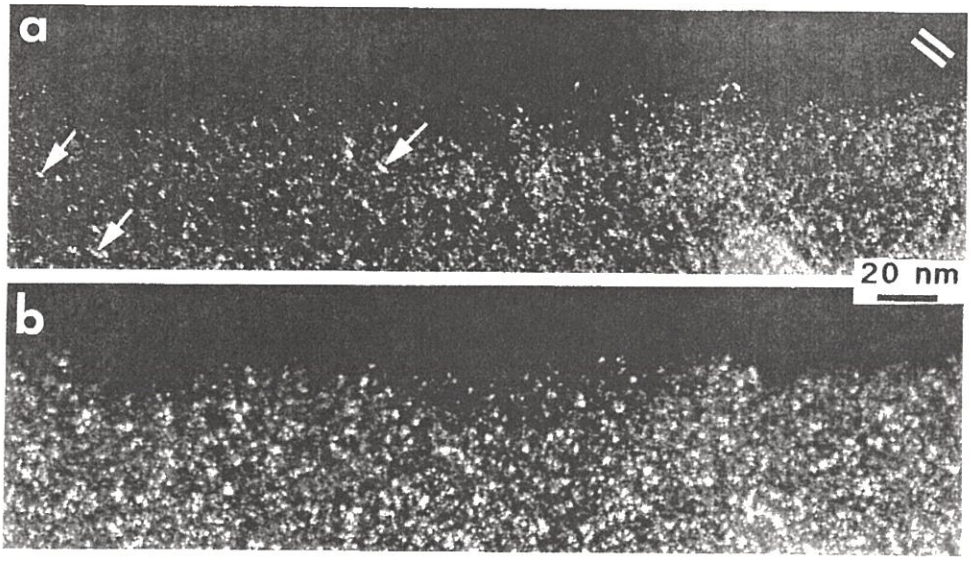

Fig. 8 : PCS heat-treated at 1050°C. DF images : a-positon 1 of the objective aperture. Arrows show associations of turbostratic carbon stacks, with their aromatic planes oriented following the direction of the double bars, b-position 2 (SiC).

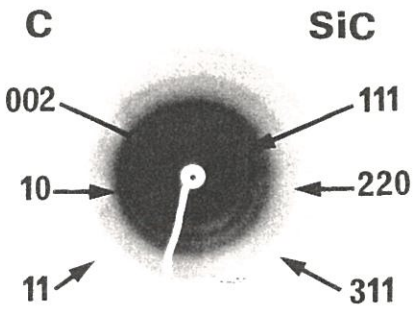

Fig. 9 : PCS heat-treated at 1050°C : overexposed SAD pattern.

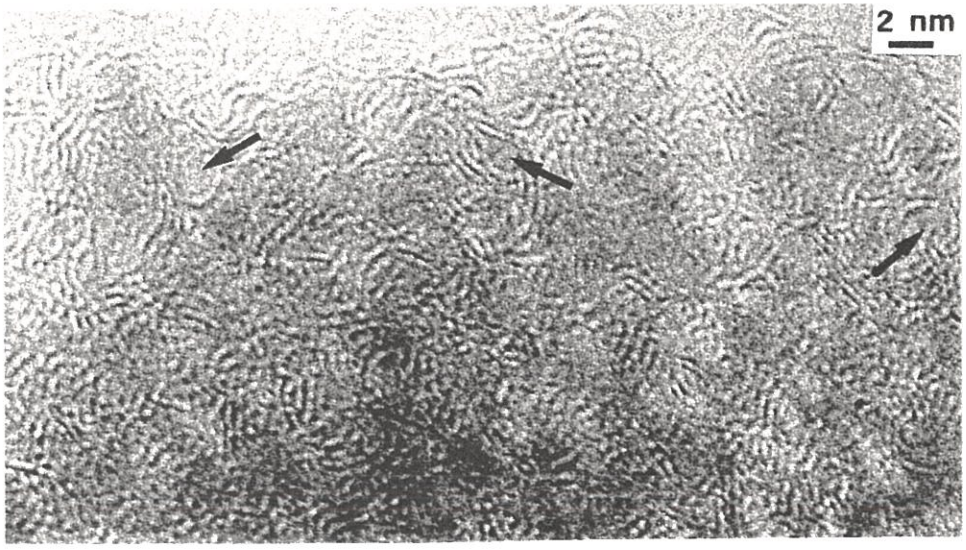

Fig. 10 : PCS heat-treated at 1050°C : LF image. Arrows show SiC crystals surrounded by turbostratic carbon stacks.

The strong contrast and the nice linearity of SiC fringes are striking. They indicate that the **SiC domains are large and very well crystallized** (sizes ranges is 4-20 nm with a mode around 5-6 nm). Correspondingly, the Debye-Scherrer rings in SAD pattern are sharp and even ponctuated. The number of fringes in a stack ranges from 2 to 6 as for 1050°C. the uncomplete carbon cages are now clearly evidenced, either around SiC crystals (single arrow) or along the broken edges of the particles (double arrow).

The micrograph of Fig 11 was taken as scattering object for an optical system equipped with a laser source. The SiC_{111} fringes acting as an internal standard at 0.251 nm, it was possible to enough accurately measure interfringe spacing of carbon in the optical diffraction patterns. The value was found to be around 0.36 nm, which is in full accordance with the hypothesis of **turbostratic carbon**, and cannot correspond to crystalline silica.

PCS heat-treated at 1400°C is again heterogeneous (ref-2 Fig. 18) since a relatively noticeable amount of less evolved particles is found, with SiC-crystal sizes having modes ranging from 3 nm (then at least equal to 1050°C) to 5-6 nm.

3. DISCUSSION- CONCLUSION

During heat-treatment, a first important step occurs before 1000°C. The material initially homogeneous and amorphous becomes crystalline in an increasing number of areas. This is typical of a phase change. It should occur at a given temperature for the whole matter except if disturbed by local changes of conditions (temperature gradients or diffusion rates of volatiles for instance). This effect could be similar to the one observed heated in fibres [14] which present a gradient of crystal size from the skin to the core. The transformations is over between 1000 and 1050°C.

The bulk histograms of size of SiC crystals for each temperature are asymmetric (the mode is not centered in the range). From 1000 to 1400°C, the mode displaced near the large values (2,3 then 5-6 nm), i.e. the smallest crystals disappear to the benefit of the largest one. This indicates a **coalescence type of growth for SiC** instead of a normal growth.

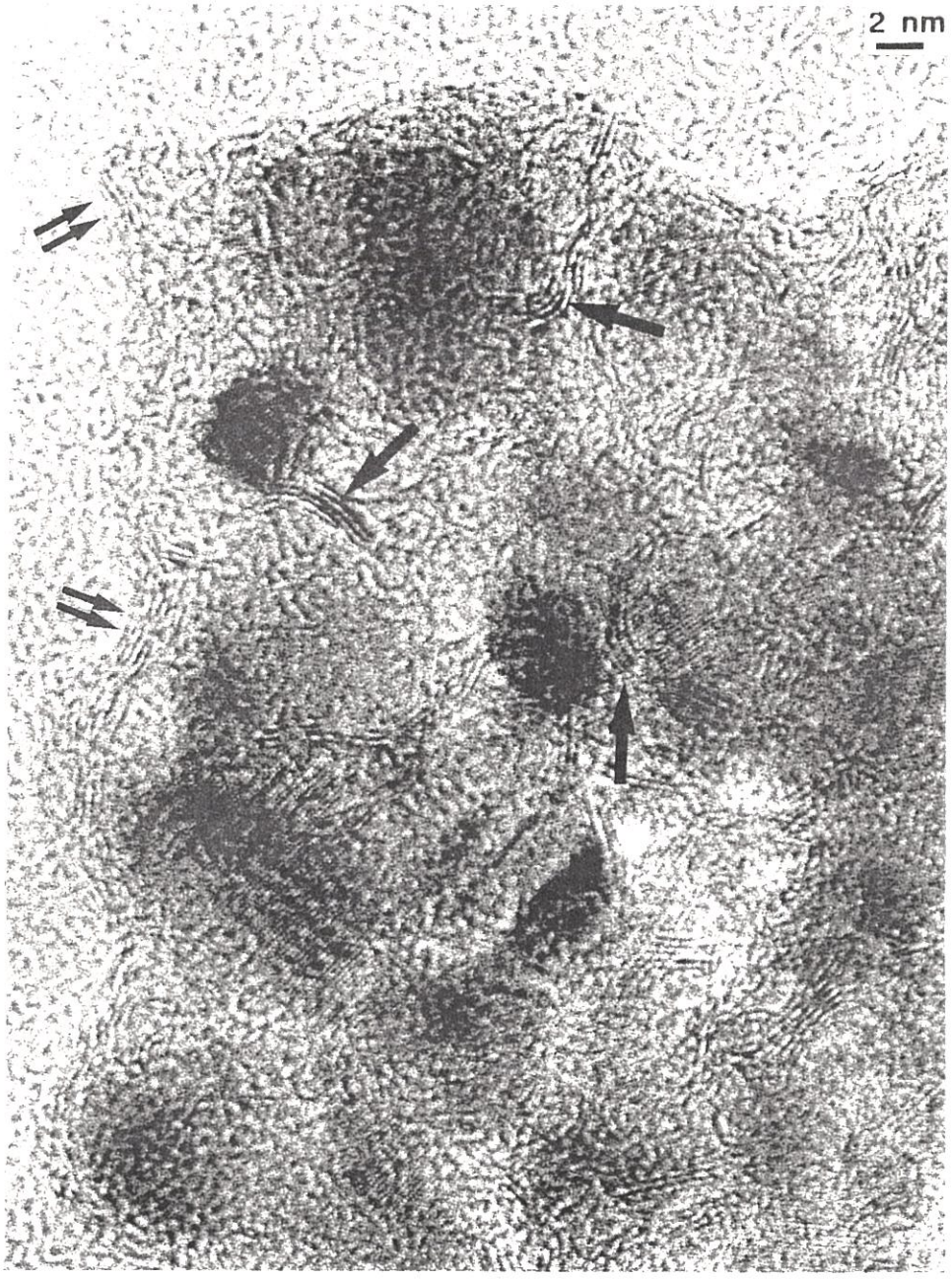

Fig.11 : PCS heat-treated at 1400°C : LF image. Single arrows show turbostratic carbon stacks surrounding SiC crystals. Double arrows show turbostratic carbon stacks along the particule edge.

At first sight, the dramatic change in conductivity [2] (Fig. 12 a) could be attributed to the crystallisation process. However, the derived curve (Fig. 12 b) shows that the maximum rate of change occurs at 1020°C, and is still very noticeable at 1050°C. An other parameter must be thus found to account for that.

Free carbon under the form of single BSU (i.e. aromatic layer stack of about 12 rings piled up by 2 to 4) suddenly appears at the very moment where amorphous state turns to crystalline. BSU increasingly associate edge-to-edge in longer distorted layer stacks from 1000°C up to 1050°C. They tend to lie **flat upon the crystal faces** as soon as SiC crystals are present (i.e. above 800°C). This behaviour is commonly encountered for other carbons, the aromatic layers of which are known to preferentially deposit flat upon any substrate [15]. Therefore, they tend to form uncomplete cages around SiC crystals. The texture of carbon increasingly improve (by progressive annealing of distorsions) up to 1400°C where the layers are nearly perfect and the cage much more complete. The increase in completion of the cage walls is obviously caused by the considerable decrease of the free SiC surface avaible for carbon deposition, as the numerous small crystals coalesce into less numerous large crystals. Thus, **the leading parameter to the conductivity increase seems to be carbon better than SiC** since formation followed by cage completion better fits with the trend of Fig. 12 b : only single BSU are majorly found at 1000°C (stage 1), cages are formed rather suddenly before 1050°C (stage 2), and partial completion occurs steadily between 1050 and 1400°C (stage 3).

An additional argument may be found in the resistivity behaviour of carbons [16]. The are insultating materials below 1000°C (Fig.12 c), which is the temperature where most of the heteroatoms among which hydrogen are removed [1]. At that point, single BSU are associated edge-to-edge and face-to-face, and the material reaches almost the graphite resistivity value. At the very moment where heteroatoms (hydrogen) fixed at the BSU boundaries are released, the free charge carriers are able to jump freely from one BSU to the next. The decrease in resistivity is about **ten decades for carbon** (Fig.12 c) and heat-treated PCS (Fig. 12a) as well. The explanation for carbons can be easily adapted to heat-treated PCS, since the release of hydrogen occurs for PCS between 1000 and 1200°C [2] as in carbons. In addition, oxygen probably leaves the bulk at the benefit of the external surface of the particles (see Fig. 5b), or

under a silicon oxide gaseous form. The formation and subsequent completion of carbon cages insure the contact between an increasing number of adjacent BSU, resulting in increasing fastly the conductivity. The mechanism for heated PCS thus approximated that established for carbons.

ACKNOWLEDGEMENTS

The authors wish to thank the Centre National de la Recherche Scientifique, the french ministry of Defence (DRET), Rhône-Poulenc, and the Société Européenne de Propulsion for their interest and their financial support.

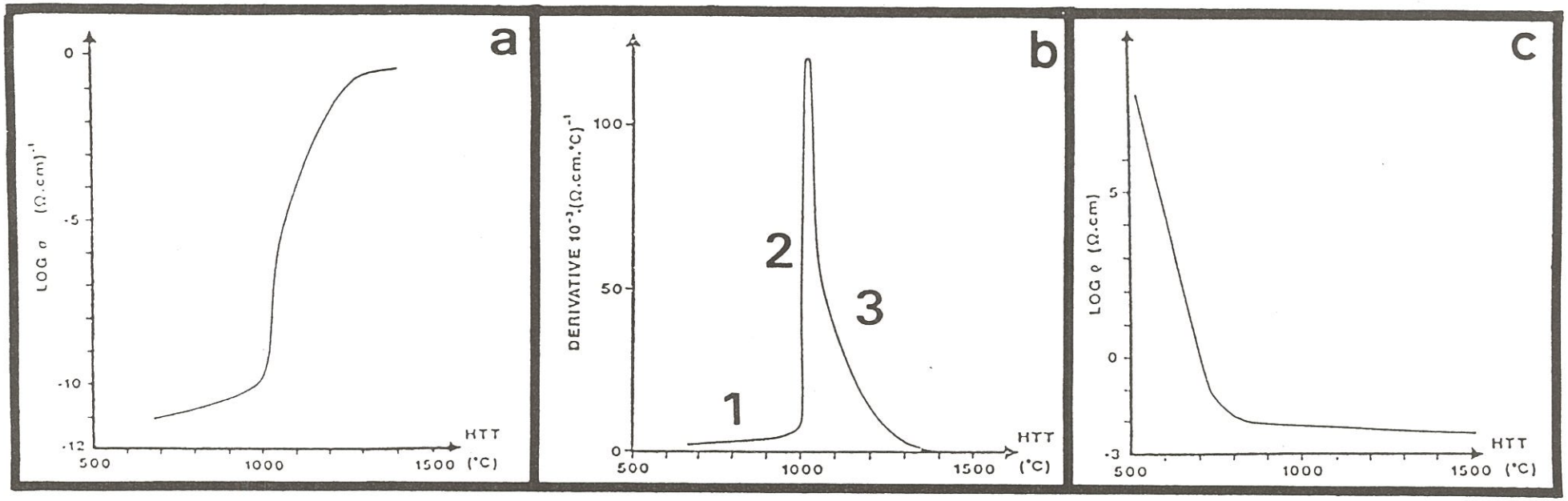

Fig. 12 : a) increase in conductivity for the PCS in function of the heat treatment temperature, b) derived curve from curve a, c) decrease in resistivity for soft carbons in function of the heat treatment temperature (from Marchand [16]).

REFERENCES

1 A. OBERLIN, Carbonization and Graphitization, **Carbon**, 22 (1984), 521-541.

2 E. BOUILLON, F. LANGLAIS, R. PAILLER, R. NASLAIN, J.C. SARTHOU, A. DELPUECH, C. LAGARDE, F. CRUEGE, P.V. HUONG, M. MONTHIOUX, A. OBERLIN On the convertion mechanisms of a polycarbosilane precursor into a SiC-based ceramic material, **J. Mat. Sci.**,(submitted)

3 A. OBERLIN, Application of dark-field electron microscopy to carbon study, **Carbon**, 17 (1979), 7-20.

4 J. AYACHE, S. BONNAMY, X. BOURRAT, A. DEURBERGUE, Y. MANIETTE, A. OBERLIN, E. BACQUE, M. BIROT, J. DUNOGUES and J.P. PILLOT, Characterization of some pyrolyzed polycarbosilanes by transmission Electron Microscopy, **J. Mat. Sci. Letters** (submitted).

5 Y. MANIETTE and A. OBERLIN. T.E.M. characterization of some crude or air heat treated SiC Nicalon fibers, **J. Mat. Sci** (submitted).

6 S. YAJIMA, K. OKAMURA, T. MATSUZAWA, Y. HASEGAWA and T. SHISHIDO, Anomalous characteristics of the microcrystalline state of SiC fibers, **Nature**, 279 (1979), 706-707.

7 Y. HASEGAWA and K. OKAMURA, Synthesis of continous silicon carbide fibre. Part 3 : Pyrolysis process of polycarbolisane and structure of the products, **J. Mat. Sci.**, 18 (1983), 3633-3648.

8 P. CHAUDHARI, J.F GRACZYK and R. HERD, electron microscope investigation of the structure of some amorphous materials, **Phys. Stat. Sol.**, 51 (1972), 801.

9 M.C. ROBERT, M. OBERLIN, and J. MERING, Lamellar reactions in graphitizable carbons, in : **Chemistry and Physics of Carbon** (ed. P.L. Walker Jr. and P.A. Thrower), Marcel Dekker Inc., New York, 1973, Vol. 10, pp 141-212.

10 J. KAKINOKI, K. KATADA T. HANAWA and T. INO, Electron diffraction study of evaporated carbon films, **Acta Cryst.** 13 (1960), 171-179.

11 R. HAGEGE, P. OLRY, J. COTTERET, M. LARIDJANI, J. DIXMIER, C. LAFFON, A. M. FLANK, J.L. MIQUEL, H. HOMMEL and A.P. LEGRAND, Study of Nicalon-based ceramic fibres and powder by EXAFS spectrometry, X-ray diffractometry and some additionnal methods, **J. Mat. Sci.** (accepted).

12 A. OBERLIN, M. OBERLIN and M. MAUBOIS, Study of thin amorphous and crystalline carbon films by electron microscopy, **Phil. Mag.**, 32 (1975), 833-846.

13 M. MONTHIOUX, and A. OBERLIN, Structural and Textural events occuring in a 800-2250°C heat-treated PCS, **J. Mat. Sci.** (to be submitted).

14 T. MAH, N.L. HETCH, D.E. Mc CULLUM, J.R. HOENIGMAN, H.M. KIM, A.P. KATZ, and H.A. LIPSIT, Thermal stability of SiC fibres Nicalon), **J. Mat. Sci.,** 19 (1984), 1191-1201.

15 J. GOMA, M. OBERLIN, A. OBERLIN, J. SCHEINEDER and C. BELOUET, Carbon-silicon interfaces studied by conventional transmission electron microscopy, **High Temp. High Press.,** 13 (1981), 263-274.

16 A. MARCHAND, Propriétés elctroniques des carbones graphitables, in : **Les Carbones** (ed. A. Pacault), Masson,Paris, 1965, Vol.1, pp 408-452.

CHAPITRE III

Composition-microstructure-property relationships in ceramic monofilaments resulting from the pyrolysis of a polycarbosilane precursor at 800-1400°C

INTRODUCTION AU CHAPITRE III

Un des axes principal de ce travail de thèse consistait à dégager les relations pouvant exister entre la **composition chimique et l'état microstructurale** d'une part et les **propriétés mécaniques** d'autre part des résidus issus des précurseurs organiques et pyrolysés à différentes températures.

Cette approche a necessité la conception et la mise au point d'un **appareillage de laboratoire** permettant une mise en forme des précurseurs de manière à obtenir les céramiques résultantes sous forme d'**éprouvettes mécaniques**. Cet appareillage a été réalisé avec Mr Loubinou de la Société ITF et Mr Olry de la SEP. Il est basé sur le principe de l'**extrusion** puis **étirage** du polymère à l'état fondu.

La mise au point des différentes étapes : (i) obtention du fil polymérique, (ii) oxydation ménagée sous air pour rendre le fil infusible et (iii) pyrolyse à haute température sous atmosphère inerte a été réalisée à partir du polymère NC_2.

L'obtention des **éprouvettes cylindriques mofilamentaires** issues du NC_2 nous a permis d'effectuer une analyse physicochimique, microstructurale et mécanique de celles-ci en fonction de la température. L'ensemble des résultats obtenus fait l'objet du **chapitre 3.**

(i) L'analyse thermogravimétrique nous a permis de mettre en évidence d'une part la **transformation organique minérale** entre 550 et 700°C et d'autre part une transition après 1200°C représentative de l'évolution de la phase oxygénée existante dans ce type de céramique.

(ii) L'analyse XPS nous a permis de confirmer la présence d'un **oxycarbure de silicium**, et d'une phase carbone libre commençant à se former vers 850°C. A cette température nous détectons aussi une faible couche de silice (environ 5 nm) en surface de fibre.

(iii) D'après les résultats de microscopie électronique en transmission nous avons une céramique qui reste **amorphe** jusqu'à 1200°C. Ensuite celle-ci cristallise entre 1200 et 1400°C et fait apparaitre des cristaux de SiC (10-20 nm) recouvert partiellement d'USB de carbone, ainsi qu'une couche de carbone turbostratique (environ 40 nm) en surface de fibre.

(iv) La mesure des propriétés électriques permet de mettre en évidence un **gap de l'ordre de quatre décades** entre 1200 et 1400°C, ce comportement étant vraissemblablement la conséquence d'un phénomène de percolation par le carbone.

(v) Les caractéristiques mécaniques des éprouvettes céramisées sont maximales pour une température de pyrolyse de 1200°C, et peu éloignée de celle de la fibre NICALON, la **contrainte à rupture** étant de **2100 MPa** et le **module d'Young** de **180 GPa.** Ces caractéristiques décroissent rapidement après 1200°C.

L'évolution de la composition chimique et de la microstructure des éprouvettes entre 1200 et 1400°C est principalement due à la **destruction de la phase oxycarbure**. Ceci se traduit par une augmentation de la phase carbone libre au sein de la céramique et par le **départ de l'espèce gazeuse SiO**.

Soumis à "Journal of Materials Science"

COMPOSITION-MICROSTRUCTURE-PROPERTY RELATIONSHIPS IN CERAMIC MONOFILAMENTS RESULTING FROM THE PYROLYSIS OF A POLYCARBOSILANE PRECURSOR AT 800-1400°C

E. BOUILLON, D. MOCAER, J.F. VILLENEUVE, R.PAILLER, R. NASLAIN
Laboratoire des Composites Thermostructuraux, (UM 47-CNRS-SEP-UB1)
Europarc, 3 Avenue Léonard de Vinci, F 33600-Pessac

M.MONTHIOUX, A. OBERLIN
Laboratoire Marcel Mathieu (UA 1205 CNRS)
Université de Pau, 2 Avenue du Président Angot, F 64000-Pau

C. GUIMON and G.PFISTER
Laboratoire de Physico-Chimie Moléculaire (UA 474-CNRS)
Université de Pau, Avenue de l'Université, F 64000-Pau

ABSTRACT

A 15 μm monofilament was extruded from a Yajima's type molten polycarbosilane, stabilized by addition of oxygen and heat-treated at 800-1400°C under argon atmosphere. Two important phenomena occur during pyrolysis. At 500-750°C, an organic-inorganic state transition takes place with a first weight loss. It yields an amorphous material stable up to about 1100°C. At this temperature, its composition is close to $Si_4C_5O_2$. It can be described as a continuum of SiC_4 or/and $SiC_{4-x}O_x$ tetrahedral species (and possibly contains free carbon), with a homogeneity domain size less than 1 nm. The amorphous filament exhibits a high strength and semi-conducting properties. Above 1200°C, a thermal decompositon of the amorphous material takes place with an evolution of gaseous species thought to be mainly SiO and CO, an important cross-section shrinkage and the formation of 7-20 nm SiC crystals which are surrounded with a poorly organized turbostratic carbon. The amorphous-crystalline state transition results in a drop in the tensile failure strength and an increase, by four orders of magnitude, in the electrical conductivity which becomes temperature-independent. The former effect is due to the crystallization of the filament and the latter to a percolation phenomenon related to the intergranular carbon. The low stiffness is also due to the presence of carbon. It is anticipated that this transition is mainly related to the decomposition of the silicon oxycarbide species. Finally, a 40-50 nm layer of turbostractic carbon is formed at filament surface at 1200-1400°C whose origin remains uncertain. It is thought to be mainly responsible for the formation of the carbon interphase in the high temperature processing of ceramic matrix composites.

Key Words *PRECERAMIC PRECURSORS, POLYCARBOSILANE PYROLYSIS, ORGANIC-INORGANIC TRANSITION, SiC-FIBER.*

1- INTRODUCTION

Ceramic Matrix Composites (CMCs) belong to a new family of ceramic materials that could be used extensively by the designers, in a near future, for structural parts submitted to severe environmental conditions (e.g. in high temperature gas turbines and reciprocating engines as well as reusable heat shields). With respect to monolithic ceramics, the main advantage of CMCs lies in their **high toughness and reliability.**

The applications of CMCs are still limited by processing considerations and availability of high performance ceramic fibers. Recent progress has been done in the field of **CMC processing**. The chemical vapor infiltration process (used for SiC-matrix composites) and the slurry impregnation/hot pressing process (used for glass or glass-ceramic matrix composites) are examples of techniques which are already utilized in industry . On the contrary, in the field of **ceramic fibers**, the progress has been very slow during the last two decades, carbon fibers remaining, as a matter of fact, the best reinforcement on the basis of their excellent mechanical properties at high temperatures and low density. Unfortunately, the strong affinity of carbon for oxygen, even at moderate temperatures, precludes the use of CMCs reinforced with carbon fibers in atmospheres containing oxygen unless a protective coating is applied on the fibers or/and the composites [1].

SiC-based fibers, obtained by pyrolysis of a polycarbosilane precursor, have been first proposed by S.Yajima and his coworkers [2-8]. They were prepared according to a procedure very similar to that already used for carbon fibers including the main following steps : (i) spinning of the precursor in the molten state, (ii) cross-linking by oxygen to make the green fiber infusible and (iii) pyrolysis under an inert atmosphere. Different products derived from the Yajima's route are now available on the market, the most common being the **Nicalon fibers** (NLP 101 and NLM 202 from Nippon Carbon). From a chemical point of view, all of them belong to the ternary Si-C-O or quarternary Si-C-N-O systems (and even to more complex systems involving e.g. titanium) and are obtained by pyrolysis of polycarbosilane (PCS) or polycarbosilazane (PCSZ) precursors [9-12]. It is worthy of note that the properties of these ceramic fibers have not been significantly improved, in terms of mechanical and thermal stability, with respect to those of the original Yajima ex-PCS fiber despite an important effort of research. This might be the result of two contradictory

considerations : (i) a high failure strength in ex-PCS fibers is thought to be related to an amorphous (or at least poorly crystallized) microstructure whereas (ii) such a microstructure is not stable at high temperatures and tends to crystallize and coarsen with a dramatic drop in failure strength.

According to **chemical analysis data**, there is both an excess of carbon (with respect to the SiC stoechiometry) and significant amount of oxygen (resulting mainly from the cross-linking step) in ex-PCS fibers. However, the nature of the forms under which these carbon excess and oxygen are present in the fibers is still a matter of controversy and seems to be different from fiber to fiber. Microcrystals of free carbon have been observed by transmission electron microscopy (TEM) in the Nicalon NLM 202 ceramic grade fiber but not in the NLP 001 grade, by M. Maniette et al. [13]. Oxygen was first assumed to be present as silica whereas recent analyses support the occurence of an amorphous Si(C,O) ternary phase [14,15]. The state of crystallization of the SiC phase is also different in the two Nicalon fibers : the NLM 202 grade being usually considered as more crystallised than the NLP 101 grade . Finally, a model of microstructure has been recently proposed by C. Laffon et al. according to which the ex-PCS fiber could be described as a nanoscale mixture of SiC and carbon embedded in a Si (C,O) amorphous matrix [16].

The **thermal stability** of ex-PCS fibers is an important property since any coarsening of the initial fine grained microstructure resulting from a heat treatment may lead to : (i) an important decrease in the fiber failure strength, as already mentioned and (ii) a change in the composition of the fiber surface modifying the fiber/matrix coupling when it takes place within a composite. This latter effect is thought to be at least partly responsible for the formation of the **carbon-based interphase** during the high temperature fabrication of most ex-PCS reinforced CMCs (e.g. SiC (Nicalon)/glass-ceramic composites) and thus for their high toughness [17-22].

As far as the strength of CMCs (which by their nature are intended to sustain long exposures at high temperatures) is concerned, ex-PCS fibers should have a high thermal stability whereas recent studies have shown that they undergo important chemical and microstructural changes above about 1100°C (i.e. far below the peritectic decomposition of SiC at about 2500°C) [23]. K.L. Luthra has shown, from thermodynamic considerations, that ex-PCS fibers are intrinsically unstable at high temperatures, their evolution towards equilibrium giving raise to the formation of carbon monoxide as main gaseous species [24]. On the other hand , S.M. Johnson et al. have established,

on the basis of their Knudsen cell/mass spectrometry data, that the main gaseous species actually formed during heat treatments of ex-PCS fibers under nitrogen up to 1400°C is **silicon monoxide** [25]. These gaseous species could result from the thermal decomposition of the ternary Si (C,O) amorphous matrix and could explain : (i) the formation of free carbon in the bulk at high temperatures, mentioned by several authors and (ii) the coarsening of the SiC grains (the SiC grains being less and less isolated by the Si (C,O) continuum as it is progressively destroyed in the C. Laffon et al. model) [16]. However, many details of the mechanism of the ex-PCS evolution at high temperatures remain unknown as well as the relations between this evolution and that of the mechanical properties.

Within the frame of a program of research on ex-PCS ceramics, we have already studied the organic/ceramic transition that occurs during the pyrolysis of **bulk** PCS and PCSZ precursors including a Yajima's type PCS and various models [26,27]. We have now spun, with a single spinneret lab-scale apparatus, a Yajima's type PCS. The aim of the present contribution is to draw tentatively a correlation between the thermal variations of the chemical and microstructural features of the **ex-PCS ceramic monofilament** on the one hand, and those of its mechanical properties, on the other hand, as a function of the pyrolysis temperature.

2 - EXPERIMENTAL

2.1 - Preparation of the ex-PCS ceramic monofilaments

The PCS precursor used in this study, of japanese origin (*) , was thought to have been prepared according to the Yajima's route, i.e. by thermal treatment in autoclave of polydimethylsilane [5]. In a first approximation, its theoretical formula is $-(HSiCH_3-CH_2)-_n$. The as-recieved product was slightly modified (Mn adjusted to 1500) in order to allow its spinning in the molten state.

The PCS precursor was spun, at a temperature of about 300°C, as a continuous monofilament, 10-15 μm in diameter, with a one single spinneret lab-scale apparatus, under an atmosphere of dry nitrogen. The green filament

(*) from Shinetsu

was then cut into lengths of about 50 mm and made infusible by oxygen cross-linking at about 160°C. Finally, the pyrolysis treatments of the stabilized samples were performed, under a flow of dry argon, at temperatures ranging from 600 to 1400°C according to a procedure which has been described elsewhere [26].

2.2 - Chemical analyses

Thermogravimetric analysis (TGA) was performed (*) under an atmosphere of dry argon, according to a heating temperature/time curve similar to that used for the preparation of the monofilaments.

The element analysis (for silicon, carbon and oxygen) was performed(**), on monofilament cross sections, by electron probe microanalysis (EPMA) in the wave lentgh dispersion mode (the curved analysers being PET for SiKα and multilayered PCI for both CKα and OKα). The method was validated on cross-sections of NLM 202 Nicalon fibers whose chemical composition has been assessed independently by conventional chemical analysis.

The XPS spectra were recorded(***) with AlKα (1486.6 eV) as excitation source, on filament tows, the irradiated surface of material having a width of about 600μm and a length of 700 μm. The analyses were performed, under a residual pressure less than 5.10^{-8} Pa, on as-spun filaments, after the oxygen cross-linking step as well as after pyrolysis at 600, 700 and 850°C. Since all the materials were insulators, the charge effect was compensated with an electron flood gun, the energy of the electrons (in the 2-10 eV range) being adjusted with respect to the nature of the material. If one excepts the green PCS filament sample whose stability was not high enough, all the samples were cleaned by Ar^+ ion bombardment (10 mA intensity ; 4 kV energy) prior to XPS analysis, as follows : (i) 10 min exposure for all samples and (ii) additional 1;20 and 30 min exposures for the samples heat treated at 850°C. Before applying this cleaning treatment, the sample surface was found to be contaminated with carbon (C1s peak at 184.6 eV ; 1-8 at. %). Finally, the XPS data recorded on the heat-treated PCS samples were calibrated utilizing the C 1s binding energy in SiC (283.3 eV) as a standard.

(*) SETARAM TAG 24
(**) CAMEBAX 75
(***) SSI/301 XPS spectrometer

Auger electron analyses were performed with an AES microanalyser (*) according to the depth profiling mode. The spectra were recorded from the heat treated filament surfaces (spot size of about 1 μm) which were progressively etched with an Ar^+ ion gun. The intensities of selected Auger electron transitions (i.e. LVV for silicon, KLL for carbon, and KLL for oxygen) were recorded as a function of the thickness of material which has been sputtered.

2.3. Nano and micro structural analyses

The nano- and micro-structural features of the heat treated PCS monofilaments were derived from **TEM analyses**(**) . The thin foils were prepared according to the following procedure : (i) the ex-PCS monofilaments were first embedded in an epoxy resin, (ii) after curing and shaping, the block of resin was cut into thin foils (less than 50 nm in thickness) with an ultramicrotom. The thin foils were set on a copper microgrid coated with a thin film of amorphous carbon (less than 10 nm) and introduced in the high resolution microscope.

The apparent diameter of the aperture in the Abbe plan of the objective lens of the microscope was : (i) 2 nm^{-1} in the dark field imaging mode and (ii) 8.2 nm^{-1} in the lattice fringe imaging mode. The selective dark field images were obtained by explorating radially and azimuthally the reciprocal space, according to a technique which has been described elsewhere [28-29]. Two aperture positions were respectively used : in position 1, the aperture is centered at 2.4 nm^{-1} and its diameter admits among others the 002 reflection of carbon (and possibly the most intense halo of amorphous SiO_2) whereas, in position 2, it is centered at 4.2 nm^{-1} and selects among others the 111 reflection of β-SiC.

2.4. Electrical conductivity

The electrical conductivity was measured up to 530°C under an atmosphere of helium. The measurements were performed on 10 monofilament tow sets on alumina plates, the electrical contacts being secured with a silver lake.

(*) Perkin Elmer PH1-590 SAM
(**) Philips EM 400

2.5. Mechanical tests

Both tensile and torsion tests were performed at room temperature, on the ex-PCS monofilaments, in order to derive the elastic Young and shear moduli as well as the ultimate tensile stress.

The **tensile tests** were performed with an apparatus similar to that used by A.R. Bunsell et al. [30]. The applied load was measured with a strain sensor directly connected to the grip whereas the strain was measured with a classical differential strain sensor fastened on the ram. The method was validated on Nicalon NLM 202 monofilaments, the data , i.e. E = 210 GPa and σ^R = 2500 MPa (gauge length 10 mm), being consistent with those generally given for this material.

The torsion tests were performed with an original apparatus which will be described in detail elsewhere [31]. In its principle, the apparatus is a micropendulum utilizing the monofilament as torsion wire. The monofilament is fastened at one end to the axis of a d.c. motor (which is used to load in torsion the monofilament) and, at the other end, to an inertial disk printed with angular sectors alternately white and black. After having been loaded in torsion, the pendulum is allowed to oscillate freely, the oscillations being recorded with an opto-electronic IR sensor acting directly on the black/white inertia disk. The shear modulus was derived from the period of the oscillations assuming that the material is isotropic. The shear modulus of the Nicalon NLM 202 filaments, measured according to this technique was 76 ± 5 GPa, a value which agrees well with that given by the fiber producer (i.e.77 GPa)

Finally, the **monofilament diameters** were measured by LASER interferometry.

3 - RESULTS AND DISCUSSION

3.1 - Chemical change during PCS filament pyrolysis

3.1.1 - As observed from TGA

As shown in fig.1, the TGA curve of a spun PCS-sample, performed after the oxygen cross-linking step, suggests that **two important transitions** occur in

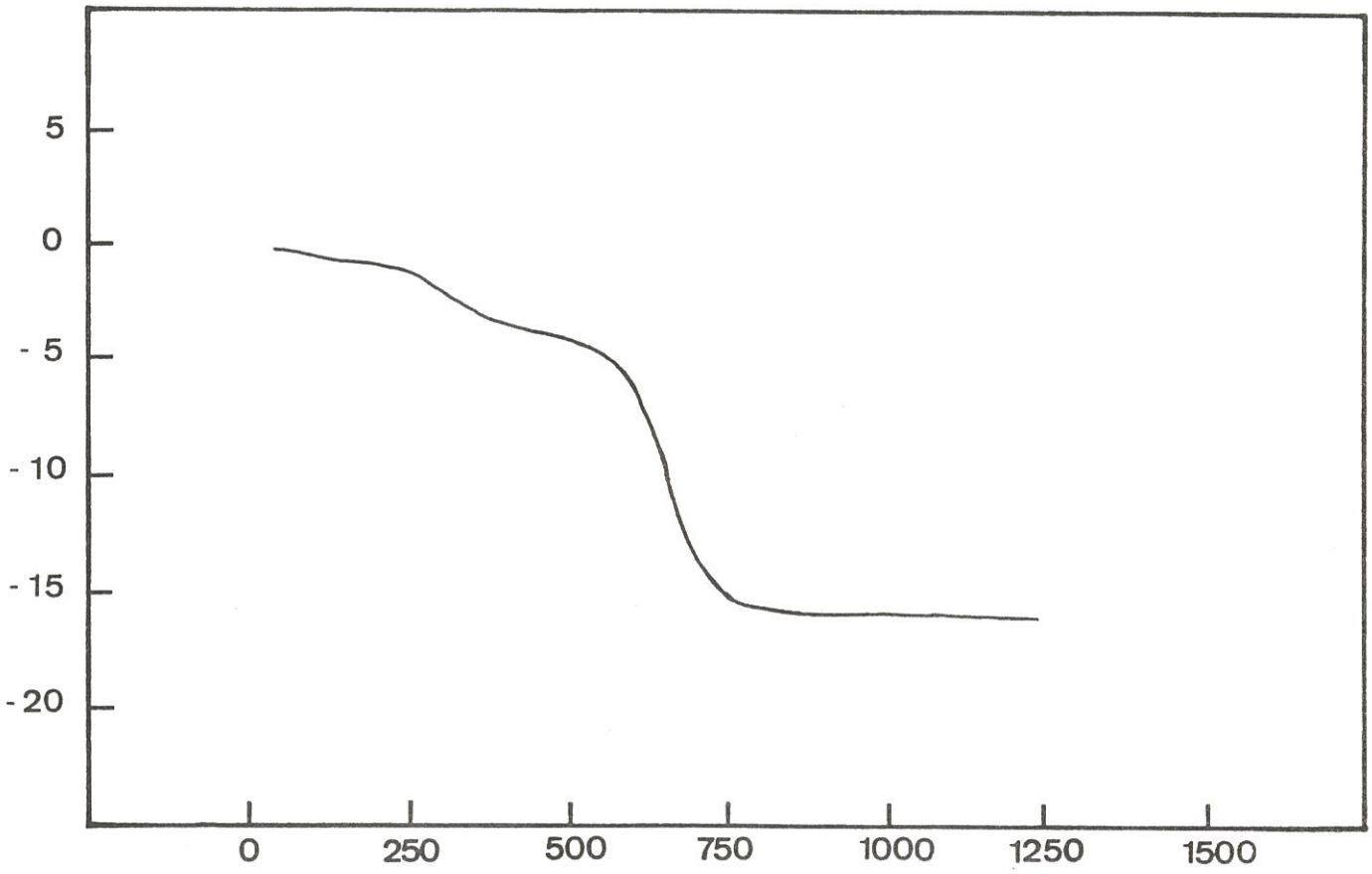

Fig. 1 : Weight loss occuring during the pyrolysis under an inert atmosphere of PCS filaments previously cross-linked by oxygen, as a function of temperature.

the material as temperature is increased respectively, at 500-750°C and above about 1100-1200°C. **The former** results in a weight loss of 10 % and is thought to correspond to the breaking of most organic bonds with formation of gaseous species (i.e. hydrocarbons and possibly silicon-based organometallic species), as previously observed during the bulk pyrolysis of the same PCS [26]. It is worthy of note that some weight loss (of the order of 4 %) already occurs before the organic --> inorganic transition (i.e. at about 250°C) which may be assigned to an evolution of polycarbosilanes of low molecular weights (either present in the material or formed during the very first steps of the pyrolysis). The **latter** transition takes place at higher temperatures, i.e. between 1200 and 1400°C, (average diameter changes from 16 μm to less than 13 μm). It results in a marked decrease in the oxygen content of the fiber (from 20 to 2 %) and to some decrease in its silicon content (which falls from 35 to 30 %), as shown in table I.

The first stages of the pyrolysis of stabilized PCS filaments (at T < 1000°C) exhibit with respect to those reported by E. Bouillon et al. for unstabilized PCS bulk samples of same origin, the following main differences : (i) the weight loss is much limited (i.e. about 16 % instead of 40 %) and (ii) the organic --> inorganic transition starts at a higher temperature (i.e. about 500°C instead of 350°C) [26]. These differences may have two origins. On the one hand, part of the low molecular weight polycarbosilanes which are responsible for the important weight loss occuring in bulk PCS at low temperatures (300-400°C), has been eliminated from the PCS precursor before filament spinning. On the other hand, the Si-O-Si chemical bonds (and probably some C-Si-O bonds) formed during the stabilization of the green PCS filament, are strong bonds which increase the thermal stability of the material.

These conclusions agree with those previously drawn by J.J. Poupeau et al. [32] or Y. Hasegawa and K. Okamura [10] from analyses performed during the pyrolysis of bulk or green fiber samples.

3.1.2 As derived from XPS and EPMA

XPS analyses performed at different stages of PCS-filament pyrolysis show that all materials are made of silicon (Si 2s and 2p peaks), carbon (C 1s peak) and oxygen (O 1s peak), as illustrated in fig. 2 for the pyrolytic residue obtained at 850°C. Hydrogen if present, which is actually the case for Tp < 850°C, is not analysed as already mentioned. The energy values corresponding

Materials	Si (at. %)	C (at. %)	O (at. %)
Nicalon NLM-202	38	49	13
PCS-filaments heated at 850°C	35	44	20
- 1200°C	36	44	19
- 1400°C	30	67	2

Table I : EPMA chemical analyses of PCS filaments after oxygen cross-linking and pyrolysis at increasing temperatures. The atomic percentages given for Tp = 850°C do not take into account hydrogen (thought to be still present in significant amount at this temperature). The data for NICALON NLM-202 (obtained at about 1200°C) are given for purpose of comparison.

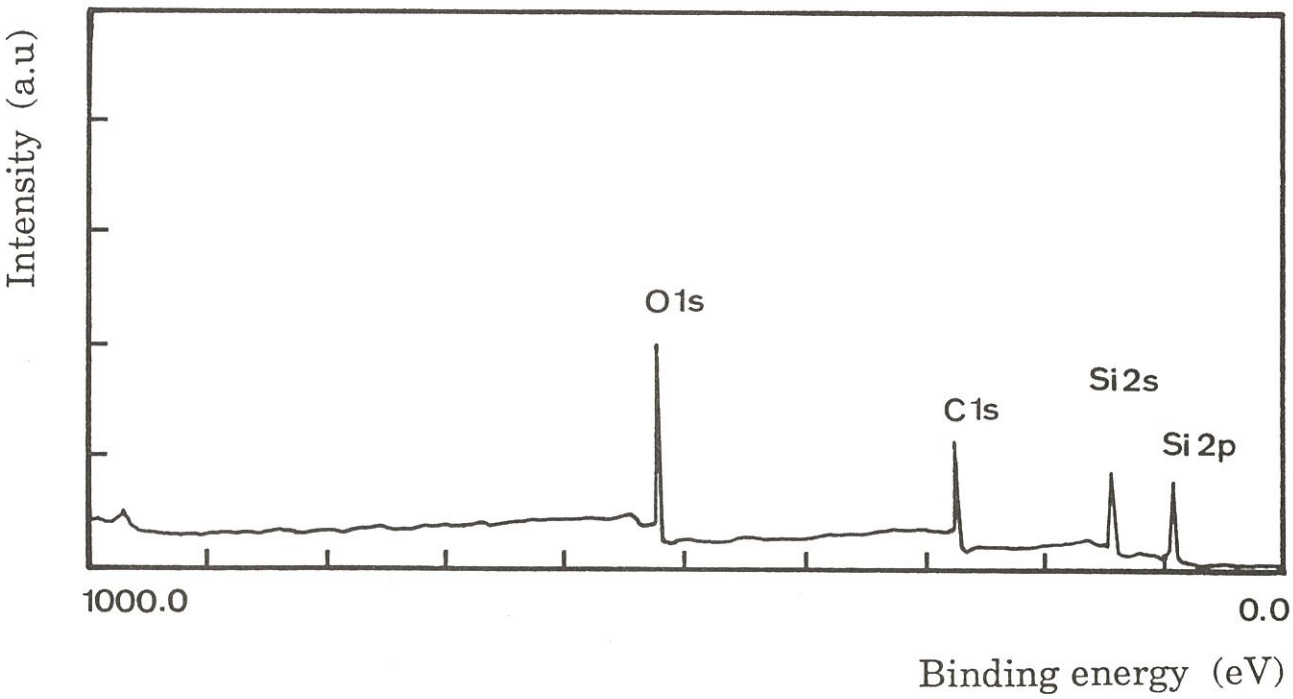

Fig. 2 : XPS spectrum of PCS filaments stabilized by oxydation and heat-treated at 850°C under an inert atmosphere (recorded after 30 min of Ar^+ ion sputtering)

to the various chemical bonds, derived from the XPS peaks (recorded in the high resolution mode) are listed in table II.

The **C 1s peak** consists of two components (fig. 3a). The first (I) at 283.3 eV, assigned to C-$(Si)_x$ bonds,and the second (II) between 284.2 and 284.4 eV,assigned to C-C and perhaps to C-$(Si)_y$ bonds ($y<x$) are present in the spectra of both the polymeric and ceramic materials Finally, a third component (III) beyond 285 eV is also observed after the cross-linking step, its intensity decreasing as Tp is raised (fig. 3b). This latter component, already mentioned by L. Porte and A. Sartre in their study on Nicalon fibers disapears after sputtering and so could be assigned to superficial carbon atoms in an electronegative environment (e.g. that of oxygen) [33].

The **Si 2p peak** consists of two or three components (fig. 4). The first (I) at about 101 eV is assigned to Si-C bonds whereas the second (II) at about 103.2 eV (fig. 4a), only observed in the spectra recorded near the surface of filaments treated at 850°C, has been assigned to Si-O bonds similar to those present in silica [34]. Finally a third component (III) at 102.3 eV for the polymeric materials and which is shifted to 101.9 eV as pyrolysis proceeds towards the ceramic state, is also observed between those corresponding to Si-C and Si-O bonds. It is assigned to a ternary Si (C,O) species. A similar component (at 101.5 eV) has been also recently reported for Nicalon fibers [33].

A shift of the Si 2p binding energy towards the low energies is observed after sputtering. This fact, already observed by Mizokawa et al. [35] could be due to a preferential sputtering of the carbon of SiC and thus to the formation of a Si-rich surface with possibly Si-Si bonds.

Our XPS data recorded from PCS filaments, cross-linked by oxygen and heat-treated under an inert atmosphere at 850°C, confirm the complex chemical nature of different ex-organosilicon precursor fibers, which has been already mentioned by several authors [14,16,33]. In order to ascertain the assignements of the XPS peak components to chemical bonds, our data are compared in table III with data available from literature for Si-based materials. The binding energies derived from components I of C 1s and Si 2p peaks are very close to those reported for **CVD β SiC** [35]. The binding energy derived from component II of C 1s peak can be assigned to C-C bonds and C-Si bonds . The binding energy corresponding to component II of Si 2p peak assigned to Si-O bonds is similar to that mentioned for silica. Finally, component III of Si 2p peak was assigned to a **ternary Si-(C,O) species** as already proposed by L. Porte and A. Sartre in their XPS study of Nicalon fibers

Filament treatment	Ar^+ ion etching	C 1s peak			Si 2p peak		
		C -Si (I)	C - Si(II)	C - O (III)	Si- C (I)	Si (C,O) (III)	Si - O (II)
before cross-linking	none	283.3	284.4	-	101.0	-	-
after cross-linking	none	283.3	284.3	285.3	100.9	102.0	-
"	10 min	283.3	284.5	-	100.7	101.9	-
at 600°C	none	283.3	284.5	285.5	101.1	102.3	-
"	10 min	283.3	284.3	285.2	100.9	102,3	-
at 700°C	none	283.3	284.4	285.4	101.3	102.5	-
"	10 min	283.3	284.3	285.3	101.0	102.3	-
at 800°C	1 min	283.3	284.2	285.2	101.1	102.1	103.2
"	10 min	283.3	284.2	-	100.8	101.9	-
"	30 min	283.3	284.2	-	100.8	101.9	-

Table II : Binding energies (in eV) derived, from the XPS peaks in untreated, cross-linked and heat-treated PCS.

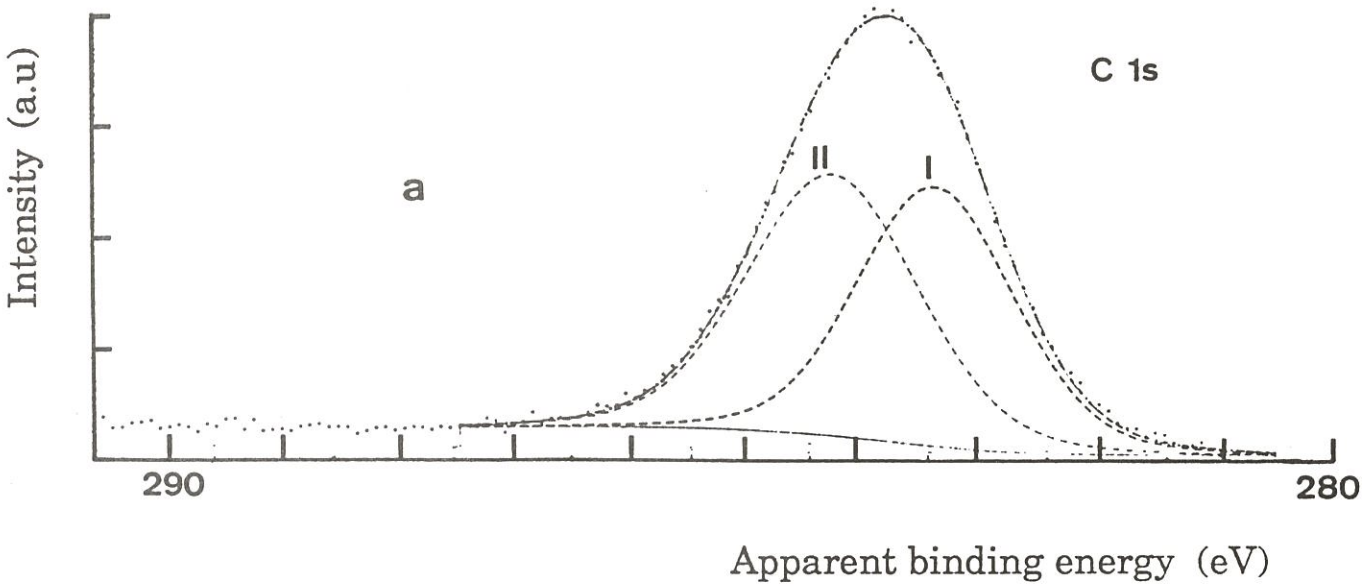

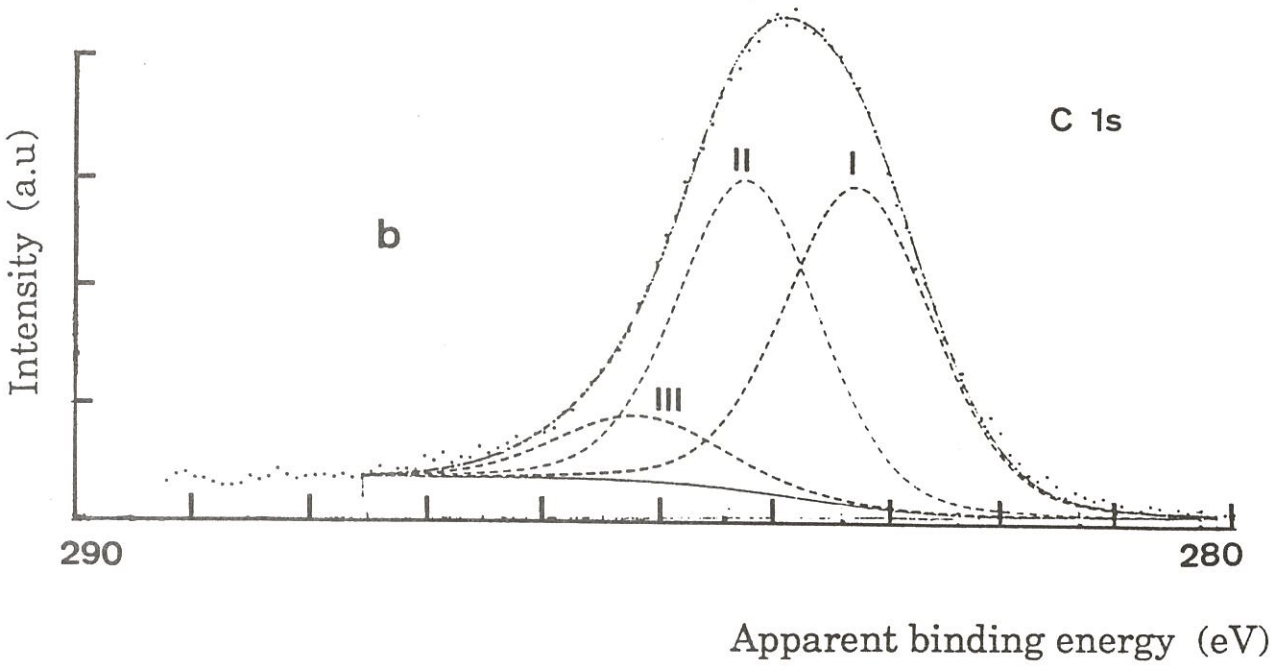

Fig. 3 : Deconvolution of the C 1s peaks of the XPS high resolution spectra of PCS filaments stabilized with oxygen and heat-treated under an inert atmosphere at : (a) 850°C (Ar^+ etching : 30 min) and (b) 600°C (Ar^+ etching : 10 min).

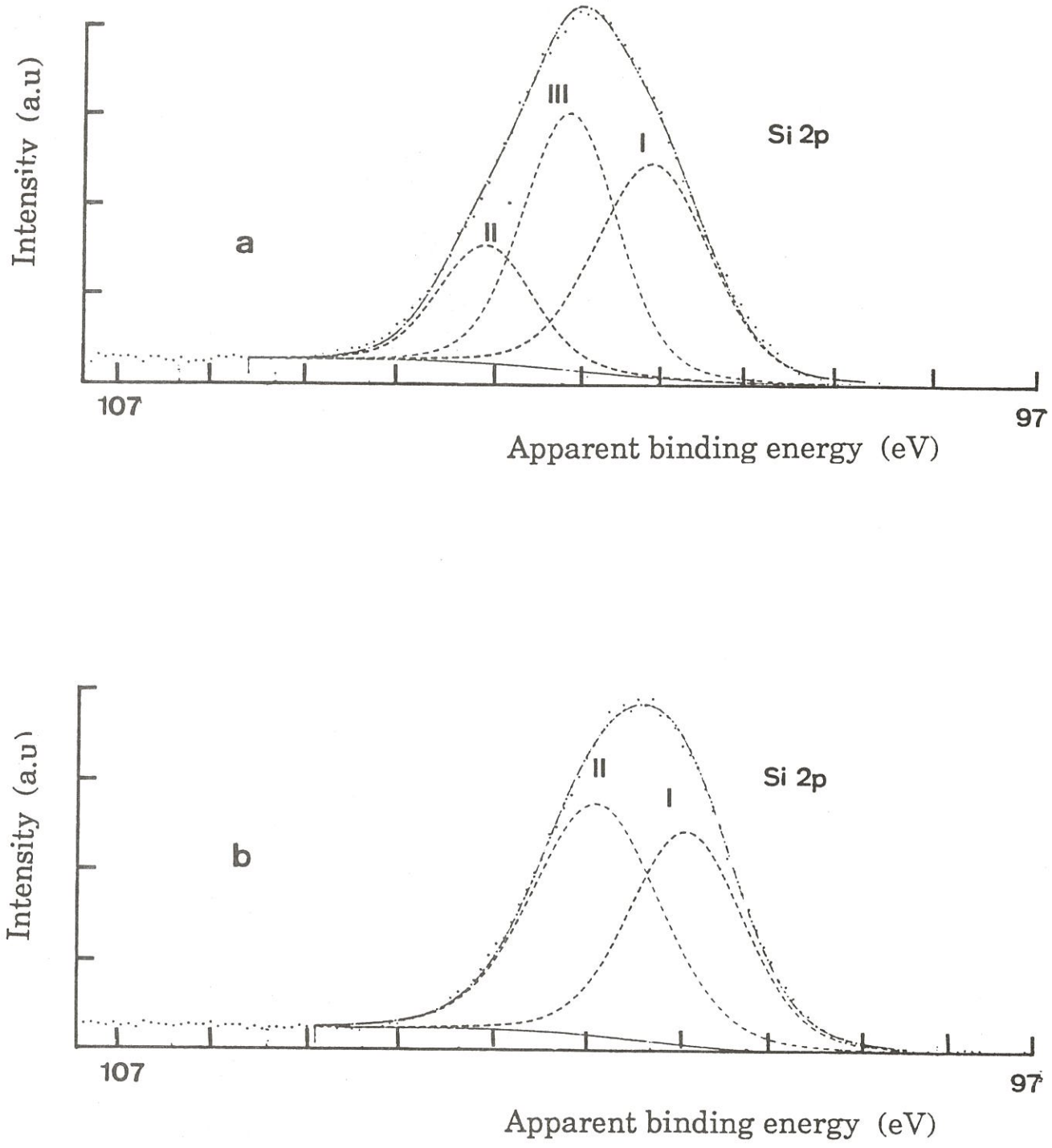

Fig. 4 : Deconvolution of the Si 2p peaks of the XPS high resolution spectra of PCS filaments stabilized with oxygen and heat-treated under an inert atmosphere at 850°C. The spectra were recorded after Ar+ etching for 1 min (a) and 30 min (b).

Materials	Si 2p peak			C 1s peak			References
	Si - C (I)	Si - (C,O) (III)	Si - O (II)	C - Si (I)	C - Si (II)	C - O (III)	
$Si_{1-x}C_x$: H films (glow discharge)	100.0			283.0	284.1		[37]
CVD SiC	101.2		103.4	283.2			[35]
CVD SiC and graphite	100.5			282.7	284.3		[36]
SiO_2 - layer on silicon	101.1	102.2	103.2	283.3	284.3	284.9	[34]
Oxidized polycristalline SiC	100.5		103.1				[35]
Oxidized SiC	100.2		103.1	282.3		284.8	[38]
Nicalon fibers surface	100.5	101.5	103.2	283.3	284.9		[33]
Bulk	100.5	101.5	103.1	283.3	284.6	285.6	
ex - PCS filament surface	101.1	102.2	103.2	283.3	284.3	284.9	Present work
Bulk	100.8	101.9		283.3	284.2		

Table III : Binding energies (in eV) corresponding to different atomic bonding in various materials containing silicon.

[33]. Such a ternary Si-(C,O) species,sometimes referred to as Si-X, was also mentioned earlier by L.C. Sawyer et al. [15] or J. Lipowitz et al. [14]. Since this component Si 2p (III) is already present in the XPS spectrum of the cross-linked PCS (table II), one could assume that the formation of the Si (C,O) bonding occurs during the stabilization of the green PCS filament by oxygen. On the other hand, the thin silica layer (thickness less than 5 nm) present at the filament surface for Tp = 850°C and which is responsible for component II of Si 2p peak (fig. 4a) is probably due to an oxidation by trace amounts of residual oxygen in the pyrolysis furnace atmosphere, during and after the organic --> ceramic transition.

A quantitative analysis of the chemical bonds in the materials at different steps of the filament processing is given in table IV. It appears that the initial PCS precursor : (i) is almost free of oxygen and (ii) shows at least two different carbons corresponding to two bonds. However, part of these C-C bonds could also be due to contamination by carbon (since no surface etching has been done prior to XPS analysis as already mentioned). The data also show that a large amount of oxygen is introduced in the PCS during the stabilization step and not removed during the organic-ceramic transition at 500-750°C. Since an important weight loss occurs during this transition, the pyrolytic residue at 850°C still contain a higher percentage of oxygen. Finally, during the transition, the percentage of silicon remains almost constant whereas that of carbon regularly decreases. This result suggests that the gaseous species which are formed during the organic-ceramic transition are mainly carbon-based organic molecules and not silicon-based organometallic molecules, in agreement with the results of gas analyses reported by several authors [7,8].

The results of the XPS quantitative analysis performed on the filaments heat-treated at 850°C are compared in table V with those obtained by EPMA on cross-sections of the same filaments. The agreement is good for silicon but rather poor for both carbon and oxygen. This discrepancy, which has been already observed by E. Bouillon et al. in their study of the pyrolysis of bulk PCS [26], could be due to a preferential sputtering of carbon and to a reoxidation during the data acquisition at about 5.10^{-8} Pa background pressure as it has been already reported by Mizokawa [35]. Finally, on the basis of EPMA bulk analysis, it appears that the chemical composition of our ex-PCS monofilaments is close to that reported by S. Yajima et al. for their first generation ex-PCS fibers [40].

Materials	Ar^+ etching time (min)	C 1s peak			Si 2p peak			O 1s peak
		C - Si(I)	C - Si(II)	C - O	Si - C	Si - (C,O)	Si - O	
(*) before cross linking	none	28	(65) 37	-	33	(33) -	-	3
after cross linking	10	25	(50) 25	-	21	(32) 11	-	18
treated at 600°C	10	22	(47) 20	5	25	(33) 8	-	18
treated at 700°C	10	18	(39) 16	5	18	(34) 16	-	27
treated at 850°C	1	12	(35) 16	7	13	(32) 13	6	33
	10	18	(37) 19	-	17	(36) 19	-	27
	30	18	(38) 20	-	16	(36) 20	-	26

(*) the analysis does not take into account hydrogen

In each case ,data given in ( ) correspond to the overall elemental percentages

Table IV : Quantitative XPS analysis of the chemical bonds (in at . %) at different steps of the organic-ceramic transition of a PCS precursor.

Materials		Si (at. %)	C (at. %)	O (at. %)
PCS monofilaments heat treated at 850°C	XPS (1)	36	38	26
	EPMA (1)	35	44	20
ex - PCS fibers obtained at ~1250°C (39)		37	40	23

(1) : hydrogen probably present in small amount, not analysed

Table V : Chemical analyses of ex-PCS fibrous materials.

The variations of the chemical composition of the filaments, calculated from XPS data for Tp < 850°C and EPMA data for Tp > 850°C, are shown in fig. 5 as a function of the temperature of pyrolysis. Two temperatures domains correspond to an important change in the chemical composition of the filaments : (i) 500 < Tp < 750°C and (ii) Tp > 1200°C. The former is related to the **organic-ceramic transition** and the latter is thought to be associated with the thermal decomposition of the Si (C,O) amorphous phase with an evolution of gaseous species. The strong increase in the C/Si ratio, observed for Tp > 1200°C, suggests that oxygen might be **preferentially removed as SiO** (rather than as CO), a result which is agreement with the conclusions of the study of S.M. Johnson et al. based on Knudsen cell/mass spectrometer experiments [25].

3.2 - Structural and microstructural change during PCS filament pyrolysis

3.2.1 - As observed from TEM analysis

PCS filaments, cross-linked by oxygen and **heat treated at 1100-1200°C** under an inert atmosphere, appear as **amorphous materials** on the basis of their electron diffraction patterns which consist of very broad rings, as shown in fig. 6 a. This result is corroborated by the fact that : (i) the bright field image shows a very smooth microstructure (fig.7) and (ii) the radial analysis of the reciprocal space yields dark field images which consist of faint dots distributed uniformly and whose mean size, i.e. less than 1 nm, is at the limit of resolution of the microscope (fig. 8a and c). However, one cannot ascertain that free carbon is not already present in the bulk of the fiber for this low Tp values, as **isolated basic structural units,** i.e. as turbostratic stacks of 2 or 3 aromatic layers of about 10 aromatic carbon cycles [41-42]. As a matter of fact, such isolated BSUs would give, in dark field imaging, dots of about 1 nm. On the contrary, **free carbon** is clearly observed, at the fiber surface as a layer whose thickness is of the order of 5 nm (arrows in fig. 8a). In this layer, the carbon BSUs are almost parallel to each others and to the fiber surface since this layer is no longer bright when the aperture is moved in a position located in a perpendicular direction (fig. 8b).

When **heat-treated at 1400°C**, the ex-PCS filaments are **well crystallized** as shown by the electron diffraction pattern which consists of the narrow diffraction rings of **β-SiC** (fig. 6b). The crystalline character of the material is

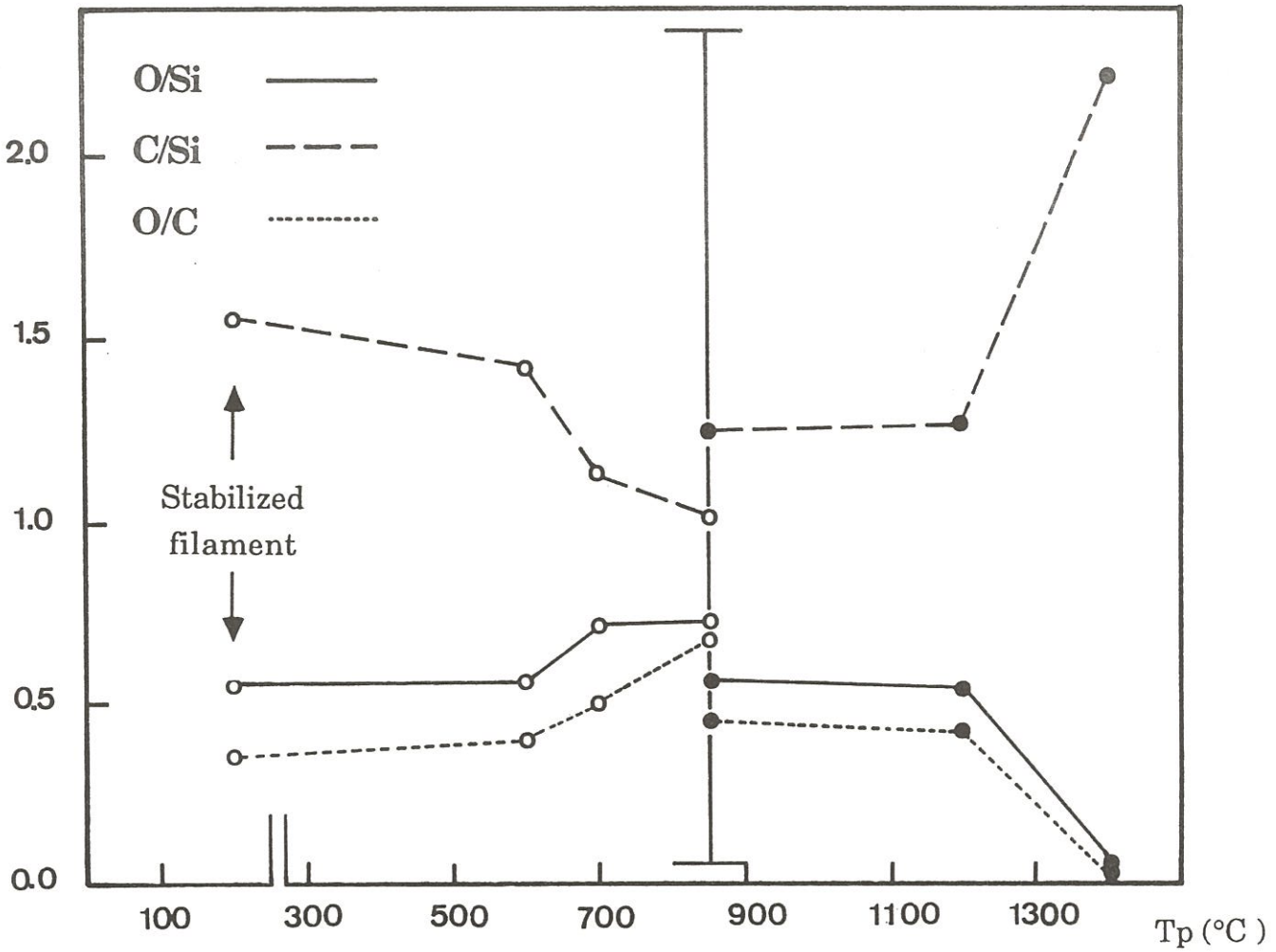

Fig. 5 : Variations of the C/Si ; O/Si and O/C atomic ratios in ex-PCS filaments as a function of the pyrolysis temperature Tp, calculated from the XPS data for Tp < 850°C and EPMA data beyond 850°C.

also evident from the bright field image which shows (i) a polycrystalline microstructure in the bulk, with a mean SiC grain size of about 7 nm (a few crystals having a size as large as 20 nm), and (ii) a layer with a different microtexture near the filament surface (arrow) and whose thickness is about 40 nm (fig. 9). This layer consists only of **carbon** since it is respectively bright or dark when the aperture is moved from position 1 to position 2 (see section 2.3) in dark field imaging (fig. 10 a and c). Amorphous silica, which the specific TEM features are not found, is excluded (texture in BF mode, brightness of dots in DF mode). Moreover, the carbon BSUs do not have any preferential orientation within this layer since the dark field images are statistically identical when the aperture in position 1 is located in two perpendicular directions (fig. 10 a and b). This 40 nm carbon skin is itself coated with a **rim of turbostractic carbon** (5 to 7 nm in thickness) whose aromatic sheets are both parallel to each others and to the filament surface (since it appears bright in fig. 10 a : arrows, and dark in fig. 10 b). The carbon dark field images also show the occurence of faint bright dots in the bulk of the fiber, which correspond **to carbon BSUs**. This carbon, surrounding the SiC microcrystals is more poorly organized than that from the 40 nm thick carbon layer at the filament surface. This latter feature is clearly apparent from the lattice fringe image shown in fig. 11. In this picture, the carbon BSUs in the 40 nm thick carbon skin (small arrows) which are associated to form a porous texture as well as those from the 5-7 nm thick carbon rim (double arrows) are clearly apparent whereas the carbon BSUs surrounding each SiC crystal (thick arrow) are hardly seen. This fact (i.e. the degradation of the internal carbon) was recently demonstrated as systematically coming with the drastic SiC crystal growth in Nicalon fibers at high temperatures [43].

Surprisingly, the degradation of free carbon is not observed in the 1400°C heat-treated bulk (uncured PCS) [26,29].

3.2.2 - As observed from AES analysis

The AES depth composition profiles, shown in fig. 12 for Tp = 1200 and 1400°C, are in their main features in agreement with the conclusions drawn above from the XPS and TEM analyses.

A carbon in excess is observed near the filament surface as a film which is very thin for Tp = 1200°C and much thicker for Tp = 1400°C. Below this carbon layer, the percentages of both silicon and carbon fall to constant values ,

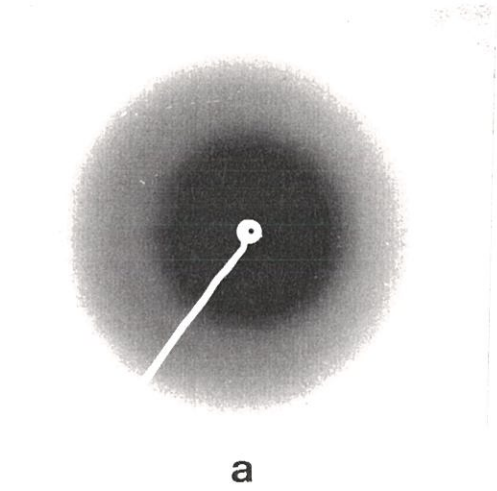

a

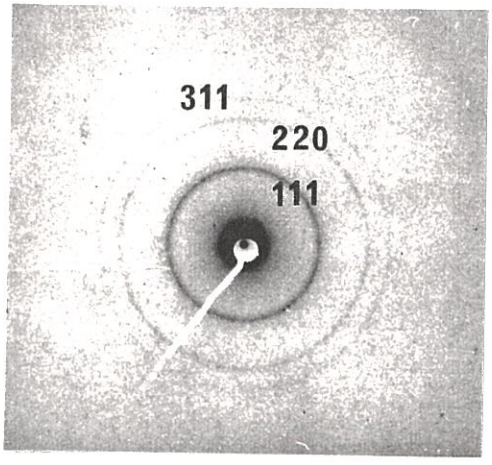

b

Fig. 6 : Electron diffraction patterns of PCS filaments stabilized with oxygen and heat-treated under an inert atmosphere at : (a) 1100-1200°C and (b) 1400°C.

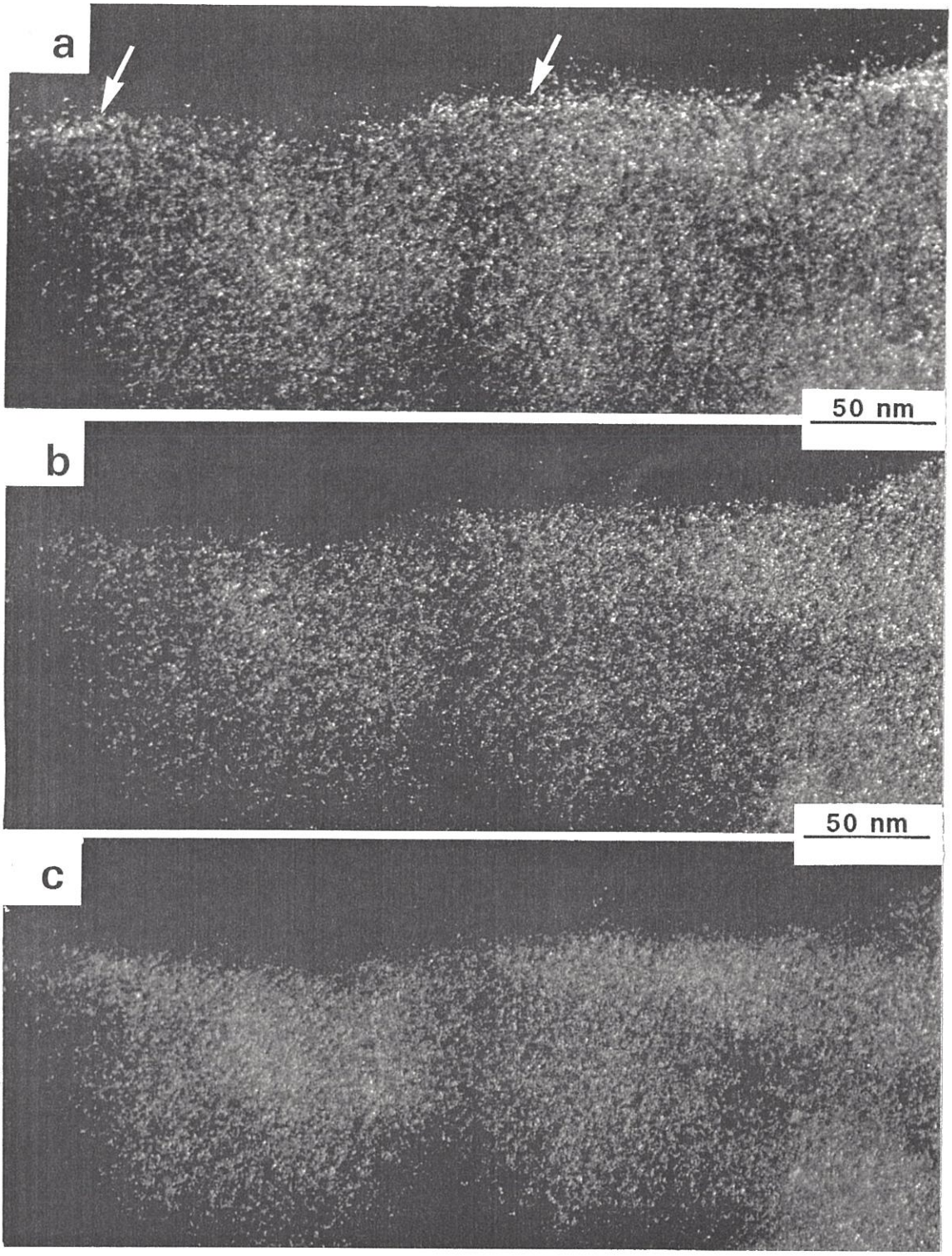

Fig. 8 : TEM analysis of a PCS filament stabilized with oxygen and heat-treated at 1100-1200°C under an inert atmosphere. Dark field images corresponding to different locations of the aperture ; (a,b): two" carbon 002 " orthogonal position ; (c): "SiC 111 " position.

Fig. 7 : TEM analysis of a PCS filament stabilized with oxygen and heat-treated at 1100-1200°C under an inert atmosphere : bright field image.

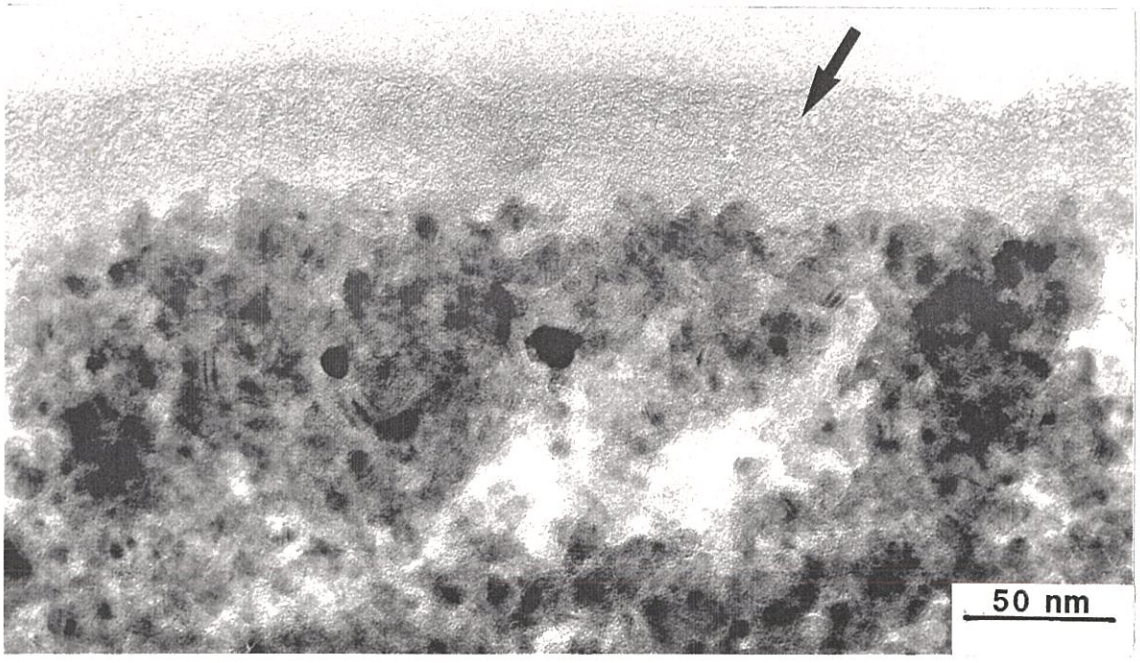

Fig. 9 : TEM analysis of a PCS filament stabilized with oxygen and heat-treated at 1400°C under an inert atmosphere : bright field image.

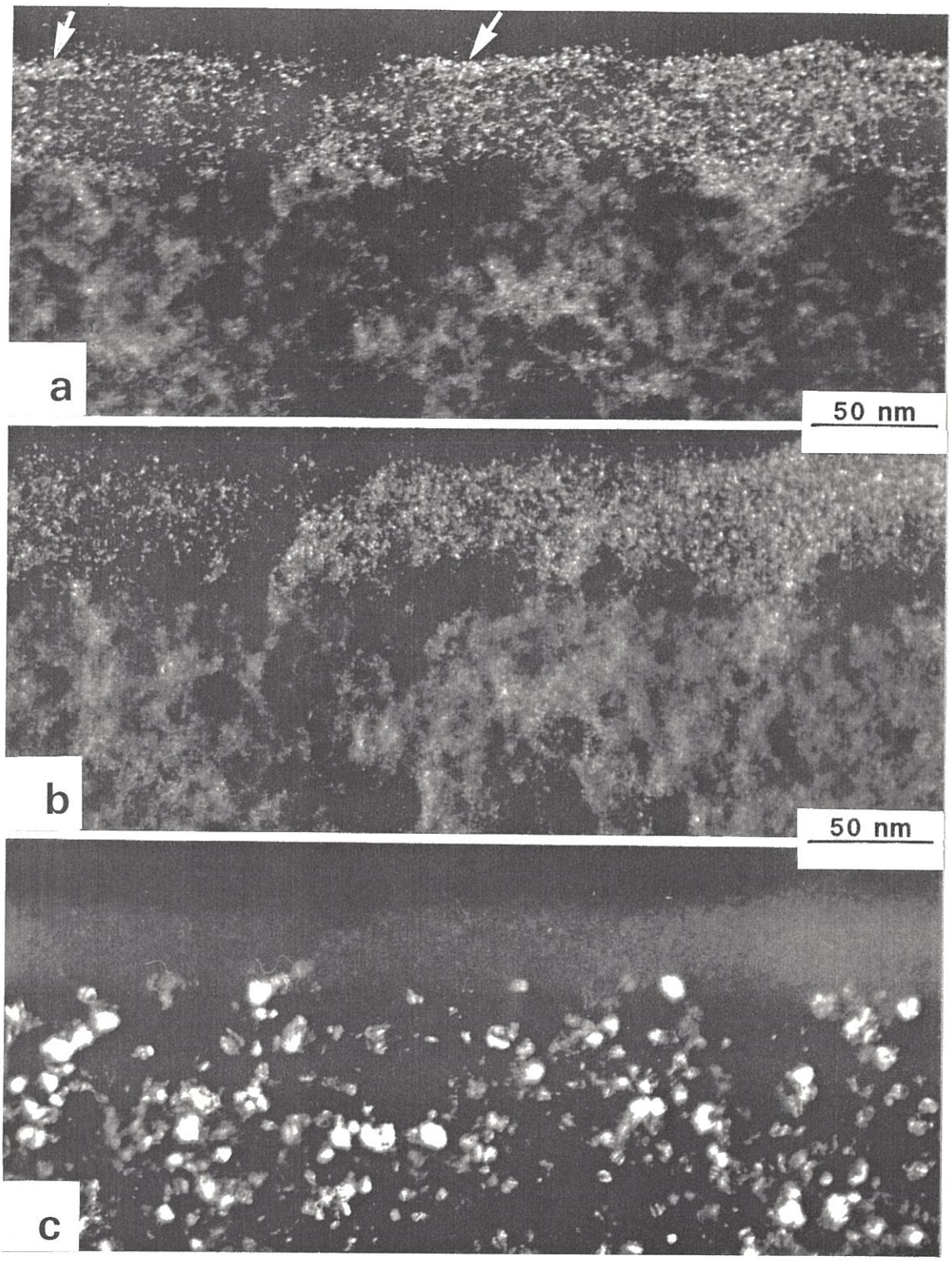

Fig. 10 : TEM analysis of a PCS filament stabilized with oxygen and heat-treated an inert atmosphere. Dark field image corresponding to different locations of the aperture (a,b) : position 1 and 1 perpendicular (carbon 002) and (c) position 2 (β-SiC 111).

Fig. 11 : TEM analysis of a PCS filament stabilized with oxygen and heat-treated at 1400°C under an inert atmosphere : lattice fringe image.

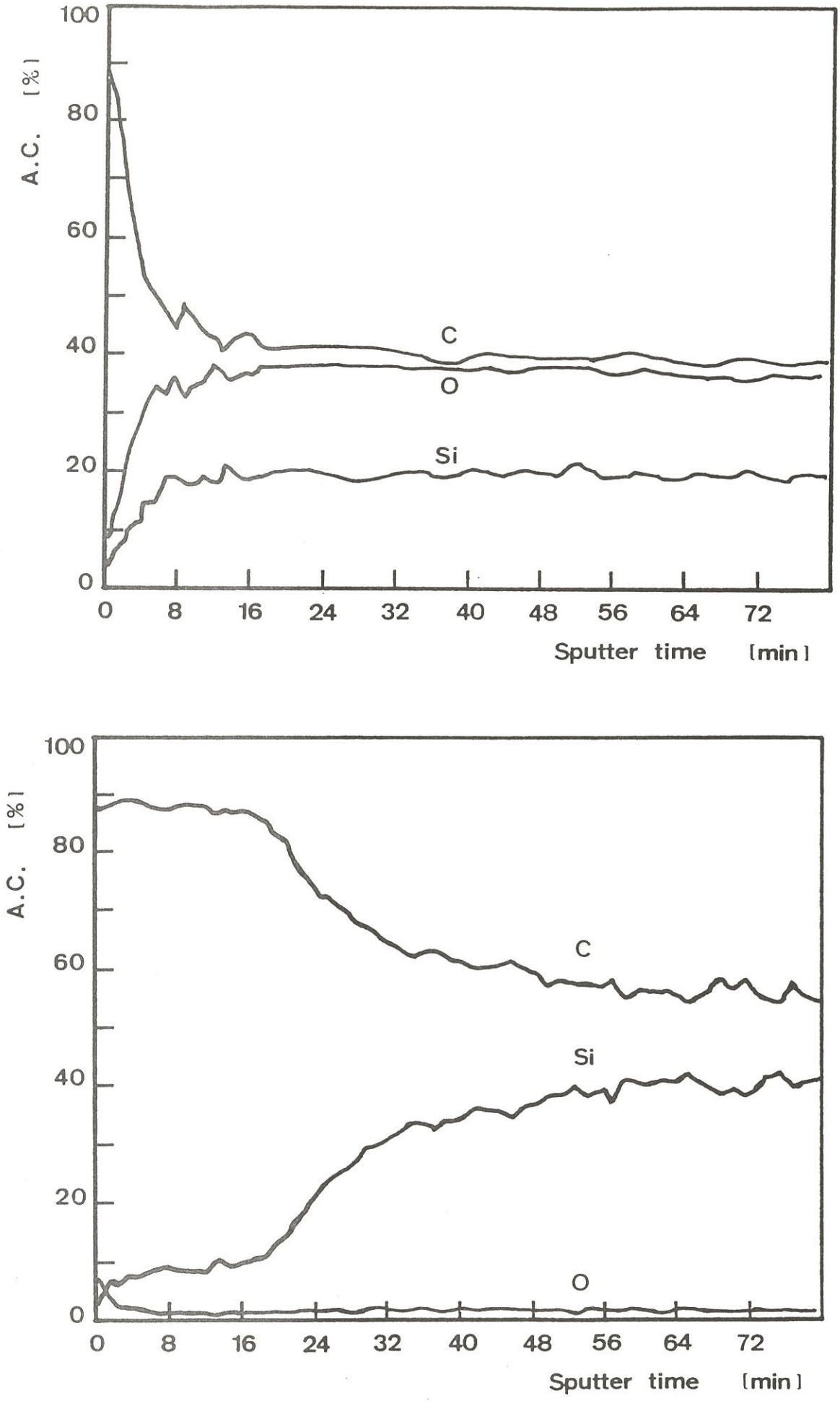

Fig. 12 : AES analysis (depth profiling mode) of PCS filaments stabilized with oxygen and heat-treated at increasing temperatures under an inert atmosphere at : (a) 1200°C and (b) 1400°C.

very rapidly for Tp = 1200°C and much slowly for Tp = 1400°C, a feature which suggest that the accumulation of carbon near the filament surface might result from a diffusion rate-controlled mechanism.

It is worthy of note that the **oxygen concentration** is almost nil in the filament heat-treated at 1400°C (as already established from the XPS and EPMA data) whereas it is very large in that heat-treated at 1200°C, a feature which confirms that the important structural/microstructural change which occurs in the 1200-1400°C temperature range is related to a chemical mechanism involving an evolution of oxygen-containing gaseous species (e.g. the thermal decomposition of the ternary Si (C,O) species).

3.3. Electrical conductivity change during PCS filament pyrolysis

The results of the electrical conductivity measurements, performed on PCS filaments, first cross-linked by oxygen addition and then heat-treated at increasing Tp (with Tp = 850, 1100, 1200 and 1400°C), are shown in fig. 13. Generally speaking, the electrical conductivity measured at a given temperature Tm increases first slowly for 850 < Tp < 1200°C and then dramatically above 1200°C i.e. by almost **four orders of magnitude** when Tp is raised from 1200 to 1400°C.

For Tp < 1200°C, the electrical behavior of the heat-treated PCS filaments is very similar to that previously reported for the solid residues resulting from the pyrolysis (up to about 1000°C) of the same PCS performed without the cross-linking step on bulk samples [26]. The main features of the $Ln\sigma = f(T^{-1})$ suggest two conduction mechanisms which are successively predominent as temperature is raised. At **low temperatures** (for Tm < 320°C), the thermal variations of the electrical conductivity are very limited and could be related to a saturation phenomenon in which the electrical conductivity is due to carriers whose number is almost independent of temperature. Such a conductivity could be associated with the C-C bonds from aromatic cycles still containing some hydrogen atoms. **At high temperatures** (Tm > 320°C), the electrical conductivity is thermally activated with an activation energy of the order of 0.4 eV, a value which falls between those characterizing SiC single crystals (ΔE = 0.3 eV) and polycristalline SiC (ΔE = 0.6 eV). However, it should be mentioned that no crystalline SiC has been observed for Tp < 1200°C on the basis of TEM analyses. Therefore, the high temperature part of the $Ln\sigma = f(T^{-1})$ curve might

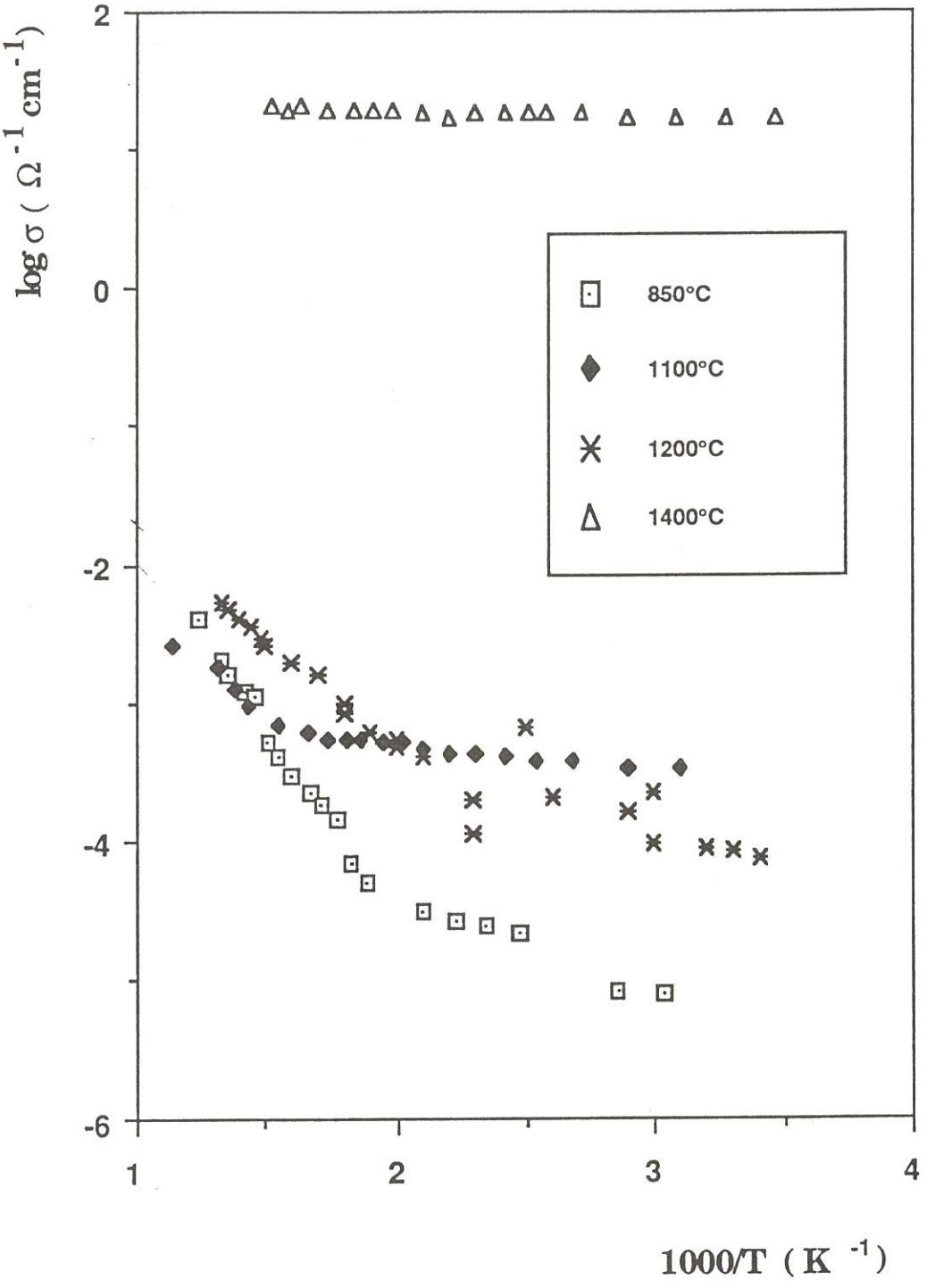

Fig. 13 : Thermal variations of the electrical conductivity of PCS filaments, stabilized with oxygen and heat-treated at increasing temperatures under an inert atmosphere, as a function of reciprocal temperature.

be better related to an amorphous material with a **semi-conducting behavior** close to that of SiC.

For Tp > 1200°C, e.g. for Tp = 1400°C, the electrical behavior exhibits a **quasi-metallic character**, i.e. it is high and almost temperature independent. The dramatic change observed in the electrical behavior when Tp is raised above 1200°C is obviously a consequence of the chemical and microstructural change that occurs in the PCS filaments in this temperature domain. Namely and as already proposed by E. Bouillon et al. [26] and Monthioux et al. [29] the increase in conductivity which is observed for Tp > 1200°C could be related to : (i) the decomposition of the Si (C,O) amorphous matrix and (ii) the formation of uncomplete shells of carbon surrounding the SiC grains and which might give rise to a **percolation effect** [26].

3.4 - Mechanical property change during PCS filament pyrolysis

The results of the **tensile** and **torsion** tests, performed at room temperature on PCS monofilaments cross-linked by oxygen and then heat-treated under an inert atmosphere, are shown in fig. 14 and 15 as a function of the highest temperature Tp at which the material was exposed during the heat treatment. The related stiffness and failure strength data are listed in table VI. The failure strength data were treated statistically on the basis of a two parameter Weibull distribution. The values of the Weibull modulus m are given in table VI.

Generally speaking, the stiffness moduli (i.e. E and G) as well as the ultimate tensile failure stress σ^R first increase with increasing Tp, then undergo maxima for Tp = 1200°C and finally decrease as Tp is still increased up to 1400°C. These experimental results are in agreement with those (for E and σ^R) reported by Y. Hasegawa et al. for ex-PCS fibers [39]. Futhermore, the values of the stiffness moduli measured in the present work for Tp = 1200°C, i.e. E = 190 GPa and G = 71 GPa are close to those given by the producer (*) i.e. E = 210 GPa and G = 77 GPa for the ceramic grade (NLM 202) Nicalon fiber thought to be produced from the same kind of PCS precursor and at a similar Tp.

(*) Nippon Carbon

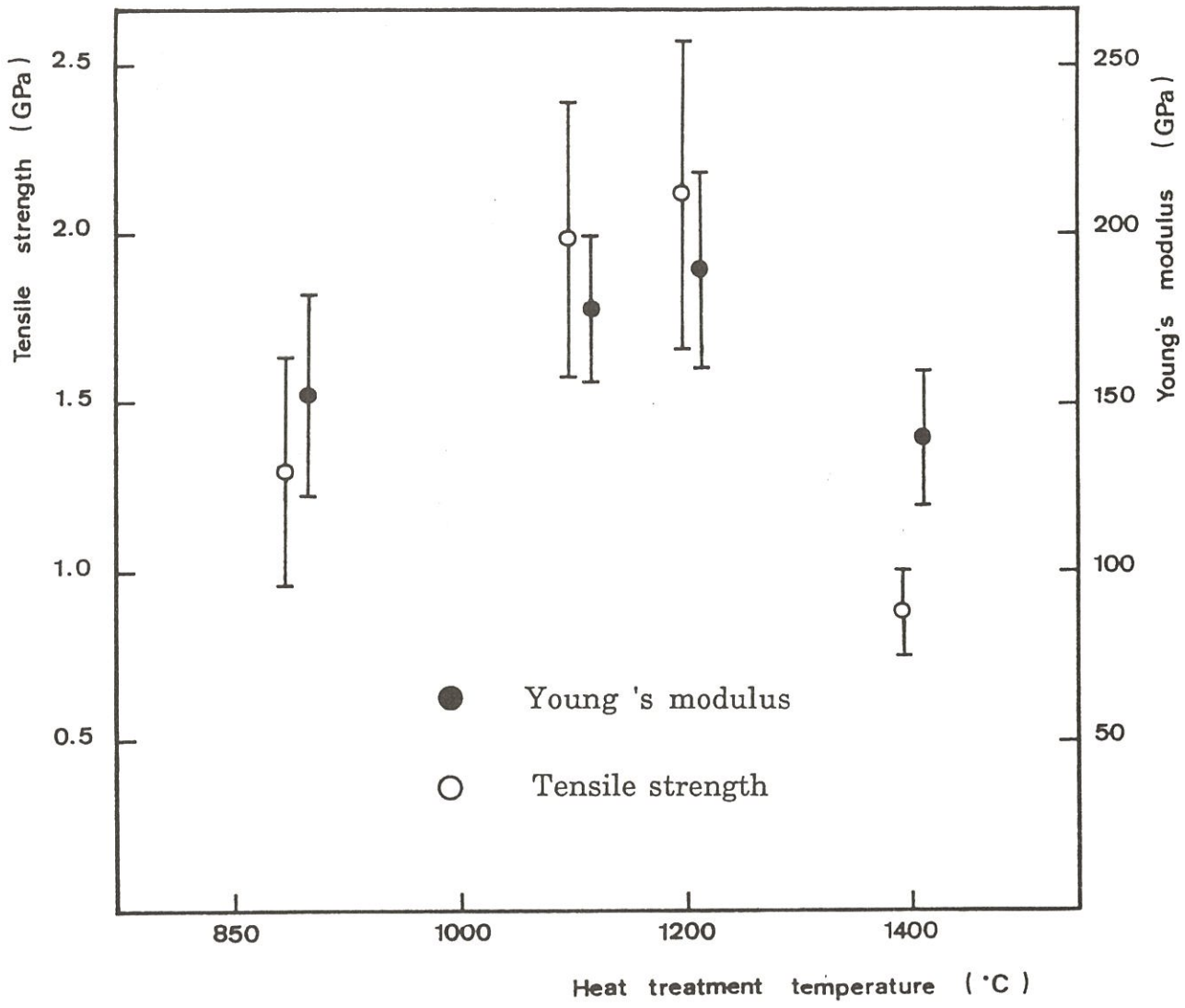

Fig. 14 : Thermal variations of the tensile ultimate stress and Young modulus measured at room temperature, of ex-PCS monofilaments as a function of the pyrolysis temperature Tp. An average of 40 samples (gange length : 10 nm) were tested for each Tp value.

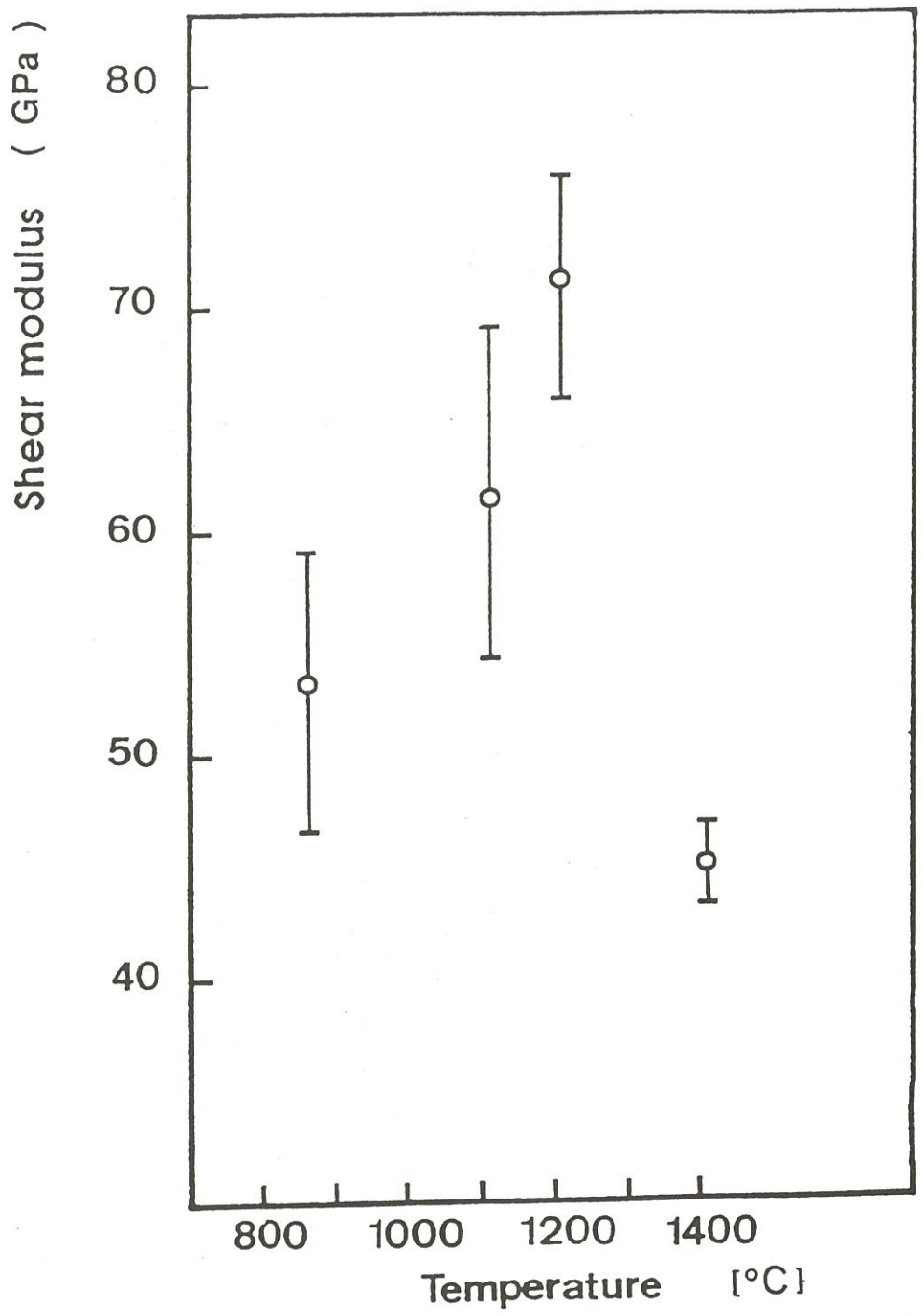

Fig. 15 : Variations of the shear modulus, measured at room temperature in torsion, of ex-PCS monofilaments as a function of the pyrolysis temperature. An average of 10 samples were listed for each Tp value;

Temperature of pyrolysis Tp (°C)	Ultimate tensile failure stress			Young modulus		Shear modulus	
	σ^R (MPa)	σ^R (%)	m	E (GPa)	$E_{rd.}$(%)	G (GPa)	$G_{rd.}$(%)
850	1300	61	4	155	82	54	75
1100	1990	94	5	180	95	61	86
1200	2120	100	5	190	100	71	100
1400	880	42	6	140	74	45	63

Table VI : Stiffness moduli and UTS of ex-PCS monofilaments, measured at room temperature, for increasing pyrolysis temperatures ($\sigma^R_{rel.}$; $E_{rel.}$ and $G_{rel.}$ are normalized values calculated taking the data obtained at 1200°C as references)

Two examples of failure surface SEM micrographs are shown in fig. 16. That corresponding to Tp = 1200°C is typical of an amorphous brittle material whereas that obtained for the filament heat-treated at 1400°C clearly shows a polycrystalline character. This difference is another evidence of the important structural/microstructural change that occurs in ex-PCS monofilaments between 1200 and 1400°C, as discussed in the above sections.

The increase in σ^R , E and G observed when Tp is raised from 850 to 1200°C, could be related to a progressive ceramization of the material which remains **however amorphous** (evolution of residual organic light species, e.g. CH_4, as well as hydrogen, with an increase in density). As a result, for Tp = 1200°C, the UTS is high and the failure surface typical of a brittle non-crystalline material. The decrease in both stiffness and failure strength which is observed for Tp > 1200°C is related to the structural/microstructural change which has been already mentioned. The dramatic UTS decrease which occurs when Tp is raised from 1200 to 1400°C results directly from the **crystallization** of the amorphous matrix still present at 1200°C followed by grain coarsening (both phenomena increasing the size of the defects which may initiate the failure of the filaments). The low values of the stiffness moduli, with respect to pure polycrystalline SiC, are probably due to the fact that the SiC grains are surrounded by uncomplete cages of poorly ordered carbon with a low rigidity.

4 - MODELLING AND CONCLUSION

During the pyrolysis of a stabilized PCS filament, performed under an inert atmosphere, two important changes occur in the material : (i) **an organic --> inorganic transition** at 500-750°C yielding an amorphous material which remains stable up to about 1100-1200°C and (ii) above this limit, a **thermal decomposition** of this amorphous material resulting in the formation of a mixture of β-SiC and carbon with an evolution of gaseous species containing oxygen. These chemical, structural and microstructural changes strongly modify the physical and mechanical properties of the filament.

The organic-inorganic transition takes place within a material made of complex polymeric structural units (PSU) cross-linked through strong Si-O-Si bonds (resulting from the oxidation of the Si-H bonds present in PCS, during the stabilization step). During this transition, most organic lateral bonds are broken with an evolution of gaseous species (e.g. hydrocarbons, silanes, hydrogen, etc...) and a significant weight loss (about 10 %). It yields a material

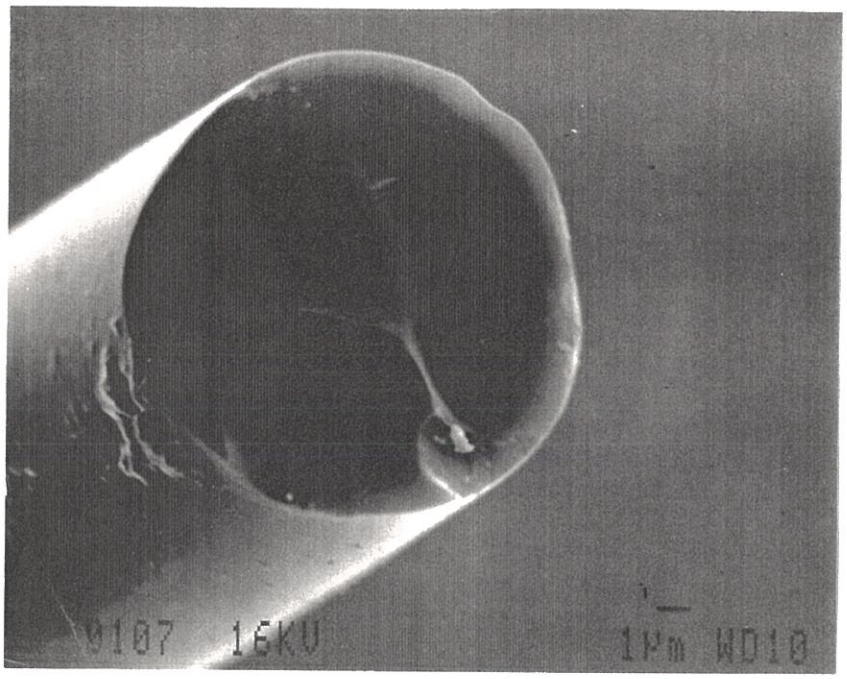

a

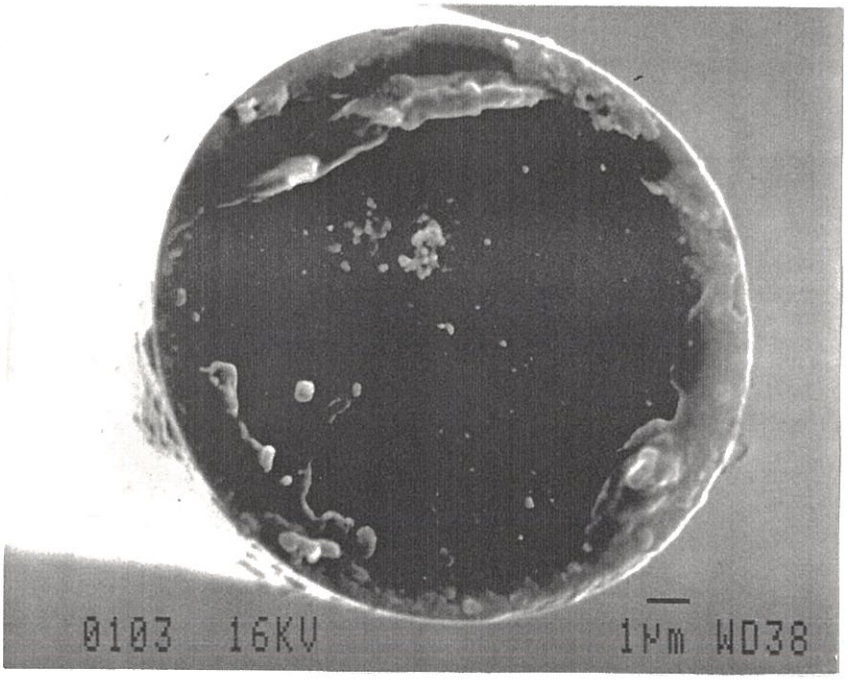

b

Fig. 16 : Failure surface of ex-PCS monofilaments, loaded in tension and tested at room temperature, as a function of the pyrolysis temperature : (a) Tp = 1200°C, (b) Tp = 1400°C.

which is **amorphous**, mainly made of silicon-based tetrahedra SiC_4 or/and $SiC_{4-x}O_x$ and containing already C-C bonds. At this stage, it is thought that the Si-C-O skeleton of the PSUs is maintained, at least in its main features.

When the amorphous filament is further heated, i.e. up to about **1100-1200°C**, the majority of the residual organic bonds are broken with a slight additional gas evolution (e.g. of H_2 and CH_4), the material remaining **amorphous**. At this stage, the overal chemical formula ($Si_4C_{4.88}O_{2.12}$, where oxygen is probably slightly over-estimated) is close to $Si_4C_5O_2$ (plus trace amounts of hydrogen) and the material can be described as a continuum of SiC_4 and $SiC_{4-x}O_x$ species which might contain, at **nanometer scale**, free carbon as isolated small BSUs. As a result of this very homogeneous microstructure, such filaments exhibit a high mechanical strength and semi-conducting properties.

At still higher temperatures, i.e. for 1200 < Tp < 1400°C, a thermal decomposition of the amorphous continuum state occurs with a new gas evolution, a significant cross-section shrinkage (i.e. about 40 %) and the formation of a mixture of carbon and SiC (mainly as the β-modification). On the basis of chemical analysis data, it is thought that the main gaseous species formed during this thermal decomposition is SiO and in less proportion CO, in agreement with the conclusion previously drawn by S.M. Johnson et al. for Nicalon fibers [25]. Therefore, the thermal decomposition could correspond to the following overall equation :

$$Si_4C_{4.88}O_{2.12} \text{ ----------> } Si_{2.15}C_{4.80}O_{0.18} + 1.85\,SiO + 0.08\,CO \quad (1)$$

with a pyrolytic residue of overall formula close to Si_2C_5. The composition of the filaments at 1400°C actually observed, i.e. $Si_2C_{4.4}O_{0.14}$ is close to that expected from equation (1) and the filaments consist indeed of a mixture of **SiC + C** almost free of oxygen. Furthermore, equation (1) should yield a weight loss of 43 % which is in rather fair agreement with the important shrinkage of the fiber diameter (from about 16 μm to about 13 μm corresponding to a weight loss of 34 %).

From equation (1), one could expect (i) an important weight loss as already mentioned, (ii) the formation of free carbon and (iii) a large and rapid growth of silicon carbide crystals (since the nanodomains of SiC which are thought to be isolated from each other by BSUs of carbon and the oxygen rich phase, according to the model of C. Laffon et al. [16] can now grow freely). It is

what has been actually observed. At last, the partial degradation of carbon BSUs surrounding SiC crystals can be explain on the basis of the oxidation of carbon by SiO species according to the following equation :

$$SiO + 2C \text{ -------> } SiC + CO \quad (2)$$

The drop in the filament failure strength occuring at 1200-1400°C is a direct consequence of the amorphous-crystalline state transition. Similarly,the dramatic increase observed in the electrical conductivity (i.e. of four orders of magnitude) associated with a semi-conductor/quasi-metal transition could be due to a percolation phenomenon related to the formation of the network of carbon at the SiC grain boundaries. Finally the low stiffness of the filaments, and more generally speaking of ex-PCS fibers (i.e. E =200 GPa instead of 450 GPa for polycrystalline SiC) could be related to the fact that the filament is not made of pure SiC but consists of a mixture of SiC and carbon of low stiffness.

A preliminary **thermodynamic study,** based on the minimization of the total Gibbs free energy of the system, has been performed(*) in order to assess : (i) the nature of the chemical species present in the gas phase and in the solid as well as (ii) the ratio of the partial pressures of CO and SiO, when equilibrium is achieved at a given temperature and within an isothermal vessel of given volume, for an overall chemical composition corresponding to that of our pyrolytic residue at 1100-1200°C, i.e. $Si_4C_{4.88}O_{2.12}$.

From the results of the calculations, shown in Table VII it appears that the solid corresponding to $Si_4C_{4.88}O_{2.12}$ should be at 1200°C , a mixture of SiC, silica and free carbon, assuming that equilibrium is reached within a vessel of small volume, CO being the main gaseous species. It is worthy of note that this result is consistent with surface AES analyses reported by Menessier et al. for Nicalon fibers annealed in sealed silica tubes at a somewhat lower temperature [44].

When both the temperature and the volume of the vessel are increased (in the calculations, a vessel of very large volume being close to an open system configuration) : (i) the proportion of SiO with respect to that of CO becomes much more important and (ii) the solid consists of pure silicon carbide only. Under such conditions, the following overall equation can be written :

$$Si_4C_{4.88}O_{2.12} \xrightarrow{1400°C} 3.4\,SiC + 1.5\,CO + 0.6\,SiO \quad (3)$$

(*) Thermodata, Saint-Martin d'Héres

Volume (l)	Temperature (°C)	P_{CO} / P_{SiO}	Phases in the solid state	Phases in the gaz phase
1	1200	572	SiC - SiO_2 - C	CO - (SiO)
1	1400	266	SiC - SiO_2 - C	CO - (SiO)
1000	1400	17	SiC - SiO_2	CO - SiO
100000	1400	2.5	SiC	CO - SiO

Table VII : Nature of the solid phases and gaseous species, and ratio of the partial pressures of CO and SiO at equilibrium, for a system of overall chemical formula $Si_4 C_{4.88} O_{2.12}$, as a function of temperature and volume of the gas phase.

which is to be compared to equation (1). On the one hand, the evolution of SiO, during the pyrolysis at 1400°C of the ex-PCS residue, has been established indirectly in the present study from chemical analyses of the solid. It has been also directly evidenced experimentally by Johnson et al., as already mentioned [25]. On the other hand, the fact that the residue actually obtained at 1400°C does not consist of pure SiC but of a SiC + C mixture, could be explained on the basis of the following remarks : (i) the thermodynamic approach does not take into account the kinetics factors and (ii) the experimental vessel actually used was not isothermal, therefore, the decomposition of SiO (into SiO_2 and Si) on the cold wall shifts reaction (2) towards the left-hand side and may favor the formation of free carbon.

Several points still remain a matter of speculation and particularly the origin of the carbon layer at the filament surface, for Tp > 1200°C. Such a carbon layer, mentioned already by several authors, is partly responsible for the high toughness of CMCs made of ex-PCS fibers and prepared at high temperatures (e.g. by CVI or hot pressing). The majority of this carbon layer is made of randomly orientated BSUs and furthermore, there exists a composition gradient between this layer of almost pure carbon and the SiC + C filament, which suggest a decomposition process governs by diffusion (possibly activated by the SiO gaseous species). Finally, the very thin films of turbostractic carbon, whose layers are parallel to the filament surface, could be the result of a CVD reaction from the residual gaseous carbosilane species present in the atmosphere of the pyrolysis furnace. Obviously, additional research would be necessary in order to confirm the origin of this so important carbon layer formed at ex-PCS filament surface during annealing treatments. A model of the filament microstructure is tentatively shown in fig. 17.

ACKNOWLEDGEMENTS

The authors acknowledge the contribution of P. Dordor to the electrical study of the filaments as well as M. Loubinou and P. Olry from ITF and SEP respectively for their assistance in setting up the monofilament extrusion apparatus. They are indebted to UA 35 for the supply of modified PCS starting material and to B. Cheynet from THERMODATA for the thermodynamic calculations. This work has been supported by AFME and SEP (grant to E. Bouillon) as well as CNRS, DRET and Conseil Régional d'Aquitaine.

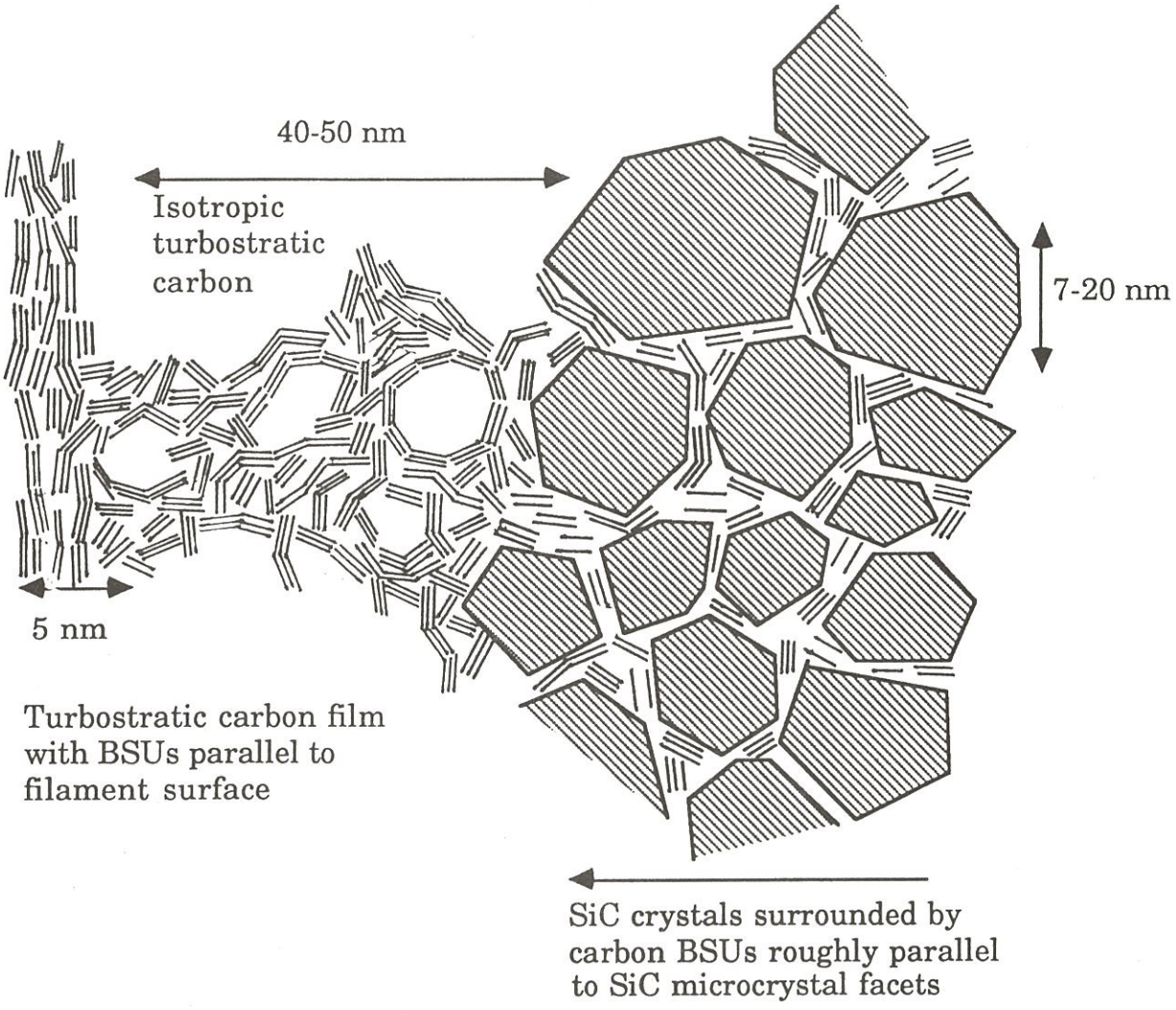

Fig. 17 : Microstructure (schematic) of ex-PCS filaments heat-treated at 1400°C under an inert atmosphere, in the vicinity of the filament surface.

REFERENCES

1 - R. NASLAIN "Introduction to Composite Materials", Tome 2, Metallic and Ceramic Matrix Composites (in french), Eds. CNRS/IMC , Bordeaux,1985.

2 - S.YAJIMA " Handbook of Composites", Vol. 1 Edited by W. Watt and B.V. Perov 1985, Elsevier Science Publishers B.V.

3 - S.YAJIMA, J. HAYASHI, M. OMORI, Chem. Letters, (1975) 931-934.

4 - S.YAJIMA, K. OKAMURA, M. OMORI, Chem. Letters, (1975) 1209-1212.

5 - S. YAJIMA, Y. HASEGAWA, J. HAYASHI, M.IIMURA, J. Mater. Sci., 13 (1978) 2529-2576.

6 - Y. HASEGAWA, M.IIMURA, S. YAJIMA, J. Mater. Sci., 15 (1980) 720-728.

7 - Y. HASEGAWA, K. OKAMURA, J. Mater. Sci., 18 (1983) 3633-3648.

8 - Y. HASEGAWA, K. OKAMURA, J. Mater. Sci., 21 (1986) 321-328.

9 - K. OKAMURA, Composites, 18 (1987) 107-119.

10 - K. OKAMURA et al., U.S. Patent 4, 650, 773, 17 ; 1987.

11 - K. OKAMURA, M. SATO, Y. HASEGAWA, T. AMANO, Chem. Letters (1984) 2059-2060.

12 - L.C. SAWYER, M. JAMIESSON, O. BRIKOWSKI, M.I. HAIDER, R.T. CHEN, J. Am. Ceram. Soc. 70 [11] (1987) 798-810.

13 - Y. MANIETTE and A. OBERLIN, J. Mar. Sci. (Accepted).

14 - J. LIPOWITZ, H.A. FREEMAN, R.T. CHEN, E.R. PRACK, Adv. Ceram. Mat. 2 [2] (1987) 121-28.

15 - L.C. SAWYER, R.T. CHEN, F. HAIMBACK, P.J. HARGET, E.R. PRACK and M. JAFFE, Ceram. Eng. Sci. Pro., 7 (1986) 914-922.

16 - C. LAFFON, A.M. FLANK, R. HAGEGE, P. OLRY, J. COTTERET, M. LARIDJANI, J. DIXMIER, J.L. MIQUEL, H. HOMMEL, A.P. LEGRAND, J. Mater. Sci.,24, (1989) 1503-1512.

17 - T.J. CLARK, R.M. ARONS, J.B. STAMMATOFF and J. RABE, Ceram. Eng. adv. Sci. Proc., 7-8 (1985) 576-588.

18 - A.S. FAREED, P.FONG, M.J. KOCZAK, F.M. KO, Am. Ceram. Soc. Bull. 66 [2] (1987) 353-58.

19 - T. MAH, N.L. HEICHT, D.E. Mc CALLUM, J.R. HOENIGMAN, H.M. KIM, A.P. KATZ, H.A. LIPSITT, J. Mat. Sci. 19 (1984) 1191-1201.

20 - L.C. SAWYER, R.ARONS, F. HAIMBACK, M. JAFFE, K.D. RAPPAPORT, Ceram. Eng. and Sci. Proc., 7-8 (1985) 567-575.

21 - G. SIMON, A.R. BUNSELL, J. Mat. Sci., 19 (1984) 3649-3657.

22 - T.J. CLARK, M. JAFFE, J. RABE and N.R. LANGLEY, Ceram. Eng. and Sci. Proc., 7,8 (1986) 901-913.

23 - Y. SASAKI, Y. NISHIMA, M. SATO, K. OKAMURA, J. Mater. Sci. 22 (1987) 443-448.

24 - K.L. LUTHRA, J. Am. Ceram. Soc., 69 [10] (1986) C-231 C-233.

25 - S.M. JOHNSON, R.D. BRITTAIN, R.H. LAMOREAUX, D.J. RAWCLIFFE, J. Am. Ceram. Soc., 71 [3] (19868) C-132 C-135.

26 - E. BOUILLON, F. LANGLAIS, R. PAILLER, R. NASLAIN, J.C. SARTHOU, A. DELPUECH, C. LAFFON, P. LAGARDE, F. CRUEGE, P.V. HUONG, M. MONTHIOUX, A. OBERLIN, J. Mater. Sci., (Submitted).

27 - E. BOUILLON, R. PAILLER, R. NASLAIN, E. BACQUE, J.P. PILLOT, M. BIROT, J. DUNOGUES, P.V. HUONG, J. Mater. Sci. (Submitted).

28 - A. OBERLIN, Carbon 17 (1979) 7-20.

29 - M. MONTHIOUX, A. OBERLIN, and E. BOUILLON, Composites Science and Technology (Accepted).

30 - A.R. BUNSELL, J.W.S. HEARLE, R.D. HUTER, J. Phy. E : Scientific Instruments 4 (1971) 868.

31 - J.F. VILLENEUVE, Internal report (1988).

32 - J.J. POUPEAU, D. ABBE and J. JAMET, ONERA Report (1982).

33 - L. PORTE, A. SARTRE, J. Mat. Sci., 24 (1989) 271-275.

34 - J.A. TAYLOR, Appl. Surf. Sci., 7 (1981) 168-184.

35 - Y. MIZOKAWA, K.M. GEIB, C.W. WILMSEN, J. Vac. Technol. A., 4 (1986) 1696.

36 - M.N. RAHAMAN, L.C. DE JONGHE, Am. Ceram. Soc. Bull. ,66 [5] (1987) 782-85.

37 - T. GOTO, F. ITOH, K. SUZUKI, T. HURUI, J. Mat. Sci. Letters, 2 (1983) 805-807.

38 - W.Y. LEE, J. App. Phys. 51 (6) (1980) 3365.

39 - R. PAMPUCH, W. PTAK, S. JONA and J. STOCH, Energy and Ceramics, Eds. P. Vinccuzini - Elsevier- Amsterdam (1980) pp 435-448.

40 - S. YAJIMA, K. OKAMURA, T. MATSUZAWA, T. SCHISHIDO , Nature 279 (1979) 706-707.

41 - A. OBERLIN, Carbon, 22 (1984) 521.

42 - A. OBERLIN, S. BONNAMY, X. BOURRAT, M. MONTHIOUX AND J.N. ROUZAUD, ACS. Symp. Ser., 303 (1986) 85-98.

43 - P.LECOUSTUMER, M. MONTHIOUX and A. OBERLIN, J. Mater. Sci, (to be submitted).

44 - E .MENESSIER, University thesis n° 216 , Bordeaux 1988

CHAPITRE IV

New polycarbosilane models. 5 : Pyrolysis of series of functional polycarbosilanes

INTRODUCTION AU CHAPITRE IV

Le chapitre IV porte sur une étude exploratoire de la céramisation de différents **polycarbosilanes (PCS) et polycarbosilazanes (PCSZ)**. Cette étude est le résultat d'une étroite collaboration avec Mr E. Bacqué, J.P. Pillot, M. Birot et Mr J. Dunogues de l'UA 35 qui ont synthétisé les polymères. Ils ont été définis dans l'objectif de posséder une **structure bien connue** de manière à cerner les relations existantes entre le précurseur de départ et le résidu minéral résultant après pyrolyse. La synthèse des PCS et PCSZ est reportée en **annexe 2.**

(i) Pour aboutir à un taux de résidus élevés, le polymère doit subir une étape de **thermolyse** ou donner lieu en début de pyrolyse à une réticulation intermoléculaire, mettant en jeu des **liaisons fortes** (e.g. Si-O).

(ii) Le pourcentage de carbone libre dans la céramique finale va dépendre essentiellement de la **stabilité thermique** des groupements hydrocarbonés des polymères.

(iii) La **voie polycarbosilazane** permet d'aboutir à une céramique contenant une phase complexe de type **oxynitrure de silicium** ou des espèces quaternaires. Elle engendre de plus un **retard à la cristallisation** qui est de l'ordre de 300°C par rapport à la céramique issue du NC_2.

(iv) Enfin, nous avons constaté que les liaisons chimiques présentes dans le squelette polymérique ne se retrouve pas systématiquement dans la céramique.

Soumis à "Chemestry of Materials"

NEW POLYCARBOSILANE MODELS. 5 : PYROLYSIS OF SERIES OF FUNCTIONAL POLYCARBOSILANES

E. BOUILLON(*) , R. PAILLER(*) , R. NASLAIN(*)
Laboratoire de Chimie du Solide du CNRS, Université de Bordeaux-I
351, Cours de la Libération, F 33405-Talence

E. BACQUE, J.P. PILLOT, M. BIROT, J. DUNOGUES
Laboratoire de Chimie Organique et Organométallique (UA 35-CNRS)
Université de Bordeaux-I, 351, Cours de la Libération, F 33405-Talence

and P.V. HUONG
Laboratoire de Spectroscopie Moleculaire et Cristalline (UA 124 - CNRS)
Université de Bordeaux-I, 351, Cours de la Libération, F 33405-Talence

ABSTRACT

Ten models of functional polycarbosilane (PCS) or polycarbosilazane (PCSZ) precursors were prepared from chlorinated poly(dimethyl-sil)methylene and pyrolysed, under inert gas flow or vacuum at temperatures up to 2300°C, in order to derive relations between the nature of the precursors and that of the ceramic residues. The organometallic/inorganic transition and the recrystallization of the pyrolytic residues were studied by a number of different analytical techniques. Linear precursors resulted in ceramic yields which are low unless a cross-linking treatment was applied prior to pyrolysis. High C-content precursors do not necessarily lead to high C-content ceramics. Ternary (Si-C-O or Si-C-N) and even quaternary tetrahedral species were present in the ceramic residues. Nitrogen was found to inhibit the recrystallization of the ex-PCSZ ceramics up to about 1400°C. Only part of the initial skeleton of the precursors was maintained in the ceramics.

(*) Present address : Laboratoire des Composites Thermostructuraux (UMR-47 CNRS-SEP-UB1), Europarc, 3, Av. Léonard de Vinci, F-33600-PESSAC.

1 - INTRODUCTION

Ceramic materials are now commonly obtained through the pyrolysis of organic- or organometallic- precursors, either as powders, fibers of fibrous composites. Carbon fibers (derived from rayon, polyacrylonitrile or pitch) can be considered as one of the first applications or the organic precursor route to the synthesis of advanced ceramics [1-9]. More recently, ceramic matrix composites (CMC), made of ceramic fibers embedded in a ceramic matrix (based on C, SiC, Si_3N_4, B_4C or BN), have been obtained according to a general procedure involving : (i) an impregnation of a fiber preform with the liquid precursors, (ii) a cross-linking step and (iii) a pyrolysis treatment at moderate temperatures [10-22]. In this field, carbon-carbon composites have already received a number of applications particularly at high temperatures.

The synthesis of a SiC-based fiber from a polycarbosilane (PCS) precursor, by S. Yajima and his coworkers in the mid-seventies, is an important milestone. This fiber, now produced by Nippon Carbon Co.Ltd under the trade mark NICALON, is obtained according to a spinning-stabilization-pyrolysis process very similar to that previously used for carbon fibers [23-33]. It is made of silicon carbide, free carbon and an oxycarbide phase mixed together at nanometer scale. The fiber exhibits high tensile strength and stiffness as well as good resistance to oxydation up to about 1100°C. Above this limit, a decrease in the mechanical properties occurs which seems to be related to a change in the microstructure of the material [34-41]. It is generally accepted that an evolution of gaseous oxygen containing species (i.e. SiO and CO) [42-43] takes place above 1100°C with simultaneously a coarsening of the silicon carbide grains and formation (or rearrangement) of free carbon at the grain boundaries [44-52]. However, the complexity of the material has precluded up to know a detailed understanding of the behavior of the fiber as well as an improvement of its mechanical characteristics at high temperatures. It is anticipated that free carbon and combined oxygen may play an important role.

In order to overcome the drawbacks of the ex-PCS SiC-based fibers, it has been suggested to use polysilazane (PSZ) or polycarbosilazane (PCSZ) precursors to prepare Si-C-N (or Si-C-N-O) fibers and even polytitanosiloxane precursors for Si-C-Ti-O fibers [53-58]. Concurrently, K. Okamura et al. have shown that Si-N-O fibers can be obtained from green PCS fibers when the pyrolysis treatment is performed under atmosphere of ammonia [59]. In all these attempts, the aim was often to form an amorphous (or poorly crystallized) phase, resulting in a high tensile strength, more stable at high temperature than that present in the NICALON fiber.

The objectives of the present work are : (i) to better understand the mechanisms involved in the pyrolysis of organosilicon precursors, (ii) to characterize the pyrolytic residue and (iii) to derive relations between the nature of the precursor, and the nature and properties of the ceramic. Our approach was to use **model functional polycarbosilanes** better defined from a structural standpoint than those obtained according to the S. Yajima's route [60-62]. These new PCS model precursors have been selected in order : (i) to verify the **concept of branching** previously suggested by C.L. Schilling et al. [19] (according to which high ceramic yields are related to a high degree of branching of the polymeric chains), by considering model precursors with functional groups able to give raise to cross-linking, (ii) to introduce **nitrogen atoms** in the precursors that may act as an inhibitor in the mechanisms responsible for the coarsening of the microstructure of the pyrolytic residue at high temperature and (iii) to increase the amount of **free carbon** in the ceramic by considering a family of precursors with different C/Si atomic ratios.

2 - MATERIALS

The model functional PCS or PCSZ precursors which have been selected for the present study are listed in Table I [62]. On the basis of the concept of branching, **polydimethylsilmethylene** (I) has almost no interest as a ceramic precursor , due to its linear structure. As a matter of fact, during heating at increasing temperatures, the linear chains are broken into low molecular weight fragments leading to a ceramic yield at 1000°C which is very low. On the contrary, polydimethylsilmethylene (I) has the capability of

being easily chlorinated according to equation (1) given in fig. 1. Taking advantage of the high chemical reactivity of the Si-Cl bonds in the chlorinated polymeric molecules (II), new functional PCS or PCSZ species having a potential as model precursors have been prepared.

In a first series of experiments, the chlorinated polymeric chains (II) have been cross-linked through the classical reactions of the Si-Cl bonds. On this basis, eight model precursors referred to as Si-Si (Na,s) ; Si-Si (Na,i) ; Si-Si (K,s) ; Si-Si (K, i) ; SiNHSi ; SiNHMe ; $SiNMe_2$ and SiOSi were prepared (Table I).

In a second series of experiments, the Si-Cl bonds of the chlorinated polymeric molecules (II) were first reduced by $LiAlH_4$ to give **a model linear polysilapropylene** (III) according to equation (2) shown in fig. 1. Based on the classical hydrosilylation cross-linking reaction, two new model precursors referred to as SiC_4Si and SiC_2ArC_2Si were prepared with butadiene and p-divinylbenzene respectively (Table I).

More details about the synthesis and characterization of the model precursors have been presented elsewhere [62].

3 - MATERIAL CHARACTERIZATION

3.1- Thermogravimetric Analysis (TGA)

For each precursor, TGA was performed(*) under flowing purified argon with a heating rate of 5°C min^{-1} up to 1000°C in order to study the organometallic/inorganic transition.

3.2- Flash Pyrolysis Gas Analysis (FPGA)

The analysis of the gaseous species evolved during the pyrolysis of some of the precursors was performed, in line, with an analytical apparatus made of a pyrolysis microfurnace, a gas phase chromatography unit and a mass spectrometer [63]. The sample (0,5 mg) was rapidly heated under flowing helium up to pyrolysis temperature (i.e. 500, 700 and 1000°C) with a platinum resistance microfurnace and then maintained at that temperature for 10 seconds. The gaseous species formed during the flash pyrolysis were first separated by gas chromatography and then identified by

(*) Perkin Elmer TGS2 apparatus

Reactants	Solvent	Theoretical formula	Reference
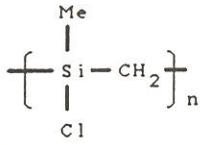 ; Na	Xylene	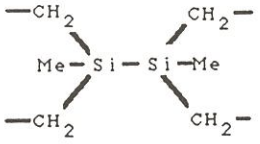	(Na, s) Si-Si (Na, i)
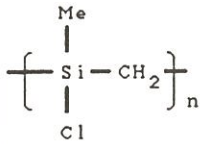 ; K	THF	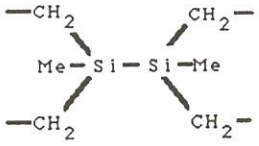	(K, s) Si-Si (K, i)
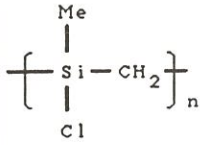 ; NH_3	CH_2Cl_2	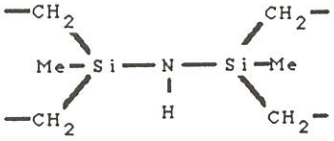	SiNHSi
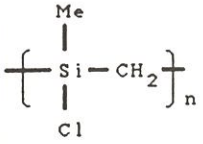 ; $MeNH_2$	CH_2Cl_2	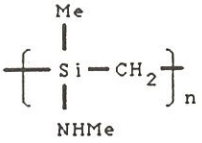	SiNHMe
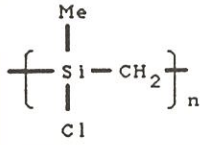 ; Me_2NH	CH_2Cl_2	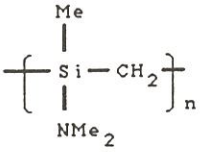	$SiNMe_2$
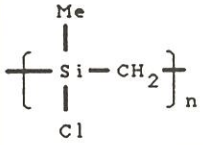 ; H_2O	None	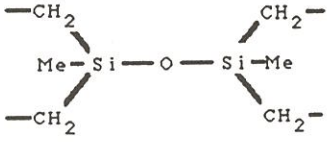	SiOSi
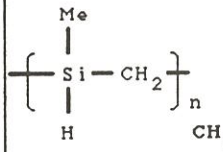 ; $CH_2=CH-CH=CH_2$	None	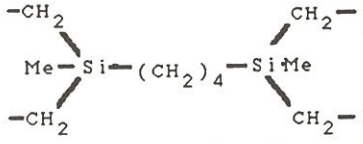	SiC_4Si
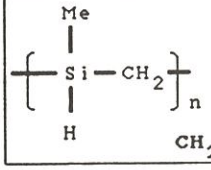 ; $CH_2=CHArCH=CH_2$	None	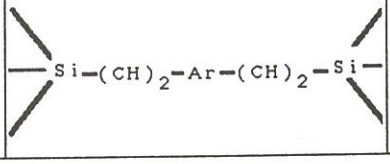	SiC_2ArC_2Si

(s) and (i) refer respectively to the soluble and insoluble fraction in said solvent.

TABLE 1 : Synthesis and identification of the model functional PCS and PCSZ precursors.

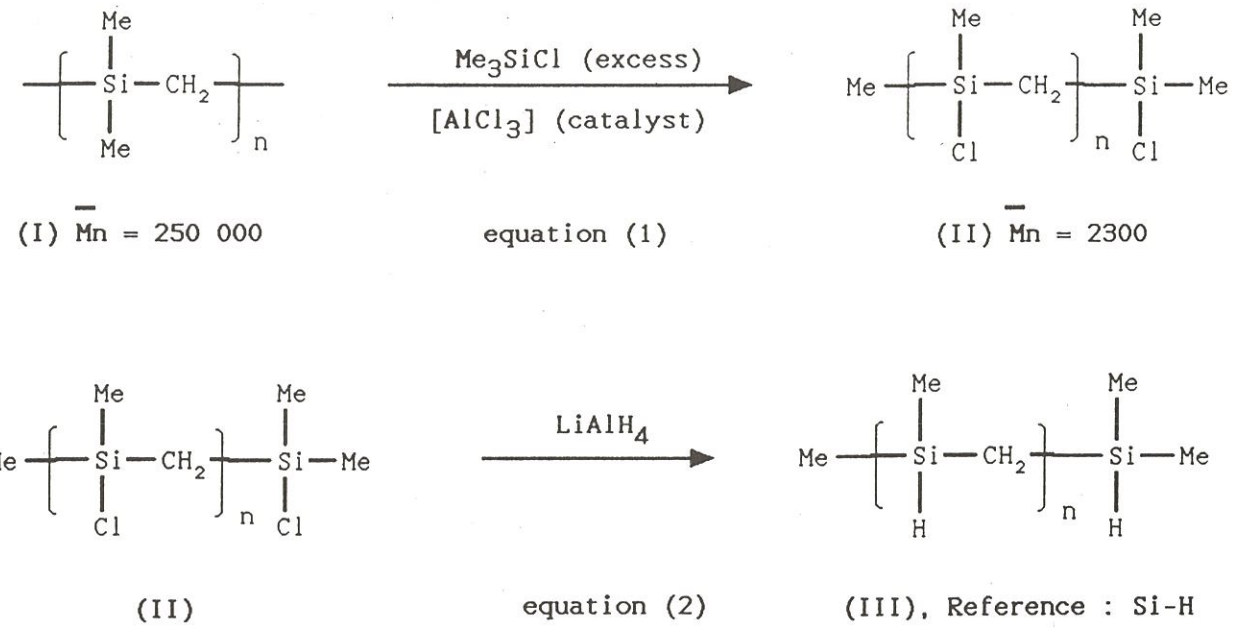

Fig 1: The important intermediates in the synthesis of the PCS or PCSZ model precursors.

mass spectrometry (*) . The effect of heating conditions specific to flash pyrolysis on (i) the chemical composition of the gas and (ii) the temperatures at which they are formed, has been already studied by E. Bouillon et al. for a PCS-type precursor and reported elsewhere [64]. It was established that the evolution of gas takes place in flash pyrolysis at a higher temperature, i.e. by 150°C, with respect to what is observed for more conventional pyrolysis performed at much slower heating rates.

3.3 - Bulk Pyrolysis Experiments

The analyses performed on the solid residues resulting from PCS or PCSZ precursors requiring rather large samples, bulk pyrolysis experiments were run on 1 to 5 g precursor samples heated in alumina crucibles under a pressure of 1-100 kPa of argon purified over P_2O_5 and magnesium (heated at 600°C). The samples were heated, at a temperature increase rate of 100°C hr^{-1} up to 700°C and 300°C hr^{-1} beyond this limit (when necessary, a few experiments were performed up to 2300°C), with a r.f. induction furnace and according to a procedure which has been described elsewhere [64]. Unless specified, the temperature plateau was usually 30-60 min.

3.4 - Elemental Chemical Analysis

The inorganic residues resulting from the pyrolysis of PCS or PCSZ precursors were analysed for silicon, carbon nitrogen, oxygen and hydrogen (**). The silicon content was established by ICP (induction coupling plasma) from an aqueous solution of sodium silicate resulting from the chemical attack of the sample, with an oxidizing melt based on sodium oxide. To determine the carbon content, the sample was burned at high temperature under oxygen, the resulting carbon dioxide being quantitatively analysed by IR spectroscopy. Similarly, the oxygen content was established through the IR spectroscopy analysis of the carbon monoxide formed during the pyrolysis of the sample at about 3000°C whereas that of nitrogen was derived according to a catharometric method. Finally, hydrogen was quantitatively analysed as H_2O by IR spectroscopy after combustion of the sample at about 1000°C under oxygen.

(*) Poropack Q gas chromatography column and CH5-DF FINNIGAN MAT man spectrometer.

(**) CNRS, Service Central d'Analyse, BP 22 F-69390 VERNAISON

3.5 - Infra Red Spectroscopy (IRS)

Some of the pyrolysis residues (i.e. those corresponding to SiNHMe and $SiNMe_2$) were analysed by IR spectroscopy, according to the conventional KBr pellet technique(*).

3.6 - Raman Spectroscopy Microanalysis (RSMA)

Raman spectroscopy analyses were performed on fragments of pyrolysis residues, with a MOLE-type microanalyser(**). The laser beam had a wavelength of 514.5 nm. The spot size was of the order of 1μm, the depth of sample analysed being a few μm. For each material, at least three fragments were analysed.

3.7 - ESCA Experiments

ESCA was performed with a X-ray microbeam apparatus (Al Kα wavelength ; spot size : 150-300μm) under ultra high vacuum (133. 10^{-9} Pa)(***). The charge effect was compensated by the use of a low energy electron gun. Each sample was submitted to an etching treatment in order to clean its surface, prior to analysis. A semi-quantitative analysis, based on the measurements of the surfaces of the Si 2p ; C 1s and N 1s peaks (high resolution mode) was performed for some of the pyrolysis residues. Conventional correction factors were applied. The best conditions for semi-quantitative analysis of the chemical bonds were found to be : a 150 μm spot size, an energy window of 25 eV and a counting time of 8 hours. As a matter of fact, it was observed that the peak width at mid-height was not significantly modified by the latter parameter, for both the Si-C and C-C bonds.

3.8 - X-Ray Diffraction (XRD)

The XRD spectra (CuKα) were recorded from the pyrolysis residues, reduced to a fine powder by grinding, with an X-ray diffractometer(*). The mean apparent grain size was calculated, from the peak width measured at mid-height, according to the Scherrer's equation.

(*) : PERKIN ELMER 983, (double beam)

(**) : Jobin-Yvon Raman Spectroscopy Microanalyser

(***) : 5950 Hewlett-Packard photoelectron spectrometer

(*) : Philips PW 1710 diffractometer control

It was assumed that the only cause of peak broadening was that related to the grain size, i.e. those due to microstraining, sample inhomogeneity and sample lack of planeity were neglected.

4 - RESULTS AND DISCUSSION

4.1 - The organometallic inorganic transition

4.1.1 - As identified from the TGA - analyses

The **Si-H model precursor,** referred to as model III in fig. 1 i.e. polysilapropylene, exhibits a progressive thermal decomposition which is almost totally accomplished at 560°C as well as a very low yield in inorganic residue (fig.2 (a) and table II). This result is in good agreement with the lack of branching in this model precursor resulting from the synthesis route which has been used [62]. Due to its purely linear structure, the polymeric chain is fragmented, during pyrolysis, in very low molecular weight species. On the contrary, when this model precursor is treated **in autoclave at 450°C,** it becomes progressively insoluble and its pyrolysis gives rise to high yields in inorganic residue, as shown in table II. It is thought that a considerable amount of rearrangement and branching occurs during the autoclave thermolysis step (as a matter of fact some of the japanese PCSs used for the preparation of NICALON-type fibers have received such a treatment in order to present an acceptable residue yield). Thus, these data confirm the relation which seems to exist between the degree of branching of the polymeric precursor and the pyrolysis yield, as previously suggested by C.L. Schilling et al. [19].

On the one hand, the autoclave thermolysis has formally a negative effect since it destroys the well characterized structure of the starting model precursor but, on the other hand, it results in a significant increase in the residue yield of the pyrolysis.

The thermal behaviors of the various **Si-Si precursors** are shown in fig. 3. As far as the soluble fractions (s) of the precursors are concerned, the Si-Si (K,s) precursor exhibits a progressive organometallic/inorganic transition which starts at about 400°C and ends at about 700°C. On the contrary, the Si-Si (Na,s) precursor shows a sharp transition at about 400°C. Futhermore, the yields in solid residue are rather different but remain low,

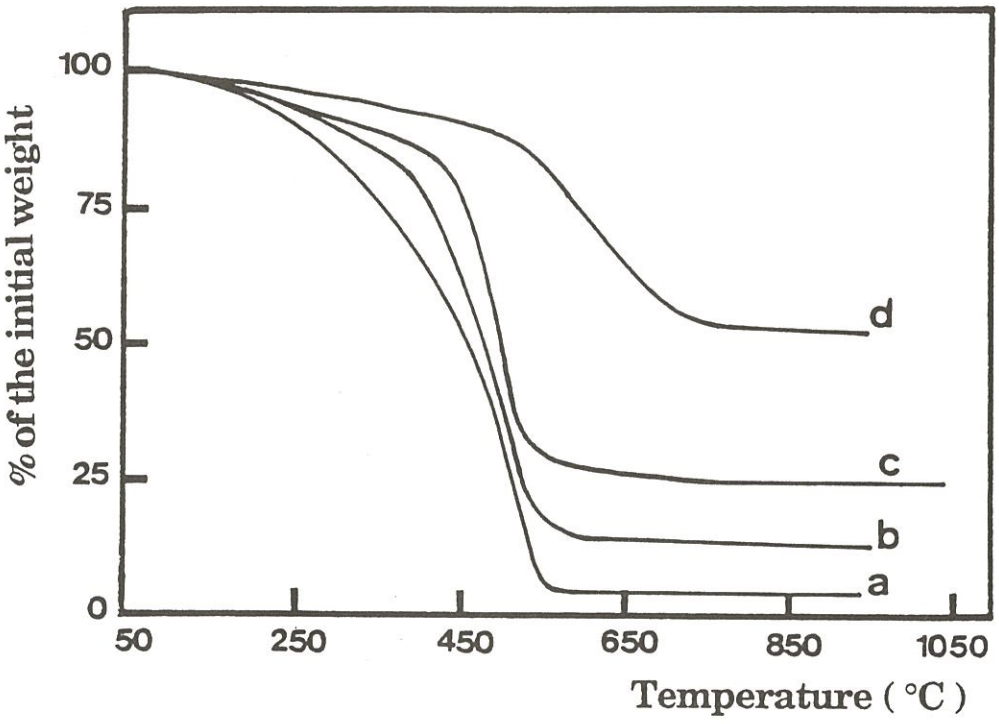

Fig.2 : TGA of the weight loss observed during the pyrolisis of PCS precursors :

a) Si-H
b) SiC_4Si
c) SiC_2ArC_2Si
d) SiOSi

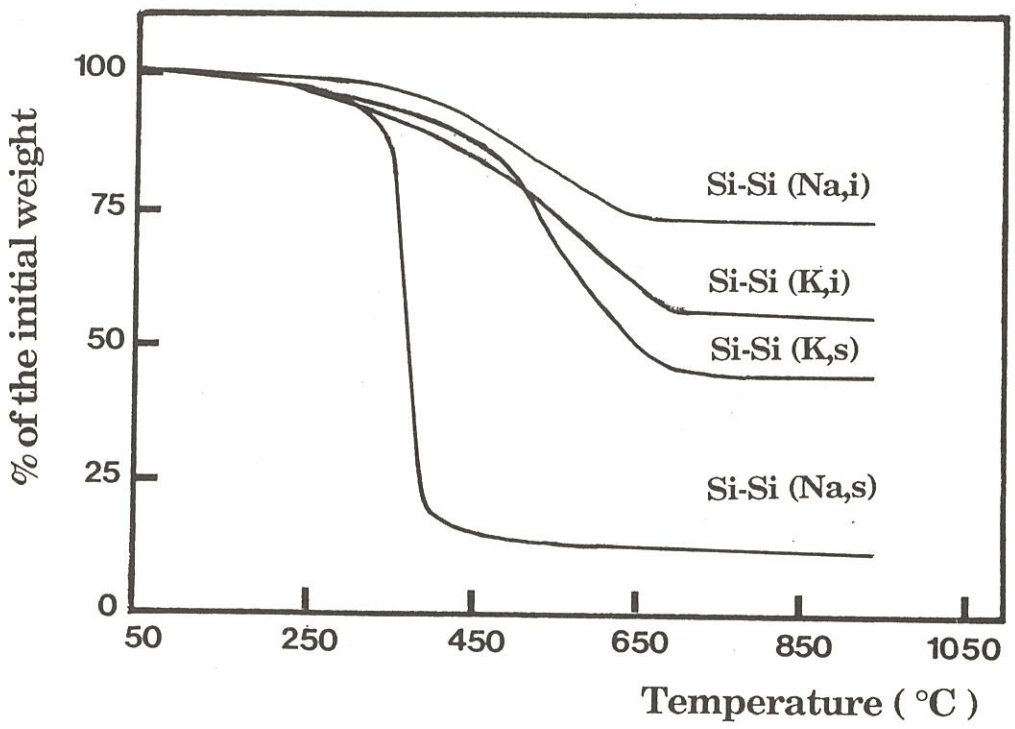

Fig. 3 : TGA of the weight loss observed during the pyrolysis of various PCS Si-Si precursors.

i.e. 11 % for Si-Si (Na, s) and 43 % for Si-Si (K, s). The yields in solid residue for the insoluble fractions are much higher, i.e. 59 % for Si-Si (K, i) and 77 % for Si-Si (Na,i). This result is in good agreement with the fact that the degree of cross-linking is higher for the insoluble fractions than for their soluble counterparts. Thus, a rather good degree of cross-linking results again in a high yield in solid residue even when it is achieved through thermally weak disilane chemical bonds.

The SiC_4Si and SiC_2ArC_2Si model precursors are characterized by organometallic/inorganic transitions which are almost totally accomplished at about 550°C and result in low yields in pyrolysis solid residue (14 % and 24 % for SiC_4Si and SiC_2ArC_2Si, respectively). On the contrary, the SiOSi model precursor is characterized by a rather high yield in solid (54 %). Therefore, the hydrocarbon chemical bridges appear to be much weaker than the oxygen ones (fig. 2).

As shown in fig. 4, the yields in solid residue of the PCSZ depend on the structure of the model precursors. When the precursor is only weakly cross-linked, i.e. when its structure is built from cycles resulting from intramolecular cyclisations, the yield in solid residue is weak. On the other hand, when the precursor is characterized by more cross-linking, the yield in solid residue is higher. As an example, a PCSZ which had been obtained without solvent by reaction between (polychloro)silmethylene and methylamine (in order to promote intermolecular cyclisation mechanisms and thus cross-linking) gave a high yield in residue, i.e. 53 %, a result which has to be compared with that i.e. 24 % mentionned in table II for the PCSZ model precursor SiNHMe obtained in CH_2Cl_2 as the solvent.

Generally speaking, it thus appears that the PCS and PCSZ model precursors considered here do not result in high yields in solid residue (with the exception of SiOSi). However, this conclusion is no longer true when the structure of the polymer moves by cross-linking to a three dimensionnal network through strong Si-O-Si or Si-N-Si bonds (and not weak hydrocarbon bridges).

4.1.2 - As identified from gas analysis

The gas formed during the flash pyrolysis of Si-H ; SiNHSi ; SiNHMe and $SiNMe_2$ were analysed by gas chromatography/mass spectrometry for the three following temperatures of the platinum

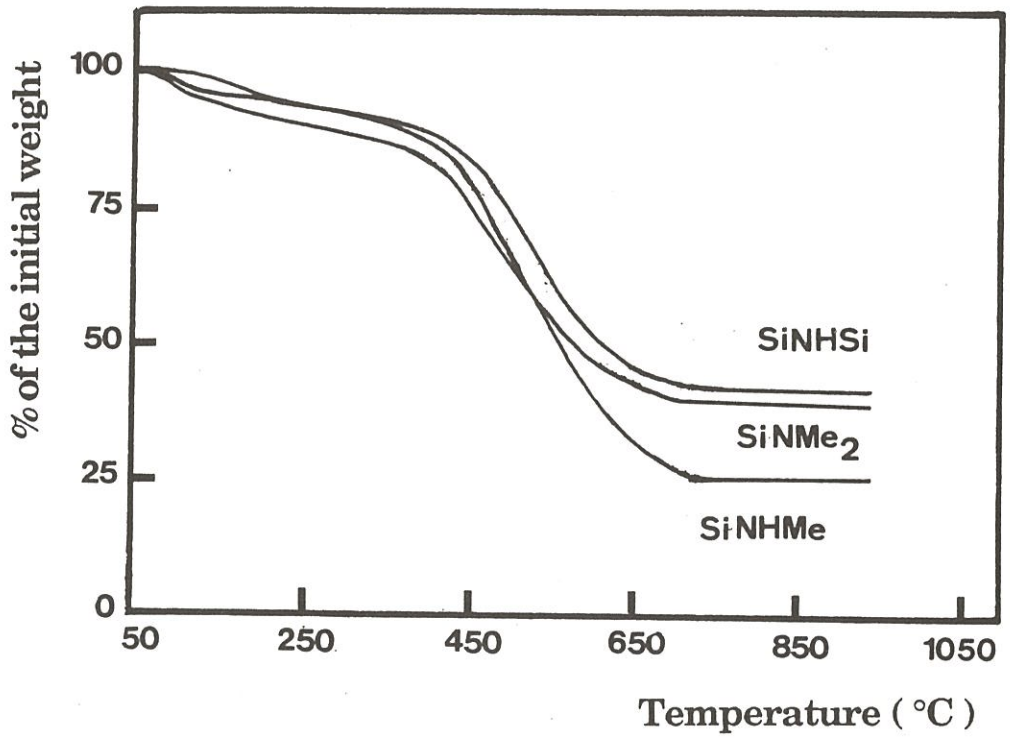

Fig. 4 : TGA of the weight loss observed during the pyrolysis of various PCSZ precursors.

Model precursor	Yield in solid residue (wt %)
Si-H	5
Si-H (*)	85
Si-Si (Na,s)	11
Si-Si (Na,i)	77
Si-Si (K,s)	43
Si-Si (K,i)	59
SiNHSi	37
SiNHMe	24
$SiNMe_2$	33
SiOSi	54
SiC_4Si	14
SiC_2ArC_2Si	24

(*) thermolyzed at 450°C

Table II : Yield in solid residue at 1000°C of the PCS and PCSZ model precursors

resistance microfurnace : 500, 700 and 1000°C. The main gaseous species which have been unambiguously identified are alcanes (methane, ethane, etc...) alkenes (ethene, butene, etc...) as well as various methylsilanes. In addition, during the pyrolysis of PCSZ precursors, different gaseous species containing nitrogen also were formed, such as acetonitrile, propionitrile and trimethylamine. Finally, one must mention the occurence of products with heavy molecular weights (which are thus difficult to detect due to their early condensation) as well as hydrogen. The results of the analysis of the main gaseous species formed during the pyrolysis of the precursors are given in table III.

From the results of the gas analyses performed at 500 ; 700 and 1000°C, the evolution of the relative amount of each main gaseous species, as a function of the pyrolysis temperature, has been tentatively drawn in fig.5 - 7. It clearly appears that at 350°C (or 500°C without correction), the thermal decomposition is still very limited for most PCS or PCSZ precursors. This result is in good agreement with that of the TGA experiments taking into account the fact that there is a temperature shift of about 150°C between flash pyrolysis and TGA pyrolysis (i.e. flash pyrolysis experiments performed at 500°C must be compared with TGA experiments run at 350°C) (Table IV).

On the contrary, at 550°C (or 700°C without correction) the relative amounts of gas are important whatever the nature of the precursor. Obviously, this temperature falls within the temperature range where the organometallic/inorganic transition occurs. This result is again in good agreement with that of the TGA analysis performed at 550°C (to take into account the temperature shift characterizing flash pyrolysis). Therefore, under such temperature conditions, the thermal degradation of most precursors is already very significant (even it is almost fully achieved for the Si-H precursor). Due to the temperature effect, the polymeric chains are broken, their fragments giving silicon- or carbon- based gaseous or low molecular weight species after intra-molecular rearrangements. It is thought that these phenomena may involve free radicals whose presence would allow numerous recombinations leading to gas formation. As an example, the formation of trimethylamine during the pyrolysis of $SiNMe_2$ could result from the recombination of $^{\circ}NMe_2$ with $^{\circ}Me$. Therefore, incorporating nitrogen in the polymeric chain as in $SiNMe_2$ (see table I)

Nature of the precursors	500°C	700°C	1000°C
SiNHSi	butene	methane butene	methane butene
SiNHMe	methane ethene	methane ethene tetramethylsilane	methane ethene
$SiNMe_2$	trimethylsilane trimethylamine	methane trimethylamine	methane ethene
Si-H	methane	methane dimethylsilane trimethylsilane tetramethylsilane	methane ethene dimethylsilane tetramethylsilane

Table III : Gaseous species resulting from the pyrolysis at different temperatures of various PCS and PCSZ precursors (flash pyrolysis) it should be mentioned that hydrogen ,not analysed by mass spectroscopy , is also present (as well as heavy polymeric species due to an early condensation) .

Precursor	Δm/m (%) 350	Δm/m (%) 550	Δm/m (%) 850
Si-H	23	88	95
SiNHSi	8	33	62
SiNHMe	9	54	75
$SiNMe_2$	9	53	66

Tabl IV : Weight loss at different stages of the thermal treatment of PCS and PCSZ precursors.

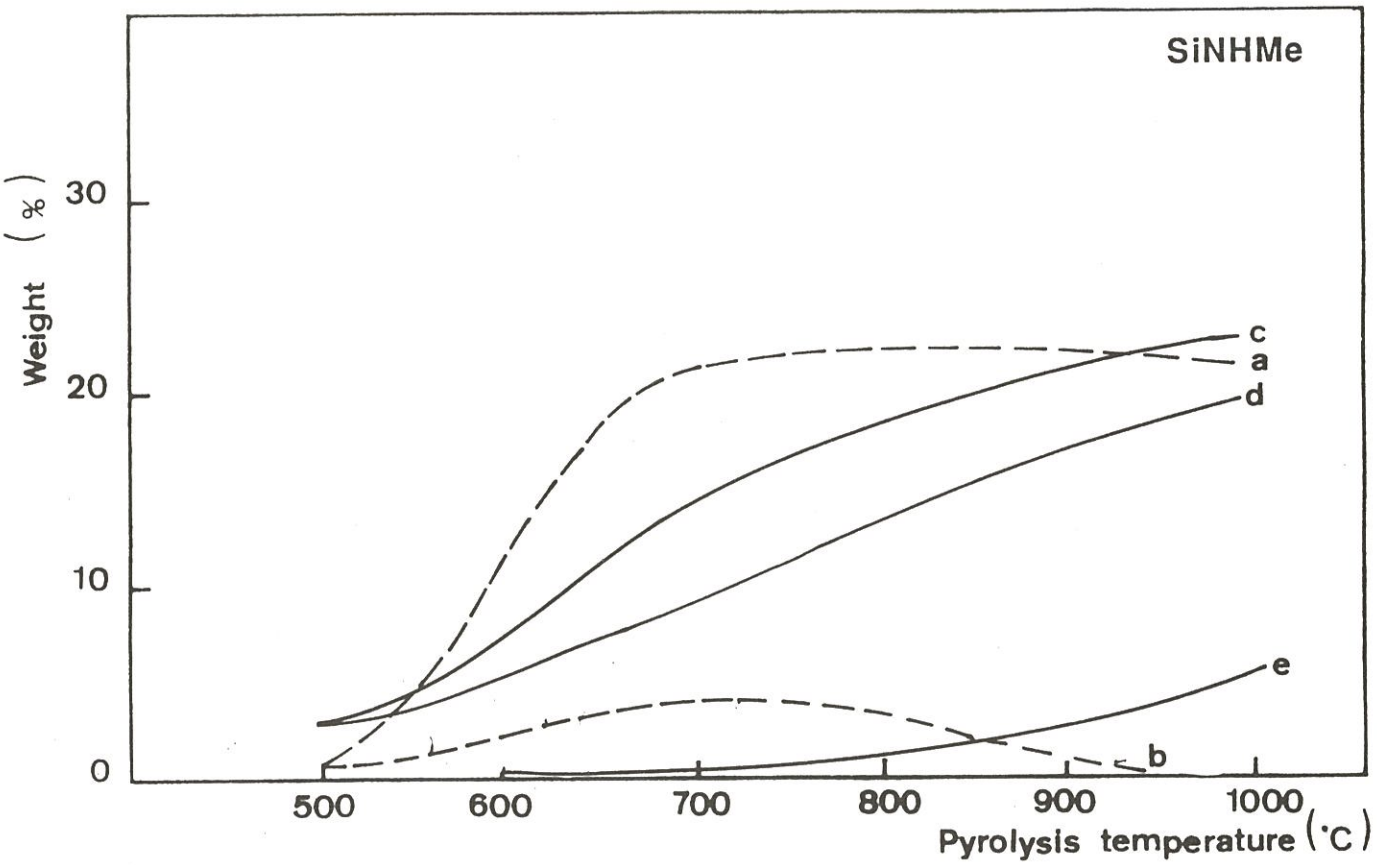

Fig. 5 : Variation of the mass of the gaseous phase evolved from 100 g precursor for the species : tetramethylsilane (a), trimethylsilane (b), ethene (c), methane (d) and butene (e).

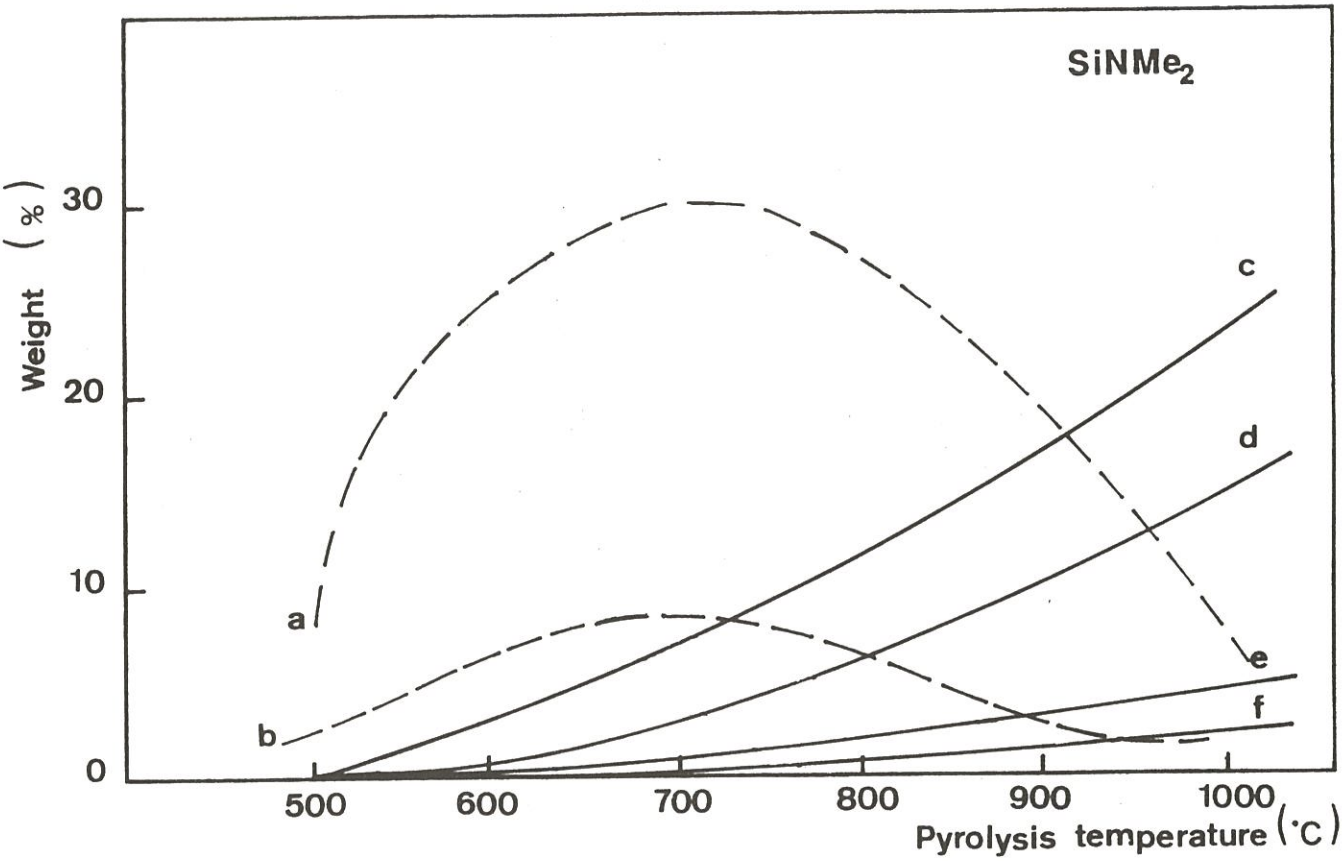

Fig. 6 : Variation of the mass of the gaseous phase evolved from 100 g of precursor for : tetramethylsilane (a), trimethylamine (b), methane (c), ethene (d), ethane (e) and butene (f) ,(from experiments performed at 500 ;700 and 1000°C).

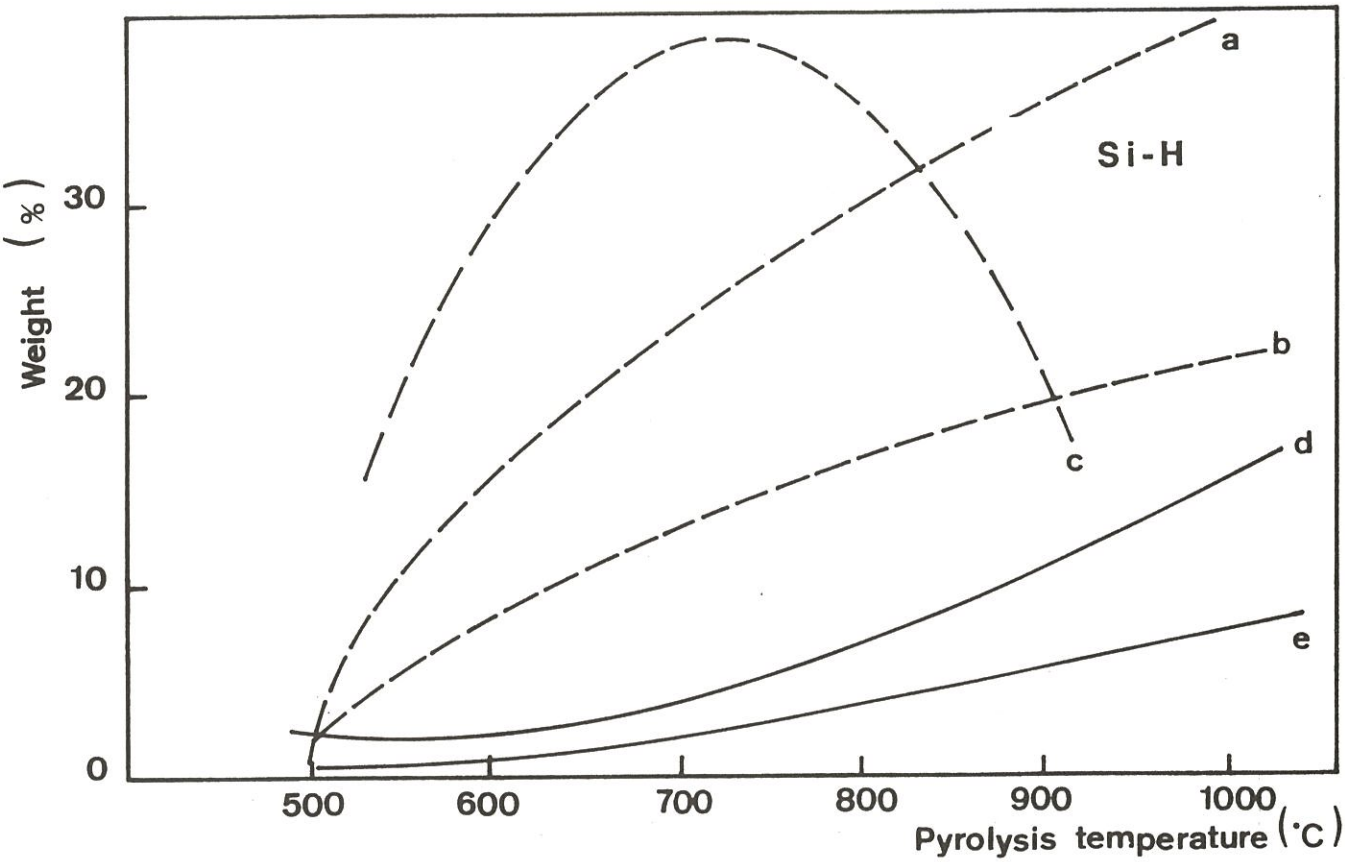

Fig. 7 : Variation of the mass of the gaseous phase evolved from 100 g of precursor for : trimethylsilane (a), dimethylsilane (b), tetramethylsilane (c), methane (d) and ethylene (e) ,(from experiments performed at 500 ;700 1000°C).

does not seem favorable enough to the synthesis of a nitrogen-based ceramic.

Finally at 850°C (or 1000°C without correction), flash pyrolysis gives rise to gaseous species which may result from recombinations between free radicals thought to be less numerous than at 550°C (or 700°C without correction). The gas evolution at this temperature, which may be considered as the end of the organometallic/inorganic transition, is still important (particularly for the Si-H precursor, as shown in fig. 7).

4.1.3 - As identified from the IR analysis

The occurence of an organometallic/inorganic transition during the pyrolysis of PCS and PCSZ precursors, which has been already identified from TGA and gas analysis, was further studied by IRS for the SiNHMe and $SiNMe_2$ precursors. The analyses were performed on the solid residues for increasing bulk pyrolysis temperatures.

As shown in fig.8 and 9, the absorption bands corresponding to the organic bonds characteristic of the starting SiNHMe and $SiNMe_2$ precursors have almost totally disappeared for a pyrolysis temperature of 700°C. For higher pyrolysis temperatures, i.e. for $700 < T_p < 1000$°C, the IR spectrum of the solid residue undergoes slight changes, its main features being maintained. As an example, for the $SiNMe_2$ precursor, the IR spectrum exhibits, for $T_p = 700$°C, a broad absorption band at 820 cm^{-1} which has been assigned to SiC (fig. 9). For $T_p = 1000$°C, the SiC absorption band is narrower and better defined whereas a shoulder is observed on its left hand side at 1100 cm^{-1} which could be assigned to Si-O bonds. The IR spectrum of silicon nitride exhibits a strong Si-N absorption band at 950 cm^{-1} which could be mixed with those due to Si-C and Si-O bonds in the pyrolysis residue of PCSZ precursors. Thus, it could be more appropriate to use a weaker absorption band at 490 cm^{-1} to identify Si-N bonds. As shown in fig.9, such a weak absorption band is present in the pyrolysis residue of $SiNMe_2$ for both $T_p = 700$°C and 1000°C. Assuming that it could be assigned to Si-N bonds, it thus appears that the three kinds of expected bonds, i.e. Si-C ; Si-O and Si-N are present in the solid residue formed during the pyrolysis at 700-1000°C of PCSZ precursors.

For still higher temperatures of pyrolysis, i.e. $T_p = 1400$°C, the occurence of SiC is still more apparent, in the solid residue formed during

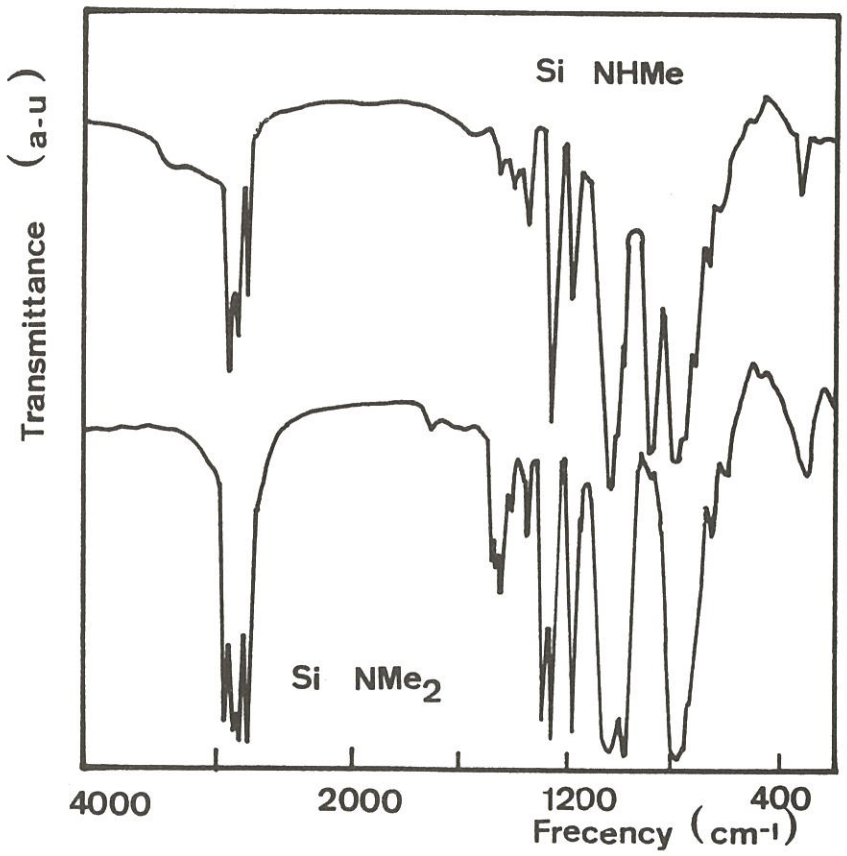

Fig. 8 : IR spectra of the SiNHMe and $SiNMe_2$ precursors

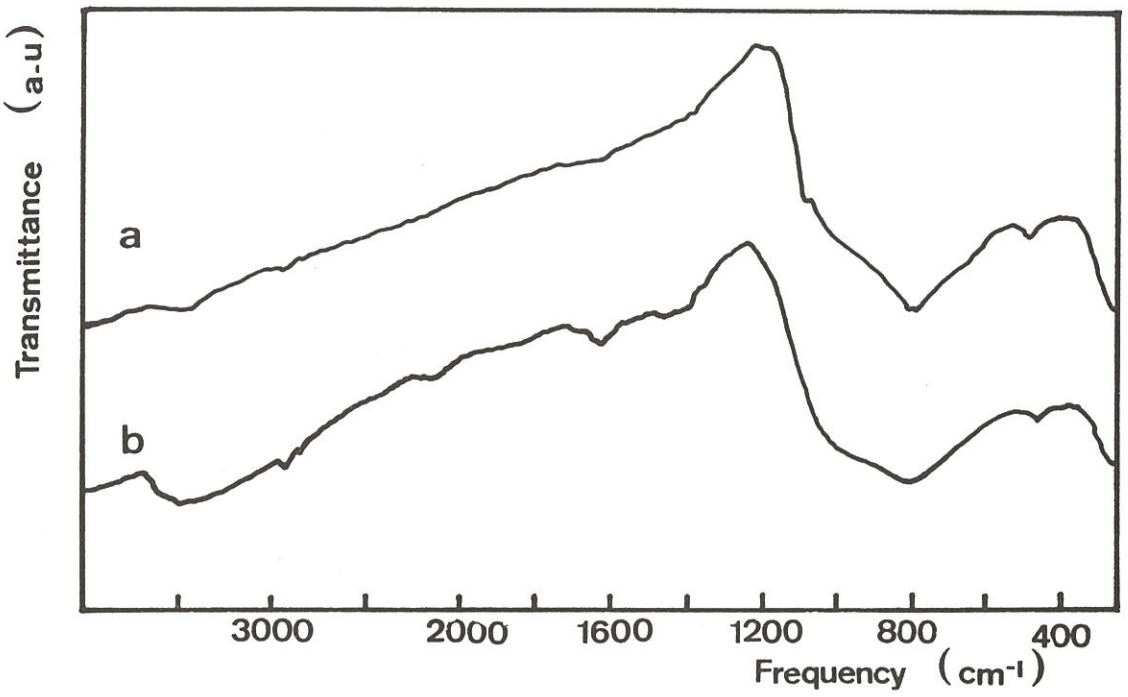

Fig. 9 : IR spectra of the SiNHMe and $SiNMe_2$ precursor pyrolysed at :
a) 1000°C
b) 700°C

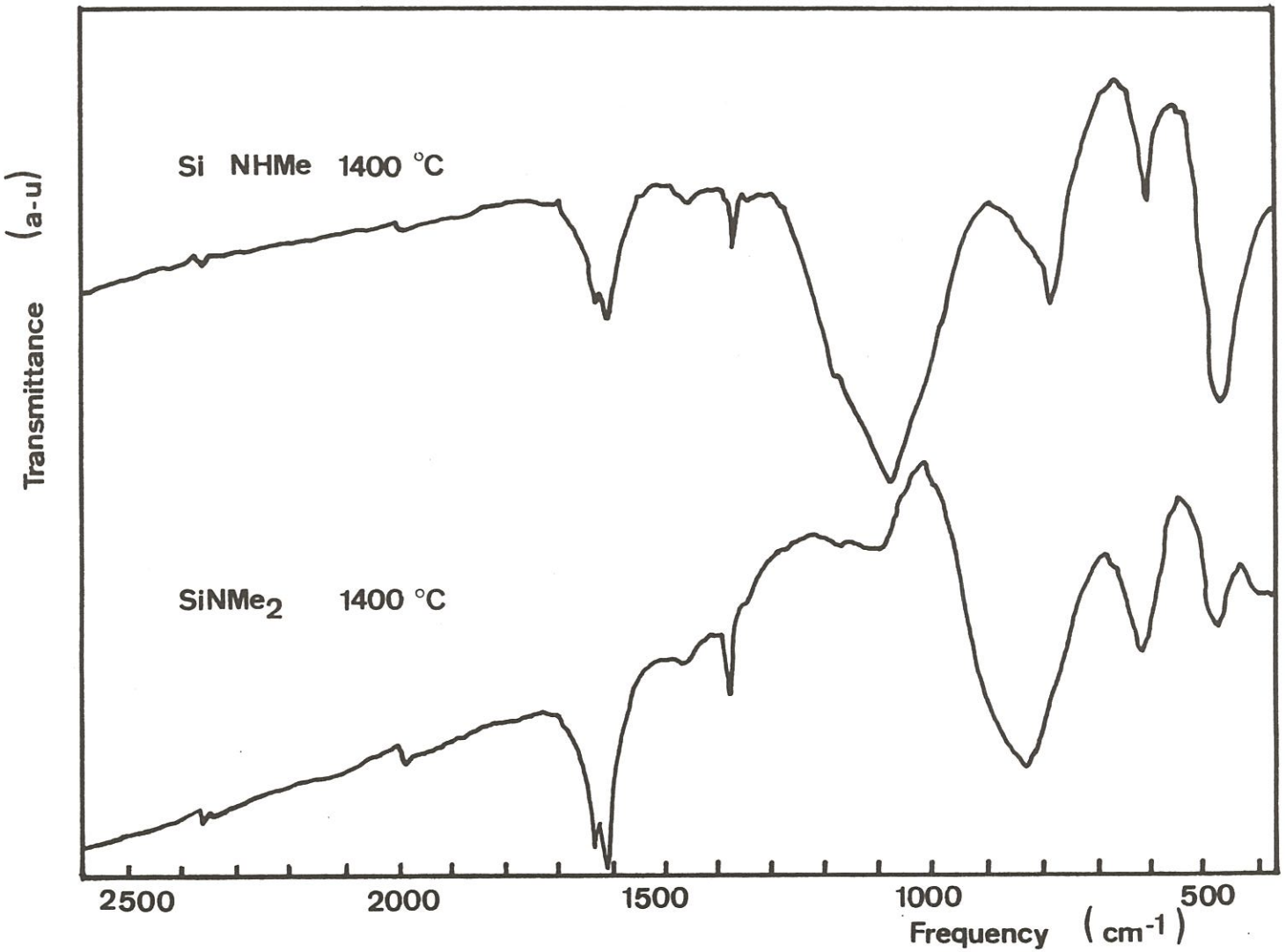

Fig. 10 : IR spectra of the SINHMe and SINMe2 precursors pyrollysed at 1400°C

the pyrolysis of $SiNMe_2$, from the strong absorption band at 830 cm^{-1} assigned to tetrahedral Si-C bonds. As discussed above, the weak absorption bands at 490 cm^{-1} and 1100 cm^{-1} could be assigned to Si-N and Si-O bonds (fig. 10). Furthermore, on the basis of the results of a study by M. Guiliano et al. the absorption bands at 1600 and 1380 cm^{-1} could be assigned respectively to C = C bonds in aromatic cycles and to CH_3 [65].

4.2 - Elemental Analysis of the Pyrolytic Residues

4.2.1 - Overall elemental analyses

The chemical compositions of the solid residues formed during the pyrolysis of the PCS and PCSZ precursors at 1200°C are given in table V and suggest the following remarks :

(i) it is noteworthy that **hydrogen** is still present in the material even for T_p = 1200°C, i.e. at a temperature well above the end of the organometallic/inorganic transition (these amount of hydrogen could contribute to the stabilization of "amorphous" SiC states as already known for amorphous silicon).

(ii) all the solid residues contain **significant amounts of oxygen** (very likely bonded to silicon). Since the initial PCS and PCSZ contain about 3 wt. % of oxygen, this feature suggests that only part of the contamination by oxygen occurs during the pyrolysis experiments themselves due to : (1) the high affinity of PCS and PCSZ for oxygen and moisture and (2) the small volume of the samples submitted to pyrolysis with respect to the volume of gas adsorded on the inner parts of the pyrolysis apparatus [64]. Less contamination by oxygen would have been observed with larger samples.

(iii) finally, assuming that oxygen and nitrogen are bonded to silicon as binary SiO_2 and Si_3N_4 species, i.e. neglecting the occurence of ternary or quaternary silicon-based species, the data given in table V suggest that the pyrolytic residues formed at 1200°C may contain significant amounts ot free carbon.

Precursors	Si (at %)	C (at %)	N (at %)	O (at %)	H (at %)
$SiNMe_2$	30.0	42.6	10.5	13.9	2.8
SiNHMe	30.8	42.2	11.5	14.5	1.8
SiNHSi	30.7	39.9	12.3	14.2	2.3
Si-Si (Na,s)	32.3	42.8	-	24.4	1.0
SiOSi	31.7	42.2	-	23.0	2.1
Si-H (*)	32.5	43.3	-	21.2	2.9

(*) heated at 450°C in autoclave and then pyrolysed at 1200°c

Table V : Chemical composition of the solid residues of PCS and PCSZ precursors pyrolysed at 1200°c

4.2.2 - ESCA analyses

Generally speaking, the ESCA spectra of the inorganic residues formed by pyrolysis of one PCS and one PCSZ precursors exhibit sharp peaks which have been assigned to silicon (Si 2s and 2p), carbon (C 1s), oxygen (O 1s) and nitrogen (N 1s), as illustrated in fig. 11 and 12. Furthermore, these peaks when recorded in the high resolution mode can be used after deconvolution, to assess the nature and relative amounts of the chemical bonds. As a matter of fact, each peak (i.e. Si 2p ; C 1s and N 1s) recorded for these ex-PCS or ex-PCSZ solids, could be analysed on the basis of the same components but with different intensities (fig. 13-14) :

(i) the Si 2p peaks exhibit three components. The first, at 98 eV (or 100.8 eV when charge effect correction is applied) is assigned to the Si-C bond in silicon carbide. The second at 100.8 eV (or 103.5 eV after correction) is related to the Si-O bond in silica. Finally, the third which falls at an intermediate position in the binding energy axis, could be assigned to a silicon atom either bonded simultaneously to both carbon and oxygen atoms (ex-PCS) or as well as to nitrogen atoms (ex-PCSZ).

(ii) the C 1s peaks exhibit also at least two components. The first at 279,7 eV and the second at 281,1 eV (or 282,7 and 284,1 eV after correction) are assigned to the C-Si bonds in SiC and C-C bonds (and to a less extent to C-H bonds) in free carbon, respectively. The others components at higher position on the bending energy axes could be related to C-O bonds from CO and CO_2 molecules adsorbed on the sample surface (due to an insufficient cleaning treatment of the surface prior to the analysis).

(iii) the analysis of the N 1s peaks (for the ex-PCSZ) shows a component at 394,5 eV (see fig. 14) corresponding to a binding energy similar to that characterizing the Si--N bonds in Si_3N_4. This result suggests that nitrogen is mainly bonded to silicon in the ex-PCSZ as it is in silicon nitride.

(iv) finally, the analysis of the O 1s peaks could not be performed due to too small chemical shifts among the binding energies related to the different oxygen-containing species.

Despite the complexity of the Si 2p ; C 1s and N 1s peaks due to that of the materials themselves, the elemental composition of the ex-PCS and

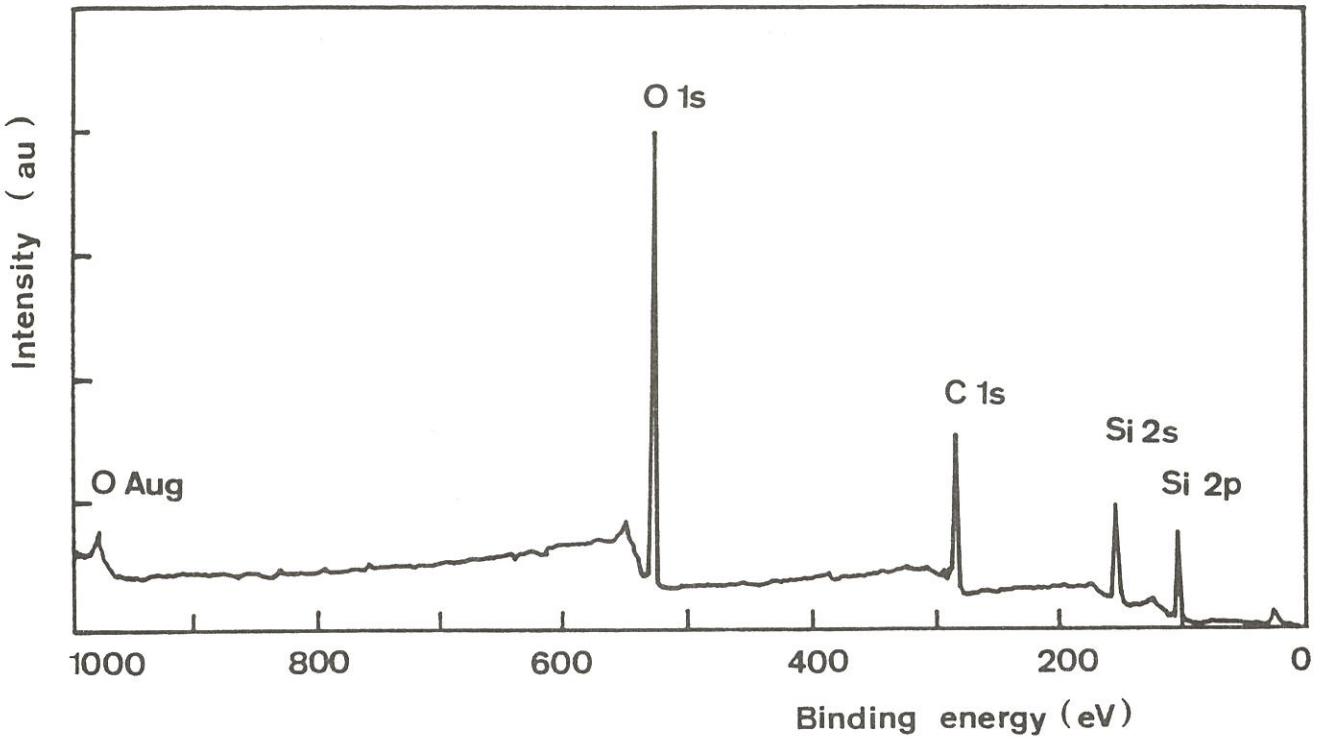

Fig. 11 : ESCA spectrum of ex- Si-Si (Na,s) pyrolytic residue (T = 1200°C)

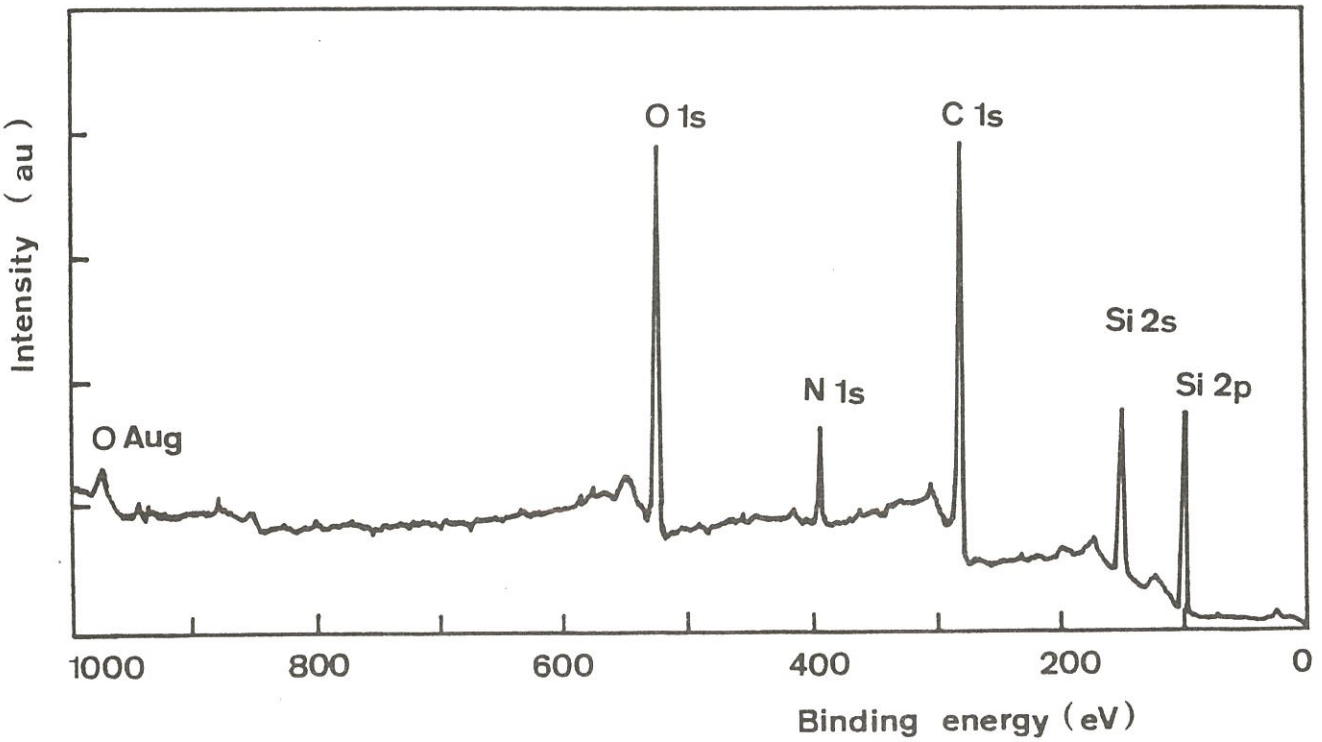

Fig. 12 : ESCA spectrum of ex- SiNHMe pyrolytic residue (T = 1200°C)

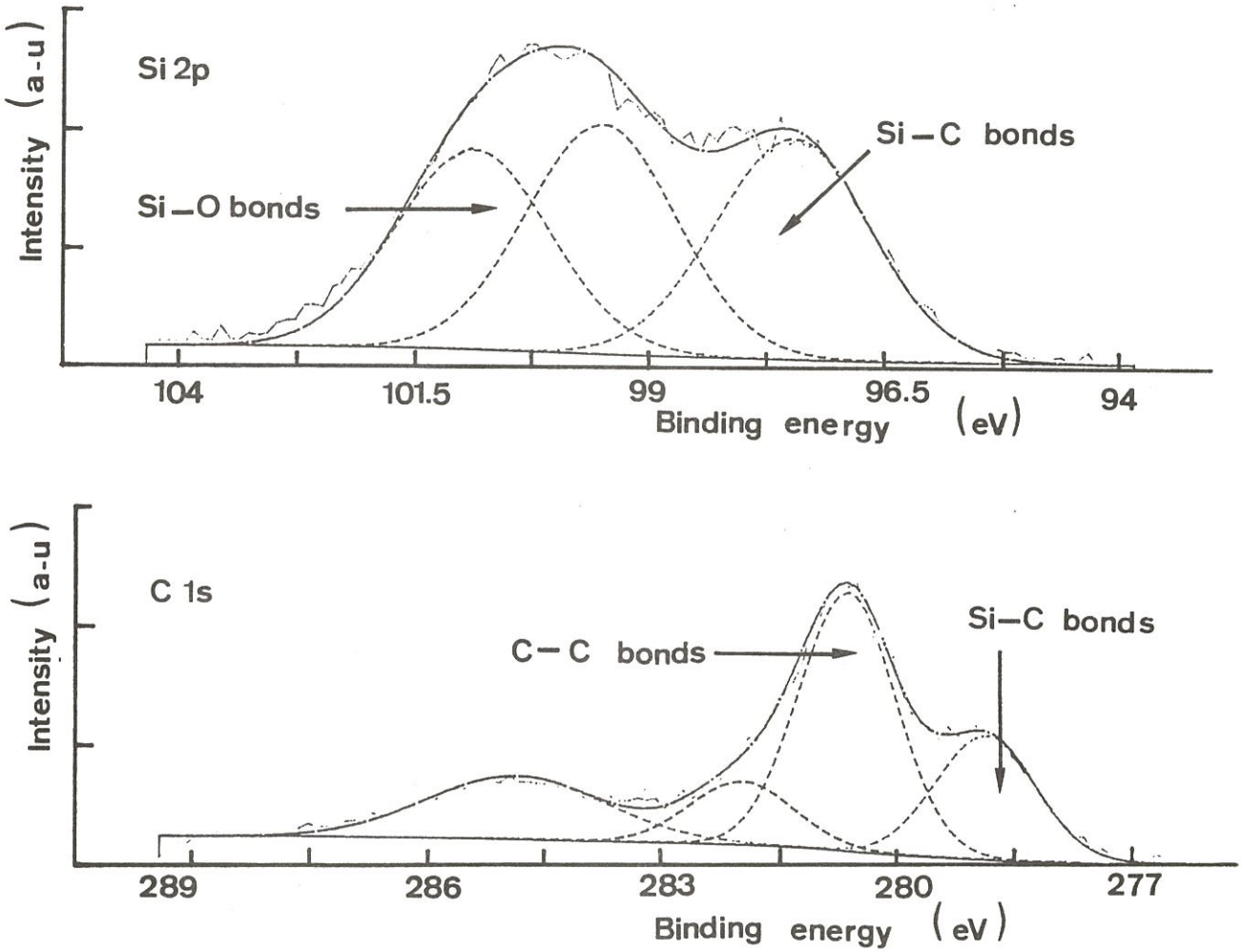

Fig. 13: Deconvolution of the ESCA Si2p and C1s peaks of ex-Si-Si (Na,s) pyrolytic residue (T = 1200°C).

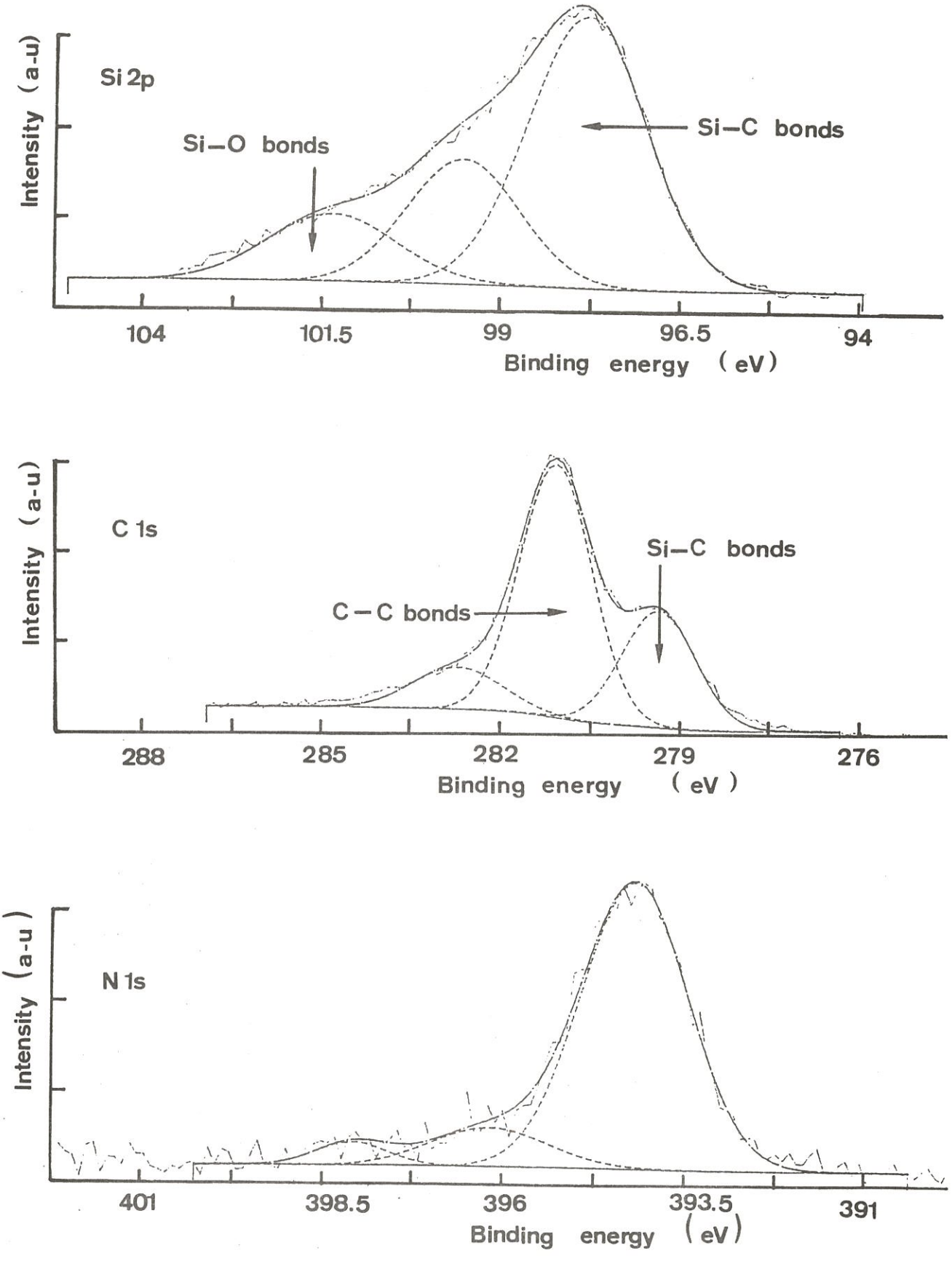

Fig. 14 : Deconvolution of the ESCA C1s, Si2p and N1s of ex-SiNHMe pyrolytic residue (T = 1200°C)

ex-PCSZ residues (for Tp = 1200°C) were assessed, semi-quantitatively, from the peak component intensities. The results of the calculations are given in table VI as : (i) the atomic percentages of silicon, carbon, nitrogen and oxygen present in the various materials and (ii) for each element, the atomic percentages of that element involved in each chemical bond discussed above. The calculations have taken into account the occurence of complex intermediate species. Such complex species have been already mentioned by E. Bouillon et al. [64], L.C. Sawyer and al. [66] or J. Lipowitz and al. [53] and are referred to SiOxCy or Si-X, for the rather simple case of the ex-PCS solids. An oxycarbide phase has been very recently identified by ESCA analyses in NICALON fibers themselves [39,67]. The situation is still more complicated for the ex-PCSZ solids due to nitrogen. On the one hand, it seems well established that a significant amount of nitrogen is bonded to silicon as it is in Si_3N_4 (i.e. as SiN_4 tetrahedron) (fig.14). On the other hand, a small amount of nitrogen also may be involved in complex SiOxNy or $SiOxCyN_z$ tetrahedral species. The chemical shifts related to these complex tetrahedral species remain unknown but probably fall within a binding energy range limited by SiO_2 and SiC, as schematically shown in fig. 15. As a result, the intermediate component observed by deconvolution of the Si 2p peak may be a mixture of different complex tetrahedral species, a feature which makes a quantitative analysis very difficult.

The contamination by oxygen of the ex-PCS and ex-PCSZ solids already established from the results of the overall chemical analysis, is clearly apparent from table VI. the higher oxygen percentages obtained from ESCA peaks could be explained by the occurence of oxygen-containing molecules adsorbed on the sample surface, as discussed above.

Surprisingly, the deconvolution of the Si 2p peak observed for the ex-SiOSi solid did not led to an intermediate component (related to ternary tetrahedral SiCxOy species) between those assigned to the Si-C and Si-O bonds, as shown in fig. 16. This result suggests that the Si-O bonds which are initially present in the SiOSi precursor may directly give rise to tetrahedral SiO_4 species in the pyrolytic residue. Therefore, the ternary tetrahedral SiCxOy species which are observed in some of the other pyrolytic residues may have their origin in C-Si-O bonds formed during the synthesis or/and at the beginning of the pyrolysis of those precursors.

Finally, the chemical composition of the ex-PCS and ex-PCSZ pyrolytic residues expressed as SiC ; "SiO_2" ; free carbon and Si_3N_4 weight

Nature of the precursor	Si (at. %)			C (at. %)			N (at. %)		O (at. %)
	Si-C	Si-X	Si-O	C-Si	C-C C-H	C-O C=O	Si-N	(1)	
$SiNMe_2$		23.9			44.5		7.2		25.3
	14.6	6.7	2.6	10.3	29.4	4.8	6.4	0.8	
SiNHMe		25.6			36.6		5.5		32.2
	13.8	6.7	5.1	10.8	21.8	4.0	4.5	1.0	
SiNHSi		25.1			37.8		6.1		30.7
	14.6	6.1	4.4	10.6	22.6	4.6	5.0	1.1	
Si-Si (Na,s)		21.4			31.9		-		46.8
	7.4	7.4	6.6	7.3	13.9	10.7	-	-	
SiOSi		23.7			30.6		-		45.6
	10.7	-	13.0	8.4	16.7	5.53	-	-	45.6

Table VI : Elemental atomic percentages (overall and per chemical bond) in the inorganic solids resulting from the pyrolysis at 1200°C of PCS and PCSZ precursors, as semi-quantitatively derived from the component intensities of ESCA peaks.

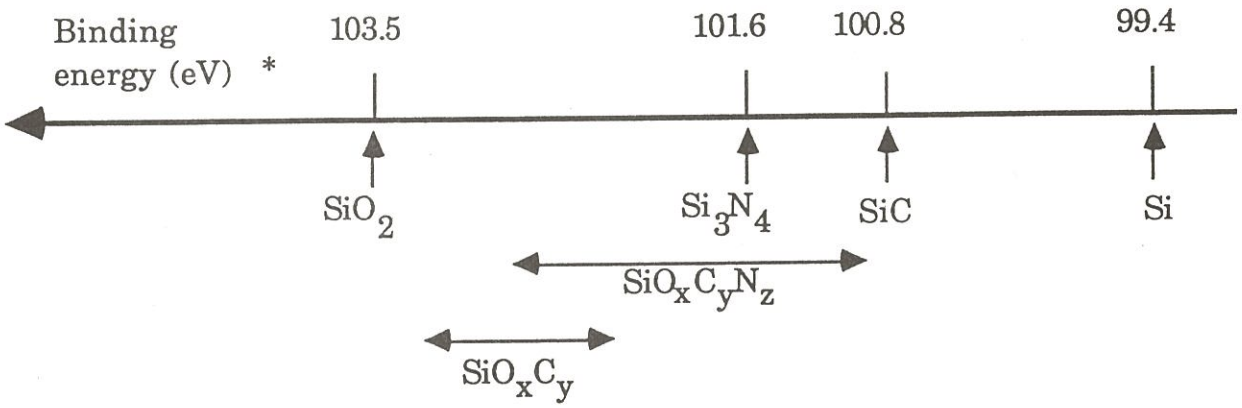

(*) Charge effect correction is applied

Fig. 15 : Binding energies (Si2p) in binary and ternary tetratredral species containing silicon (schematic), as derived from ESCA analysis.

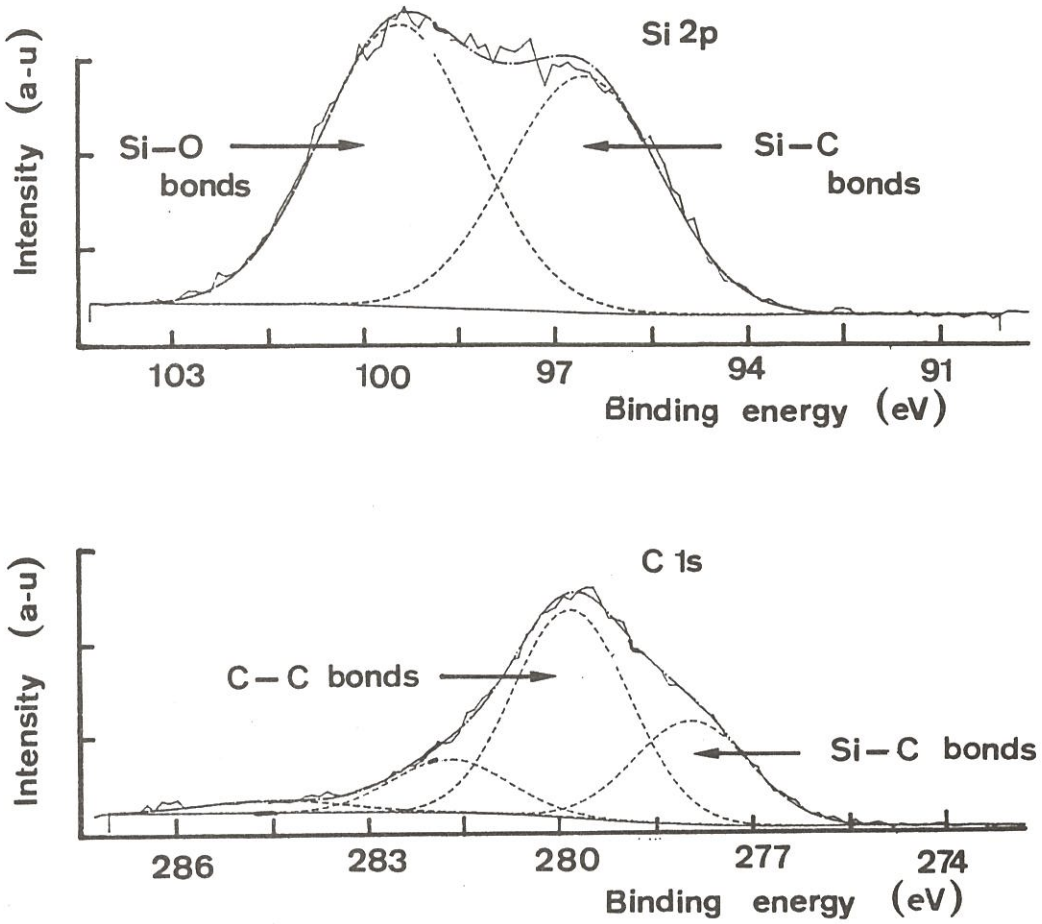

Fig. 16 : Deconvolution of the ESCA Si2p and C1s peaks of ex-SiOSi pyrolytic residue (T = 1200°C).

percentages, was derived from the ESCA data, neglecting the occurence of the ternary or quaternary tetrahedral species. The amounts of SiC ; SiO_2 and free carbon were calculated from the Si 2p and C 1s peak components and that of Si_3N_4 from the N 1s peak, as discussed above. The results are given in table VII for the inorganic residues resulting from the pyrolysis at 1200°C of Si-Si (Na,s) ; SiNHSi ; SiNHMe and $SiNMe_2$ precursors. It clearly appears that the SiC percentage in inorganic residue is almost the same whatever the nature of the precursor. Furthermore, the SiO_2 and free carbon percentages calculated for the ex-$SiNMe_2$ pyrolytic residue are respectively lower and higher than those obtained for the other materials. This result could be explained by the fact that the $SiNMe_2$ precursor has a lower cross-linking capability and then less sites to fix oxygen atoms during the first part of the pyrolysis, i.e. between 200 and 500°C.

4.3 - Structure and Microstructure of the Pyrolytic Residues

4.3.1 - From XRD analyses

When heated for one hour **under argon flow** (P = 100 kPa), according to a procedure described elsewhere [64], the solid residue resulting from the organic/inorganic transition remains **amorphous** up to 1400°C for SiNHSi ; SiNHMe and $SiNMe_2$ precursors, as shown in fig. 17 and 18a. In constrat, when treated under the same conditions, the pyrolytic residue of the Si-Si (Na,s) precursor is characterized by broad XRD lines : three assigned to cubic β-SiC ((111) ; (220) and (311)) and one (002) to pyrocarbon, as shown in fig. 19. As a matter of fact, the state of crystallization in this latter case is comparable to that of the NLM 202 NICALON fiber (obtained from a related PCS precursor), the apparent mean grain size (calculated according to the Scherrer's equation) being of the order of 3 nm. When heated at higher temperatures, e.g. 1600°C, the ex-Si-Si (Na,s) ceramic is better crystallized, as shown by narrower XRD peaks and a larger mean grain size (15 nm).

Furthermore, thermal treatment at 1400°C (duration : 1 h) when performed **under high vacuum** (133.10^{-6} Pa) led, for all the nitrogen-based precursors, to ceramics in which the β-SiC phase is well crystallized (mean grain size larger than 100nm), as shown in fig. 18 b for $SiNMe_2$. Moreover, under these conditions, the oxygen concentration in the pyrolytic residue is

Nature of the precursor	SiC (wt. %)	SiO_2 (wt. %)	C (wt. %)	Si_3N_4 (wt. %)
Si-Si (Na,s)	34	23	20	-
SiNHSi	38	23	24	14
SiNHMe	38	26	23	13
$SiNMe_2$	38	13	31	17

Table VII : Massic concentrations of the various species present in inorganic residues obtained by pyrolysis at 1200°C of some PCS and PCSZ precursors, as calculated from the results of ESCA analysis (neglecting the occurence of complex tetrahedral ternary or quaternary species)

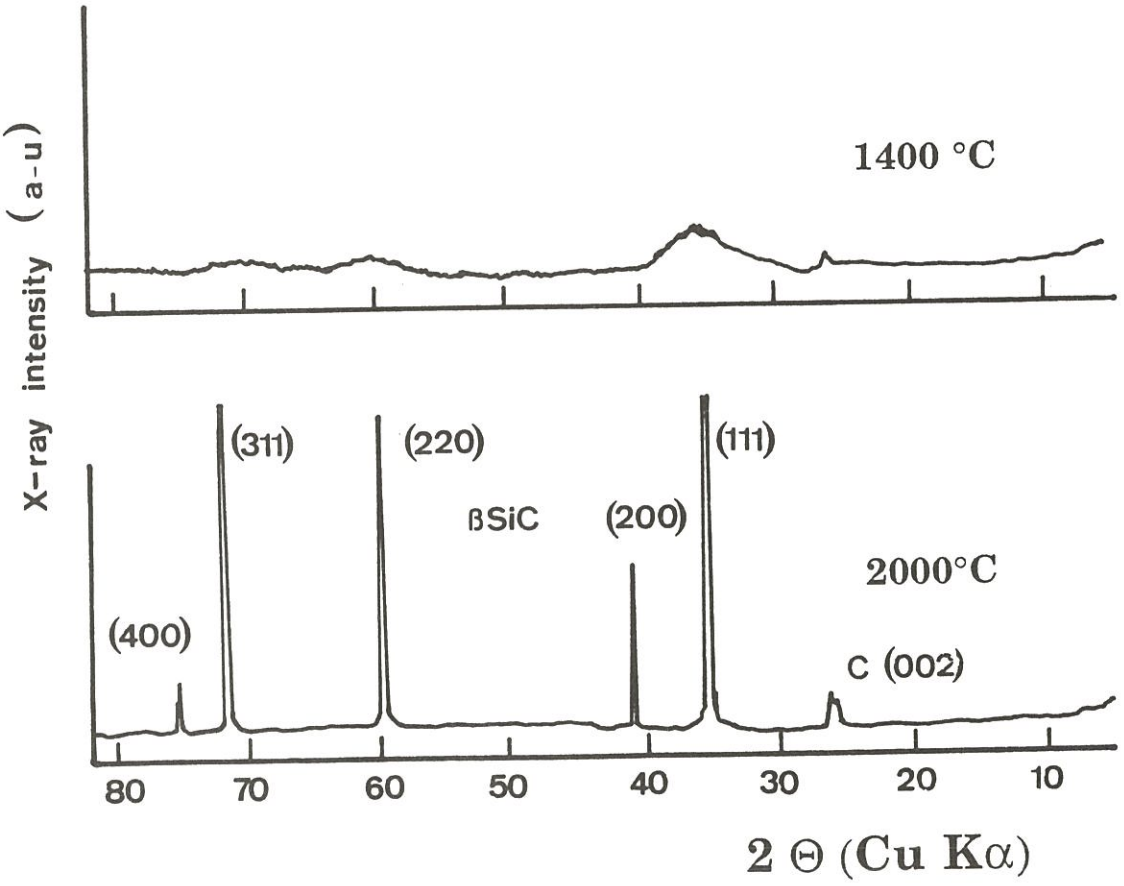

Fig. 17 : X-ray diffraction patterns of the solid resulting from the pyrolysis of SiNHSi under argon flow.

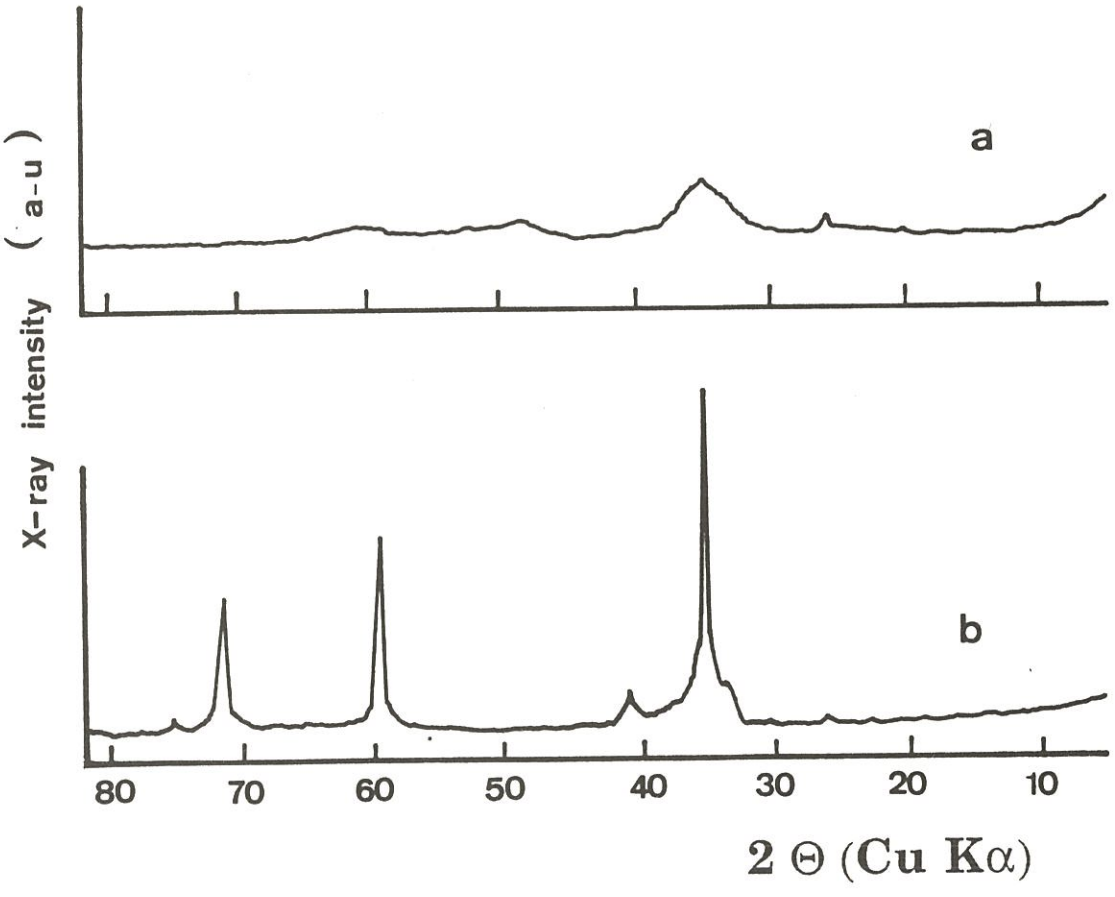

Fig. 18 : X-ray diffraction patterns of the solid resulting from the pyrolysis of SiNMe2 : a) under argon flow at 1400°C
b) under vacuum (133.10^{-6} Pa at 1400°C)

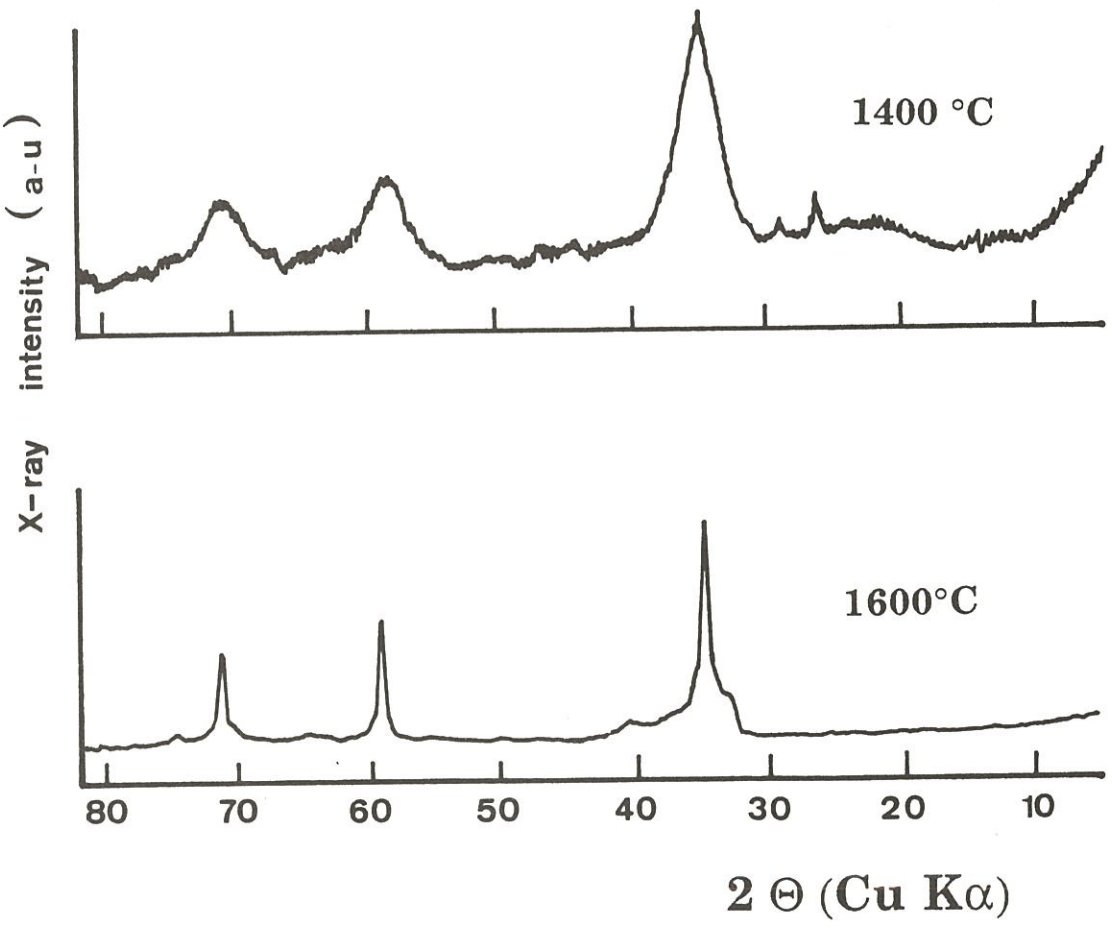

Fig. 19 : X-ray diffraction patterns of the solids resulting from the pyrolysis of Si-Si (Na, s) precursors, under argon flow.

only 8 at. % (instead of 14 at.% when treated under argon flow). From these results, it seems that the simultaneous presence of the oxygen and nitrogen heteroatoms inhibits the grain growth of β-SiC.

As could be expected, a thermal treatment performed under argon flow at very high temperatures, i.e. 2000°C, still improves the state of crystallization of the β-SiC phase, as shown in fig. 17 for SiNHSi. However, even under such conditions the XRD lines of Si_3N_4 are not observed. On the contrary, the 002 line of carbon is clearly present with a d value of 3.42 Å. Assuming that d(002) is respectively equal to 3.44 Å for a fully disordered carbon and 3,35 Å for graphite, the degree of disorder g of a carbon is often defined as [68] :

$$g = 1\,[\,(3.44 - d(002)obs.)/(3.44 - 3.35)] \qquad (1)$$

on the basis of the d value measured from XRD pattern shown in fig. 17, the degree of disorder of carbon in the ex-SiNHSi ceramic treated at 2000°C under argon, as calculated from equation (1) is only 20 %. Furthermore, the apparent mean grain size along the c-axis, as calculated from the 002 peak width at mid-height according to the Scherrer's relation, is of the order of 9 nm, a value which corresponds to a stack of about 25 graphitic layers. Therefore, one may conclude assuming that the carbon phase in ceramics derived from nitrogen-containing precursors is rather well crystallized when they have been treated at 2000°C under argon flow.

4.3.2 - From Raman Spectroscopy Microanalysis (RSMA)

Raman spectroscopy is known to be a suitable method to characterize poorly crystallized solids (e.g. materials prepared at low temperatures). As an example, it has been used to study SiC CVD-filaments [69-70] as well as SiC-based yarn fibers derived from PCS-precursors [71]. It has been particularly successful in the characterization of the poorly graphitized carbon which is present in such materials.

In the present study, the RSMA has been used to characterize the ceramics obtained by pyrolysis of various PCS (i.e. Si-Si (Na,s)) and PCSZ (i.e. SiNHSi ; SiNHMe and $SiNMe_2$) precursors, performed at 1400°C under argon flow (100 kPa). The duration of the thermal treatment at 1400°C was one hour. Some of the Raman spectra are shown in fig.20. Their main

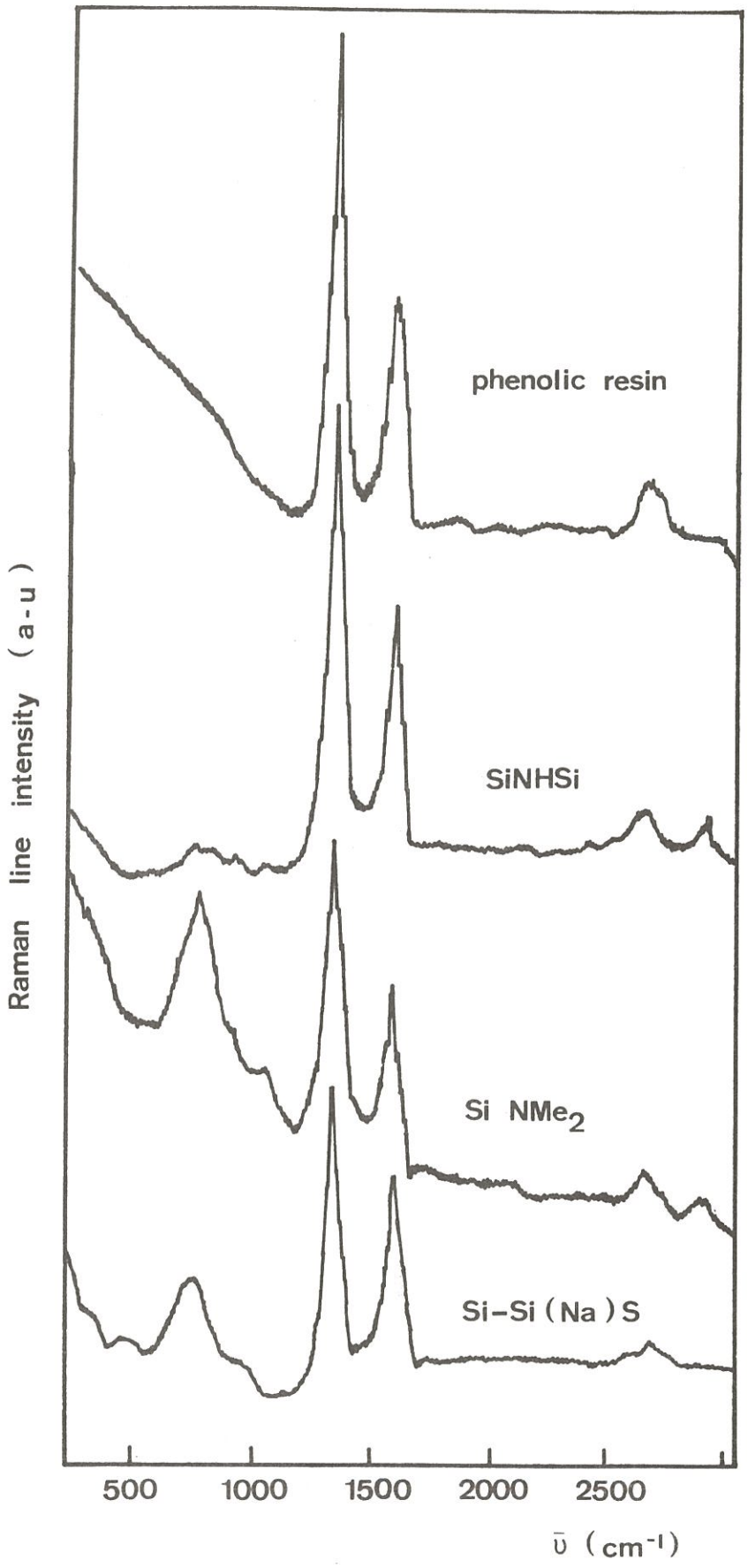

Fig. 20 : Raman Spectra of the residues resulting from the pyrolyses at 1400°C of various precursors.

features are : (i) two strong peaks between 1300 and 1600 cm^{-1}, (ii) one (or two) weak peak(s) between 2500 and 3000 cm^{-1} and (iii) a complex broad band between 500 - 1000 cm^{-1} whose shape and intensity are different from one material to another.

The above mentioned peaks in (i) and (ii) were assigned to **free carbon** by reference to litterature [72- 76]. On the contrary, the assignment of that (or those) falling in the 500 - 1000 cm^{-1} range remains uncertain as discussed below. Since the Raman peaks due to carbon were known to be sensitive to the degree of graphitization of carbon [75], the residue of the organometallic/inorganic transition for SiNHMe was heat treated under argon flow at increasing temperatures up to 2300°C. The corresponding Raman spectra, given in fig. 21, show that the heat treatment has : (i) modified the intensity and width of all the peaks and (ii) resulted in slight shifts of their positions in the wave number scale (tableVIII). It appears from litterature, that most of these features may be related to the graphitization of the poorly crystallized carbon formed during the organometallic/inorganic transition, as discussed below.

It is usually admitted that graphitization **takes place mainly in two steps** : stage I (extension of the ordering within the graphitic planes) and stage II (ordering of the graphitic layers along the c-axis) [75]. The Raman spectrum of a pyrolytic carbon is made of two peaks of strong intensity at 1350 and 1600 cm^{-1} (first order) and one broad peak of much weaker intensity at 2700 cm^{-1} (second order). As the degree of graphitization increases ; (i) the intensity of the 1350 cm^{-1} peak (due to grain size effects) progressively decreases to become nil, (ii) the E_{2g} peak is shifted from 1600 to 1580 cm^{-1} (as a matter of fact this peak is a doublet : the intensity of its 1600 cm^{-1} component increases, as graphitization proceeds) and (iii) the peaks become sharper [75].

As shown in fig. 20, the Raman spectrum of carbon present in the pyrolytic residues of PCS and PCSZ **obtained at 1400°C** is similar to that of carbon resulting from the pyrolysis of a phenolic resin (performed under the same conditions). From the position of the 1350 cm^{-1} peak (which is still higher than that of the E_{2g} peak, as shown in fig.20), one could conclude that such a carbon is in a state of graphitization corresponding to the beginning of stage I. However, for this state of graphitization, the spectrum should exhibit only one broad peak (reported to be as broad as 140 cm^{-1} [75]) in the second order at 2700 cm^{-1} whereas our data (fig. 20 ; table VIII)

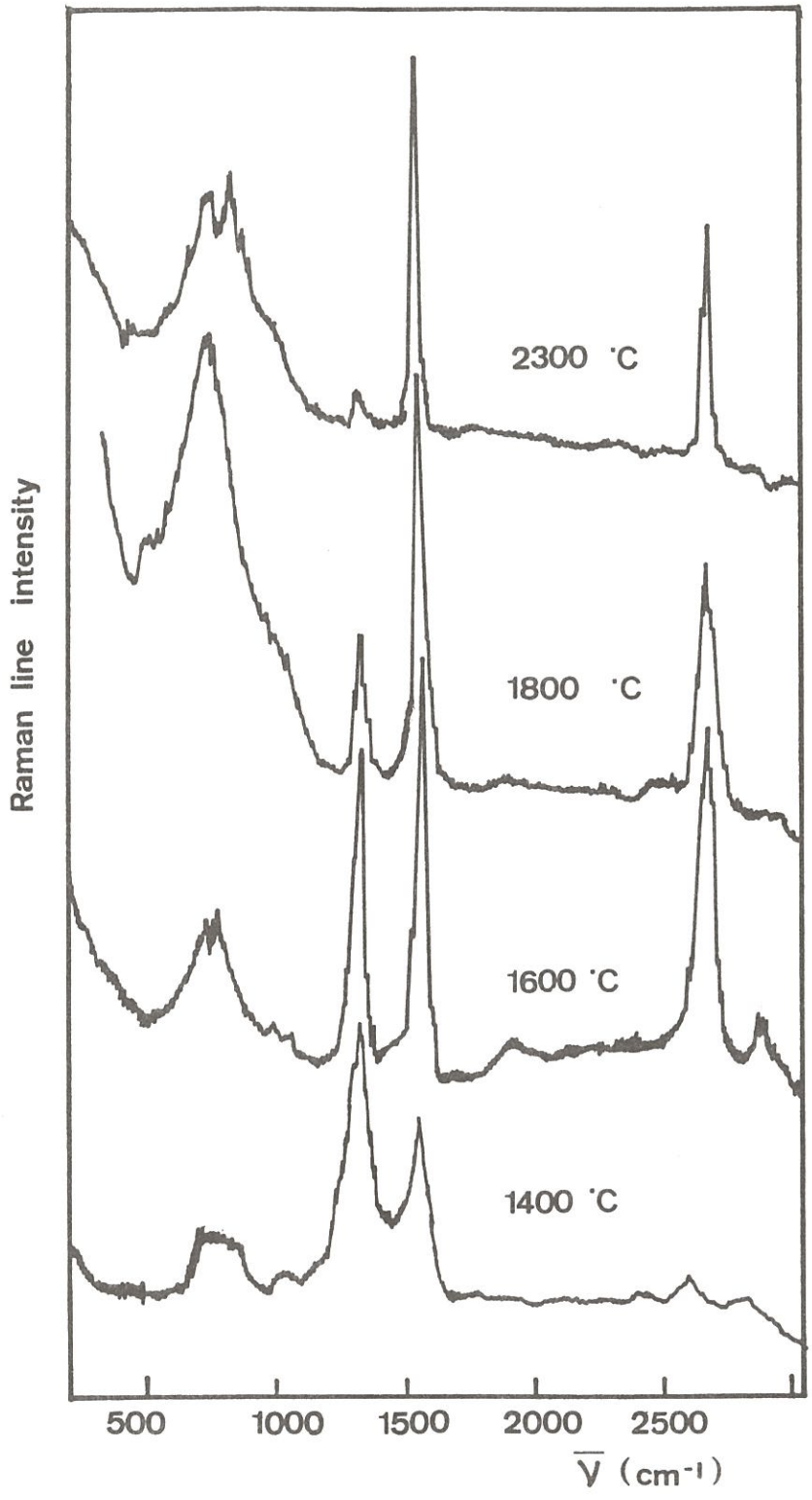

Fig. 21 : Evolution with Tp of the Raman spectra of the solid residue resulting from the pyrolysis of the SiNHMe precursor.

Nature of the precursor	T(pyr.) (°C)	Wave number ν (cm^{-1})					
		(a)		(b)		(c)	
Phenolic resin	1400	-	-	1350	1590	2700	
Si-Si (Na,s)	1400	750	950	1350	1600	2650	2890
$SiNMe_2$	1400	780	1000	1350	1590	2650	2890
SiNHSi	1400	780	910	1350	1605	2650	2905
SiNHMe	1400	750	-	1350	1600	-	
	1600	780	-	1350	1585	2670	2870
	1700	700	-	1350	1580	2670	
	1800	800	1080	1350	1580	2694	
	2000	800	1100	1350	1575	2694	
	2300	780	980	-	1580	2720	

Tabl VIII : Wave number of the Raman peaks for solid residues resulting from the pyrolysis of various precursors in wave number ranges that may correspond to : silicon carbide (a), carbon first order (b) and carbon second order (c)

support rather the occurence of two peaks, at 2650 and 2890 cm^{-1} respectively.

The spectra shown in fig. 21 clearly illustrate the progression of **the graphitization of carbon** (mainly stage I), in the ex-SiNHMe residues, as the temperature of pyrolysis is raised from 1400 to 2300°C which results in : (i) a decrease in intensity of the 1350 cm^{-1} peak (the intensity being almost nil for 2300°C) and (ii) a shift of the E_{2g} peak from 1600 to 1580 cm^{-1} (as soon as the temperature of pyrolysis is higher than 1700°C).

On the other hand, the occurence of the second stage in the graphitization process (stage II) of carbon in ex-SINHMe residues is not as well supported by the Raman spectroscopy data (although, our XRD data suggest a rather high degree of graphitization for materials treated at 2000°C, as discussed above). According to A. Marchand et al. the occurence of stage II can be assessed from a detailed analysis of the Raman peak at 2700 cm^{-1}. As a matter of fact, this peak is doublet. One of its component, with a strong intensity, is shifted from 2700 to 2730 cm^{-1} and the other, of weaker intensity, is shifted from 2680 to 2690 cm^{-1}, as graphitization proceeds to completion. Thus, there is a wave number gap of about 50 cm^{-1} between the two component for well graphitized carbons [75]. The data given in table VIII show that : (i) there is indeed a shift of the second order peak of carbon as the temperature of pyrolysis increases but (ii) this peak, if it is a doublet, remains unresolved even at 2300°C.

The graphitization of carbon in ex-PCS or ex-PCSZ residues can be followed, as it proceeds, by plotting the variations of the Raman peaks intensity ratios,i.e. I(1350)/I(1600) and I(2700)/I(1600), versus the pyrolysis temperature. It is noteworthy that the accurate measurement of the intensity of the Raman peaks is particularly difficult for carbon (since the orientation of the carbon microcrystals with respect to the Laser beam must be taken into account due to polarization effects). Therefore, the measurements have been performed, for each pyrolysis temperature, on several samples. The data, shown in fig. 22, illustrate the progression of the graphitization process with a singularity for a pyrolysis temperature of 1700-1800°C.

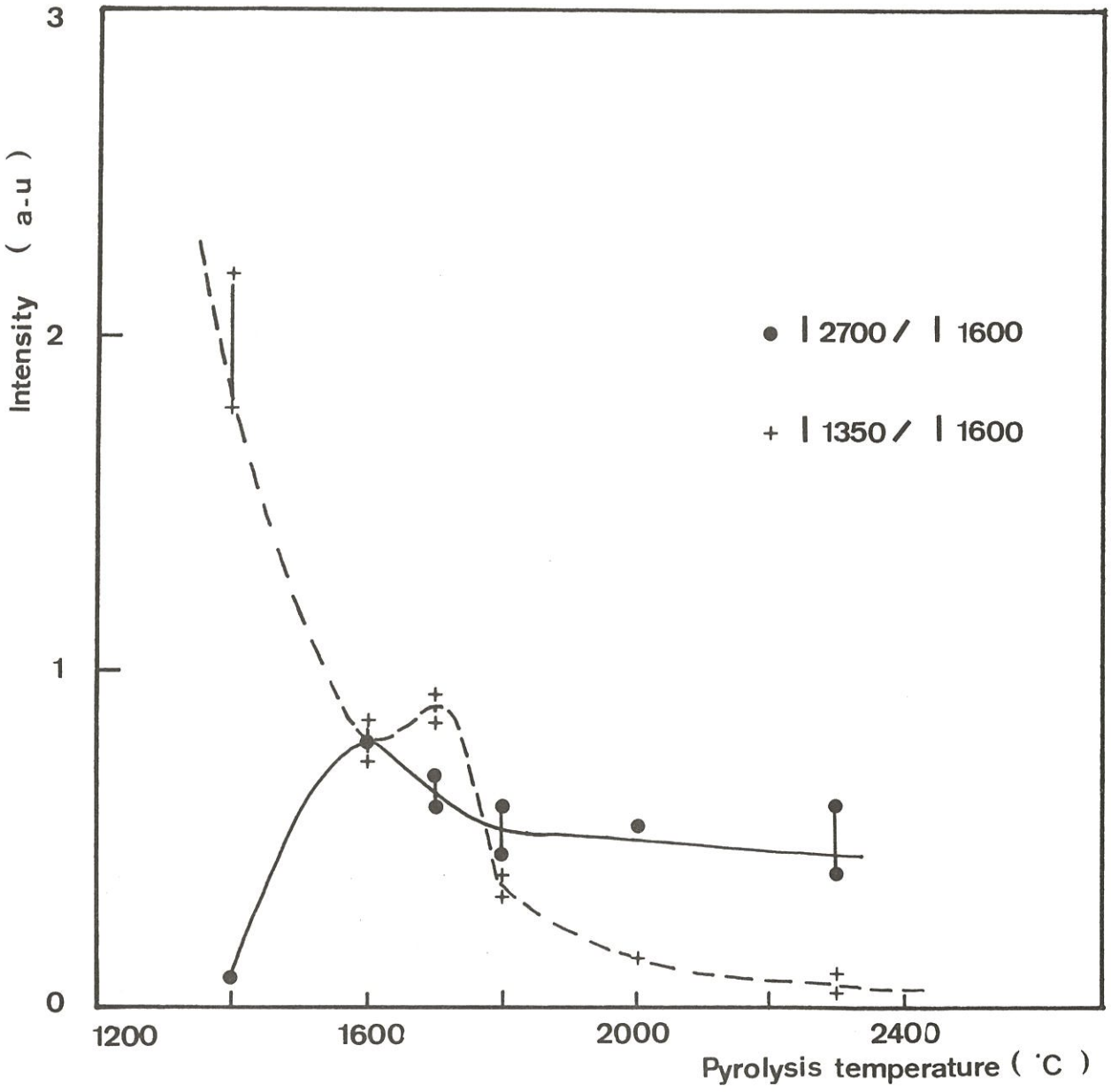

Fig. 22 : Evolution with Tp of the I_{2700}/I_{1600} and I_{1350}/I_{1600} ratios for the solid residues resulting from the pyrolysis of the SiNHMe precursor

Generally speaking it seems, from the above discussion, that the graphitization process of the carbon phase present in small amount in the pyrolytic residues of PCS and PCSZ precursors does not exactly proceeds as for pure carbon. This difference could be related to the presence of heteroatoms (e.g. oxygene, nitrogen or silicon) which may alter the vibrations of the C-C bonds in their vicinity. As schematically shown in fig.23, a heteroatom X can be bonded either to a carbon atom located within a graphite layer (position I) or to a carbon located at a layer edge (position II). In the first case, the heteroatom would have an effect on the stage II of graphitization (and on the second order Raman spectrum) while in the second, the effect would be rather on the stage I (and on the first order Raman spectrum).

As previously mentioned, the assignment of the broad peak(s) present in the 400-1100 cm^{-1} range, to silicon carbide remains uncertain particularly at low T_p values (e.g. 1400°C). According to a study by Y.Sasaki et al. on ex-PCS fibers, the Raman spectrum of the 3C polytype of SiC (the most commonly observed from SiC below 2000°C) is made of two broad bands at 400 and 800 cm^{-1} (whose widths may reach 600 cm^{-1} for T_p <1400°C and are still of the order of 200 cm^{-1} for $T_p \leq 1500°C$), on the one hand, and of two sharp peaks at 795 and 975 cm^{-1} (observed when the grain size becomes larger than 10 nm), on the other hand [72]. Futhermore, silica itself gives rise to a Raman spectrum with two peaks falling in the same wave number range, i.e. at 500 and 1100 cm^{-1}. Finally,the Raman spectrum of amorphous silicon nitride is also characterized by two peaks, very broad at 400 and 900 cm^{-1} [71].

As shown in fig. 20, the Raman spectra of the ex-Si-Si (Na,s) and ex-SiNMe residues obtained at 1400°C do exhibit several broad peaks of significant intensity in the 400-1100 cm^{-1} range. On the contrary, these peaks are almost inexistent in the related ex-SiNHSi residue. Although an accurate assignment of the peaks cannot be done, as discussed above, the lack of sharp peaks at 795 and 975 cm^{-1} suggests that silicon carbide formed at this temperature remains poorly crystallized as observed by XRD.

When the temperature of pyrolysis raises, the intensities of the peaks in the 400-1100 cm^{-1} range increases (fig.21). Above 1600°C, a peak of strong intensity, but which remains rather broad, is observed at 800 cm^{-1} with a shoulder on its right hand side at 1000 cm^{-1}. This peak could be assigned to silicon carbide.

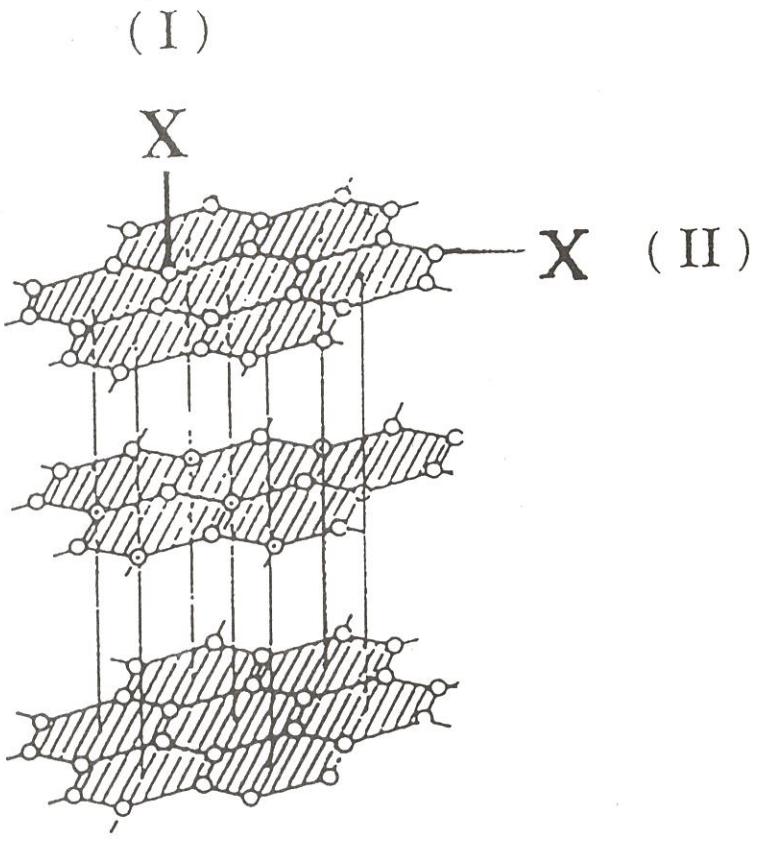

Fig. 23 : Possible locations of heteroatoms X in the crystal structure of graphite-like carbons.

5 - CONCLUSION

From the above results and discussion, the following conclusions can be drawn concerning the relations that may exist between PCS (or PCSZ) precursors and their residues of pyrolysis :

(i) As already suggested by C.L. Schilling et al., a PCS precursor with a **linear structure** (e.g. the Si-H model precursor) does not lead to a high inorganic residue by pyrolysis under an argon pressure of one atmosphere. Under these conditions, the linear polymeric chain is progressively broken into short fragments which give rise to an evolution of low boiling point species (presumably according to rearrangements involving free radicals). Therefore, such polymers must be submitted to a **cross-linking treatment** (which could be performed either thermally or chemically) before pyrolysis, to increase the ceramic yield . Such a treatment is known to be an important step in the S. Yajima's route to ex-PCS fibers. The ceramic yield will be high when the precursor will contain strong chemical bonds (e.g. Si-O bonds), when the degree of cross-linking will be sufficient or more generally speaking, when the precursor will exhibit a marked ability to give rise to a three dimensional polymeric network at the beginning of the pyrolysis (which is actually the case for the SiNHSi model precursor with respect to the other nitrogen-containing precursors here studied).

(ii) Precursors with a high percentage of organic carbon do not necessarily lead to ceramics with a high percentage of **free carbon**. As a matter of fact, the result depends strongly on the thermal stability of the hydro carbon linkages which have been introduced into the precursor.

(iii) Introducing **nitrogen** in the organometallic precursors (PCSZ precursors) results in ceramics containing significant percentages of nitrogen which is thought to be bonded to silicon (as Si_3N_4 or more probably as oxycarbide or oxycarbonitride tetrahedral species). In such ceramics, nitrogen seems to act as **an inhibitor** with respect to the recrystallisation mechanisms. As a result, the ex-PCSZ ceramics are thought to keep their poorly crystallized microstructure (known to be responsible for high

strength in the fibrous materials) at temperatures higher than those previously reported for ex-PCS ceramics (e.g. Nicalon-type fibers).

(iv) **Free carbon**, in ceramics obtained by pyrolysis of PCS or PCSZ precursors at 1400°C, has some common structural and microstructural features with carbon resulting from the pyrolysis of a phenolic resin. Its graphitization (mainly stage I) is effective at 1800-2000°C.

(v) Generally speaking, the main chemical bonds from the initial polymeric skeleton are not all maintained in the inorganic solid obtained by pyrolysis. As an example, the Si-Si bonds present in the various Si-Si precursors are no longer observed in the residues of pyrolysis.

(vi) The Si-O-Si chemical bridges from polysiloxane precursors give rise, after pyrolysis, to ceramics which contain silica and not silicon oxycarbide. Therefore, it is thought that silicon oxycarbide, which is present in most ex-PCS ceramics, may result from C-Si-O chemical bonds already present in the precursor or formed during the beginning of the organometallic/inorganic transition.

ACKNOWLEDGMENTS

The authors are indebted to acknowledge the contribution of M.M Delpuech and Sarthou, from CEA-CESTA, for the gas analysis of the pyrolysis products as well as that for M. SARTRE from Science et Surface, to the ESCA analyses. This work has been supported by AFME, CNRS, DRET and SEP.

REFERENCES

1 : Carbon Fibers (J.B. Donnet and R.C. Bansal, eds), M. Dekker, Inc., New York 1985.

2 : J. Delmonte, in "Technology of Carbon Graphite Fibers Composites" Chap 2, pp 41-87, Van Nostrand Reinbold Co, New York, 1981.

3 : P.J. Goodhew, A.J. Clarke and J.E. Bailey, Mater. Sci. and eng., 17 (1985) 3-30.

4 : P.J. Rose, in Processing and uses of Carbon fibre Reinforced Plastics, pp 5-39, VDI Verlag, Dussldorf 1981.

5 : J.B. Barr, S. Chwastiack, R. Didchenko, I.C. Lewis, R.T. Lewis, L.C. Singer, Applied Polymer Symposium, 29 (1976) 161-173, John Wiley et Sons.

6 : (a) L.S. Singer, Carbon, 16 (1978) 409-415.
(b) L.S. Singer, Fuel, 60 (1981) 839-847.

7 : I.C. Lewis, J.Chimie Phys., 81 (1984) 751-758.

8 : S. Otami, Mol. Cryst. Liq. Cryst., 63 (1981) 249-264.

9 : L. S. Singer, Brevet U.S. 4.005. 183, 25 Janvier 1977.

10 : E. Fitzer, W. Fritz et R. Gadow, Actes Réunion "Advanced Ceramic Materials Tokyo Inst. Technol. Yokoama, Oct. 1983.

11 : R. West, L.D. David, P.I. Djurovich, H. Yo,and R. Sinclair, Ceram. Bull. 62/8 (1983), 916-923.

12 : S. Yajima, Cer. Bull., 62/8 (1983) 893-915.

13 : R.C. Rice, Cer. Bull., 62/8 (1983) 889-892.

14 : J.Jamet, J.R. Spann, R.W. Rice, D.Lewis, W.S. Goblenz, Actes 8 th Annual Conf., Composites and Advanced Ceramics, Mater., Janv. 1984 Cocoa Beach (F.L.) pp 677-94.

15 : R.R. Wills, R.A Mackle et S.P Makhajee, Cer. Bull. 62/8 (1983) 904-905

16 : B.E. Walker, R.W. Rice, P.F. Becher, B.A. Bender, W.S. Goblenz, Cer. Bull., 62/8 (1983), 916-923

17 : E. Fitzer, Act. Symp. Int., Factors in Densification and Sintering of Oxide or Non-oxide Ceramics, Hakone, Japan 1978, pp. 618-673

18 : E. Fitzer and J. Schlichting, High Temp. Sci., (1980) 149-172

19 : C.L. Schilling, J.P. Wesson and T.C. Williams, Cer. Bull, 62/8 (1983) 912-915

20 : Y. Hasegawa and K. Okamura, J. Mat. Sci., 18 (1983) 3633-3648

21 : B.J. Penn, F.E. Ledbetter, J.H. Clemous, J.G. Daniles, J. Appl. Polym. Sci., 217 (1982) 3751-3761.

22 : B.A. Bender, R.W. Rice, J.R. Spann, Com. Am. Ceram. Soc., 70 (3) C. 58- C.60 (1987)

23 : S.Yajima, Y. Hasegawa, J. Hayashi and M. Iimura, J. Mat. Sci., 13 (1973) 2529-2576.

24 : Y. Hasegawa, K. Okamura, J. Mat. Sci., 18 (1963) 3633-3648.

25 : Y. Hasegawa, M. Imura et S. Yajima, J. Mat. Sci., 15 (1980) 720-728.

26 : K. Okamura, M. Sato and Y. Hasegawa, J. Mat. Sci. Lett., 2 (1983), 769-771

27 : S.Yajima, K. Okamura, J. Hayashi et M. Omon, J. Am. Ceram. Sci., 59 (7-8) (1976) 324-77.

28 : H. Ichikawa, F. Machino, S. Mitsuno, T. Ichikawa, K. Okamura, Y. Hasegawa, J. Mat. Sci., 21 (1986) 4352-4358

29 : H. Ichikawa, H. Teranishi, T. Ichikawa, J. Mat. Sci. Lett., 6 (1987) 420-422.

30 : K. Okamura, T. Matsuzawa, Y. Hasegawa, J. Mat. Sci. Lett., 4 (1985) 55-57.

31 : S. Yajima, K. Okamura, J. Hayashi, Chemistry letters, pp 1209-1212 (1975).

32 : S. Yajima, J. Hayashi, M. Omori, Chemestry Letters, pp 931-934 (1975).

33 : K. Okamura, M. Sato, T. Matsuzawa, ACS Polymers Preprints, Vol 25 (1) pp 6-7 (1984).

34 : G. Simon, A.R. Bunsell, J. Mat. Sci., 19 (1984) 3649-3657.

35 : G. Simon, A.R. Bunsell, J. Mat. Sci. Lett., 2 (1983) 80-82.

36 : S. Yajima, K. Okamura, T. Matsuzawa, T. Schishido, Nature, Vol 279 (1979) 311-13.

37 : M. Guimon, Revue. Phys. Appl. 23 (1988) 229-238.

38 : Y. Maniette, A. Oberlin, J. Mat. Sci. (Accepted).

39 : C. Laffon, A.M. Flank,R. Hagege, P. Olry, J. Cotteret, S. Dixmier, M. Laridjani, A.P Legrand, B. Hommel, J. Mat. Sci. (Submitted).

40 : O.J. Pysher, K.C. Goretta, R.S. Hodder, R.E Tressler, presented at the 89 th Annual Meeting, the American Ceramic Society Pittsburgh, PA, April 29, 1987 (N°-145-C-87).

41 : R. Chaim, A.H. Hewer, R.T. Chen, J. Am. Ceram. Soc. 71 [11] 960-69 (1988).

42 : S.M. Johnson, R.D. Brittain, R.H. Lamoreaux, D.J. Rowcliffe, J. Am. Ceram. Soc., 71 [3] C-132-C-135 (1988).

43 : K.L.Luthra, J. Am. Ceram. Soc., 69 [10] C-231-C-233 (1986).

44 : E. Fitzer, R. Gadow, Am. Ceram. Soc.Bull., 65 (2) 326-35 (1986).

45 : R. Hamminga, G. Grathwolth, F. Thummler., J. Mat. Sci., 18 (1983) 353-364.

46 : H. Fukunaga, K. Goda, Progress in advanced Materials and Process Elswier Science Publishers, B.V. Amsterdam, 1985, 125-134.

47 : A.S. Fareed, P.Fang, M.J. Koczak, F.M.Ko, Am. Ceram. Soc. Bull., 66 (2) 353-58 (1987).

48 : T. Mah, N.L. Heicht, D.E.Mc. Cullum, J.R. Hoenigman, H.M. Kim, A.P. Katz, H.A. Lipsitt., J. Mat. Sci., 19 (1984) 1191-1801.

49 : B. Catoire, M. Sotton, G. Simon, A.R. Bunsell, Polymer, 1987, Vol 28, April 751-54.

50 : L.C. Sawyer, R. Arons, F. Haimbach, M. Jaffe, K.D. Rappaport Ceram. Eng. and Sci. Proc. 7-8 A85 567-75.

51: T.J.CLark, R.M. Arons, J.B. Stamatoff, Ceram. Eng. and Sci. Proc. 7-8 A 85, 576-88.

52 : T.J.CLark, M. Jaffe, J. Rabe, N.R. Langley, Ceram. Eng. and Sci. Proc. 7-8- A86, 901-914.

53 : J. Lipowitz, H.A. Freeman, R.T. Chen, E.R. Prack, Ad. Ceram. Mat., 2 (2), 121-28 (1987).

54 : D. Seyferth, G.H. Wiseman, C. Prud'Homme, Com. Am.Ceram. Soc. (1983) C 13-C 14.

55 : J.E. Legrow, T.F. Lim, J. Lipowitz, R.S. Reach, Am. Ceram. Soc. Bull., 66 (2) 363-67 (1987).

56 : J.E. Ledbetters, J.G. Daniells, J.M. Clemons, N.H. Hundley, B.G. Lenn, J. Mat. Sci. Lett., 3 (1984) 802-804.

57 : L.C. Sawyer, M. Jamieson, D. Brikowski, M.I. Aider, R.T. Chen, J. Am. Ceram. Soc., 70 (11) 798-810 (1987).

58 : K. Okamura, M. Sato, Y. Hasegawa, U.S. Patent 4. 650. 773., Mar 17. 1987.

59 : K. Okamura, M. Sato, Y. Hasegawa, T.Amano, Chem. Lett. pp 2059-2060, 1984.

60 : E. Bacque, J-P. Pillot, M. Birot and J. Dunogues, Macromolécules 1988, 21, 30-34.

61 : E. Bacque, J-P. Pillot, M. Birot and J. Dunogues, Macromolécules 1988, 21, 34-38.

62 : E. Bacque, J-P. Pillot, M. Birot , J. Dunogues, E. Bouillon, R. Pailler, R. Naslain, Chem. of Mat. (Submitted).

63 : J-C. Sarthou, University thesis n° 155, Bordeaux (1984)

64 : E. Bouillon, F. Langlais, R. Pailler, R. Naslain, J.C. Sarthou, A. Delpuech, C. Laffon, P. Lagarde, F. Cruege, P.V. Huong, M. Monthioux, A. Oberlin, J. Mat. Sci. (Submitted) .

65 : M. Guiliano, G. Mille, J. KIster, H.J.M. Dou Analusis, 1984, v. 12; n°4, pp 201-204.

66 : L.C. Sawyer, R.T. Chen, F. Haimback, P.J. Hargert, E.R. Pracks and M. Jaffe, Ceram. Eng. Sci. Proc., 7, 7-8 (1986) 914.

67 : L. Porte, A. Sartre, J. Mat. Sci. , 24 (1989) 271-275

68: Les Carbones, Tome 1, édité par le Groupe Français d'Etude des Carbones, Masson 1965.

69 : M. Gorman, S.A. Solin, Solid State Commun., 15, 4 (1974) 761.

70 : A. Morimoto, T. Kutaoka, M. Kumada, T. Schimiza, Philosophical Magazine B, 50, 4 (1984) 5.

71 : P. Martineau, M. Layaye, R. Pailler, R. Naslain, M. Couzi, F. Cruege, J. Mat. Sci. 19 (1984) 2731.

72 : Y. Sasaki, Y. Nishima, M. Sato, K. Okamura, J. Mat. Sci., 22 (1987) 443-448.

73 : F. Tuinstra, J.L. Koenig, J. Chem. Physics, Vol 33, Num 3.1 (1970) 1126.

74 : J.N. Rouzaud, A. Oberlin, C.B. Bassez, Thin Solid Films, 105 (1983) 75-96.

75 : P. Lespade, A. Marchand, M. Couzi. and F. Cruege, Carbon 22 (1984) p 375.

76 : C. Galiotis, D. N. Batchelder, J. Mat. Sci. Lett., 7 (1988) 545-547.

CONCLUSIONS GENERALES

CONCLUSIONS GENERALES

Ce travail, sur la transformation de précurseurs organosiliciés en céramique base SiC s'inscrivait dans le cadre général des études poursuivies au Laboratoire de Chimie du Solide (LCS) du CNRS sur les composites fibreux du type **céramique-céramique** destinés à des applications thermostructurales notamment dans l'industrie aéronautique et spatiale.

L'étude de la pyrolyse de polymères organosiliciés était un axe nouveau pour le groupe Matériaux Composites du LCS puisque les études précédentes concernaient plutôt l'élaboration des matrices céramiques par dépôt chimique en phase vapeur. Il est apparu clairement, après une étude bibliographique (i) que la voie pyrolytique mettait souvent en oeuvre des procédés d'élaboration simples en ce qui concerne l'obtention de matrices céramiques, (ii) qu'elle était la voie principale de synthèse des fibres céramiques de faible diamètre et qu'enfin, (iii) elle permettait d'accéder à des systèmes originaux tels Si-C-N ou Si-Ti-C-O difficilement abordables par la voie gazeuse.

Notre objectif était d'approfondir la connaissance de la transformation de précurseurs de type polycarbosilanes (PCS) et polycarbosilazanes (PCSZ) en céramiques de manière à (i) mettre en évidence les différents mécanismes qui régissent ce type de transformation, (ii) étudier l'évolution des céramiques résultantes en fonction de la température et (iii) trouver les relations existantes entre, d'une part, la structure du polymère et, d'autre part, la microstructure et le comportement mécanique des céramiques.

Il s'est orienté autour de trois axes :

(i) - Nous avons réalisé une étude fine de la pyrolyse **du polycarbosilane (NC_2) commercialisé** par la société NIPPON CARBON et qui est probablement le précurseur de la fibre actuellement commercialisée sous le label NICALON. Les pyrolyses ont été conduites jusqu'à 2200°C, et un ensemble de techniques d'analyses fines (EXAFS,TEM, XPS, AUGER, RAMAN) a été mis en oeuvre.

(ii) - Ensuite nous avons élaboré et caractérisé d'un point de vue physico-chimique et mécanique des **éprouvettes monofilamentaires issues du précurseur NC_2**. Nous nous sommes attachés à comprendre les phénomènes se produisant durant les étapes de réticulation, de pyrolyse et de céramisation.

(iii) - Enfin, nous avons contribué à la définition et à l'étude d'un ensemble de **précurseurs modèles de type PCS et PCSZ** en vue de dégager le rôle tenu par l'azote et l'oxygène liés au silicium et par le carbone libre dans les céramiques et leurs propriétés (stabilité de l'état amorphe/microcristallisé).

1 -) L'étude de la pyrolyse du précurseur NC_2 peut être décrite suivant trois étapes prédominantes : (i) la transition organométallique/minérale (550°C < Tp < 800°C), (ii) le passage du résidu amorphe à la céramique microcristallisée (800°C < Tp < 1200°C), (iii) la cristallisation importante de la céramique. Deux étapes intermédiaires (800°C < Tp < 1000°C et 1200°C < Tp < 1400°C) existent, elles correspondent respectivement à une faible variation de composition chimique et à une faible variation de la microstructure.

- Pour 20°C < Tp < 550°C, le polymère évolue peu. Il se produit une réticulation au sein du précurseur, rendant celui-ci infusible. Les spectres infra-rouge restent invariants jusqu'à cette température, la perte de masse importante observée est donc attribuable au départ de PCS de faibles masses moléculaires.

- Pour 550°C < Tp < 800°C, le polymère se dégrade quasiment totalement pour aboutir à un résidu minéral où il reste cependant une quantité importante d'atomes d'hydrogène liés ainsi que des groupes méthyls. Cette transformation organométallique-minérale est bien illustrée par l'observation des spectres IR puisque dès 700°C, les bandes caractéristiques des liaisons de types organiques

ne sont plus visibles. Cette transformation se traduit au niveau de l'analyse des gaz par le départ d'espèces siliciés provenant certainement de ruptures de bouts de chaines et par le départ important de molécules hydrocarbonées (i.e. CH_4, C_2H_6...)

- Pour 800°C < Tp < 1000°C. Le résidu minéral à 800°C peut être considéré comme étant totalement amorphe et constitué d'entités tétraédriques de carbure de silicium, d'oxycarbure de silicium et de silice incluant des groupements résiduels carbonés (e.g. CH, CH_2, CH_3) et des atomes d'hydrogène. L'évolution de ce système vers 1000°C se fait essentiellement par élimination de molécules hydrocarbonées (e.g. CH_4, C_2H_6...) comme le montre l'analyse des gaz. On observe une diminution de la quantité de phase oxycarbure, une augmentation de celle de carbone libre et une augmentation du nombre de tétraèdres de carbure de silicium. D'autre part, on peut penser qu'il se produit des phénomènes chimiques conduisant à la formation de carbone libre. Enfin, le caractère isolant du matériau est attribuable à la faible mobilité des porteurs de charges ou à une concentration faible de ces porteurs.

- Pour 1000°C < Tp < 1200°C. On observe un changement de comportement électrique du matériau. D'un caractère isolant marqué, le résidu évolue rapidemment vers un comportement quasi-métallique, un saut de conductivité de l'ordre de dix décades est observé lors de cette transition. L'étude par microscopie électronique en transmission met bien en évidence l'apparition d'unités structurales de base de carbone autour de cristallites de cabure de silicium de taille pouvant aller jusqu'à 3 nm. D'autre part, il reste une phase amorphe qui peut être la silice et/ou l'oxycarbure. Les propriétés électriques de ce matériau à 1200°C peuvent donc résulter essentiellement d'un phénomène de percolation par le carbone.

- Pour 1200°C < Tp < 1400°C. Les traces d'hydrogène incluses dans le matériau disparaissent. La taille moyenne des cristallites de carbure de silicium augmente (environ 6 nm). Le phénomène d'apparition de carbone autour du SiC s'accentue, et celui-ci s'organise de plus en plus. Parallélement le pourcentage global de la phase oxygénée diminue.

- Pour 1400°C < Tp < 1600°C. La cristallisation du carbure de silicium se poursuit, la taille des cristallites étant supérieure à 50 nm pour 1600°C. Simultanément le pourcentage global d'oxygène dans le matériau devient inférieur à 2 % traduisant la décomposition des phases oxygénées (e.g. l'oxycarbure de silicium) avec probablement départ des formes gazeuses SiO et CO.

2-) Nous avons, dans un second temps, synthétisé par extrusion /réticulation/pyrolyse, **des éprouvettes monofilamentaires cylindriques** afin d'accéder aux propriétés mécaniques de la céramique issue du polycarbosilane NC_2. L'étude XPS effectuée sur des éprouvettes pyrolysées jusqu'à 850°C a permis de caractériser : (i) l'oxygène introduit lors de l'étape de réticulation (i.e. environ 18 % combiné essentiellement avec le silicium) et (ii) la formation d'une phase complexe oxygénée (un oxycarbure de silicium) et probablement du carbone libre dès 850°C. Il faut noter qu'à cette température, le taux d'hydrogène dans les résidus solides doit être encore important.

Sur la base des résultats de l'analyse chimique et XPS, nous pouvons considérer que le matériau à 850°C est formé d'entités minérales dont la taille est voisine des molécules polymériques de base, les entités étant reliées entre elles par les ponts Si-O-Si. D'autre part, elles possédent à leurs périphéries des atomes d'hydrogène ainsi que des groupements méthyls résiduels.

Les caractéristiques mécaniques en traction des éprouvettes pyrolysées à cette température sont de 1500 MPa pour la contrainte à rupture (σ^R) et de 150 GPa pour le module d'Young (E). Lorsque l'on augmente la température finale de traitement, ces caractéristiques augmentent, et la conductivité électrique croît légérement.

On obtient un optimum pour une température de 1200°C (σ_R = 2100 MPa et E = 180 GPa). A ce stade de traitement, les éprouvettes sont constituées (i) dans la masse, d'une phase amorphe parsemée d'unités structurales de base de carbone en formation, (ii) à la surface, d'une couche de 5 nm de pyrocarbone orientée parallélement à celle-ci. La couche superficielle de carbone provient probablement d'un phénomène de dépôt chimique en phase vapeur, à partir d'espèces organiques résiduelles se trouvant dans le four de pyrolyse. Lorsqu'on augmente la température finale de traitement des éprouvettes, la phase oxycarbure se dégrade, elle se transforme principalement par le départ de SiO, en carbure de silicium et carbone libre (on peut envisager aussi le départ de la forme CO). Ce qui permet d'aboutir, à 1400°C, à une céramique formée de cristallites de SiC dont la taille est d'environ 10 nm entre lesquelles se trouve du carbone libre turbostratique. D'autre part, les éprouvettes présentent à cette température une couche de carbone turbostratique en surface, d'épaisseur de l'ordre de 50 nm, et qui peut provenir de la décomposition du carbure de silicium en carbone et silicium volatil. Les

transformations s'opérant au sein de la céramique entre 1200 et 1400°C entrainent une chute des propriétés mécaniques des éprouvettes ainsi qu'une augmentation de la conductivité électrique.

3 -) La synthèse de **précurseurs modèles** à l'UA 35 par l'équipe de Mr Dunogués a été réalisée dans le souci de pouvoir corréler la structure du polymère avec les propriétés des céramiques résultantes. Cette démarche a permis de cerner les facteurs qui détermineront le taux de résidu, l'état de cristallisation ou bien encore le taux de carbone libre dans la céramique après pyrolyse.

(i) Nous avons constaté qu'un polymère possédant une structure linéaire ne pouvait conduire à un rendement élevé en céramique, celui-ci se dégradant quasiment totalement en espèces volatiles par fragmentations successives des chaines au cours de la pyrolyse. Par contre, si celui-ci subit une étape de thermolyse, le rendement en céramique peut aller jusqu'à 80 % (suivant le degré d'avancement de la thermolyse). Ce type de traitement est une étape importante dans le procédé d'obtention de la fibre NICALON. Il est aussi possible d'aboutir à des taux de résidu élevés si le précurseur peut donner lieu à une réticulation intermoléculaire, mettant en jeu des liaisons fortes (e.g. Si-O), au début de pyrolyse.

(ii) Le pourcentage de carbone libre dans la céramique n'est pas directement lié au pourcentage de carbone dans le polymère. Il dépend du type de groupements hydrocarbonés et de leur emplacement dans le précurseur. Ces groupements doivent présenter une stabilité thermique suffisante pour ne pas donner lieu à des espèces gazeuses lors de la pyrolyse.

(iii) L'introduction d'azote dans le précurseur permet d'aboutir à une céramique azotée. La phase comprenant l'azote n'est pas spécifiquement Si_3N_4 mais plutôt un oxynitrune de silicium ou des espèces quaternaires. La voie polycarbosilazane conduit donc à une céramique encore plus complexe que celle résultant de la voie polycarbosilane, cependant elle engendre un retard à la cristallisation qui est de l'ordre de 300°C. En effet, à 1400°C les résidus issus de PCSZ sont encore amorphes.

(iv) Les ponts Si-O-Si des polysiloxanes ne conduisent pas après pyrolyse à une phase complexe de type oxycarbure. Cette phase qui est observée dans les autres céramiques peut donc provenir de ponts O-Si-C présents dans le précurseur de départ ou se forment en début de pyrolyse.

De manière générale, les liaisons chimiques présentes dans le squelette polymérique ne se retrouvent pas systématiquement dans la céramique. Citons pour exemple, l'absence de liasions Si-Si dans les résidus issus de précurseurs possédant ce type de liaisons.

En résumé, cette étude est une première approche des relations existant entre polymères de départ et microstructure/propriété mécanique de la céramique résultante. Les différentes investigations menées sur ce thème ont montré qu'il était nécessaire de faire appel à des méthodes d'analyses fines pour la compréhension de la transition organométallique/minéral et pour celle de l'évolution microstructurale des résidus de pyrolyse. D'autre part, les caractéristiques mécaniques mesurées sur la céramique issue du NC_2 ont démontré que nous possédions un moyen simple et efficace de tester mécaniquement les céramiques qui seront issues de polymères originaux.

ANNEXE I

Study of the polymer to ceramic evolution induced by pyrolysis of organic precursor

Published in SPRINGER-VERLAG, International Symposium EXAFS 5
(SEATTLE 21-25 August 1988)

STUDY OF THE POLYMER TO CERAMIC EVOLUTION INDUCED BY PYROLYSIS OF ORGANIC PRECURSOR

C.LAFFON*, A.M. FLANK*, P. LAGARDE*, E. BOUILLON** (°)
* LURE, Bâtiment 209 D, U.P.S., 91405-ORSAY (France)
** Laboratoire de Chimie du Solide, Université de Bordeaux I,
F- 33405-Talence

ABSTRACT

The structure of a precursor : the polycarbosilane, has been followed during pyrolysis up to 1600°C. A continuous evolution is observed, leading to a nucleation of SiC clusters followed at higher temperature by a growth of the SiC crystalline phase. The structure keeps the memory of the precursor up to 1400°C.

Much work has been done on preparing heat resistant silicon carbide materials in fibrous form, since plastics or metals can be reinforced with them in order to obtain very heat resistant composite of great mechanical strength. Thus Nicalon and related fibers have been described as heterogeneous materials containing SiC microcrystals linked together by a more complex SiC_xO_y phase [1]. But these fibers loose their oxidation resistance for temperature higher than 1000°C and have to be improved.

The synthesis of such materials implies the conversion of organometallic polymers (the precursors) to inorganic substances which is realised by pyrolysis. Few studies have been devoted to the organic-mineral transition. The knowledge of the crystallisation process might be interesting to understand the mechanical properties. In the present study, attention is given to the structural evolution about Si atoms in one type of precursor, the polycarbosilane (PCS), during pyrolysis up to 1600°C.

(°) Present address : Laboratoire des Composites Thermostructuraux (UMR-47 CNRS-SEP-UB1) Europarc, 3 Av. L. de Vinci, F-33600 PESSAC

EXPERIMENTAL AND DATA ANALYSIS

The polycarbosilane precursor has been prepared by Nippon Carbon according to the Yajima route [2] pyrolysis treatments at different temperatures, each one half an hour long, were performed in a RF induction furnace under a pressure of argon carefully purified. Samples were powdered, and deposited on "Nucleopore" membranes.

EXAFS measurements have been carried out at the silicon edge by transmission on the InSb two-crystal monochromator of the ACO storage ring, using an ion chamber filled with a low pressure of air as a detector. The absorption spectra have been analysed in a conventional manner, in order to extract the EXAFS oscillations which were k^2 weighted and Fourier transformed. A Hanning window is chosen from 1.6 $Å^{-1}$ to 8.5 $Å^{-1}$. For the atoms Si the work function is less than 10 eV. Normalisation, background removal, Fourier transforms of unknowns and references were done over similar K ranges. Crystalline silicon, crystalline silicon carbide c-SiC (β-SiC and α-SiC), amorphous and crystalline SiO_2, were used as model compounds.

RESULTS

** Initial structure of the polycarbosilane precursor.*

The molecular structure of the starting precursor can be described in a first approximation by the formula $-(HSiCH_3-CH_2)-_n$. Actually, EXAFS results which are represented qualitatively in figure 1 by the Fourier Transfom of the data indicates that an unneglectible proportion of Si-O bonds is already present. It can be quantified by a fitting procedure of the first peak (A) and evaluated to be more than 12 % (Table 1). We must point out that the total coordination number of Si atoms is found to be less than 4 indicating the presence of Si-H bonds undetectable by EXAFS. The second (B) peak is attributed to two major componants Si ---> C neibhourgs (by bonds $_{SI}{}^{C}{}_{C}$) and Si ---> Si neibhourgs (by bonds $_{Si}{}^{C}{}_{Si}$). The second and third (C) peaks point at distances lesser and upper than the one of c-SiC.

** Structural evolution of the polycarbosilane precursor (table 1).*

EXPERIMENTAL AND DATA ANALYSIS

The polycarbosilane precursor has been prepared by Nippon Carbon according to the Yajima route [2] pyrolysis treatments at different temperatures, each one half an hour long, were performed in a RF induction furnace under a pressure of argon carefully purified. Samples were powdered, and deposited on "Nucleopore" membranes.

EXAFS measurements have been carried out at the silicon edge by transmission on the InSb two-crystal monochromator of the ACO storage ring, using an ion chamber filled with a low pressure of air as a detector. The absorption spectra have been analysed in a conventional manner, in order to extract the EXAFS oscillations which were k^2 weighted and Fourier transformed. A Hanning window is chosen from 1.6 $Å^{-1}$ to 8.5 $Å^{-1}$. For the atoms Si the work function is less than 10 eV. Normalisation, background removal, Fourier transforms of unknowns and references were done over similar K ranges. Crystalline silicon, crystalline silicon carbide c-SiC (β-SiC and α-SiC), amorphous and crystalline SiO_2, were used as model compounds.

RESULTS

** Initial structure of the polycarbosilane precursor.*

The molecular structure of the starting precursor can be described in a first approximation by the formula $-(HSiCH_3-CH_2)-_n$. Actually, EXAFS results which are represented qualitatively in figure 1 by the Fourier Transfom of the data indicates that an unneglectible proportion of Si-O bonds is already present. It can be quantified by a fitting procedure of the first peak (A) and evaluated to be more than 12 % (Table 1). We must point out that the total coordination number of Si atoms is found to be less than 4 indicating the presence of Si-H bonds undetectable by EXAFS. The second (B) peak is attributed to two major componants Si ---> C neibhourgs (by bonds $_{SI}{}^{C}{}_{C}$) and Si ---> Si neibhourgs (by bonds $_{Si}{}^{C}{}_{Si}$). The second and third (C) peaks point at distances lesser and upper than the one of c-SiC.

** Structural evolution of the polycarbosilane precursor (table 1).*

1) For the samples resulting from pyrolysis at 800°C and 1000°C (figure 1), the evolution concerns the very near environment of Si atoms (the second peak implies more $_{Si}{}^{C}{}_{Si}$ bonds) but they conserve mainly the original structure of the PCS.

2) After heating at 1200°C (figure 2), one can observe a crystalline structure identical to c-SiC. The peaks are in coincidence up to the 8th distance. From the apparent coordination number of the second shell, besides the hypothesis of spherical crystallites, and taking into account the proportion of surface atoms, one can deduce the size of the crystallites. It has been evaluate to about 20 Å.

3) Beyond 1400°C of pyrolysis temperature (figure 2) no more difference exists between the EXAFS spectra of c-SiC and the pyrolysis residues. Diffraction techniques give a crystallite size of 50 Å for 1400°C and 500 Å for 1600°C. By comparing to c-SiC (α-SiC, β-SiC and two other SiC polytypes) we can conclude that the present crystallisation does not correspond to a pure cubique phase.

CONCLUSION

By following the structural temperature evolution of the pyrolysis residus, we observe that the first step of the crystal growth of the ceramic products takes place in between 800°C to 1000°C. The SiC crystalline phase expanses to the detriment of the PCS structure.

	PCS	800	1000	1200	1400	1600	NF2	NF1
Si-O (%)	12	15	19	8	3	1	4	7
nuclei SiC size		nuclei SiC	< 7 Å	< 20 Å	< 50 Å	500 Å	15 Å	7 Å

Table 1

1. C. LAFFON, A.M. FLANCK, P. LAGARDE, J. de Physique , 47 (1986) C8-383

2. Y. HASEGAWA, K. OKAMURA, J. Mater. Sci. , 21 (1986) 321

Figure 1

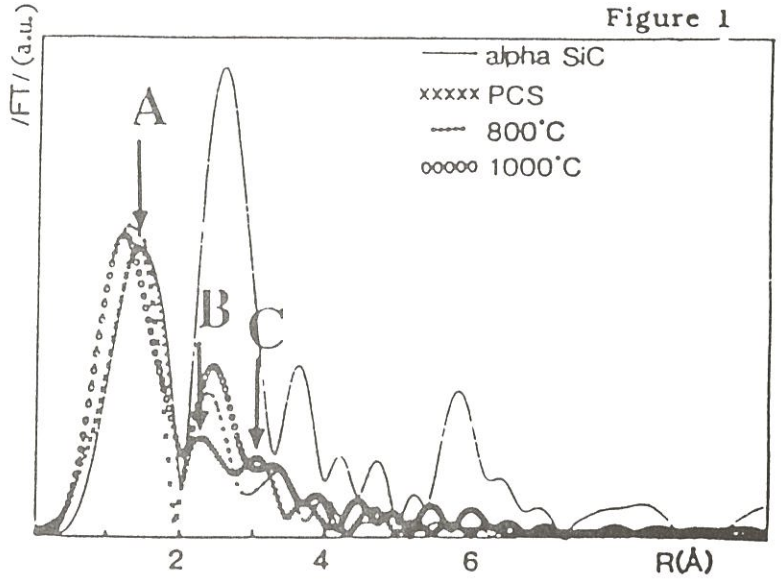

Figure 2

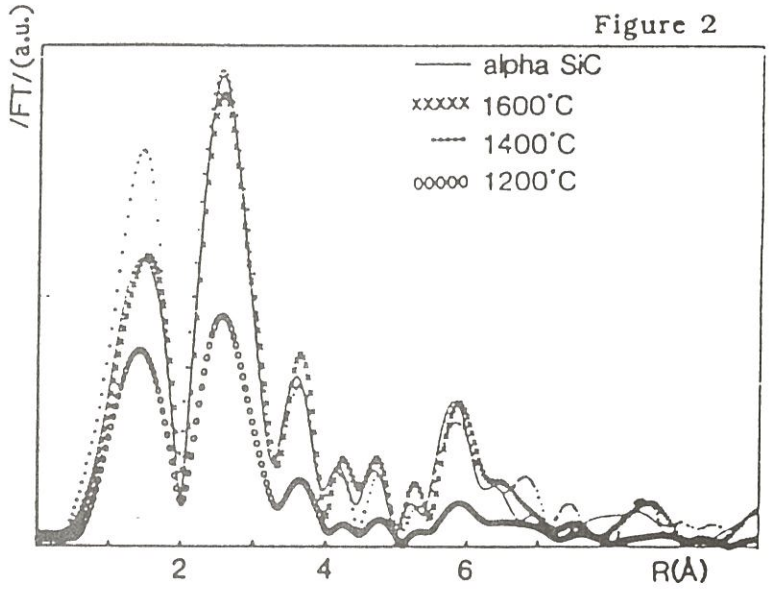

ANNEXE II

New polycarbosilane models. 4 : Derivatization of linear (polymethylchloro)silmethylene and application to the synthesis of functional polycarbosilanes

NEW POLYCARBOSILANE MODELS. 4 - DERIVATIZATION OF LINEAR (POLYMETHYLCHLORO) SILMETHYLENE AND APPLICATION TO THE SYNTHESIS OF FUNCTIONAL POLYCARBOSILANES

J.P. Pillot, E. Bacqué, M. Birot and J. Dunoguès
Laboratoire de Chimie Organique et Organométallique
U.R.A. 35 (CNRS), Université de Bordeaux I
351 Cours de La Libération, F-33405 TALENCE Cedex.

E. Bouillon(*) and R. Pailler(*)
Laboratoire de Chimie du Solide du CNRS, Université de Bordeaux I
351 Cours de La Libération, F-33405 TALENCE Cedex.

ABSTRACT

New functional polycarbosilane precursors of SiC ceramics were synthesized in order to study the role of the chemical composition and the branching stucture on the pyrolysis features and the properties of the ceramics. Thus, polycarbosilanes possessing a linear skeleton of alternate silicon atoms and methylene groups and disilane, disilazane, disiloxane and hydrocarbon bridges were obtained upon derivatization of (polymethylchloro) silmethylene.These polymers were characterized by physico-chemical methods (IR, NMR, GPC and TGA).

(*) present address : Laboratoire des Composites Thermostructuraux
Europarc : 3, avenue Léonard de Vinci
F-33600 PESSAC.

(*)

1 - INTRODUCTION

Nowadays, the need of ceramic matrix composite materials offering enhanced properties requires new production processes. Thus, the preparation of SiC fibers upon pyrolysis of polycarbosilanes (PCS), as reported by Yajima, is an important demonstration of the interest of organometallic precursors in this field [1].

Even if it has led to the production of continuous silicon carbide fibers at an industrial scale, the Yajima's route suffers of several drawbacks. For example, the low thermal stability of these fibers is responsible for the dramatic drop in their mechanical properties above 900-1000°C [2]. Another limitation lies in the fact that the structure of the starting PCS has not yet been clearly established : its representation according to the simple linear polysilapropylene formula, -(-MeHSi-CH_2)n- [3], must be ruled out. Similar carbosilane patterns are undoubtely present, as it can be inferred from spectroscopic data, but they likely are included into a strongly branched skeleton. Thus, this precursor is now better viewed as a complex framework of alternate carbon and silicon atoms forming ring structures joined by chains, as previously assumed by Hasegawa et al. [4]. Moreover, very little is known concerning the mechanism of the thermal conversion of PCS into silicon carbide, so that it remains difficult to establish any precise correlation between the framework of such an organometallic precursor and the microstructure or the properties of the final ceramic. In order to have a better understanding of the chemistry of the conversion of PCS into silicon carbide, investigations on the pyrolysis of suitable models was an alternative. Thus, we have previously described the conversion of (polydimethyl)silmethylene (I) into a (polymethylchloro)silmethylene, (II) and the subsequent reduction of this last polymer, affording a new linear polysilapropylene (III) which could be regarded as a convenient model of the ideal Yajima's PCS (Scheme 1) [5,6].

In this paper, we report the preparation and the characterization of a series of functional PCS upon the derivatization of II and III, as depicted in Schemes 2 and 3.

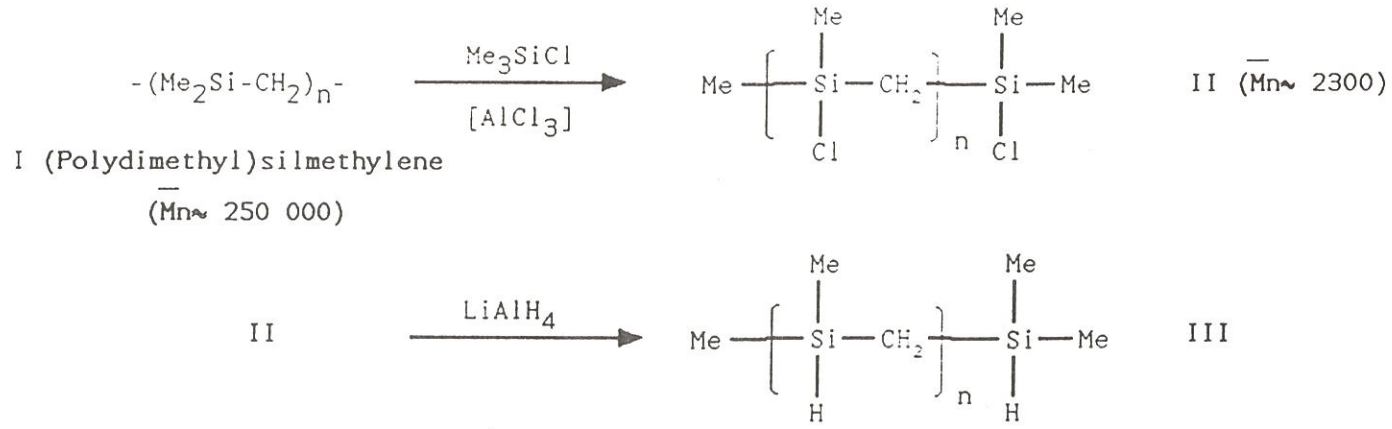

Scheme 1: Synthesis of (Polymethylchloro)silmethylene (II) and Polysilapropylene (III)

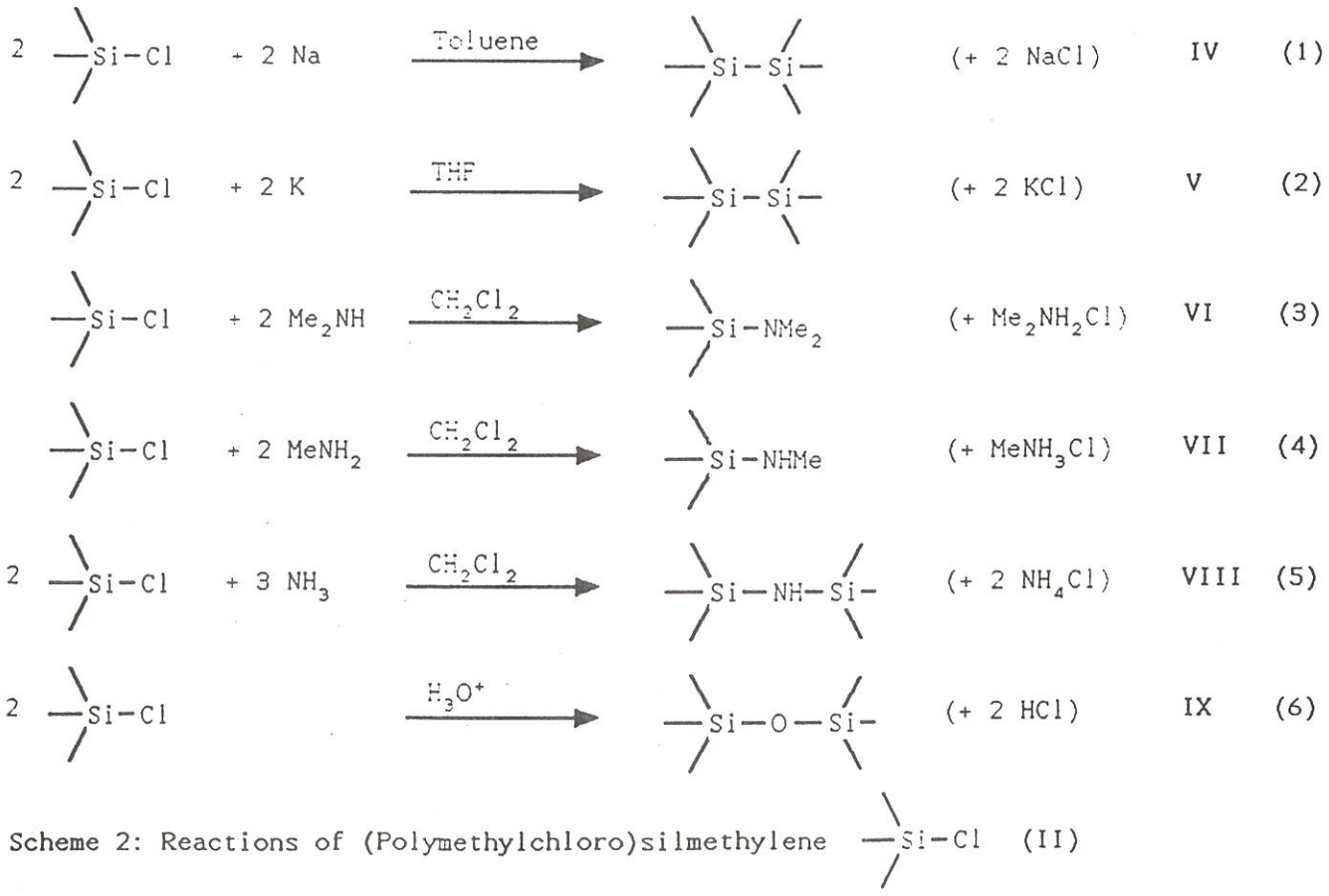

Scheme 2: Reactions of (Polymethylchloro)silmethylene —Si—Cl (II)

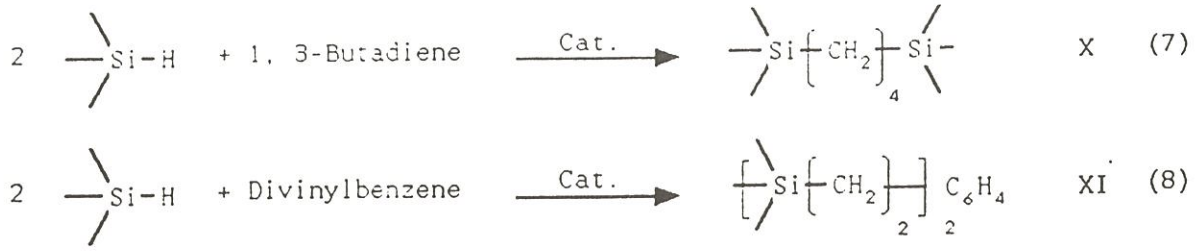

Scheme 3: Hydrosilylation of Polysilapropylene (III) in the Presence of Speier's Catalyst

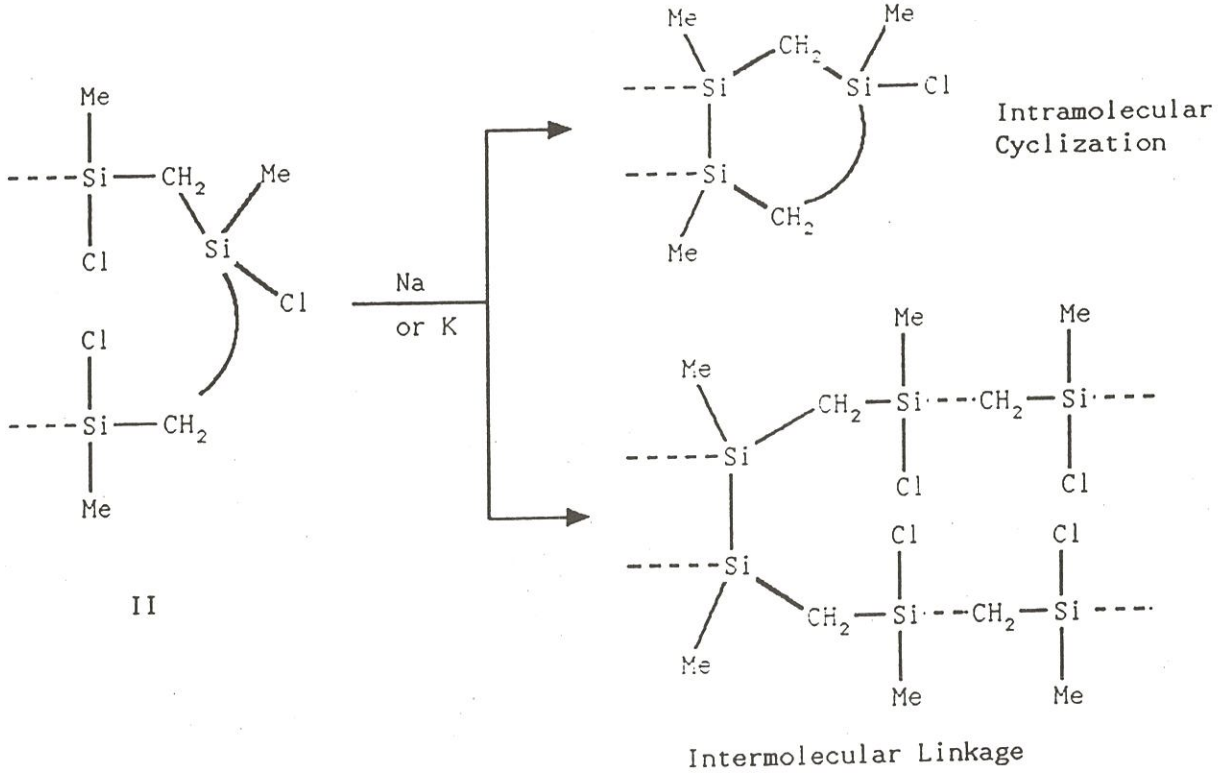

Scheme 4: Cross-linked Structures from II *via* the Formation of Disilanyl Linkages in the Presence of Sodium or Potassium

- EXPERIMENTAL

Solvents.

All the solvents were distilled before use and kept on molecular sieves.

Apparatus.

All the reaction vessels were thoroughly dried and purged with inert gas prior to use.

Characterization

Polymer molecular weights were determined by gel permeation chromatography (GPC) using four μ-styragel columns (porosity ranges of 500, 10^3, 10^4 and 10^5 Å) and THF as the eluent at a flow rate of 1 mL/mn(*).

Proton NMR spectra were checked(**) on polymer solutions in deuteriochloroform or benzene-d_6, using TMS as the external standart.

Infrared spectra were examined(***) with product films respectively between NaCl and TiBrI plates.

Thermogravimetric analyses(****) were performed under the following conditions : heat rate : 5 deg/mn ; argon flow rate : 40 mL/mn.

Synthesis

Obtention of IV_s and IV_i.

The apparatus consists of a 100-mL three-necked flask equipped with a magnetic bar, fitted with a dropping funnel, a thermometric well and a condenser cooled by decalin at -10°C, connected to a $CaCl_2$ column. Xylene (10 mL) and sodium in excess (3.45 g, 0.15 mol) were successively introduced under an argon stream and heated to reflux under vigorous stirring. A solution of chlorinated polycarbosilane II (9.26 g, approx. 0.1mol) in xylene (40 mL) was then added over a period of 10 mn on the suspension of molten sodium and the reactional mixture kept at reflux during five days. After cooling, the

---

(*) The detection system was a Waters Associates Differential Refractometer (R 401)

(**) Hitachi Perkin-Elmer R 24 B spectrometer (60 MHz) or a Bruker AC 200 spectrometer

(***) Perkin-Elmer 1420 spectrometer (in the region 4000-600 cm^{-1}) or Perkin-Elmer 983 spectrometer (in the region 4000-200 cm^{-1})

(****) Perkin-Elmer TGS 2 analyser (data station 3600)

mixture was centrifugated in order to separate the solid and liquid phases. The solid was washed with xylene and centrifugated twice and the combined solutions concentrated with a rotavapor and then devolatilized under reduced pressure affording a yellow grease IV_s (2.25 g). The solid fraction was successively treated by methanol and water, and then filtered. The residual solid was then washed with acetone and ether and dried under vacuum. Weight of this insoluble unmeltable part IV_i : 4.5 g.

Obtention of V_s and V_i.

Using a similar apparatus, 10 g of polymer II (about 0.173 mol) in 70 mL of THF were added on a suspension of molten potassium (6.8 g, 0.174 mol) in refluxing THF (100 mL) over a period of 50 mn. After 75 h of reflux the mixture was allowed to cool at room temperature. A similar workup afforded V_s as an unmeltable solid (4.82 g) and an unmeltable insoluble solid V_i (7.3 g).

Preparation of VI.

A 500-mL three-necked flask was fitted with a reflux condenser cooled by ethanol at - 30°C and connected to a potassium hydroxide column, a thermometric well and a dropping funnel. After carefull purging with argon, dichloromethane (50 mL) and dimethylamine (9.75 g, 0.221 mol) were introduced (using a syringe for the amine) before cooling at - 40°C with a dry ice-acetone bath. A solution of II (9.5 g, 0.102 mol) in dichloromethane (100 mL) was then added over 75 mn under vigorous stirring. The mixture was allowed to warm again, kept at room temperature during 20 h and the solvent removed under high vacuum. This crude product was treated with pentane and filtred in order to separate any residual hydrochloride, and this workup repeated several times. After careful devolatilization a viscous orange colored oil was recovered and stored under argon at - 20°C (9.8. g, 94.4 % yield) ; residual chlorine percentage : 0.7 %.

Preparation of VII.

A solution of PCS II (9.5 g, 0.103 mol) in dichloromethane (200 mL) was placed into a similar vessel under argon flow and cooled with an ice-bath. The gaseous amine was then introduced and the internal temperature gradually

raised to 12°C before falling again slowly. After one hour, the limpid yellow mixture containing a large part of condensed monomethylamine was allowed to come back at room temperature and the excess of amine evolved slowly under partial vacuum. The precipitate of hydrochloride was filtered off and washed twice with dichloromethane. The organic solutions were combined, concentrated with a rotavapor and trace of solvent eliminated overnight under high vacuum, affording a yellow solid which was strored at -20°C VII_a (8.94 g, 90.6 % yield).

A similar experiment was performed without solvent starting from 13.7 g of II. The usual workup yielded a yellow viscous liquid VII_b (6.25 g, 43,9 % yield).

Preparation of VIII.

A similar apparatus as for dimethylamine was used, but the dropping funnel was replaced by a gas inlet prolonged by a glass pipe for the bubbling of ammonia inside the vessel. After careful purging of the system with argon, a solution of polymer II (16.6 g, 0.179 mol) in dichloromethane (250 mL) was introduced and ammonia allowed bubbling at 20°C under vigorous stirring. The initially brown solution readily turned to a white color, whereas the maximal inside temperature raised up to 41°C before it fell again to 20°C. After one hour more at this temperature, the mixture was refluxed during three hours and allowed to cool at room temperature. After centrifugation, a white solid and an orange liquid were separated. The solid part was washed with dicloromehtane and filtered off twice. The solutions were combined and filtered again. The filtrate was concentrated with a rotavapor and devolatilized overnight, affording a yellow solid VIII (8.95 g), melting interval : 90-100°C. On the basis of the theoritical formula, the yield was 69.2 % (expected weight : 12.93 g). The elemental analysis gave a very low residual chlorine ratio (0.6%). VIII was found to give an insoluble unmeltable polymer when kept at room temperature within a few days. So it must be stored under argon at -20°C. The insoluble part was treated by water affording a grey solid (6.1 g) which was not further characterized.

Preparation of IX.

A solution of PCS II (5.05 g 0.054 mol) in THF (25 mL) was slowly poured onto a mixture af water (10 g) and THF (10 mL) under vigorous stirring. After refluxing overnight, the solvent and water were removed under high vacuum during several hours, affording a brown solid (3.48 g, 98 % yield) ; softening range : 120-140°C.

Preparation of X and XI

1,3 - butadiene (1.4 g, 0.026 mol) was condensed into a 500 mL glass tube carefully purged with argon . Polymer II (3 g, 0.051 mol) and a very small amount of catalyst ($H_2Pt\ Cl_6$. 6 H_2 O) were then introduced, and the glass tube frozen in liquid nitrogen and sealed tube was opened and the excess of butadiene removed under high vacuum at a temperature of 200°C, affording an insoluble, unmeltable yellow solid X (4.39 g, 96.8 % yield).

A similar experiment was carried out with PCS II (2.9 g, 0.05 mol) and divinylbenzene (3.3 g, 0.0253 mol) yielding an insoluble, unmeltable polymer XI (5.92 g, 96 % yield).

3 - RESULTS AND DISCUSSION

3.1 Dechlorination of Polymer II by alkaline Metals

Alcaline metals are known to produce the formation of disilane bonds by chlorosilane condensation [7]. Owing to the formation of such linkages between silicon atoms belonging to different linear chains, this route was expected to lead to crosslinked structures.Consequently, we have investigated the behavior of polymer II successively in the presence of sodium in xylene or potassium in THF.

3.1.1. Preparation of polymer IV,

Upon treatment with sodium in boiling xylene, polymer II afforded a soluble greasy product IV_s, which did not flow at room temperature, and an insoluble unmeltable (below 250°C) fraction IV_i (IV_i/IV_s ratio = 2). The overall

weight of the polymer which was recovered after careful devolatilization slightly exceeded the expected value, suggesting that the solvent was not inert and was incorporated to polymer IV to a small extend, as confirmed by ^1H NMR and IR data.

^1H NMR spectrum (60 Mhz) of IV_s exhibited two broad peaks centered at 0.6 and 0.1 ppm, respectively assigned to remaining CH_3SiCl and CH_3Si-Si plus CH_2Si-Si protons, whereas the presence of a small amount of aromatic and benzylic protons was also detected. IR spectrum of this product (Fig. 1) was in good agreement with these observations ; moreover, we observed a strong absorption at 477 cm^{-1} and a shoulder by 440 cm^{-1}, respectively assigned to ν_{Si-Cl} and ν_{Si-Si} vibrations, whereas a strong band at 2100 cm^{-1} (ν_{Si-H}) revealed that the reduction of Si-Cl groups occurred as a side-reaction. At least, the GPC curve of the soluble fraction IVs was similar to the distribution observed in the case of the starting material for the main hump (but with the difference of a noticeable lovering of molecular weight), whereas a smaller hump corresponding to higher molecular weights products was also observed.

The IR spectrum of IV_i (Fig 1) exhibited a strong ν_{Si-H} band and a weak ν_{Si-Si} band respectively at 2100 cm^{-1} and 441 cm^{-1}, whereas the ν_{Si-Cl} absorption could not be detected in the spectrum. Characteristic absorptions of aromatic and benzylic units also were visible.

3.1.2 - Preparation of polymers V

Dechlorination of polymer II using potassium in THF afforded an orange soluble unmeltable solid V_s, and an insoluble, unmeltable solid V_i, (V_i/V_s ratio = 1,5). V_s was initially soluble in THF but could not be entirely dissolved again when the solvent had been removed.

The IR spectra of V_s and V_i (fig.1) exhibited the characteristic absorptions of Si-H (2100 cm^{-1}), Si-Si (430 cm^{-1}), whereas Si-O-Si, Si-O-C (broad absorption between 1050 and 1200 cm^{-1}) and alkane units (1450 cm^{-1} for example) were also visible. The incorporation of THF was probably responsible for the presence of oxygen as well as of the alkane bands. This side-reaction accounts for the fact that the overall weight of the product exceeded the expected value. Finally, a small band corresponding to the remaining Si-Cl bonds (474 cm^{-1}) was observed only in the case of V_s. This was corroborated by the elemental analysis which revealed the presence of a very low residual chlorine ratio (less than 5 %) as in the case of IV_s. Therefore potassium in THF

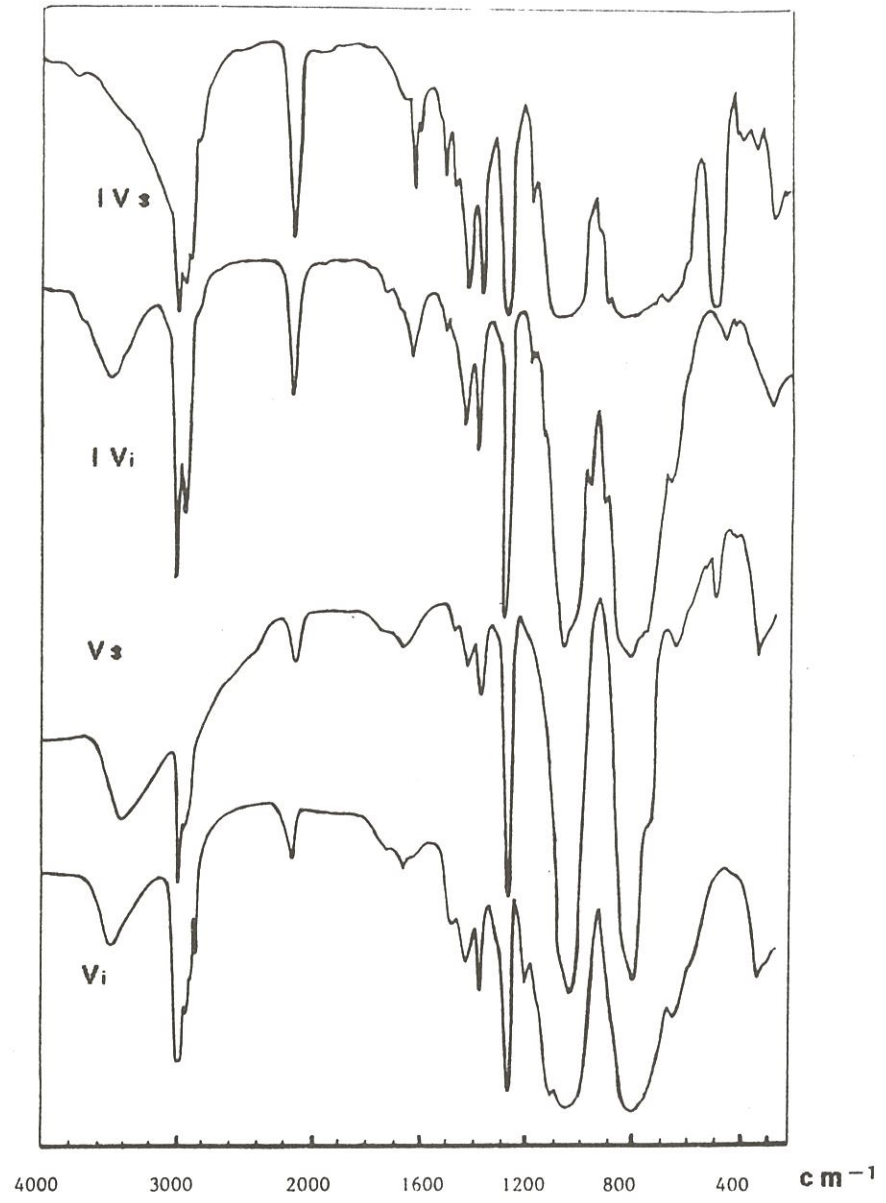

Figure 1 IR Spectra of the Polysilacarbosilanes Obtained upon Treatment of II Respectively in the Presence of Sodium (IV_s, IV_i) or Potassium (V_s, V_i).

was more efficient than sodium in xylene to afford crosslinked polymers from the chlorinated PCS II, as only unmeltable products were obtained (i.e. more branched polymers). However side reactions occured so the structure of these compounds were more complex than initially expected.

From these results it can be assumed that intramolecular as well as intermolecular condensations could occur simultaneously upon treatment of II by alkaline metals, resulting in the obtention of cyclic structures (Scheme 4). The former process accounts for the fact that the first hump of the GPC profile of IV_s was quite similar to the curve of the starting compound, but with a slightly downweight shifted Mn value. In the second case, the condensation of at least two molecules via the creation of silicon-silicon bond belonging to different chains should lead to a significant increase in the average molecular weights affording insoluble unmeltable high molecular weight products. So, the resulting PCS could be regarded as a complex framework formed with linear and condensed cyclic structures having different sizes. There is also good evidence that the solvent is incorporated into the products. Similar phenomena were previously mentioned by Schilling et al. in the case of Na/K alloys [8], whereas the formation of Si-H bonds suggested that the silicon-centered radicals were involved during the dechlorination by alkaline metals (as previously inferred by Zeigler [9]). The poor ability of such radicals towards coupling might be a consequence of the steric hindrance as well as the lack of motion when rigid cyclic structures were involved, and resulted in competitive hydrogen abstraction reactions from the solvent. It is likely that, in such rigid structures, the residual silicon-chlorine bonds became less and less accessible when the steric hindrance and the insolubility increased.

4 - REACTION OF POLYCARBOSILANE II WITH AMINES

We turned then to the synthesis of new PCSZ possessing a skeleton of alternate silicon and carbon atoms and bearing nitrogen atoms on each silicon, by reacting the chlorinated polymer II with amines.

4.1 - Preparation of VI

The action of dimethylamine on polymer II in dichloromethane as the solvent readily resulted in the precipitation of a white solid (dimethylamine

hydrochloride), and an orange viscous oil VI which slowly flowed at room temperature (95 % yield upon careful devolatilization ; residual chlorine ratio 0.7 %). This product was very sensitive to moisture.

Characterization of VI

The IR spectra of VI and of the monomeric derivative $Me_3Si\text{-}NMe_2$ were very similar, at the exception of the additional characteristic absorption of the $Si\text{-}CH_2\text{-}Si$ units at 1040 cm^{-1} in the case of VI (Fig. 2). Its ^1H NMR spectrum (200 MHz) was consistent with the expected linear structure of VI : the NMe protons appeared stereosentive as they exhibited three singlets in the range of 2.39-2.42 ppm, as well as the Me-Si signals in the range of 0.10-0.18 ppm.

$Si\text{-}CH_2\text{-}Si$ protons appeared as an AB spectrum (J_{AB} = 14.2 Hz and a broad singlet (A_2 spectrum) both centered at -0.18 ppm. These patterns resulted from dyad effects induced by the two adjacent asymmetric silicon atoms, and their respective intensities roughly corresponded to the statistical ratio, i.e. 0.6;0.3. This is consistent with the fact that VI was a statistic polymer, as it was also the case for the starting chlorinated PCS II [5,6].

The ^{29}Si NMR spectrum of VI exhibited a broad singlet at 4.95 ppm and a very small singlet at 5.95 ppm respectively assigned to the internal and to the terminal silicon atoms (δ^{29} Si = 5.9 ppm for the monomeric compound $MeSiNMe_2$ [10]). As expected , the average number molecular weight of II and VI, as well as their polydispersity indexes, were similar : (II : Mn = 2330, ρ = 2.7 ; VI : Mn = 2480, ρ = 1.7).

4.2 -Preparation of VII

(Polymethylchloro)silmethylene was reacted with monomethylamine under similar conditions, affording a yellow soluble solid after separation of the amine hydrochloride and evaporation of the solvent (91 % yield according to Scheme 2, eq. 4 ; melting interval : 50-60°C). Residual chlorine ratio : 0.2 %. The IR spectrum of VII was consistent with the expected structure (Fig.3). Its ^1H NMR spectrum (200 MHz) was very similar to the spectrum of VI : for example, AB and A_2 patterns also were given by the methylene protons. On the other hand, integration of the signals showed a significant lowering for the intensity of the NMe peak, indicating that Si-NMe-Si bridges also were formed

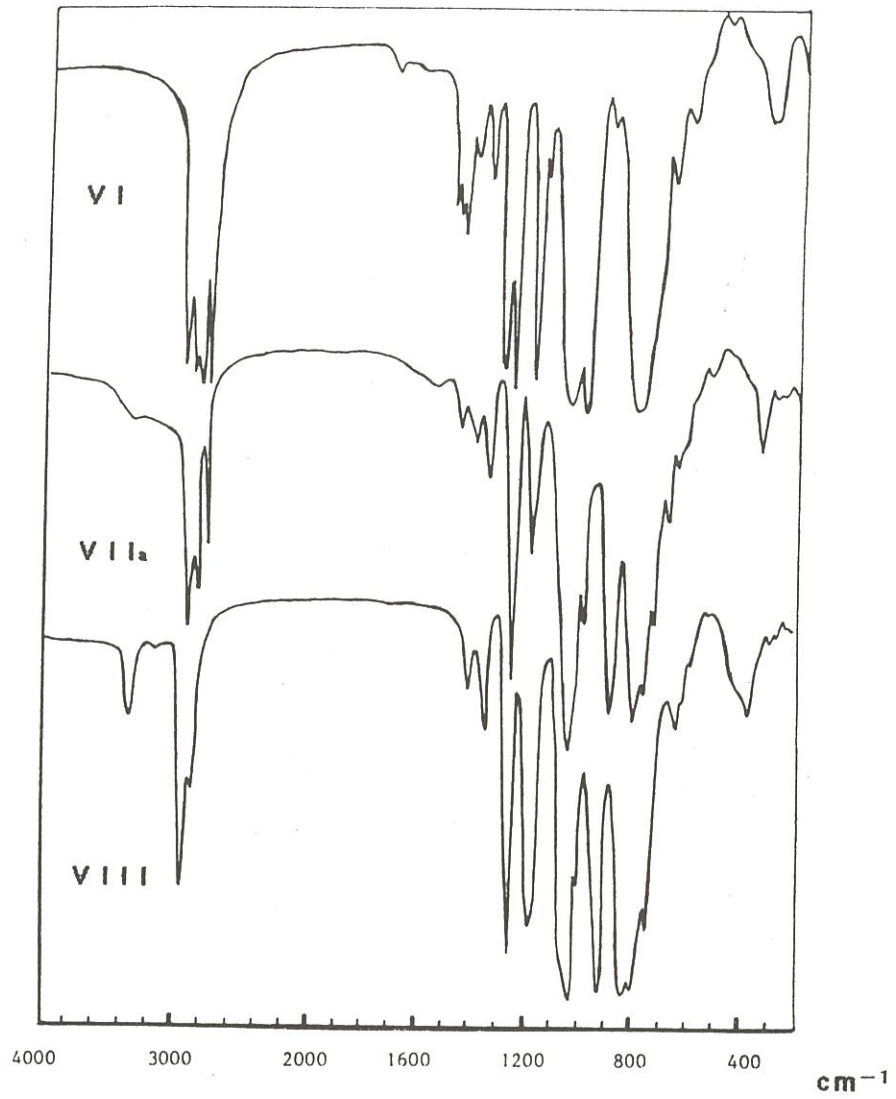

Figure 2 IR spectra of the Polycarbosilazanes Obtained upon Treatment of II Respectively by Dimethylamine (VI), Monomethylamine (VII_a) or Ammonia (VIII).

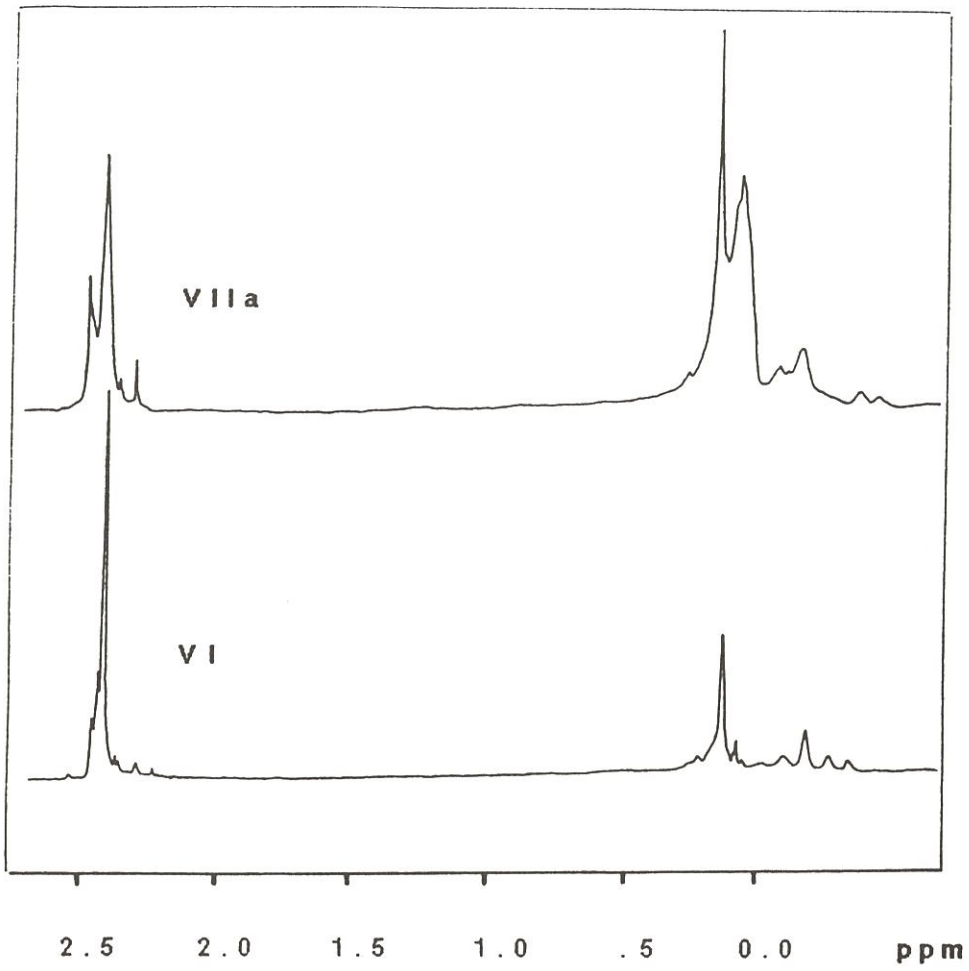

Figure 3 ^{1}H NMR Spectra (200 MHz) of Polycarbosilazanes VI and VIIa

to a large extend affording a new PSCZ with ring structures via intramolecular or intermolecular condensations, as depicted in Scheme 5.

This pathway accounted for the solid aspect of the product as well as for the broadening of the signals which was observed in the ^1H NMR spectrum. Moreover, the GPC curve was in good agreement with these phenomena as a considerable increase of the average molecular weights was observed (Mn = 3585). When the reaction was performed in the absence of solvent, the ratio of the insoluble fraction increased as expected (VII_i/VII_s =1) ; this result was consistent with intermolecular condensations which became predominant under these conditions.

4.3. Preparation of VIII

When reacted with anhydrous gaseous ammonia in dichloromethane as the solvent, II afforded a soluble fraction $VIII_s$ in 70 % yield after filtration and evaporation of the solvent and an insoluble fraction $VIII_i$ (30 % yield) which was not separated from the ammonium chloride. Subsequent aqueous workup of this last mixture led to an insoluble unmeltable, polycarbosiloxane : its elemental analysis revealed the presence only of carbon, silicon and oxygen thus demonstrating that all the initially present silicon nitrogen bonds were hydrolyzed. The yield of the soluble polymer was found to decrease strongly when prolonging the reaction time, suggesting that further reticulation pathways occured slowly, even at room temperature, likely via transamination processes involving either silylamino groups or disilazane linkages (scheme 6).

Although elemental analysis were generally aberrant in these series, particularly for silicon and carbon, because of incomplete combustion, the residual chlorine ratio was found to be less than 1 %. Polymer VIIIs was very sensitive to moisture and became gradually insoluble and unmeltable after a few days when kept at room temperature, even under argon, but remained unchanged over several weeks at - 20°C. This reticulation could be ascribed to stepwise transamination pathways wich occured very slowly in the solid state, affording trisilylated nitrogen centers (Scheme 6).

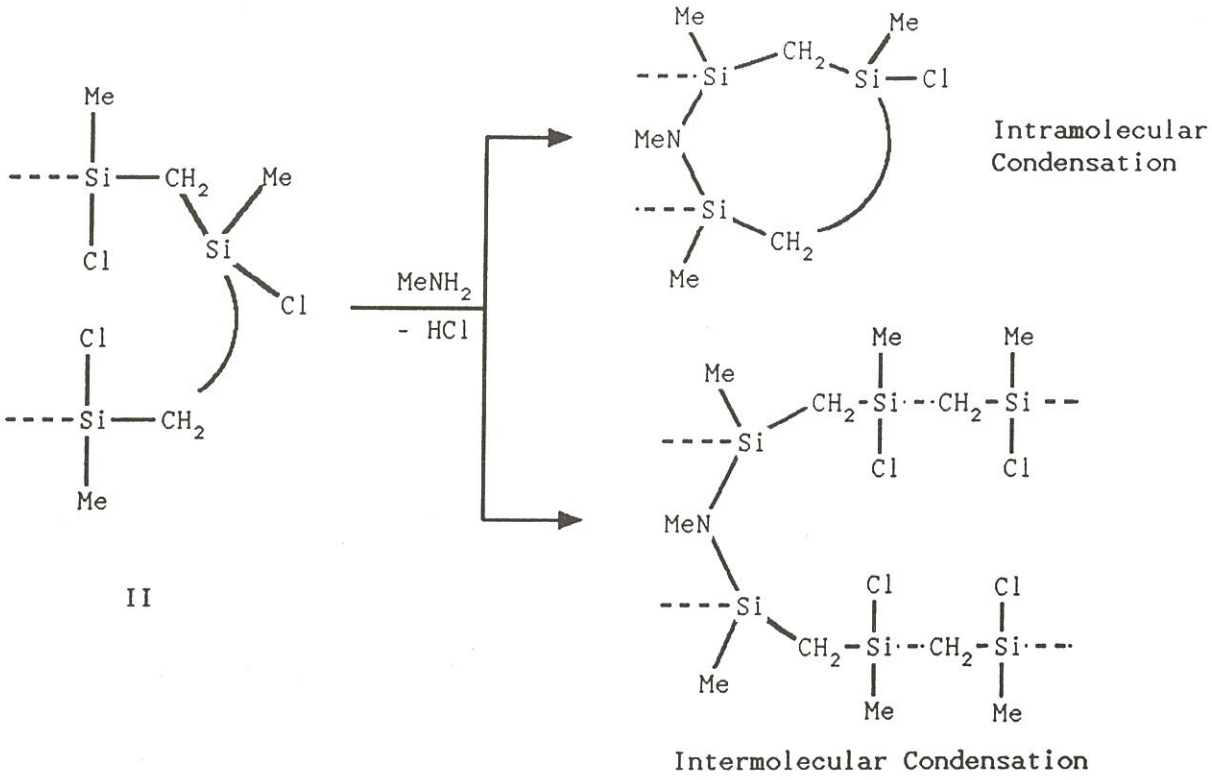

Scheme 5: Formation of Disilazane Bridges upon Reaction of Monomethylamine on II *via* Intramolecular or Intermolecular Condensations

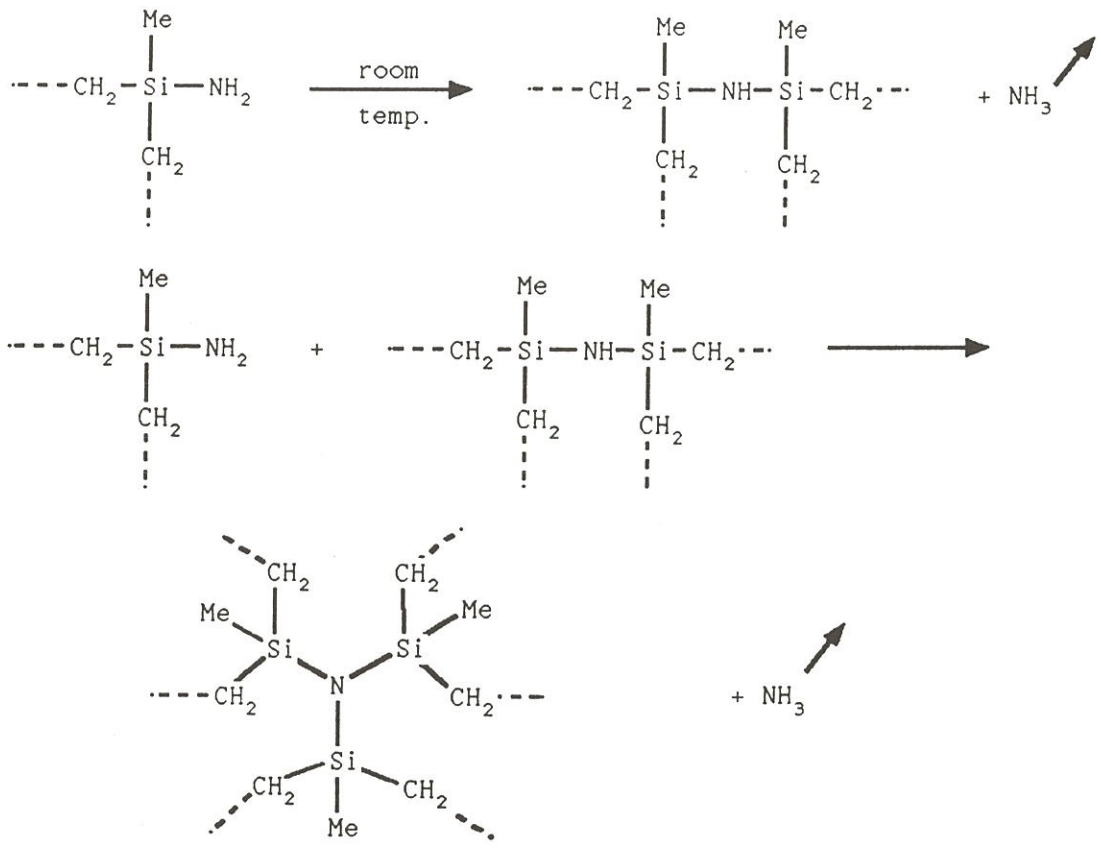

Scheme 6: Reticulation of Polycarbosilanes *via* Transamination Pathways

Characterization of $VIII_s$.

The IR spectrum of VIIIs displayed the characteristic bands of the disilazane units (3380, 1180 and 980 cm^{-1}), while no significant $Si-NH_2$ absorption was detected.

^1H NMR spectrum (200 MHz) of VII_s exhibited two broad peaks centered at 0.15 and -0.13 ppm, respectively assigned to CH_3Si plus Si-NH protons and $Si-CH_2-Si$ protons (integration ratio : 4:2). The broadening of the signals might arise from the quadrupolar effect of nitrogen as well as the complex structure of the product ; it is likely that the actual framework of $VIII_s$ was better viewed on the basis of $Si-CH_2-Si$ units linked at the silicon atoms by nitrogen bridges, and that a wide range of ring structures might arise from the silylamine and silazane condensations, as already depicted in Scheme 6 and 7, and that intramolecular ring closure might occur as well as intermolecular condensation. This assumption was also supported by the GPC profile of the soluble fraction, showing a significant increase in the molecular weight and a stronger polydispersity (Mn = 4121, ρ = 8.9). However, the relatively small change of the Mn value led us to assume that, under our conditions, the intramolecular condensations were predominant yielding only a weakly reticulated skeleton for the soluble part. This result was in good agreement with the TGA curve, as the low ceramic yield upon pyrolysis at 1000°C was only 37.5 %.

5 - HYDROLYSIS OF II : OBTENTION OF IX

In order to collect some information on the role of oxygen in the silicon carbide based ceramics, the chlorinated PCS II was hydrolysed under acidic conditions. A controlled introduction of oxygen at known positions, via disiloxane bridges was expected from this experiment, IX was a brown solid (98 % yield according to eq. 6, Scheme 2, soluble in organic solvents, softening interval : 120-130°C, Mn = 2960, ρ = 2.5).

Characterization of IX.

The ^1H NMR spectrum of IX (60 MHz) exhibited a unique signal (very broad) centered at 0.1 ppm. The IR absorption $\nu_{Si-O-Si}$ overlapped the band of the deformation of $Si-CH_2-Si$ units between 1000 and 1050 cm^{-1}. No remaining

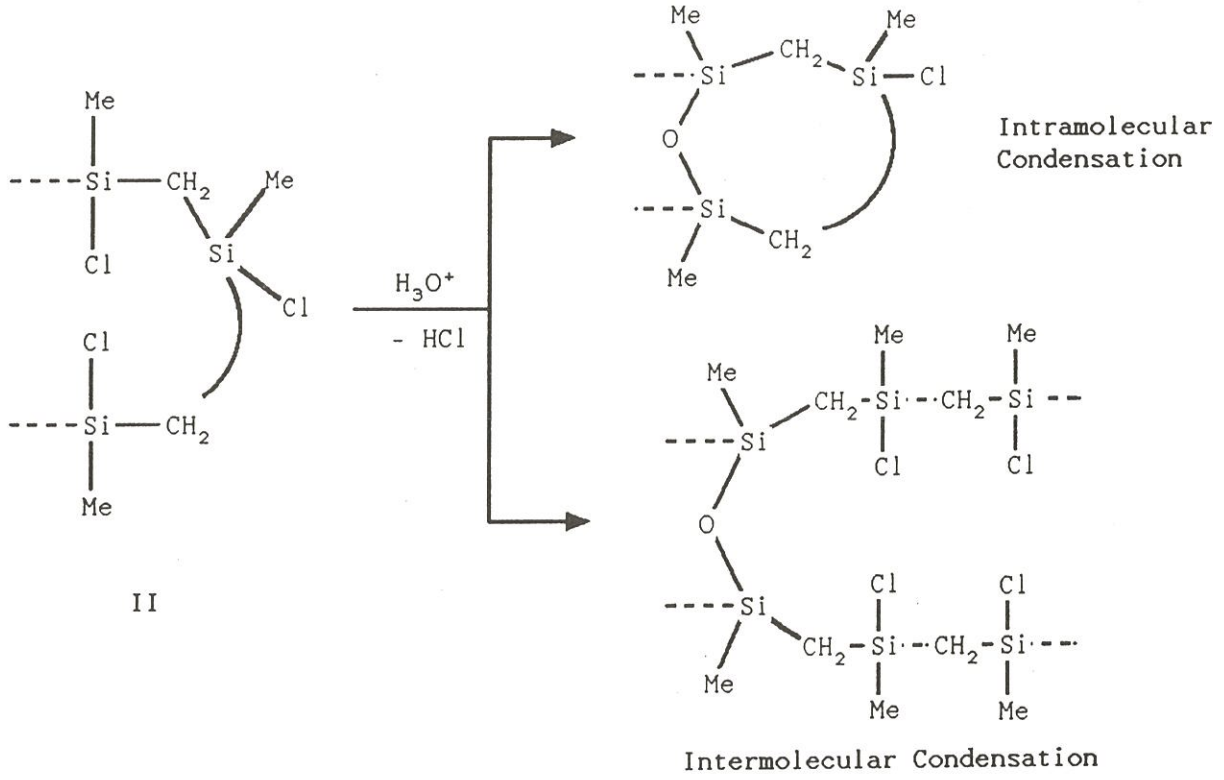

Scheme 7: Hydrolysis of II and Formation of Siloxane Bridges *via* Intramolecular or Intermolecular Condensations

TABLE I Ceramic Yields at 1000°C of the Functional Polycarbosilane Models

pro-ducts	I	III	IV_i	IV_s	V_i	V_s	VI	VII_a	VII_b	VIII	IX	X	XI
yield wt. %	3.5	5	11.4	77.6	43.5	59.3	33.5	24.7	53	37.5	54.3	14	24.7

Si-Cl absorbtion was observed in the range of 400-500 cm^{-1}. These spectroscopic data as well as the very low remaining chlorine ratio led to assume that the Si-Cl bonds were hydrolyzed. The GPC curve led to Mn = 2694 and ρ = 2.55 ; this value suggested that, in our conditions, intramolecular condensations affording the disiloxane bridges were predominant with respect to intermolecular condensation (Scheme 7).

6 - HYDROSILYLATION REACTIONS OF III

Very little information was available on the microstructure of the free carbon and its influence on the thermomechanical properties of the resultant silicon carbide ceramics. Thus polysilapropylene II was a convenient starting material in the perspective of preparing preceramic polymers with alternate silicon atoms and methylene groups, as encountered in the case of the Yajima's PCS but also offering hydrocarbon bridges. It was inferred that these last would increase the free carbon ratio in the final ceramic. Hydrosilylation reactions of 1, 3-butadiene and divinylbenzene with III were performed at 200°C in sealed vessel in the presence of Speier's catalyst [11]. In both cases, insoluble unmeltable solids were obtained respectively in 97 % yield for X and 96 % yield for XI, according to equations 7 and 8 in Scheme 3. Unfortunately the ceramic yield was very low (see Table I).

IR characterization of X and XI

The IR spectrum of X is consistent with the IR data reported for the monomeric derivative $(Me_3SiCH_2CH_2)_2$ [12]. In the case of XI, it can be observed that both Si-H bonds and vinyl groups remained.

7 - CERAMIZATION OF THE POLYCARBOSILANE MODELS

The ceramic yields were determined from the results of thermogravimetric analysis (Table 1). The data illustrate the branching concept developed by Schilling i.e. the more branched the polymer, the better its ability to give a high ceramic yield [13]. Thus I and II are linear and consequently are unsuitable precursors, whereas the ceramic yields given by the soluble products are generally poor. On the contrary, the more reticulated polymers in this series i.e. IVi and Vi are effective precursors. This result

showed that disilanyl linkages despite the reactivity, favoured high conversion rates. However it is noteworthy that the PCS having disiloxane linkages in their skeleton afforded fair ceramic yields. Such disilane or disiloxane bridges have been suggested by Okamura et al. in PCS fibers cured by electron irradiation or oxidation respectively [14].

CONCLUSION

We have synthetized original functional PCS upon derivatization of (polymethylchloro)silmethylene and polysilapropylene, in order to study the influence of the chemical composition and the nature of the reticulation patterns on the resultant ceramics. Polymers having disilane, disilazane, disiloxane and hydrocarbon chemical bridges were obtained. Futher studies on the ceramics prepared upon pyrolysis of this models will be reported in a forthcoming paper.

Acknowledgements

We thank Société Européenne de Propulsion (S.E.P.) and Centre National de la Recherche Scientifique for a grant (E. Bacqué and E. Bouillon). Also we are indebted to Conseil Régional d'Aquitaine (C.R.A.) for financial support, and Société Rhône-Poulenc Industries for providing us strating materials. We are grateful to M. Pertraud and B. Barbe at the Centre d'Etudes Structurales et d'Analyse des Molécules Organiques (C.E.S.A.M.O.) who recorded most of our NMR spectra for fruitful discussions.

References

1. S.YAJIMA, Ceram. Bull. 62 (1983) 993.

2. G. SIMON and A. BUNSELL, J. Mater. Sci. Lett. 2(1983) 80.

3. S.YAJIMA, in "Advanced Fibers and Composites for Elevated Temperature" ed. by I. AHMAD and B.R. NOTON (Conferences Proceedings 1979) p 29.

4. Y. HASEGAWA and K. OKAMURA, J. Mater. Sci. 21 (1986) 321.

5. E. BACQUE, J.P. PILLOT, M. BIROT and J. DUNOGUES, Macromolecules 21 (1988) 30.

6. E. BACQUE, J.P. PILLOT, M. BIROT and J. DUNOGUES, ibid. 21 (1988) 34.

7. C. EABORN, in "Organosilicon Compounds" (Butterworths Scientific, London, 1960).

8. C.L. SCHILLING Jr., ONR Technical Report N° AD-A141649 (1983).

9. J.M. ZEIGLER, Polym. Prepr. 27(1) (1986) 109.

10. H. MARSMANN, in "NMR Basic Principales and Progress" ed. by P. DIEHL, E. FLUCK and R. KOSFELD (Springer Verlag Berlin, Heidelberg, New-York 1981) p 65.

11. J.L. SPEIER, J.A. WEBSTER and G.H. BARNER, J. Amer. Chem. Soc. 79 (1957) 974.

12. Y.P. EGOROV, K.S. PUSHCHEVAYA, E.D. LUBUZH, V.M. VDOVIN and A.V. PETROV, Izv. Akad. Nauk SSSR Otd. Khim. Nauk, (1963) 822.

13. C.L. SCHILLING Jr., J.P. WESSON and T.P. WILLIAMS, ONR Technical Report N° AD-A099030 (1981).

14. K. OKAMURA, M. SATO and Y. HASEGAWA, in "High Tech Ceramics" ed. by P. VINCENZINI (Elsevier Science Publishers B.V., Amsterdam, 1987) p. 747.

Vu et approuvé

Talence, le

Le Président de

l' Université de Bordeaux I

RESUME :

Les procédés d'obtention des céramiques thermostructurales par pyrolyse de précurseurs organométalliques sont le sujet, depuis une quinzaine d'années, de recherches actives. On citera, à titre d'illustration, le développement et l'industrialisation des fibres à base de carbure de silicium obtenues à partir de polycarbosilanes branchés (voie S. Yajima) au Japon.

Ce travail avait pour objectif d'approfondir la connaissance de la transformation des précurseurs de type polycarbosilanes (PCS) et polycarbosilazanes (PCSZ) en céramiques à base de SiC et de Si (C,N) et de tenter de faire le lien entre la structure du précurseur, la microstructure de la céramique obtenue par pyrolyse et ses propriétés mécaniques. Il s'est orienté autour de trois axes principaux :

(i) - mise en évidence des diverses étapes et des mécanismes intervenant lors de la pyrolyse et de la céramisation d'un précurseur commercial (NC2) de type polycarbosilane branché. Il a été montré que la pyrolyse conduit d'abord à un résidu minéral amorphe qui cristallise à plus haute température. L'étude a été faite par ATG, analyse des gaz, IR, ESCA, Raman, Auger, XRD, TEM.

(ii) - élaboration et caractérisation en traction d'éprouvettes monofilamentaires issues de ce précurseur. Compréhension des phénomènes se produisant durant les étapes de réticulation, de pyrolyse et de céramisation, relation microstructure-comportement mécanique.

(iii) - contribution à la définition et à l'étude de précurseurs modèles de type PCS et PCSZ en vue de dégager le rôle tenu par l'azote et l'oxygène liés au silicium et par le carbone libre dans les céramiques et leurs propriétés (e.g. stabilité de l'état amorphe/microcristallisé).

MOTS CLES :

Précurseurs de céramique
Polycarbosilanes, polycarbosilazanes
Pyrolyse
Transition organique-inorganique
Fibre à base de SiC
Caractérisation physico-chimique
Propriétés mécaniques